Identifying lineage relationships in human T cell populations

by

Celia Lara Menckeberg

A thesis submitted to
The University of Birmingham
for the degree of
DOCTOR OF PHILOSOPHY

School of Immunity and Infection
College of Medical and Dental Sciences
The University of Birmingham
December 2010

ABSTRACT

$CD4^+$ and $CD8^+$ T cell populations can be divided into subpopulations based on expression of surface markers CCR7 and CD45RA. The resulting populations are referred to as naive, central memory, effector memory and effector memory RA^+ (EMRA). The aim of this study was to identify potential lineage relationships between these subpopulations for both $CD4^+$ and $CD8^+$ T cells through microarray analysis. The genes found to distinguish between these subpopulations include many molecules with known functions in T cell differentiation, including CCR7, CD45RA, granzymes, L-selectin and TNF receptors. Several genes from the tetraspanin family of proteins were found to be differentially expressed at mRNA and protein level; suggesting a possible role for these genes in $CD4^+$ and $CD8^+$ T cell activation, migration and lysosomal function. Other genes identified, such as LRRN3 and CXCR5 which were expressed highest on naive and CM T cells respectively, provide interesting gene targets to follow up on their function in these T cell populations. Microarray data was validated through Real Time PCR and suggests that both $CD4^+$ and $CD8^+$ T cells differentiate along a linear pathway of naive to central memory to effector memory. The transcriptional programmes responsible for these differentiation steps were distinct between $CD4^+$ and $CD8^+$ T cells, although additional elements were common to both subsets.

Dedicated to Mama en Papa

ACKNOWLEDGEMENTS

First I would like to thank my supervisor Dr. John Curnow for guiding me through this project and for adopting me when it was very much needed. The encouragement and advice he has given have helped me grow as a scientist and as a person. I would also like to thank Professor Mike Salmon, without whom this project would not have been possible.

Huge thanks to Steve (*Stev*) Kissane for all his help throughout these years, not only was he my microarray specialist but also a source of knowledge in many different topics. Thanks for always being there to help with any questions I had and for the countless lab bench and lunch time chats. I would like to thank Dr. Graham Wallace for all his support throughout and helpful discussions along the way and Dr. Ewan Ross for being a source of knowledge and always ready to help.

Also I want to thank all my lovely friends that I made working on the 3rd floor IBR. You were my family away from home and made living in Brum for four years so very special. Fern (*Barry*) Barrington, thank you for being my Harborne and vacation buddy; I loved our movie and Sunday cooking nights! Dr. Sarah (*Chuckles*) Essex thank you so much for being the smiling face I saw sitting across from me for almost four years, as well as for introducing me to the wonder that is a lemon drizzle cake. Katherine (*Kaaath*) Howlett for being my gym and pub buddy and subsequent fellow Harbonite! And for the many, many, many excellent cakes in these past four years. Lorraine (*Lore*) Yeo thank you for taking over from Sarah when it was needed and of course for the excellent white chocolate and raspberry muffins. To all my other friends, Dr. Peter Hampson, Dr. Jason Lee, Dr. Sian Lax, Siobhan Restorick, Hema Chahal, Emma Yates and many others, thank you for being a huge part in why the department of Rheumatology was such a nice place to work. I would like to acknowledge Professor Janet Lord and Professor Chris Buckley in their roles as head of the Marie Curie TRIFID project and head of the Department of Rheumatology respectively.

To my lovely friends and family back home, Ranjeeta Bendter, Francis Saridin and Serge Parabirsing, thank you for always supporting me and for always being only a phone call away. Jeeta, thank you for sticking with me for almost 25 years (playground buddies for life!) and Francis, my study-buddy, 10 years and counting! Serrie thanks for staying positive throughout everything that has happened.

I want to thank my sister Tanja and her husband Rodney for all their help along the way and for giving me the best gift ever by making me the proud auntie of Rafaël. Mostly I would like to thank my parents for always believing in me and encouraging me; for instilling in me a thirst for knowledge from a very young age and for being my rock to fall back on. You are my heroes.

ABBREVIATIONS

ADD2	Beta-adducin
AEBP1	Adipocyte Enhancer Binding Protein 1
ANOVA	Analysis of Variance
APC	Antigen Presenting Cell
BCR	B Cell Receptor
BHLHB2	Basic Helix-Loop-Helix protein B2
BM	Bone Marrow
BSA	Bovine Serum Albumin
CLIP	Class-II-associated Ii peptide
CLP	Common Lymphoid Progenitor
CM	Central Memory
CMP	Common Myeloid Progenitor
Cn	Calcineurin
CTLA-4	Cytotoxic T lymphocyte antigen-4
Cy3/Cy5	Cyanine 3 or 5
DAG	Diacylglycerol
DC	Dendritic Cells
DN	Double Negative
DP	Double Positive
EAE	Experimental Autoimmune Encephalomyelitis
EBV	Epstein-Barr virus
EDTA	Ethylenediaminetetraacetic acid
EM(RA)	Effector Memory (RA)
ER	Endoplasmic Reticulum

ETP	Early Thymic Progenitor
FACS	Fluorescent Activated Cell Sort
FDC	Follicular Dendritic Cell
FDR	False Discovery Rate
GPS	Glutamine Penicilin Streptomycin
GZM	Granzyme
HCL	Hierarchical Clustering
HEV	High Endothelial Venules
HLA	Human Leukocyte Antigen
HSC	Hematopoietic Stem Cell
HVEM	Herpesvirus entry mediator
ICAM1	Intracellular Cell Adhesion Molecule 1
IFNγ	Interferon γ
Ig	Immunoglobulin
Ii	MHC-II specific chaperone invariant chain
IL	Interleukin
IP3	Inositol 1,4,5-triphospahate
IS	Immunological synapse
KLRB1	Killer Cell Lectin-like Receptor subfamily B member 1
KLRC4	Killer Cell Lectin-like Receptor subfamily C member 4
KLRF1	Killer Cell Lectin-like Receptor subfamily F member 1
LAT	Linker for T cell Activation
LFA-1	Lymphocyte Function-associated Antigen-1
LIGHT	homologous to LTs, exhibits inducible expression, and competes with HSV gD for herpesvirus entry mediator, a receptor expressed by T lymphocytes or TNSF14
(p)LN	(peripheral) Lymph Node
Lo/Ld	Liquid order/Liquid disorder

LRRN3	Leucine Rich Repeat Neuronal protein 3
LTα$_1$β$_2$	Lymphotoxinα$_1$β$_2$
LTβR	Lymphotoxinβ Receptor
LTi	Lymphotoxin inducer
LTo	Lymphotoxin organiser
MAdCAM-1	Mucosal Addressin Cell Adhesion Molecule-1
MALT	Mucosal-Associated Lymphoid Tissue
MHC	Major Histocompatibility Complex
MLP	Multilymphoid Progenitor
MTMR8	Myotubularin related protein 8
MVB	Multivesicular Body
MTUS1	Mitochondrial Tumor Suppressor 1 isoform 3
MYBL1	Myb-related protein A
MYO1F	Myosin-If
NFAT	Nuclear factor of activated T cells
NGFRAP1	Nerve Growth Factor Receptor (TNFRSF16) Associated Protein 1
NK cell	Natural Killer cell
NKG7	Natural Killer Cell protein 7
PALS	Periarteriolar lymphoid sheath
PAMP	Pathogen Associated Molecular Patterns
PBMC	Peripheral Blood Mononuclear Cells
PBS	Phosphate Buffered Saline
PCA	Principal Component Analysis
PCR	Polymerase Chain Reaction
PF	Primary Follicles
PIP$_2$	Phospholipid phosphatidylinositol-4,5-biphosphate
PLEKHK1	Pleckstrin homology domain containing family K member 1

PKC	Protein Kinase C
PLCγ1	Phospholipase C-γ1
PNAd	Peripheral Lymph Node Addressin
PP	Peyer's Patches
PRDM8	PR domain zinc finger protein 8
PRR	Pattern Recognition Receptor
RORγt	RAR-related orphan receptor gamma
RT	Reverse Transcription
SAM	Significance Analysis of Microarrays
SH3BP5	SH3 domain-Binding Protein 5
SLC22A17	Solute carrier family 22 member 17
SLO	Secondary Lymphoid Organs
SLP-76	SH2 domain containing leukocyte protein of 76 kDa
SMAC(c/p-)	Central/peripheral supramolecular activation cluster
SP	Single Positive
TAP	Transporter associated with antigen processing
TCR	T Cell Receptor
TEM	Tetraspanin Enriched Membrane
T_{FH}	T follicular helper
Th	T helper
TLR	Toll like Receptor
TNFα	Tumour Necrosis Factor α
TRANCE(R)	TNF-related activation-induced cytokine (receptor)
(n/i) Treg	(Natural/inducible) T regulatory cell
VCAM1	Vascular Cell Adhesion Molecule 1
ZAP70	ζ-associated protein of 70kDa
ZNF	Zinc Finger

TABLE OF CONTENTS

LIST OF FIGURES

Chapter One: Introduction

Chapter Three: Examining gene expression profiles of $CD4^+$ and $CD8^+$ T cell populations during differentiation

Chapter Four: Validating gene expression profiles of $CD4^+$ and $CD8^+$ T cell populations by Real Time PCR

Chapter Five: Expression of tetraspanin family members on $CD4^+$ and $CD8^+$ T cell populations

Chapter Six: General Discussion

LIST OF TABLES

Chapter One

Introduction

1 INTRODUCTION

The immune system consists of many different cell types and organs, all of which work together to protect the body from infection. The cells of the immune system are constantly communicating with their surroundings by sending and receiving signals and by responding to those signals. The immune system itself has several levels of protection which a pathogen has to breach in order to cause damage. First there are external and chemical barriers, such as the skin and stomach acids. And then there are two branches of immune responses, the innate and adaptive [1]. Innate immunity is the first line of defence against pathogens and depends on a fixed number of germline encoded receptors. The adaptive immune response requires some time after activation to clonally expand, but it is capable of specifically recognising a wider variety of pathogens and of forming immunological memory [1-3].

1.1 Innate Immunity

As mentioned above the innate immune system is the first cellular defence mechanism the body has to protect itself from pathogens. It consists of cells which can be tissue residing (*e.g.* dendritic cells and macrophages) or patrolling (*e.g.* neutrophils and monocytes) and display immediate and non-specific effector functions [1;4]. The cells classified as innate immune cells are neutrophils, monocytes, macrophages, dendritic cells (DCs) and natural killer cells. These cells have several ways of detecting and clearing a pathogen. They express receptors on their cell surface, referred to as pattern recognition receptors (PRRs) which recognise several evolutionary conserved molecular structures, referred to as pathogen associated molecular patterns (PAMPs) [5]. Toll-like receptors (TLRs) are very important to

innate immune cells, since they are capable of recognising a variety of organisms. There are ten human TLRs described so far and these can be expressed on the cell surface (such as TLR1, 2, 4, 5 and 6) or within intracellular compartments (such as TLR3, 7, 8 and 9). The nucleotide organisation domain (NOD) family of receptors are mostly expressed in the cytoplasm and react to intracellular pathogen derived molecules. Through phagocytosis innate immune cells are capable of engulfing a pathogen and trapping it within a vesicle, in which the pathogen is destroyed by digestive enzymes or reactive oxygen species [1]. Almost all cells of the innate immune system are capable of phagocytosis. Innate immunity can also activate a humoral response through the complement system [6;7]. The complement system uses antimicrobial peptides and opsonins to target and lyse the pathogen, and produces chemoattractants. The result of this is that more cells are attracted to the site of inflammation and cause the classical signs of inflammation, such as swelling, redness, pain and heat [7].

1.2 Adaptive Immunity

In contrast to the cells in the innate immune system, cells of the adaptive immune system (T and B cells) are capable of recognising specific antigens due to the expression of antigen specific receptors on their cell surface [6]. B cells express on their cell surface a B cell receptor (BCR), which is an antibody unique for an antigen. When a B cell recognises its antigen, it is stimulated to proliferate and differentiate into plasma cells and memory B cells. Plasma cells produce large amounts of soluble antibodies (immunoglobulins) of a defined specificity, these antibodies are then released into the blood [1]. Immunoglobulins are produced through somatic recombination and mutation of a limited set of gene segments, resulting in an almost infinite diversity. Immunoglobulins are Y shaped molecules consisting of two heavy chains and two light chains which are linked together by disulfide bonds. Both the heavy and light chains have a constant and a variable region. The class of antibody (isotype) is determined by the heavy chain, of which there are five resulting in five isotypes IgA, IgD, IgE, IgG and IgM. IgM antibodies are low affinity and are produced in the primary response. In a secondary response, resulting from B cell activation through T cell help, the higher affinity IgG antibodies are produced. Antibodies will bind to their antigen and neutralise them in this way [1].

T cells are divided into a $CD4^+$ and a $CD8^+$ compartment, both $CD4^+$ and $CD8^+$ T cells express an antigen specific T cell receptor (TCR) on their cell surface. The TCR is very similar to an immunoglobulin, being composed of immunoglobulin-like domains, however a different set of genes is involved in producing the TCR. When the TCR is activated the T cells can be induced to produce cytokines as well as exert effector functions. $CD8^+$ T cells are cytotoxic through the secretion of perforin and granzymes resulting in the death of an

infected cell. $CD4^+$ T cells upon activation can secrete cytokines and differentiate into several subsets which can exert either effector or regulatory functions [1]. DCs are classically innate immune cells, but they provide an important link between innate and adaptive immunity [5]. When residing in tissue, DCs are capable of taking up antigens, which they then present on their cell surface. They subsequently migrate to lymphoid organs where they can present the antigen to T cells initiating the adaptive response [1;5]

1.3 Hematopoiesis

Hematopoiesis is the process in which the cells of the blood are generated in the bone marrow. This process is classically thought to start out with a hematopoietic stem cell (HSC) which divides and gives rise to progenitor cells which will differentiate into one of the blood lineages [8-10]. A linear model for hematopoiesis was adopted after Kondo *et al* (1997) described a clonogenic common lymphoid progenitor (CLP) in mice and Akashi *et al* (2000) found a clonogenic common myeloid progenitor (CMP) [11;12]. This classical model of hematopoiesis starts with an HSC which differentiates into either of the multipotent progenitors CLP or a CMP committed to either the lymphoid or myeloid lineage (Fig. 1.1A). With the identification of mouse progenitors capable of giving rise to both lymphoid and myeloid lineages the question arose whether the split between the progenitors capable of giving rise to these distinct lineages was as clear cut as suggested in the classical model. Doulatov *et al* (2010) compared the developmental potential of seven progenitor populations in humans and suggested an adapted model of hematopoiesis in humans (Fig. 1.1B) [10]. They found that the CLP which was thought to only give rise to cells of lymphoid origin, was also

capable of giving rise to cells of myeloid origin and termed it a multilymphoid progenitor (MLP).

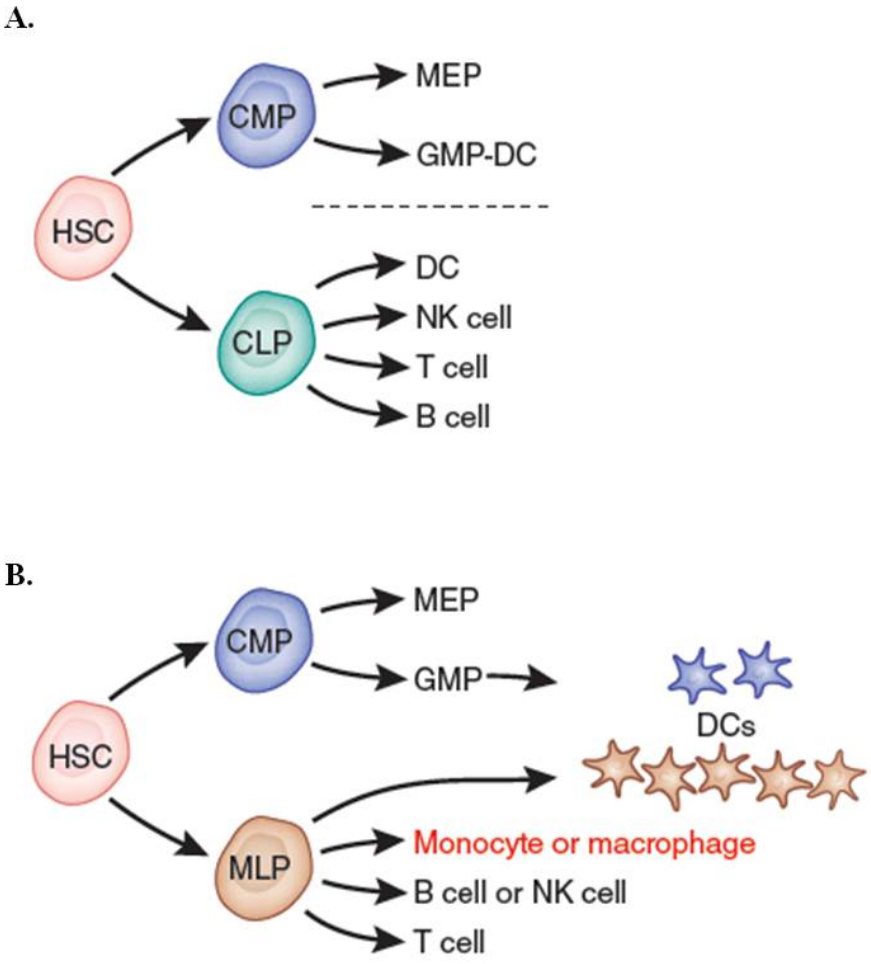

Figure 1.1. Schematic overview of hematopoiesis in humans, adapted from Dorshkind 2010 [13]. The classical view of hematopoiesis assumed an early split between lymphoid and myeloid lineages **(A)**, whereas more recent data suggests that there is some degree of multi-lineage potential even in the more differentiated subpopulations **(B)**.

It is thought that hematopoiesis occurs in two specialised stem cell niches in the bone marrow, namely the osteoblastic niche and the vascular niche [14;15]. A stem cell niche is thought to provide a microenvironment to stem cells, which supports self renewal and proliferation (Fig. 1.2). The development of adult blood lineages from HSCs is dependent on a balance between the self renewal capacity of the cells and the capacity to differentiate. One way in which this is achieved is by asymmetric division of the HSC; when dividing one daughter cell will become an HSC whereas the second daughter cell will differentiate along a pathway. The other factor influencing this balance is thought to be the microenvironment provided to the HSCs. Among HSCs there are long term (LT) and short term (ST) HSCs, in which the LT HSCs are mainly kept in a quiescent state and ST HSCs are proliferating cells [14]. Several mouse studies have shown that an increase in osteoblastic cells in the bone marrow correlates to an increase in the number of LT HSCs found, suggesting a role for the osteoblastic niche in the generation and maintenance of LT HSCs [16;17]. The vascular niche does so by providing a nutrient rich environment, which is less hypoxic compared to the osteoblastic niche [14;18]. The vascular niche also provides stimuli which help the HSC migrate across the endothelium (*e.g.* SDF-1) and migrate to peripheral sites as well as home back to the bone marrow.

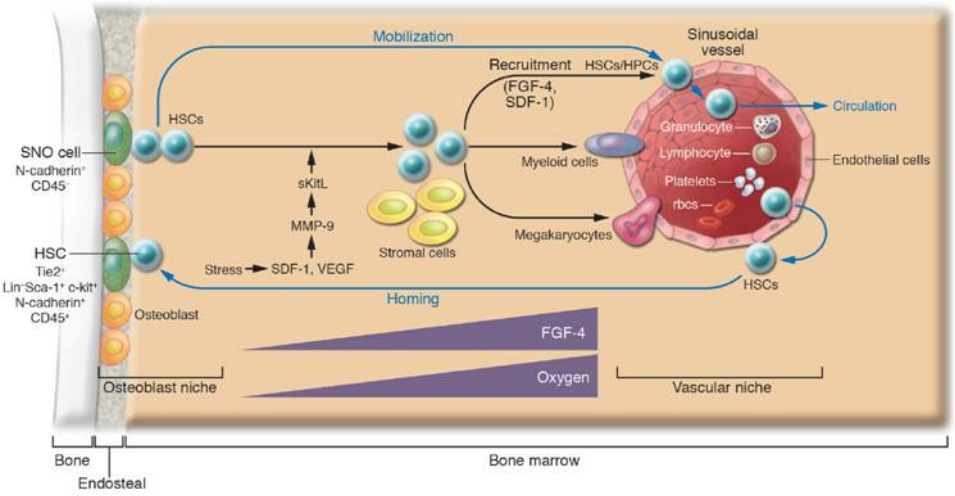

Figure 1.2. Osteoblastic and vascular niches in bone marrow, adapted from Yin and Li 2006 [14]. Hematopoiesis can occur within two distinct niches in the bone marrow. The osteoblastic niche is thought to provide a microenvironment which keeps the HSCs in a quiescent state, whereas the vascular niche helps with the HSC migration across the endothelium as well as providing an environment which promotes proliferation and differentiation of the cells.

1.4 Lymphoid organs

The cells of the immune system arise in the bone marrow from a hematopoietic stem cell, they then travel between the blood and lymphoid organs until they encounter antigen. The lymphatic system consists of lymph nodes which are connected by lymphatic vessels [19]. Since the bone marrow and thymus are the sites of lymphocyte generation in the immune system they are referred to as primary lymphoid organs [20]. Lymphoid cells, such as B and T cells travel through lymphatic vessels from tissues to secondary lymphoid structures [19].

As opposed to primary lymphoid organs there are also secondary lymphoid organs (SLOs). Spleen, lymph nodes (LN) and mucosal-associated lymphoid tissue (MALT) are examples of these lymphoid structures. Secondary lymphoid organs are involved in the retention of foreign antigens and subsequent presentation of these antigens to lymphoid cells (Fig.1.3). These lymphoid organs are spaced throughout the body in such a manner that ensures optimal capture of antigen [21]. The spleen plays a pivotal role in detection and clearance of blood-borne antigens. Lymph nodes on the other hand are important in detecting interstitial antigens and MALT does so at mucosal surfaces [22].

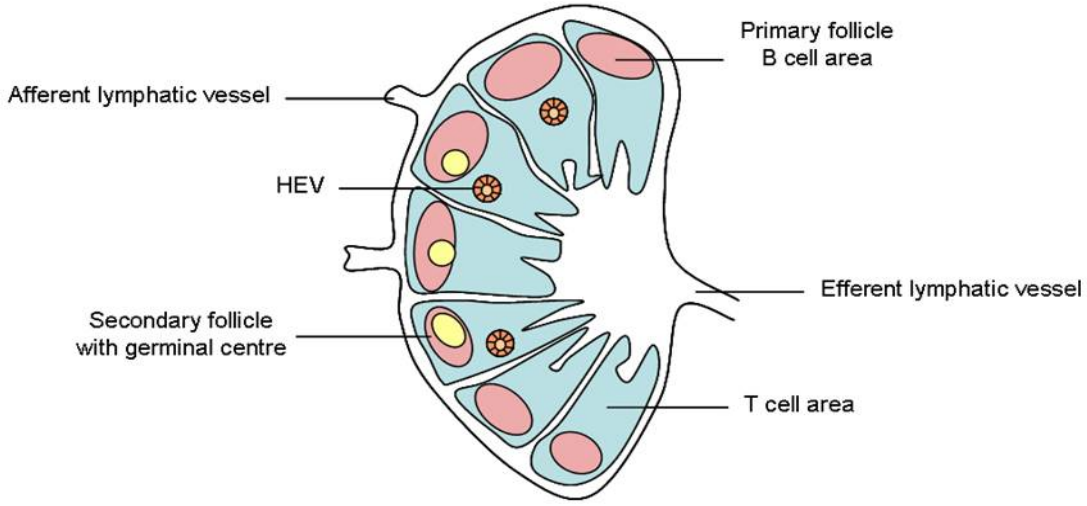

Figure 1.3. Structure of secondary lymphoid organs (SLO). The cortex of a SLO has T and B cell areas, consisting of primary follicles and, after antigen challenge, secondary follicles containing germinal centres. Afferent lymphatic vessels form the entry route for antigen loaded DCs and naive B and T cells extravasate through High Endothelial Venules (HEV) and lymph leaves the SLO through the efferent lymphatic vessels.

The development of LNs occurs after lymph sacs are formed from endothelial cells during early development [23]. From these lymph sacs the lymphatic network is formed under the control of the transcription factor Prox1, which is expressed by lymphatic endothelial cells. $CD4^+CD3^-IL\text{-}7R\alpha^+$ lymphotoxin inducer (LTi) cells form aggregates near endothelial cells at sites where a LN will develop. The LTi cells trigger the differentiation of $VCAM\text{-}1^+ICAM\text{-}1^+$

(vascular cell adhesion molecule 1, intracellular cell adhesion molecule 1) lymphotoxin organiser (LTo) cells by binding to the lymphotoxin beta receptor (LTβR) on these cells. This results in the production of the chemokines CXCL13, CCL19 and CCL21 which attract circulating hematopoietic cells resulting in the formation of an early lymph node anlagen [24]. From the 12th week of gestation T cells are starting to appear in the periphery and the number of circulating cells that enter the lymph node increases [25]. After week 14 CD4^{+} T cells can be found in the lymph node anlagen, whereas very few CD8^{+} T cells can be found. The B cells that are present at this stage are not organised into lymphoid follicles yet, this occurs during the subsequent weeks when primary follicles (PF) are formed. In these PF precursors for follicular DCs (FDCs) are present. The first fibroblastic reticulum cells (FRC) are found in the paracortical regions of the lymph node after the 16th week, this marks the formation of a T cell zone [25]. FRCs form a reticular network together with reticular fibres and fibrous extracellular matrix, the reticular network functions as a scaffold for the structure of a lymph node [26;27].

An adult lymph node consists of B and T cells and APCs arranged into specific compartments; an outer cortex and inner medulla which are surrounded by a capsule and a lymphatic sinus [28]. The B cells and follicular dendritic cells can be found in the cortex, whereas T cells and dendritic cells can be found in the paracortical region. The subcapsular sinus and medullary cord contain the macrophages (Fig. 3) [29;30].

The B cells are organised into primary follicles, which can form germinal centres when a B cell is activated with its antigen. Within the paracortex near the border with the B cell area there are high endothelial venules (HEVs), through which B and T cells enter from the

circulation, if they do not get activated the cells leave the LN via the efferent lymphatic vessels [28;31].

The spleen can be divided into two areas, the splenic red pulp and white pulp. The red pulp functions primarily as a filter where aged or damaged erythrocytes are removed from the blood. The white pulp is organised into T and B cell areas and has a single vascular supply, the splenic artery. The splenic artery branches into central arterioles which enter the white pulp.

The central arterioles are surrounded by a T cell compartment called the periarteriolar lymphoid sheath (PALS). After the central arteriole leaves the PALS it forms a marginal sinus which contains endothelial cells expressing mucosal addressin cell adhesion molecule-1 (MAdCAM-1). The B cells in the white pulp are organised into two compartments, one which consists of naive B cells and the other consists of follicle associated cells, which are organised into primary follicles [28].

1.5 T cell development

The development of T cells in the thymus can be divided into several distinct phases. The first phase entails thymic colonisation and committing to the T cell lineage. The second phase sees the development of two distinct T cell lineages based on the T cell receptor (TCR) expressed on their cell surface. T cells which express a αβ TCR respond to antigen presented on MHC molecules and require the co-receptors CD4 and CD8, whereas T cells with a γδ TCR can recognise antigen which is not presented on an MHC molecule. During the third phase both the αβ and γδ lineages complete their differentiation [32;33]. Early thymic progenitors (ETPs) are thought to colonise the thymus while retaining some myeloid potential. The environment in the thymus is thought to drive the cells to become committed T cells in a gradual process in which the cells become less multipotent in each subsequent stage. The double negative (DN) stage in which the cells do not express CD4 or CD8 on their cell surface, can be divided into four stages based on the expression of CD44 and CD25. The ETPs are cells in the DN1 stage and exhibit a $CD44^{+}CD25^{-}$ phenotype, these cells can give rise to T cells, B cells, NK cells and DCs. ETPs and DN2 ($CD44^{+}CD25^{+}$) cells undergo a burst of proliferation, they may also initiate some V(D)J rearrangement but this does not result in the full rearrangement required for expression of a functional TCR on the cell surface. When the cells reach the DN3 stage ($CD44^{-}CD25^{+}$) they stop proliferating and the TCR gene rearrangement is increased resulting in the first fully rearranged TCR loci. The DN3 stage can be further divided into a DN3a and DN3b stage, the DN3a cells have not yet successfully rearranged the TCR gene, whereas DN3b cells have. The DN3b cells subsequently undergo TCR dependent selection, referred to as β-selection, after which the cells switch on CD4 and CD8 expression and become double positive (DP) TCR αβ cells. If

the DN3b cells express a γδ TCR they are selected as γδ T cells, which do not express the co-receptors CD4 or CD8 [32;33].

DP cells are subjected to a process called positive selection, in which cells are presented with self antigen expressed on MHC molecules. DP cells are the first to express a fully assembled αβ TCR and the ligand specificity of this TCR will determine their fate during positive selection. The generation of αβ TCRs through V(D)J rearrangements results in a huge repertoire of antigen specific TCRs, most of which will not be able to recognise self antigen and therefore result in the death of the cell expressing this TCR during positive selection. DP cells undergoing positive selection are required to only respond to survival signals downstream from TCR ligation and remain unresponsive to other survival signals, such as IL-7. The CD4 and CD8 co-receptors are transmembrane molecules whose extracellular domain binds to the MHC-II or MHC-I molecules respectively. Their intracellular domain binds to protein tyrosine kinase Lck, which initiates TCR signalling when activated. The progression from the DP stage to the SP stage is a result of positive selection, in which thymic epithelial cells express self antigen on MHC molecules and trigger TCR signalling [34;35]. The TCR binding with self antigen on MHC is required to be a low affinity bond otherwise the cells undergo programmed cell death.

There are several models on how TCR specificity determines whether a DP cell will become a $CD4^+$ or a $CD8^+$ single positive (SP) T cell. In the classical stochastic model it was thought that the lineage choice was random and would result in halted gene expression of one or the other co-receptor as a consequence of the same signalling event (Fig. 1.4A). After this first step a second TCR rescue step would be needed to assure that only SP cells with matched TCR and co-receptor survive [36]. This model requires the new SP cells to be short lived if their TCR and co-receptor do not match, however this has been contradicted by experiments that

show SP cells with mismatched TCRs and co-receptors are in fact not short lived but capable of differentiating into mature T cells.

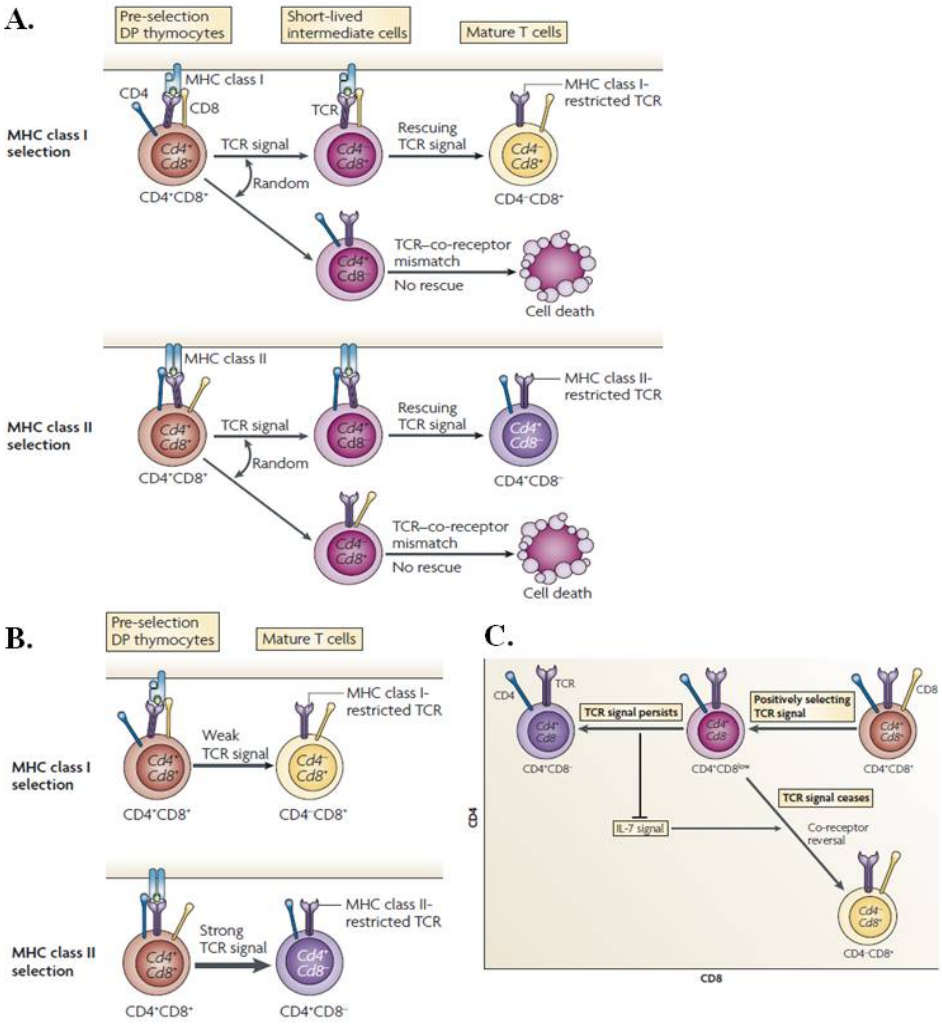

Figure 1.4. Models of positive selection of double positive (DP) thymocytes, adapted from Singer *et al* 2010 [36]. During positive selection DP αβ T cells are presented with antigen on MHC-I or MHC-II molecules, depending on which co-receptor gets activated during positive selection the cell differentiates into either a $CD4^+$ T cell or a $CD8^+$ T cell. **A)** The classical stochastic model assumes that positive selecting T cell receptor (TCR) signals randomly stop the expression of one or the other co-receptor molecule, creating short lived intermediate cells which require a second TCR signal for their rescue. **B)** The strength of signal model suggests that a weak TCR signal halts Cd4 expression, whereas a strong TCR signal halts Cd8 expression. **C)** The kinetic signalling model postulates that regardless of the specificity of their TCR, a TCR signal induces the DP cell to become $CD4^+CD8^-$ intermediate cells. If the TCR signal persists in this intermediate cell it will differentiate into a $CD4^+$ T cell, if not it will become a $CD8^+$ T cell.

The strength of signal model assumes that CD4 and CD8 co-receptors provide signals of a different strength during positive selection (Fig. 1.4B). The intracellular tail of CD4 is capable of binding more Lck than that of CD8 therefore the engagement of TCR and CD4 generates stronger signals than TCR engagement along with CD8. When engineering a CD8α gene in mice to express the cytosolic tail of CD4, it was shown that expression of this engineered gene resulted in more MHC-I T cells being rescued, but that there was no effect on CD4/CD8 lineage choice because all the MHC-I T cells in the engineered mice were $CD8^+$ T cells [36].

The kinetic signalling model suggests that TCR signal duration and cytokines of the common γ chain family acting as sensors to detect the duration of the TCR signal determine CD4 *versus* CD8 lineage choice. Based on experimental observations it was proposed that in the kinetic signalling model DP cells switch off CD8 gene expression and then assess the effect of a lack of CD8 on TCR signalling (Fig. 4C). If a TCR signal persists in the absence of CD8, the cell differentiates into a $CD4^+$ T cell, if no signal is detected then the cell becomes a $CD8^+$ T cell. This model proposes that persistence of the TCR signal stops IL-7 signalling allowing the differentiation of $CD4^+$ T cells, whereas a lack of TCR signalling leads to IL-7 signalling allowing the differentiation of $CD8^+$ T cells [36]. A round of negative selection occurs in which cells which have migrated to the cortico-medullary junction are exposed to self antigen. Cells which bind with high affinity to the self antigen, hence are auto-reactive, will then undergo apoptosis [35;37].

1.6 T cell memory

Before antigen activation naive T cells circulate through the body between secondary lymphoid organs via the blood and lymph. This circulation of naive cells is necessary to increase their chances of encountering antigen [38]. Without antigen activation naive T cells have a prolonged lifespan, this is a result of continuous recognition of several ligands which deliver sufficient signals to keep the T cells from dying. The main survival factor for naive T cells is the cytokine IL-7, *in vitro* culture of naive T cells showed IL-7 kept the cultured naive cells alive, whereas naive cells cultured without IL-7 died [26]. Three subsequent events occur when a naive cell homes to peripheral lymph nodes (pLN), first the cell starts rolling due to interaction of CD62L with its ligand PNAd (Peripheral Lymph Node Addressin). The cell then adheres by the ligation of CCR7 with its ligand CCL21, resulting in the activation of the integrin LFA-1. LFA-1 binding to ICAM-1 results in firm adhesion of the cell, allowing extravasation of the cell [39;40]. After recognising antigen presented on APCs the naive T cells undergo clonal expansion and differentiate into effector cells. $CD8^+$ T cells differentiate into cells capable of producing IFN-γ, TNF-α and several chemokines as well as directly killing their target cells. $CD4^+$ T cells differentiate into either of several subsets of T helper cells, Th1, Th2, Th17, T follicular helper (T_{FH}) and regulatory T cells (Treg).

The immune response is divided into several phases based on the accumulation and/or disappearance of antigen specific cells during the response [41]. After antigen stimulation occurs, a lag phase in which antigen specific cells are stimulated to become activated, but do not divide. During the expansion phase that follows the antigen specific cells expand and differentiate. The cells eventually reach a plateau stage which is followed by a contraction phase [41]. After clearance of the antigen the majority of effector cells are removed since they

are no longer required [38;39]. A small number of T cells persists after antigen clearance and become long-lived memory cells. Memory T cells provide long-term protection to re-exposure to antigen, resulting in a faster and stronger response after re-exposure [38;39;42]. As opposed to the naive T cell pool, the memory T cell pool has a narrower TCR repertoire. Another striking difference between memory T cells and naive T cells is that memory cells are able to produce a wider variety of cytokines than naive cells. The exact route of memory T cell formation is not yet clearly understood, one possibility is that memory cells are descendants from the effector population. There might also be a group of activated cells which are either predestined to become memory cells or driven to become memory cells [42]. Memory T cells can be further divided into two subsets of memory cells (central and effector), based on their rate of proliferation and surface marker expression [38]. Sallusto *et al* (1999) describe four T cell populations based on the expression of CCR7 and CD45RA; naive, central memory (CM), effector memory (EM) and EMRA populations [43]. The EMRA population ($CCR7^{-}CD45RA^{+}$) shares many of the features of the EM cells but are thought to be terminally differentiated cells.

The naive population described by Sallusto *et al* (1999) is double positive for both CCR7 and CD45RA, whereas the central memory population expresses $CCR7^{+}CD45RA^{-}$ and has a lower rate of proliferation [43]. The effector memory cells have a fast turnover and exert cytotoxic effector functions. These cells express the activation markers CD69 and CD25 and have lost expression of lymph node homing receptors CCR7 and CD62L expressing a $CCR7^{-}$ $CD45RA^{-}$ phenotype. Memory T cells are more metabolically active than naive T cells, suggesting that these cells receive constant signals essential for providing a survival stimulus. Even though memory T cells show a higher rate of proliferation total numbers of memory T cells remain fairly constant through life. Moreover after each infection a new memory subset

is formed, resulting in a redistribution of the number of memory T cells already present, so as to maintain a similar total number of memory cells [44].

1.7 T cell activation

When a T cell recognises its antigen on the surface of an APC an adaptive immune response is initiated. Antigen, in the form of peptides, is presented to the T cells on a major histocompatibility complex (MHC) molecule present on the cell surface of an APC, such as DCs or B cells. DCs express several molecules needed for efficient activation of T cells, especially naïve cells, such as the costimulatory molecules CD80 and CD86, the adhesion molecules ICAM-1 and ICAM-3 as well as high levels of MHC class I and MHC class II molecules [45;46]. As described above, a TCR present on a $CD4^+$ T cell will recognise antigen presented on MHC-II whereas a $CD8^+$ T cell will recognise antigen presented on MHC-I. CD4 and CD8 are coreceptors which will directly bind to non-polymorphic regions of MHC-II or MHC-I respectively, thereby strengthening the interaction between the T cell and APC.

T cell activation is a direct result of the recognition by the TCR of antigen presented in the peptide binding groove of MHC-I and MHC-II molecules. The way in which peptide is acquired differs between MHC-I and MHC-II. MHC-I is primarily thought to present intracellularly acquired peptides, as a result of the presence of a viral infection, an intracellular bacteria or changes within the cell. In comparison MHC-II is thought to present extracellular antigens. There is also the process of cross-presentation by certain specialised APC particularly plasmacytoid DC, where extracellular antigens are presented by MHC-I. MHC molecules are heterodimeric proteins, consisting of an α and β chain and which span the plasma membrane [47;45]. Newly synthesised MHC-II dimers are chaperoned by binding

with the MHC-II specific chaperone invariant chain (Ii), this prevents the MHC-II heterodimer from forming aggregates which is a result of not having bound peptide in the binding groove. The Ii protein has a classII-associated Ii peptide (CLIP) which occupies the binding groove as well as sorting signals which direct the MHC-II molecule to the endocytic system [45]. Within an endosome the Ii protein is degraded by proteases, except for the CLIP region, which stays bound to MHC-II. CLIP can be removed by non-classical MHC-II protein HLA-DM, when HLA-DM colocalises with MHC-II in an endosome it catalyses the dissociation of CLIP from the MHC-II molecule [45].

MHC-II molecules encounter their antigen after APCs take it up from the extracellular milieu, the antigen is then contained within a phagosome. The phagosome fuses with a lysosome, giving rise to a phagolysosome, in which the contents of the phagosome are degraded by lysosomal acid hydrolases and cathepsins. In the phagolysosome the degraded contents of the phagosome can be loaded onto the MHC-II molecules which were present in the lysosome. MHC-II molecules loaded with antigen are then transported to the cell surface where they can present their load to circulating $CD4^+$ T cells [47].

The MHC-I molecule consists of an α (heavy chain) and β_2 microglobulin chain, of which the α chain is membrane spanning. MHC-I molecules present antigen derived from cytosolic proteins that they encounter in the endoplasmatic reticulum (ER) where both chains are synthesised. Proteins which are destined for degradation are ubiquitinated and processed by a proteasome within the cytosol. The degraded proteins are then transported into the ER by the transporter associated with antigen processing (TAP) complex. In the ER the peptides can interact with the newly synthesised MHC-I molecule [47].

As described above (**1.5 T cell development**) a TCR can consist of either αβ or γδ chains. The TCR forms a complex together with CD3. CD3 consists out of four subunits of ε, γ, δ and ζ and these subunits associate with the TCRαβ as three dimers, namely εγ, εδ and ζζ [48]. When a TCR binds to its antigen on an MHC molecule, the TCR:CD3 complex undergoes a conformational change, resulting in CD3 protein intracellular domains becoming accessible to phosphorylation. When several TCRs on the same T cell are engaged in binding to antigen, TCR clustering occurs. This creates the possibility for the CD4 or CD8 coreceptors, which are associated with the Src kinase Lck, and the membrane protein Fyn to phosphorylate ITAM motifs on the CD3 chains [49]. Phosphorylation of the ζ chain creates docking sites for the ζ-associated protein of 70 kDa (ZAP70) and subsequent phosphorylation of ZAP70 by Lck activates ZAP70, which in turn phosphorylates the membrane protein linker for T cell activation (LAT) as well as the SH2 domain containing leukocyte protein of 76 kDa (SLP-76). Together SLP-76 and LAT form a docking site for phospholipase C-γ1 (PLCγ1), PLCγ1 is activated by the kinase Itk and activated PLCγ1 cleaves phospholipid phosphatidylinositol-4,5-biphosphate (PIP_2) to form inositol 1,4,5-triphosphate (IP3) and diacylglycerol (DAG). IP3 binds to IP3 receptors on the endoplasmic reticulum (ER) resulting in the release of intracellular calcium stores. Calcium itself is involved in many biological processes and the rise in calcium concentration in the cell results in cell membrane calcium released activated calcium channels (CRACs) allowing extracellular calcium to enter the cell [49;50]. Calcineurin (Cn) is a serine-threonine protein phosphatase which can transduce the calcium signal. The nuclear factor of activated T cells (NFAT) family of transcription factors are principal targets of Cn. When a cell is activated the NFAT proteins are dephosphorylated by Cn, this results in a conformational change which exposes a nuclear localisation signal. NFAT is then translocated to the nucleus where it can activate gene transcription.

It has been shown that during the interaction between T cells and APCs the surface molecules are organised in a specific manner, forming what is referred to as an immunological synapse (IS). The IS on the surface of a T cell consists of two concentric rings, the centre ring or central supramolecular activation cluster (c-SMAC) contains the TCR:CD3 complex, the costimulatory molecule CD28 and the kinase Lck. In the outer ring or peripheral supramolecular activation cluster (p-SMAC) there are high levels of the integrin leukocyte function-associated antigen 1 (LFA-1), the p-SMAC thus provides anchoring of the T cell to the APC [45]. There is another ring of proteins formed outside of the p-SMAC, where proteins such as CD43 and CD45 accumulate. These proteins are quite big and therefore stick out of the plasma membrane which would make it impossible for the much smaller TCR to stay in contact with the MHC molecule [45;50]. Optimal T cell activation requires there to be a second signal from co-stimulatory molecules in addition to TCR recognition of antigen. CD28 is a potent co-stimulatory molecule and it binds to its ligands CD80 (B7-1) and CD86 (B7-2) present on the cell surface of APCs [51]. As mentioned before, CD28 co-localises with the TCR within the c-SMAC, where together with the TCR signal it enhances the gathering of lipid rafts as well as tyrosine phosphorylation of molecules involved in T-cell activation [51;52]. The actual signalling pathways used by both the TCR and CD28 have common characteristics and this suggests that CD28 signalling can lower the threshold for T cell activation. Cytotoxic T lymphocyte antigen-4 (CTLA-4) structurally resembles CD28 and also binds to CD80 and CD86, but ligation of CTLA-4 leads to an inhibitory signal limiting T cell activation [51;52]. CTLA-4 is not normally expressed on the cell surface of a resting T cell, but its expression is induced by T cell stimulation via the TCR; the one exception is on the surface of regulatory T cells. CTLA-4 has a much higher affinity for binding to CD80 and CD86, thus making it possible to inhibit further T cell activation as a result of TCR and CD28 signalling. Since CD86 is constitutively expressed on the cell surface of APCs, whereas CD80 is induced upon

stimulation, it is thought that CD86 functions primarily as a ligand for CD28 and CD80 as a ligand for CTLA-4. PD-1 (CD279) is another inhibitory protein related to CD28 and it is expressed on activated T and B cells. The ligands for PD-1 are PD-L1 and PD-L2 and both ligands have different expression patterns. PD-L2 expression can be induced on DCs and monocytes, while PD-L1 expression is constitutive on T cells, APCs as well as on non-hematopoietic cell types such as vascular endothelial cells [51].

1.8 $CD4^+$ T cells

$CD4^+$ T cells are classically described as helper T cells, since they provide several signals to activate other immune cells. They promote isotype switching and somatic hypermutation in B cells. They also induce B cell differentiation to plasma cells and memory cells in germinal centres [53]. Another role attributed to $CD4^+$ T cells is helping naive $CD8^+$ T cells to allow differentiation into effector and memory cells [54-56]. $CD4^+$ T cells also provide help to macrophages and APCs [53].

After antigen stimulation naive $CD4^+$ T cells become activated and differentiate into effector cells. Several $CD4^+$ effector T cell subsets have been described based on cytokine production (Fig.1.5). Th1 cells are identified by their production of IFN-γ and the expression of transcription factor T-bet, Th2 cells predominantly produce IL-4, IL-5 and IL-13 and express the transcription factor GATA-3, whereas the Th17 subset most notably produces IL-17 and requires the expression of transcription factor RORγt [57]. The development of the different subsets of T helper cells can be driven by $CD4^+$ T cells response to different cytokines. Polarisation towards the Th1 phenotype can be achieved by stimulating the cells with IL-12 and IFN-γ, whereas it is inhibited by the addition of IL-4. The Th2 subset is promoted by IL-4 and can be inhibited by IFN-γ. Th17 cells develop after stimulation with IL-6 and require IL-23 to be maintained; their development is inhibited by the Th1 and Th2 cytokines, IFN-γ and IL-4 respectively (Fig. 1.5). Once the subsets are formed their own cytokine production will skew subsequent effector cells towards that specific phenotype [53]. Follicular T helper (T_{FH}) cells are involved in regulating B cell maturation. IL-21 and the transcription factor Bcl-6 are required for the differentiation of T_{FH} cells. T_{FH} are localised within germinal centres and express high levels of the chemokine receptor CXCR5 [58]. They have been shown

to be able to produce the Th2 cytokine IL-4, which promotes isotype switching to IgG. IL-21 and IL-6 can induce T_{FH} differentiation as well as Th17 differentiation, but T_{FH} produce very low levels of IL-17. It was shown that overexpression of Bcl-6 led to suppression of IL-17 production by non-polarised and Th17 polarised $CD4^+$ T cells *in vitro* [58].

Regulatory T cells are another subset of $CD4^+$ T cells which are involved in regulating the effector responses of the T helper subsets and are thought to be important in controlling autoimmunity, by their suppressive action on self-reactive T cells [59-61]. Tregs are characterised by the expression of the transcription factor Foxp3. There are two subsets of Tregs which can be described, the naturally occurring Tregs (nTregs), which develop in the thymus and express CD25 and the inducible Tregs (iTregs) which develop in the periphery induced by TGF-β expression [57;59].

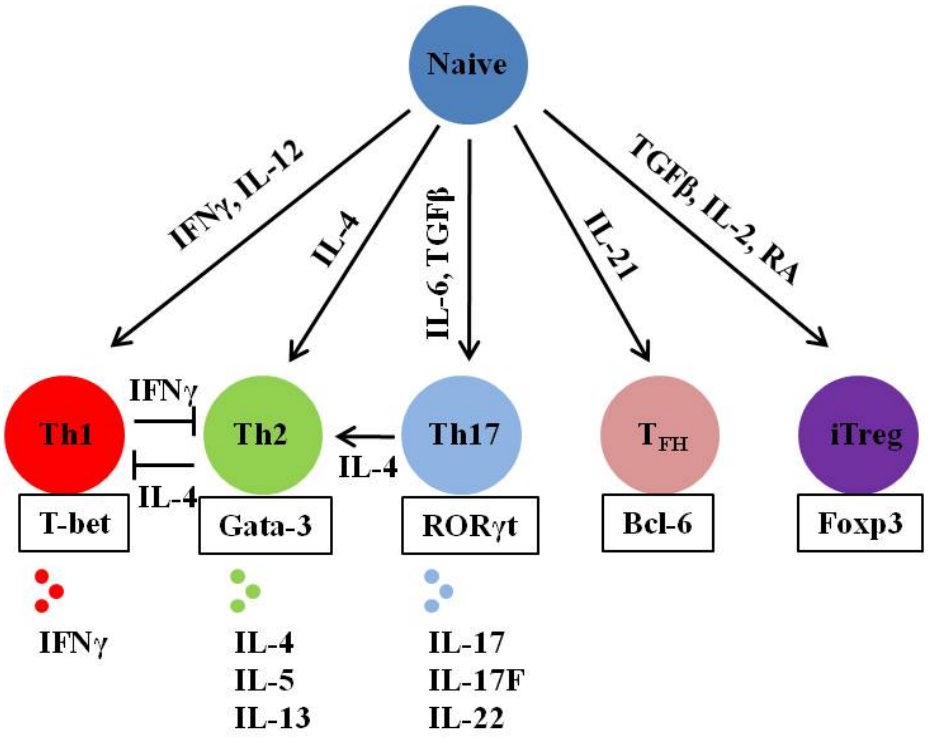

Figure 1.5. Model of CD4$^+$ effector cell differentiation, based on the production of cytokines. A naive CD4$^+$ T cell recognises its antigen and becomes activated, depending on the cytokines produced by the micorenvironment, it can give rise to one of five effector lineages.

As described above CD4$^+$ T cell populations have not only been described based on their cytokine production profiles, but also on the expression of cell surface markers. Frequently used markers are the chemokine receptor CCR7, the costimulatory molecules CD27 and CD28, CD62L and CD45RA [62-64]. Amyes *et al* (2005) described the CD4$^+$ T cell compartment using CCR7, CD45RA and CD28 [63]. They described the eight possible populations when using these three markers and looked at the relative numbers of cells in each population and also analysed their cytokine production. Using CCR7 and CD45RA four populations can be described, a naive population that is CCR7$^+$CD45RA$^+$, a central memory population which is CCR7$^+$CD45RA$^-$, an effector memory population of CCR7$^-$CD45RA$^-$ cells and a terminally differentiated subset of cells which re-expresses CD45RA (CCR7$^-$ CD45RA$^+$, also called EMRA population). When adding in CD28 these four populations

were further subdivided into either $CD28^+$ or $CD28^-$ cells. The authors found that the naive and central memory populations consisted of mostly $CD28^+$ cells. When analysing the cytokine production of these populations, it was found that the naive and central memory cells could produce cytokines but did this to a limited extent compared to the effector memory and EMRA populations. Naive and central memory cells preferrentially expressed IL-2 and TNF-α, while effector memory cells were more likely to produce IFN-γ than the EMRA population.

The study by Amyes *et al* (2005) and other studies have described $CD4^+$ T cell populations based on different strategies, either looking at cytokine production or expression of cell surface markers [63]. These studies have resulted in the description of various $CD4^+$ T cell populations, such as Th1, Th2, CM and EM.

1.9 $CD8^+$ T cells

$CD8^+$ T cells are important mediators in protection against virally infected cells, tumour cells and other damaged cells. Most $CD8^+$ T cells are cytotoxic, capable of directly killing the target cell and producing cytokines, some are found to have regulatory functions [65;66;67]. As mentioned above the $CD8^+$ T cell compartment can be divided into four T cell populations based on the expression of CCR7 and CD45RA (Sallusto *et al* 1999), however as was the case in the $CD4^+$ compartment other markers can be used to describe $CD8^+$ T cell populations [68;69].

Hamann *et al* (1997) describe that using an array of surface molecules, including CD45RA, CD27 and CD28; they were able to find three $CD8^+$ T cell populations, a naive ($CD45RA^+CD27^+CD28^+$), a memory ($CD45RA^-CD27^+CD28^+$) and an effector subset ($CD45RA^+CD27^-CD28^-$) [68]. The naive subset expressed high levels of CD62L, whereas the effector subset downregulated CD62L expression. The three cell populations also differed in their ability to produce cytokines, with the naive population producing the narrowest repertoire of cytokines. Appay *et al* (2002) also describe three populations of $CD8^+$ T cells using only CD27 and CD28 as markers, an early population of $CD27^+CD28^+$, a late population of $CD27^+CD28^-$ cells and an intermediate population of $CD27^-CD28^-$ cells [69;70]. They suggest that these three subsets overlap with the CM, EM and EMRA populations respectively.

A subpopulation of $CD8^+$ Treg cells has been described using a mouse model [65;71], this Treg was capable of binding to Qa-1 (HLA-E in humans) on B cells which resulted in the suppressive activity of $CD8^+$ T cells; $CD4^+$ T cells were subsequently inhibited in their response. There are no good surface markers to distinguish $CD8^+$ Tregs from effector $CD8^+$ T cells, however CD28 expression has been implicated with $CD8^+$ Tregs. It was shown that depletion of $CD8^+$ T cells from CD28 deficient mice resulted in experimental autoimmune encephalomyelitis (EAE), adoptive transfer of $CD8^+CD28^-$ T cells into CD8 knockout mice resulted in disease suppression [72]. The $CD8^+$ Treg which is based on Qa-1 recognition suppresses EAE development [65]. The exact mechanisms through which $CD8^+$ Tregs work or are induced are not known.

1.10 Tetraspanins

Tetraspanins are a family of membrane spanning proteins, consisting of 33 family members in humans and mice [73;74]. Tetraspanins can be found in a wide range of multicellular organisms, such as plants, schistosomes and *Drosophila melanogaster* [75]. *Drosophila melanogaster* has 36 known tetraspanins, whereas *Schistosoma* has 25 [76]. Unicellular fungi do not express tetraspanins, compared to multicellular fungi which do express tetraspanins. The presence of tetraspanins in such a wide range of organisms suggests that they play a very fundamental role in the organisation of the cell membrane. Mammalian tetraspanins consist of four transmembrane domains, a small and a large extracellular loop and two short intracellular amino and carboxyl tails (Fig.1.6). The large extracellular loop (EC2) consists of a constant region, containing three α-helices (A, B and E) and a variable region. The variable region contains most of the known tetraspanin protein-protein interaction sites [77].

Many tetraspanins are postranslationally modified by the addition of palmitate to the cysteine residues closest to the membrane. This addition of palmitate allows the formation of tetraspanin-enriched microdomains (TEMs) at the cell surface. Tetraspanins have been implicated in having a role in many biological functions, such as cell activation, membrane fusion, adhesion, differentiation and metastasis [78-82].

Several tetraspanins have been shown to have a widespread expression, such as CD81 on almost all cell types and CD151 on epithelial, endothelial and fibroblastic cells. Other tetraspanins such as CD37 have been shown to have a narrower expression pattern only on lymphocytes. Tetraspanins are thought to be involved in many cellular processes as master organisers of the cell membrane, through the formation of TEMs [77].

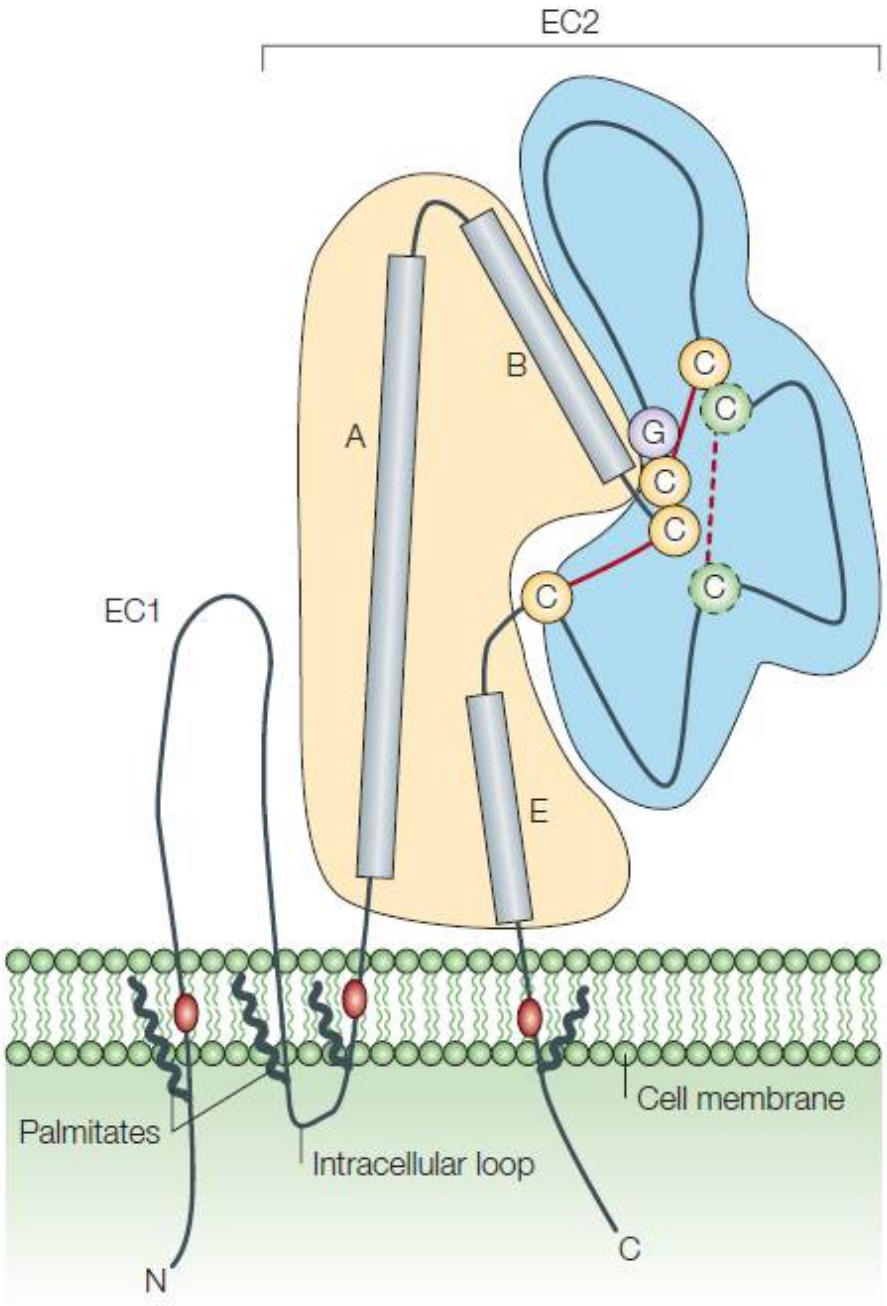

Figure 1.6. Representation of tetraspanins, adapted from Hemler (2005). Tetraspanins contain four transmembrane domains, a short extracellular loop (EC1) and a longer extracellular loop (EC2). EC2 is divided into a constant region (yellow) and a variable region (blue). The variable region contains several protein interaction sites.

The tetraspanin CD9 has been described to be involved in membrane fusion, metastasis suppression and sperm-egg fusion [80;81;83] and CD81 in cell migration, hepatitis C infection and also membrane fusion [80;84-86]. CD63 is highly expressed on late endosomes and exosomes [78]. It has been suggested that there are several levels of interaction which can occur in the 'tetraspanin web' [76;87]. It was shown that when using different detergents to extract tetraspanin complexes direct or first level interactions can be revealed by using stronger detergents, whereas using more gentle detergents results in identifying second level interactions [81;87]. The first level interactions are quite rare and these include tetraspanin homodimers and homotrimers as well as heterointeractions between tetraspanins. The second level interactions are mostly between tetraspanins and integrins. Yanez-Mo *et al* (2008) showed direct association of CD9 with ICAM-1 as well as recruitment of VCAM-1 into TEMs by its association with CD151 [87;88]. CD151 is also described to associate with α3β1 and α6β4 and by doing so is involved in regulating integrin-dependent cell morphology, migration and adhesion [89].

As mentioned above CD9 has been implicated in several cellular reactions and several binding partners for CD9 have been described. Among these are several integrins, proteins of the EWI family and the epidermal growth factor receptor (EGFR) [90]. Miyado *et al* (2000) generated a $CD9^{-/-}$ mouse and found that male and female $CD9^{-/-}$ mice were born healthy and showed no developmental differences with their wild type controls [91]. They did, however, find that $CD9^{-/-}$ females produced smaller litter sizes (less than 2%) than the wild type females did. No difference was found between the $CD9^{-/-}$ males, as well as no difference could be found in the frequency of copulation vaginal plugs between $CD9^{-/-}$ and wild type females. The knockout females also showed no histochemical changes compared to the wild type females and when treated with hormones, no difference in ovulation could be found.

They then isolated oocytes from both wild type and knockout females and applied *in vitro* fertilisation with wild type sperm. Analysing the cells 6 hours after insemination revealed that for both the wild type and the knockout cells the sperm had penetrated the zona pellucida of the eggs. A difference in the ability of the $CD9^{-/-}$ eggs to fuse with the sperm and from pronuclei was found, since almost all of these eggs failed to fuse with sperm [91]. Recently Jégou *et al* (2011) suggested that CD9 could be providing adhesion sites where fusion of sperm and egg will take place [92].

CD9 and CD81 seem to be very closely related in several of their functions, as exhibited by the exacerbation of the phenotype of CD9 and CD81 double knockout mice compared to the respective single knock outs [93]. CD9 and CD81 double knockout mice were found to spontaneously develop pulmonary emphysema and as the mice aged, symptoms outside of the pulmonary tract could be identified, such as weight loss and osteopenia. Takeda *et al* (2008) show that CD9 and CD81 expression is reduced in the macrophage cell line RAW264.7 after smoking-related stimuli. Since smoking reduces the expression as well as the activity of histone deacetylases (HDACs) in the macrophages of chronic obstructive pulmonary (COPD) patients, they analysed the effect of HDACs on the expression of both CD9 and CD81 in RAW264.7 cells. Using the HDAC inhibitor TSA they found that protein levels for both CD9 and CD81 were lower after treatment with TSA. An increase in matrix metalloproteinase production in macrophages of COPD patients is involved in the pathology seen in these patients and Takeda *et al* found that the downregulation of CD9 and CD81 by TSA correlated with the upregulation of MMP-2 and MMP-9. They further supported this finding by using specific siRNA's for CD9 or CD81, which led to a similar increase in MMP production. They analysed the phenotype of CD9/CD81 double knockout mice and found that these mice developed pulmonary emphysema and showed signs of alveolar destruction and

remodelling. More inflammatory cells could be isolated out of the lungs from the double knockouts and there was a higher activity of MMPs found in these lungs. Macrophages from the double knockout mice showed impaired motility compared to those from wild type mice.

CD63 has been described as a marker for exosomes, these vesicles can be formed when endosomes fuse with the plasma membrane and release their contents into the extracellular space [94]. Recent data suggests that exosomes are not just a way for cells to rid themselves of unwanted contents, but that exosomes are important for intercellular communication, cellular adhesion and migration. Koumangoye *et al* showed that the detachment of cells to their surroundings induces the release of CD63 positive exosomes [94]. A vector encoding a GFP-tagged CD63 was transfected into a human breast cancer cell line (BT-549) and the uptake and release of CD63 positive exosomes was analysed. Firstly cells which were kept in a cell suspension were found to release 5 to 6 times more exosomes compared to cells which were kept in an adherent culture for 16 hours. They then analysed the effect of detaching the cells from the culture dishes, by adding ethylenediaminetetraacetic acid (EDTA) to the culture. The addition of EDTA to the cells results in contraction of the cells followed by the release of CD63-GFP positive exosomes, seen under the microscope as green vesicles projecting out of the plasma membranes of the cells [94]. Exosomes are also described to express MHC molecules as well as some co-stimulatory molecules, such as CD86. CD63 is expressed on endosomes positive for MHC-II and it could be involved in regulating peptide loading of MHC-II [95]. Petersen *et al* (2011) knocked down CD63 expression in both the Epstein-Barr virus (EBV) transformed B lymphoblastoid cell line and the HeLa-CIITA (Class II major histocompatibility complex transactivator) cervical cancer cell line. Surprisingly they found that loading both CD63 deficient cell lines with EBV synthetic peptides resulted in better T cell recognition of the peptide compared to the control cells. They then analysed the effect of

CD63 deficiency on the surface expression of MHC-II peptide complexes and found that this was not affected. They concluded that CD63 may very well be involved in the trafficking and fusion of endosomes as well as exosomes, but not in the formation of these vesicles, since they can still form in the absence of CD63 [95].

CD81 has been described in both B and T cell activation. It associates with the B cell signalling complex consisting of CD19, CD21 and Leu-13. CD19 expression has been shown to be reduced in CD81 deficient B cells. Shoham *et al* (2003) show that this reduction in CD19 expression is especially pronounced on $CD81^{-/-}$ small pre-BII cells [96]. The $CD81^{-/-}$ small pre-BIII cells did express mRNA for CD19 at levels which were similar to those expressed in wild type cells, this suggests that CD81 may be regulating normal cell surface expression of CD19. The CD19 defect could be rescued by transfecting human CD81 back into the $CD81^{-/-}$ cells, restoring CD19 surface expression back to wild type levels. CD81 binding to CD19 is thought to lower the threshold for B cell activation by linking two processes on the cell surface of the B cell; namely antigen recognition and CD21 mediated complement activation [79]. Boismenu *et al* described a role for CD81 in T cell development in the thymus [97]. Using a monoclonal antibody which was generated against a, at that time still unknown, surface marker of the PAM 212 epithelial cell line, they found that addition of this antibody led to halted T cell development in fetal thymus organ cultures. The ligand for this monoclonal antibody was found to be CD81. In the fetal thymus organ cultures no development of $CD4^{+}CD8^{+}$ TCRαβ thymocytes could be found [97]. After 7 days of cell culture in the presence of either medium alone or a control monoclonal antibody 80% $CD4^{+}CD8^{+}$ cells could be found in the culture. This compared to 0.5% of $CD4^{+}CD8^{+}$ cells found when the cells were cultured in the presence of the anti-CD81 antibody. No effect was

found on the development of γδ T cells. Todd *et al* (1996) analysed CD81 expression on thymocytes and found that it was expressed at all stages of thymocyte development. Using co-immunoprecipitation, they found that CD81 on thymocytes was strongly associated with both CD4 and CD8, but more weakly associated with CD3 [98]. When CD81 was ligated on these cells by the addition of an antibody against CD81, this resulted in cell adhesion and cell aggregation. This cellular adhesion and aggregation could be blocked by antibodies against both LFA-1 and ICAM-1. The upregulated cellular adhesion and aggregation is thought to aid in T cell-APC contact; strengthening the contact between the two cells will enhance the ability for the APC to stimulate the T cell [98].

CD151 expression can be found on epithelial cells and muscle cells, as well as on platelets [75]. In endothelial cells CD151 is found in the cell-cell junctions. CD151 is also the tetraspanin with the most pronounced interaction with laminin binding integrins, such as α3β1 and α6β1 [99]. Interactions between CD151 and laminin binding integrins are necessary to recruit these integrins into TEMs [100]. Through these interactions with integrins CD151 is thought to regulate cell motility and adhesion [101]. Wright *et al* (2004) were the first to generate and describe the phenotype of a $CD151^{-/-}$ mouse [102]. Analysing the blood and bone marrow compartments of these mice, Wright *et al* found that compared to wild type mice a significant increase of immature myeloid cells could be found in the bone marrow. This increase of immature myeloid cells corresponded with a decrease in the number of lymphocytes. Histological analysis of tissues from the mice showed that there was no significant difference between tissues from wild type mice and those from the $CD151^{-/-}$ mice. Absence of CD151 also did not seem to result in reduced expression of the α3, α6, β1 and β4 integrin chains on the cell surface. A difference in the ability of $CD151^{-/-}$ keratinocytes to migrate was seen,

however these cells had the same proliferative capacity as their wild type counterparts. Based on tail bleeding experiments these mice were found to display abnormal hemostasis, signified by longer bleeding times of the tails, as well as the amount of blood lost during the tail bleeding time. They concluded that this bleeding effect indicates an underlying defect in endothelium and/or platelet function [102].

1.11 Transcriptome analysis

DNA microarrays provide a useful strategy to analyse the gene expression of cells. Microarrays allow the analysis of thousands of genes or even the whole genome at the same time. This results in microarray analysis producing large data sets and it is therefore important to utilise appropriate statistical analysis to be able to draw any conclusions [103]. Depending on the aims of the study microarray analysis can be sorted into three groups, namely class comparison, class discovery and class prediction. Class comparison studies try to identify genes that are differentially expressed between two or more groups; this can be used when wanting to compare two cell types to each other. Class discovery tries to classify groups using the samples or genes examined; one can envisage using this when analysing samples from patients who have yet to be diagnosed. Class prediction tries to predict whether a sample belongs to a certain group, by comparing gene expression profiles [104].

Several groups have used microarrays to try and delineate different cell populations in humans. Most groups have sorted cells based on the expression of surface markers and subsequently taken the mRNA of these sorted cells and used this to analyse on an array. Holmes *et al* (2005) used microarray analysis to investigate the relationship between naive, effector and memory $CD8^+$ T cells [105]. They sorted these three populations based on CD27 and CD45RA expression and analysed the samples on arrays. Identification of genes which were differentially expressed between the populations found that memory cells show gene expression patterns intermediate between naive and effector T cells. Du *et al* (2006) used microarray analysis to compare gene expression between $CD4^+$ T cells, $CD8^+$ T cells, $CD19^+$ B cells, $CD56^+$ natural killer (NK) cells and $CD14^+$ monocytes. They also selected a number

of genes that have previously been reported to be involved in ischemic stroke, Tourette syndrome and migraine and used these genes to analyse if cell specific expression of these genes could be found [106]. They concluded that most blood cells express a similar pattern of genes but that there are also genes which seem specific to a certain cell type. Palmer *et al* (2006) also looked at cell type specific gene expression in blood cells. They compared B cells, $CD4^+$ T cells, $CD8^+$ T cells, granulocytes and lymphocytes on microarrays containing 18,000 human genes [107]. Their analysis showed that differentially expressed genes could be found when comparing the different populations to each other, resulting in gene expression signatures for each cell type. Haining *et al* (2008) identified an evolutionary conserved gene expression pattern for $CD8^+$ memory differentiation which was shared by B cells. The gene expression of $CD4^+$ and $CD8^+$ naive and memory T cell populations in human and mouse were analysed [108]. Comparing the results from these analyses resulted in a list of genes which were conserved in mouse and human memory T cell differentiation. When comparing this conserved gene list to the gene expression of human B cells it was found that the expression of these genes were also conserved in B cells. These studies show that microarray analysis is a useful strategy to utilise when trying to identify differences between cell populations sorted based on expression of surface markers.

Quantitative Real Time polymerase chain reaction (PCR) is a more accurate way of utilising PCR analysis to quantify the expression level of a certain gene in a sample. The addition of fluorescent probes to Real Time PCR allows accurate measurement of a fluorescent signal during the PCR reaction, hence the addition Real Time [109]. Real Time PCR has been used to validate gene expression results obtained from microarray analysis because it allows the researcher to focus on several specific genes without the costs associated with microarray analysis. Wang *et al* (2008) used Real Time PCR to validate their microarray results, when

comparing the gene expression levels of the bulk CD3 population to the bulk $CD4^+$ and $CD8^+$ T cell populations. They found that the Real Time PCR data corresponded very well with the microarray data [110]. Chtanova *et al* (2001) validated the gene expression results from their microarray experiment through Real Time PCR as well and the data from the Real Time PCR corresponded with the data from the microarrays [111]. To this date Real Time PCR remains the gold standard for validating microarray results [109;112].

1.12 AIMS

The separation of T cell populations based on cell surface marker expression is a relatively blunt tool. We therefore formed the working hypothesis that microarray analysis of purified populations of human blood cell populations will further extend our understanding of T cell subsets and provide novel targets to control immune responses.

The main aim of this study was to examine lineage relationships between human $CD4^+$ and $CD8^+$ T cell populations. To address this specifically:

(a) The gene expression patterns of T cell populations based on the cell surface markers CCR7 and CD45RA will be examined by microarray to identify genes shared between the $CD4^+$ and $CD8^+$ T cell compartments as well as genes which are unique;
(b) The microarray analysis will be validated by Real Time PCR;
(c) The role of genes of interest in $CD4^+$ and $CD8^+$ T cells will be examined.

Chapter Two

Material and Methods

2 MATERIAL AND METHODS

2.1 Peripheral blood

Samples from peripheral venous blood from healthy controls were collected with informed consent, into a 50 ml Falcon tube with Heparin (CD Pharmaceutical Ltd).

2.1.1 Cell isolation

Peripheral Blood Mononuclear Cells (PBMC) were isolated from fresh, heparinised, venous blood from healthy controls using ficoll (GE Healthcare) density centrifugation. Peripheral blood was diluted 1:1 in RPMI-1640 (Sigma) 1% GPS (Sigma, 2 mM Glutamine, 100 u/ml penicillin, 100 µg/ml streptomycin), 1% HEPES (Sigma) and 10 ml were layered onto 15 ml of ficoll and centrifuged at 320 g for 30 minutes at 20ºC. The resulting buffy layer of mononuclear cells was removed by Pasteur pipette and washed 3 times in RPMI-1640 1% GPS, 1% HEPES. The cells were then counted on a haemocytometer and used in staining for flow cytometry.

2.2.1 Antibody Dilutions for flow cytometry

CD3 FITC	1:20	Immunotools
CD3 PE	1:20	Immunotools
CD4 PECy7	1:10	BD Pharmingen
CD8β PECy5	1:20	Beckman Coulter
CD8α FITC	1:20	Immunotools
CD8α PE	1:20	Immunotools
CD9 PE	1:20	Biolegend
CD14 PE	1:50	Immunotools (dilution used for sorts)
CD14 PE	1:100	Immunotools (dilution used for FACS)
CD14 PECy5	1:100	Immunotools
CD27 FITC	1:20	BD Pharmingen
CD37 PE	1:20	ImmunoTools
CD45RA ECD	1:80	Beckman Coulter
CD53 PE	1:20	BD Pharmingen
CD63 PE	1:20	Biolegend
CD62L PE	1:50	BD Biosciences
CD69 FITC	1:10	Beckton Dickinson
CD81 PE	1:20	BD Pharmingen
CD82 PE	1:20	Biolegend
CD151 PE	1:20	BD Pharmingen
CCR7 FITC	1:10	R&D systems
TCR γ/δ	1:20	BD Biosciences
IgG1 FITC	1:20	Dakocytomation

IgG1 PE	1:20	BD Biosciences
IgG2a PECy5	1:20	Immunotools
IgG2a PE	1:20	eBioscience

2.2.2 Flow cytometry

PBMC were used for flow cytometry, 2 x 10^5 cells were seeded per tube in 5 ml polypropylene tubes (Falcon 352063). The tubes were spun for 3 min at 320 *g* at 4 ºC, after which the supernatant was discarded and the tubes were briefly vortexed to resuspend the cells. Subsequently 50 µl of antibody dilution was added and the cells were incubated on ice for 20 minutes. The cells were then washed twice, by adding 500 µl of PBS (Sigma) 2% BSA (Sigma) and centrifuging the tubes for 4 minutes at 320 *g* and 4 ºC. Finally the cells were taken up in 400 µl of PBS 2% BSA and run through the flow cytometer, Beckman Coulter, Cyan.

2.2.3 Flow cytometry intracellular cytokine staining of stimulated $CD4^+$ and $CD8^+$ T cell populations

PBMCs where isolated from whole blood as described above, the cells were plated in a 96 well flexiplate at 1x10^6 cells/well in 50 µl culture media. The cells were then stimulated with PMA (500 ng/ml) and Ionomycin (500ng/ml) and Brefeldin A (2 µg/ml) was added to the wells after which the cells were cultured for 3 hours at 37°C.

The cells were subsequently stained for the relevant antibodies for the surface markers CD3, CD4, CD8, CCR7 and CD45RO and incubated on ice for 20 minutes, after which the cells were fixed and permeabilised using the FIX & PERM® cell fixation kit from Invitrogen. The cells were subsequently stained for the relevant antibodies for the intracellular markers IFN-γ, IL-17 and IL-22 and incubated on ice for 20 minutes in the dark. The cells were subsequently washed and taken up in 400 µl of PBS 2% BSA and run through the flow cytometer, Beckman Coulter, Cyan.

2.2.4 FACS sorting of $CD8^+$ CCR7/CD45RA populations

120 ml of blood was collected from a healthy control and PBMC were isolated as previously described. Compensation between two colours used in the staining was achieved by staining 2 x 10^5 cells with single antibodies. The cells for the population sort were stained with an antibody cocktail of CD8β PECy5, CD45RA ECD and CCR7 FITC in a volume of 1 ml. The cells were stained for 20 minutes on ice, after which they were washed and filtered through a 50 µm filter (CellTrics®) and put into 5 ml polypropylene tubes (Falcon 352063). The cells were sorted on the Mo-Flo MultiLaser flow cytometer (DakoCytomation), after being gated on forward and side scatter profiles to include only live lymphocytes, and on cell surface marker combinations to select the cell populations of interest. These populations included only $CD8\beta^+$ cells and were based on expression of CCR7 and/or CD45RA, $CCR7^+CD45RA^+$ (Naive), $CCR7^-CD45RA^+$ (Effector Memory RA), $CCR7^-CD45^-$ (Effector Memory) and $CCR7^+CD45RA^-$ (Central Memory).

2.2.5 FACS sorting of $CD4^+$ CCR7/CD45RA populations

120 ml of blood was collected from a healthy control and PBMC were isolated as previously described. Compensation between two colours used in the staining was achieved by staining 2 x 10^5 cells with single antibodies. The cells for the population sort were stained with an antibody cocktail of CD4 PECy7, CD14PE, CD45RA ECD and CCR7 FITC in a volume of 1 ml. The cells were stained for 20 minutes on ice, after which they were washed and filtered through a 50 µm filter (CellTrics®) and put into 5 ml polypropylene tubes (Falcon 352063). The cells were sorted on the Mo-Flo MultiLaser flow cytometer (DakoCytomation), after being gated on forward and side scatter profiles to include only live lymphocytes, and on cell surface marker combinations to select the cell populations of interest. These populations included $CD4^+CD14^-$ cells and were based on expression of CCR7 and/or CD45RA, $CCR7^+CD45RA^+$ (Naïve), $CCR7^-CD45RA^+$ (Effector Memory RA), $CCR7^-CD45^-$ (Effector memory) and $CCR7^+CD45RA^-$ (Central memory).

2.2.6 Sorting CD9 subsets from $CD4^+$ T cells

120 ml of blood was collected from a healthy control and PBMC were isolated as previously described. Compensation between two colours used in the staining was achieved by staining 2 x 10^5 cells with single antibodies. The cells for the population sort were stained with an antibody cocktail of CD4 PECy7, CD9PE, CD45RA ECD and CCR7 FITC in a volume of 1 ml. The cells were stained for 20 minutes on ice, after which they were washed and filtered through a 50 µm filter (CellTrics®) and put

into 5 ml polypropylene tubes (Falcon 352063). The cells were sorted on the Mo-Flo MultiLaser flow cytometer (DakoCytomation), after being gated on forward and side scatter profiles to include only live lymphocytes, and on cell surface marker combinations to select the cell populations of interest. The sorted populations were $CD9^{-}CCR7^{+}CD45RA^{-}$ central memory T cells and $CD9^{-}CCR7^{-}CD45^{-}$ effector memory T cells.

2.3 RNA extraction

Samples were lysed using 350 µl of lysis buffer (Qiagen, RNeasy® RLT buffer) and were frozen down at -80 ºC, for at least a day. The samples were then defrosted at room temperature and 350 µl of 70% Ethanol was added and mixed in. This mix was then applied to a filter cartridge and spun for 1 minute at 11000 g. The filter was then washed with 700 µl of buffer RW1 (Qiagen, RNeasy®) and spun for 1 minute at 11000 g. The filter was washed again with 500 µl of buffer RPE (Qiagen, RNeasy®) and spun for 1 minute at 11000 g after which a final wash was done using 500 µl of buffer RPE (Qiagen, RNeasy®). The sample was then spun for 2 minutes at 11000 g, after which the filter cartridge was transferred to a clean eppendorf. 35 µl of H_20 was added to the filter and which was subsequently spun for 1 minute at 11000 g. The RNA was then used in a DNase I kit (Ambion) treatment to remove any contaminating DNA.

2.3.1 DNase I treatment

3.5 µl of 10x DNase I buffer and 1 µl of DNase I were added to the RNA samples and the samples were incubated at 37 °C for 30 minutes. Following this, 5 µl of DNase inactivation reagent was added and samples were incubated at room temperature for 2 minutes, before being centrifuged for 1 minute at 11000 g. The supernatant containing the RNA was transferred into a fresh tube. The yield of RNA was quantitated using a spectrophotometer (Eppendorf Biophotometer, Helena Biosciences) at a wavelength of 260 nm. Isolated RNA was stored in DEPC treated water at -20°C until needed.

2.3.2 Reverse transcription

cDNA was reverse transcribed from the isolated RNA samples using the cDNA synthesis kit Superscript VILO® (Invitrogen). The equivalent amount of RNA to $1x10^5$ cells was used in the reaction, together with 4 µl 5x VILO® Reaction Mix, 10x Superscript® Enzyme Mix and DEPC treated water to make up the reaction volume to 20 µl. Samples were kept at 25°C for 10 minutes, 2 hrs at 42°C and 5 minutes at 85°C. The resulting cDNA was then PCR purified and used for microarray analysis or Real Time PCR.

2.3.3 PCR product purification

After reverse transcription the cDNA was purified using NuceleoSpin® Extract II (Macherey-Nagel). First the cDNA was bound to the column by mixing 1 volume of sample with 2 volumes of Buffer NT and spinning the sample for 1 minute at 11000 g. The silica membrane was then washed by adding 700 µl of Buffer NT3 and spinning for 1 minute at 11000 g. The membrane was dried by a subsequent spin of 2 minutes at 11000 g, after which the cDNA was eluted in 50 µl DEPC H_2O by spinning for 1 minute at 11000 g. The eluted cDNA was then quantitated with a spectrophotometer (Eppendorf Biophotometer) at 260 nm and tested for purity via electrophoresis gel and stored at -20^0C.

2.4 Real Time PCR

Gene expression profiles of purified total RNA from sorted cell populations were analysed using TaqMan Low Density Arrays (www.appliedbiosystems.com). A working solution was prepared per sample; this consisted of 50 µl cDNA (equivalent to $1x10^5$ cells) and 50 µl Taqman Gene Expression Master Mix. Approximately 95 µl of each sample's working solution was then pipetted into two ports of the card. The cards were then centrifuged twice at 300g for 1 minute to allow adequate distribution of the sample over the probes. The plate was then sealed and the ports cut off. The Applied Biosystems 7900HT Fast Real-Time PCR System was used to perform the real time-PCR with the following cycle conditions: 50°C for 2 minutes, 94.5°C for 10 minutes and then 45 cycles of 97°C for 30 seconds and 59.7°C for 1 minute.

Data was analysed using SDS 2.2 (Applied Biosystems). Relative quantification of signal per gene was achieved by setting thresholds within the logarithmic phase of the PCR for the control gene and the target gene. The cycle number (Ct) at which the threshold was reached was then determined. The Ct for the target gene was subtracted from the Ct for the control gene and the relative quantity was calculated as $2^{-\Delta CT}$.

2.5 Microarray spotting

The probes used for the arrays were Operon Human Genome Array-Ready Oligo Set™ V4.0 (AROS) and were spotted by the Liverpool microarray facility, University of Liverpool. The oligos were spotted using a TAS microgrid II robot (BioRobotics). AROS contains 35,035 oligonucleotide probes, representing approximately 25,100 unique genes and 39,600 transcripts excluding control oligos.

2.5.1 CyDye labelling

cDNA samples were labelled with Cy3-dCTP and Cy5-dCTP prior to hybridization. 500 ng of sample cDNA was added to 20 µl of random primer mix from the Bioprime Labelling Kit (Invitrogen) and the volume was made up to 43 µl with de-ionised water. The mix was heated to 94 °C for 5 minutes and then cooled on ice before adding 1.2 µl (10 mM) dATP, 1.2 µl (10 mM) dTTP, 1.2 µl (10 mM) dGTP, 0.72 µl (10 mM) dCTP, 0.68 µl de-ionised water, 1 µl of either Cy3 dCTP or Cy5 dCTP (Amersham Biosciences), and 1 µl (40 U/µl) Klenow enzyme (from the Bioprime

Labelling Kit, Invitrogen). The reaction was kept at 37°C for 2 hours before labelled cDNA was purified using the NucleoSpin® Extract II. Labelled cDNA was eluted in 70 µl de-ionised water instead of using the elution buffer supplied. The quantity of labelled product was determined using a spectrophotometer (Pharmacia Biotech Ultrospec 2100 pro) at a wavelength of either 550nm (Cy3-dCTP) or 650nm (Cy5-dCTP). The picomole (pmol) yield was calculated as follows:

Cy3 = Abs550 x dilution factor /0.15

Cy5 = Abs 650 x dilution factor /0.25

Labelled cDNA was stored in the absence of light at 4°C until hybridisation, which was performed later on the same day.

2.5.2 Hybridisation

The microarrays were pre-hybridised to GAPS II coated slides (Corning) for 2 hours at 42 °C. Pre-hybridisation solution consisted of 12.5 ml of formamide (Sigma), 12.5 ml of 20 x SSC, 0.25 ml of 20% SDS and 50 µl of 100 mg/µl Fraction V BSA (Sigma), made up to a volume of 50 ml with de-ionised water. Equal quantities (100 pmol) of labelled cDNA from the test and reference samples were added together and concentrated using a Microcon YM-30 concentration column (Millipore). The column was centrifuged for 10 minutes, inverted into a fresh tube and the concentrate was eluted in a final volume of 30 µl of de-ionised water. The hybridisation mix was made up using the instructions provided with the GAPS II coated slides and contained 20 µl

of formamide, 20 µl of 20 x SSC, 0.4 µl of 20% SDS, 2.5 µl (2 mg/ml) of PolyA DNA (Invitrogen) and 4 µl (2 mg/ml) of Cot1 DNA (Invitrogen). This was added to 30 µl of labelled cDNA and the volume was made up to 80 µl with de-ionised water. The solution was then denatured at 95 °C for 5 minutes and kept on ice.

Pre-hybridised slides were dipped in de-ionised water and then ethanol, centrifuged until dry and placed into a hybridisation chamber (Corning), which had been prepared by using 10 µl of de-ionised water to moisten the seal. The hybridization mix was added to the surface of the slides and a Lifter Slip (VWR International) was applied. The hybridisation chamber was then sealed, wrapped in a dampened paper towel and foil and kept in a hybridisation oven for 16-20 hours at 42 °C. After hybridisation, the Lifter Slip was removed by immersing the slide in a solution of 2 x SSC (0.3M sodium citrate + 3M NaCl, pH 7.0) + 0.1% SDS at 42 °C. The slides were then washed for 2 minutes at 42 °C in 2 x SSC + 0.1% SDS and for 2 minutes at room temperature in 0.2 x SSC. This was followed by 4 washes of 2 minutes at room temperature in 0.05 x SSC, before the slides were dipped into de-ionised water, followed by ethanol, and then centrifuged until dry. After hybridization, the arrays were scanned using a Perkin Elmer Scanarray Gx Plus scanner and Scanarray express.

2.5.3 Microarray data analysis

Slide scans were processed first using Scanarray express. A prepared (and thoroughly checked) GAL file was used to interpret the slide image and the intensity data was extracted. This was then exported as a gpr file. The resulting files were then uploaded

into the Gene Expression Pattern Analysis Suite v2.0 (GEPAS) analysis software (http://gepas.bioinfo.cipf.es/) for normalisation. Normalisation was performed using print-tip normalisation with background subtraction. This was performed first within slide, and then between slide. Data for the normalised data was then exported to TIGR Multiexperiment Viewer (TMEV), which allowed the data to be analysed by SAM analysis, hierarchical clustering and PCA.

2.5.4 Statistical tests

For analysis of the sorted T cell populations supervised statistical tests were used, SAM (Significance Analysis of Microarrays). SAM is a supervised statistical test. The test results in a list of genes significantly different between the samples and the samples were then clustered together based on gene expression profiles, using hierarchical clustering (HCL). Hierarchical clustering analysis clusters genes or samples together based on similar expression profiles. An HCL could then be visualised using Principal Component Analysis.

Statistical analysis of flow cytometry data was carried out using GraphPad Prism computer software (GraphPad Software, Inc., San Diego, CA) and performing a *t*-test.

Chapter Three

Examining Gene Expression Profiles of $CD4^+$ and $CD8^+$ T Cell Populations During Differentiation

3 EXAMINING GENE EXPRESSION PROFILES OF $CD4^+$ AND $CD8^+$ T CELL POPULATIONS DURING DIFFERENTIATION

3.1 Introduction

After recognizing antigen presented on mature dendritic cells naive T cells undergo clonal expansion and differentiate into effector cells. $CD8^+$ T cells differentiate into cells capable of producing IFN-γ, TNF-α and several chemokines as well as directly killing their target cells. $CD4^+$ T cells can differentiate into several subsets of T helper cells (Th) Th1, Th2, Th17 and regulatory T cells (T regs) [57;113]. $CD4^+$ and $CD8^+$ T cell populations have been described based on their cytokine production profiles (T helper subsets) and on the expression of cell surface markers. Based on the expression of CCR7 and CD45RA the $CD4^+$ and $CD8^+$ T cell compartments can be divided into a double positive naive population ($CCR7^+CD45RA^+$), a single positive central memory population ($CCR7^+CD45RA^-$), a double negative effector memory population ($CCR7^-CD45RA^-$) and a single positive effector memory RA population terminally differentiated cells ($CCR7^-CD45RA^+$) [43].

Other frequently used markers are the costimulatory molecules CD27 and CD28, CD62L and CD45RA. Using these markers several populations also designated naive, central memory and effector memory populations can be described [62-64].

Several groups have used microarrays to delineate different cell populations in humans. Most groups have sorted cells based on the expression of surface markers and subsequently reverse transcribed the mRNA of these sorted cells to cDNA for use in an array. Holmes *et al* (2005) used microarray analysis to investigate the relationship between naive, effector and memory

$CD8^+$ T cells in humans [105]. They sorted these three populations based on CD27 and CD45RA expression and determined genes which were differentially expressed between the populations. It was found that genes expressed in memory cells show intermediate levels of expression between naive and effector T cells. Wang *et al* (2008) examined gene expression for human $CD3^+$, $CD4^+$ and $CD8^+$ T cell populations [110]. The cells were stimulated and the gene expression on the different time points was analysed and Wang *et al* described a list of upregulated and downregulated genes during activation. Chtanova *et al* (2001) analysed the gene expression of murine $CD4^+$ Th1 and Th2 and $CD8^+$ type 1 and type 2 cell populations [111]. Their analysis resulted in lists of genes differentially expressed between the four cell types studied. These previous studies have shown that microarray analysis is a useful strategy to utilise when trying to identify differences between cell populations sorted based on expression of surface markers.

The aim of the experiments in this chapter was to identify shared and unique genes during the differentiation of both $CD4^+$ and $CD8^+$ T cell populations. We set out to sort the T cell populations based on CCR7 and CD45RA and describe the gene expression profiles for each subset. Genes that are shared in both $CD4^+$ and $CD8^+$ T cell differentiation will come up in gene lists generated when comparing the differentiation states within their compartment and genes which are unique to differentiation states in either $CD4^+$ or $CD8^+$ will not.

3.2 Results

3.2.1 Sorting CCR7 and CD45RA based $CD4^+$ and $CD8^+$ T cell populations for gene expression analysis on microarrays

$CD4^+$ and $CD8^+$ T cell populations were sorted based on expression of CCR7 and CD45RA. Since monocytes express low levels of CD4 (Fig 3.1) an antibody against CD14 was included in the protocol to exclude these cells. Sorting of the $CD8^+$ T cell populations was based on CD8β expression which allowed the analysis of CD8αβ T cells and exclude any natural killer (NK) cells which express CD8α as a homodimer (Fig. 3.2). After sorting, the populations were all more than 95% pure. As can be seen in both Fig. 3.1 and Fig. 3.2, the sorting gates used differ slightly from the gates used to analyse the purities of the sorts. This was due to trying to ensure the purest populations during the sort by setting a very tight gate around the population of interest. When the purities were analysed after the sort, it was therefore warranted to use a gate which was slightly bigger than the sorting gate used.

Six healthy donors were used to sort six replicates of each population and the mRNA of 100,000 cells from each population was reverse transcribed and the resulting cDNA was then used to run on a microarray. The $CD4^+CCR7^-CD45RA^+$ population gave less than 10,000 cells when sorted, which would have required amplification of the samples to get enough material to put on the arrays and therefore this population was not analysed.

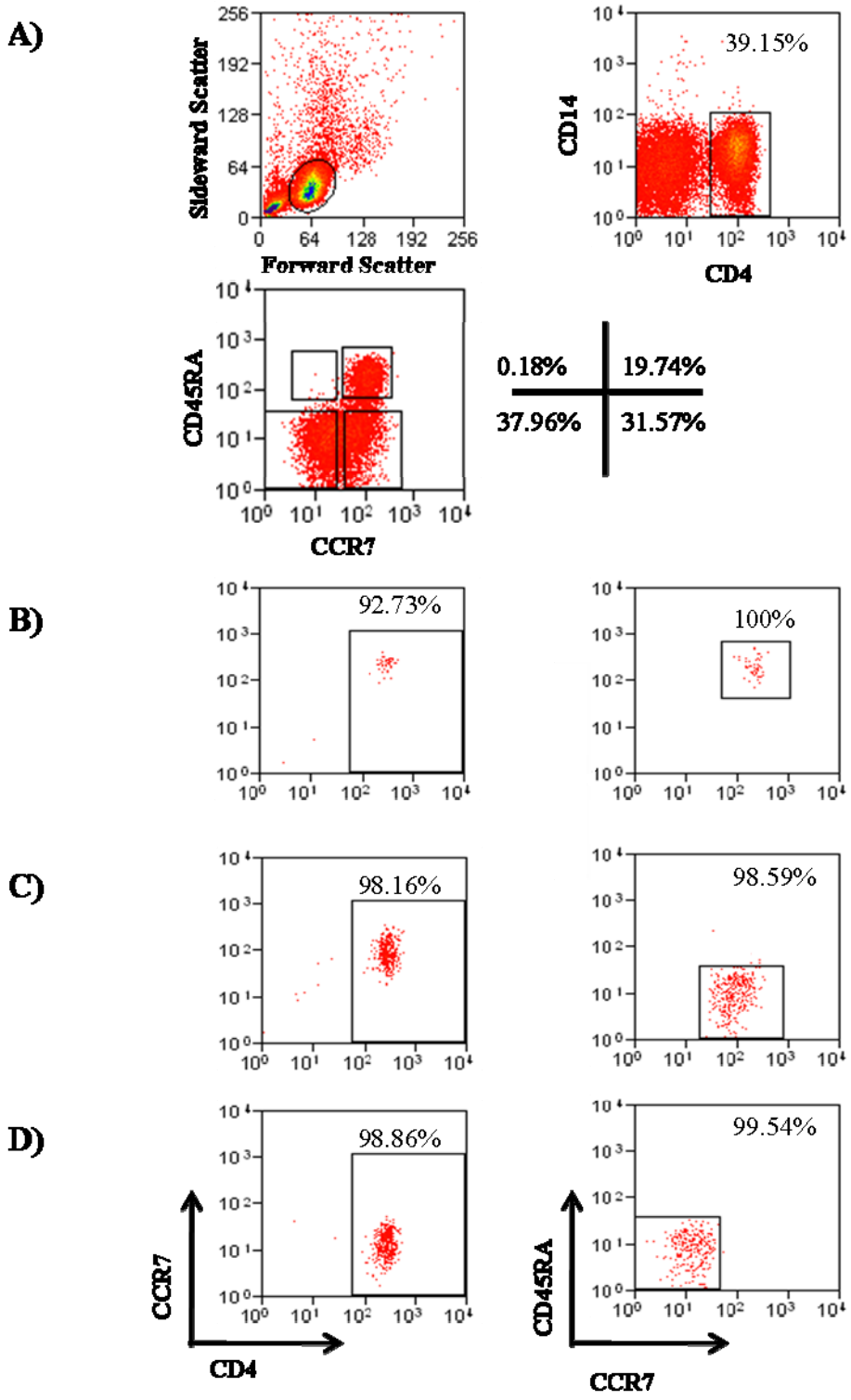

Figure 3.1. Sorting populations based on the expression of CD4, CCR7 and CD45RA. A) Representative donor (n=6) showing the gating used during the sort and representative percentages of each population. **B)** Representative purities for sorted $CD4^+$ naive T cells. **C)** Representative purities for sorted $CD4^+$ central memory T cells. **D)** Representative purities for sorted $CD4^+$ effector memory T cells.

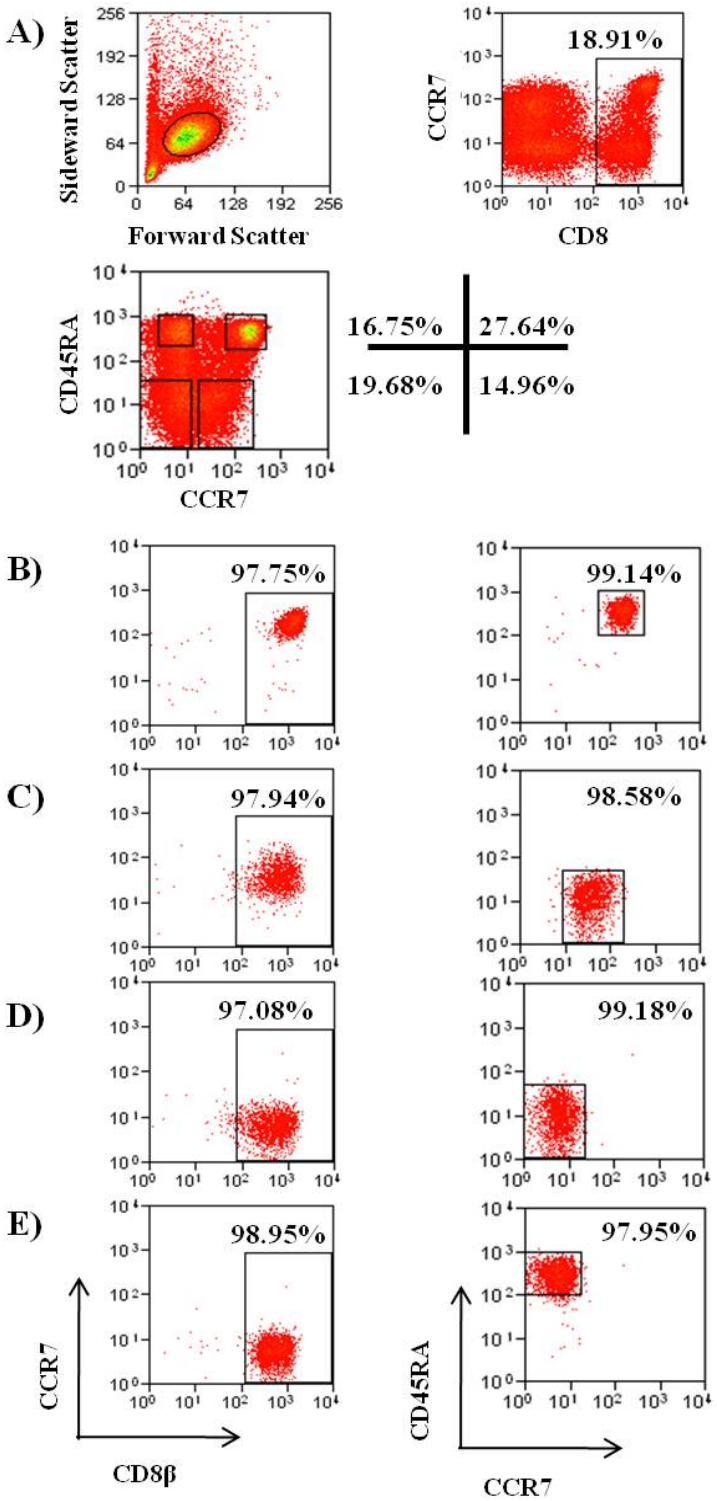

Figure 3.2. Sorting populations based on the expression of CD8, CCR7 and CD45RA. A) Representative donor (n=6) showing the gating used during the sort and representative percentages of each population. **B)** Representative purities for sorted $CD8^+$ naive T cells. **C)** Representative purities for sorted $CD8^+$ central memory T cells. **D)** Representative purities for sorted $CD8^+$ effector memory T cells. **E)** Representative purities for sorted $CD8^+$ effector memory RA T cells.

3.2.2 Microarray analysis of sorted $CD4^+$ and $CD8^+$ T cell populations

To address the question of which genes allow the best distinction between the four described $CD4^+$ or $CD8^+$ T cell populations, the cDNA from each population was run on a full human genome microarray which contained 35,035 oligonucleotide probes, representing approximately 25,100 unique genes and 39,600 transcripts excluding control oligos. Each microarray analysed a single sample and a human reference sample, labelled with different Cy-dyes hybridised. The human reference sample consisted of a low number of RNA transcripts for 99% of genes expressed on the arrays. The addition of a reference sample allowed for the comparison of different slides to each other, since the reference sample should give a similar signal every time. The expression levels of the genes on the array are therefore expression values relative to the human reference sample. The expression value of a particular gene was calculated by taking the human reference value for that gene and dividing by the sample value for that gene. This means that if the gene in question has a very low level of expression in the sample the expression value relative to the human reference will be a positive number, whereas if the gene is expressed very high in the sample, the expression value becomes a smaller minus number.

3.2.3 Comparing the four differentiation states without distinguishing between $CD4^+$ and $CD8^+$ T cell populations

SAM analysis was performed, dividing the samples into the four differentiation states: naive, central memory (CM), effector memory (EM) and effector memory RA (EMRA). The samples were not divided between $CD4^+$ and $CD8^+$, therefore each SAM group contained 12 samples (six $CD4^+$ populations and six $CD8^+$ populations), except for the EMRA group which only contained six $CD8^+$ populations. This analysis resulted in a SAM gene list of 115 genes which differed significantly in their expression between the differentiated T cell populations and a false discovery rate (FDR) of 1% (Supplemental Table 1). This gene list was used to analyse the samples by hierarchical clustering (HCL). Fig. 3.3 shows how the samples cluster together based on these 115 genes. Based on these genes five $CD8^+$ samples were misclassified. A $CD8^+$ naive sample clustered more closely together with $CD4^+$ naive samples, however it is also clear from the clustering that all but two naive samples clustered separately from the other differentiated populations. The two $CD8^+$ naive samples which clustered together with the more differentiated populations clustered very close to the differentiated $CD8^+$ populations. One $CD8^+$ EMRA sample clustered together with the $CD8^+$ EM population from the same donor (donor F). Another $CD8^+$ CM sample clustered together with the $CD8^+$ EM population from the same donor (donor E). Lastly the $CD8^+$ EM and EMRA from donor A clustered together.

Principal component analysis (PCA) was used to visualise the clustering from the HCL (Fig. 3.4). The PCA shows the naive samples clustering very close together, regardless of whether they are from the $CD4^+$ or $CD8^+$ compartment. The more differentiated populations however showed a split between $CD4^+$ and $CD8^+$, even though this was not one of the criteria which

generated the SAM gene list. Within the $CD4^+$ compartment the EM population (red spheres) differed the most in its gene expression profile, compared to the naive samples (light blue spheres). The gene expression of the $CD4^+$ CM population shows that the expression levels of those genes are intermediate to the naive and EM population. The $CD8^+$ compartment shows a similar trend, albeit not as clear as can be seen within the $CD4^+$ compartment. This could be due to the EM and EMRA populations sharing a lot of functions and therefore having very similar gene expression profiles.

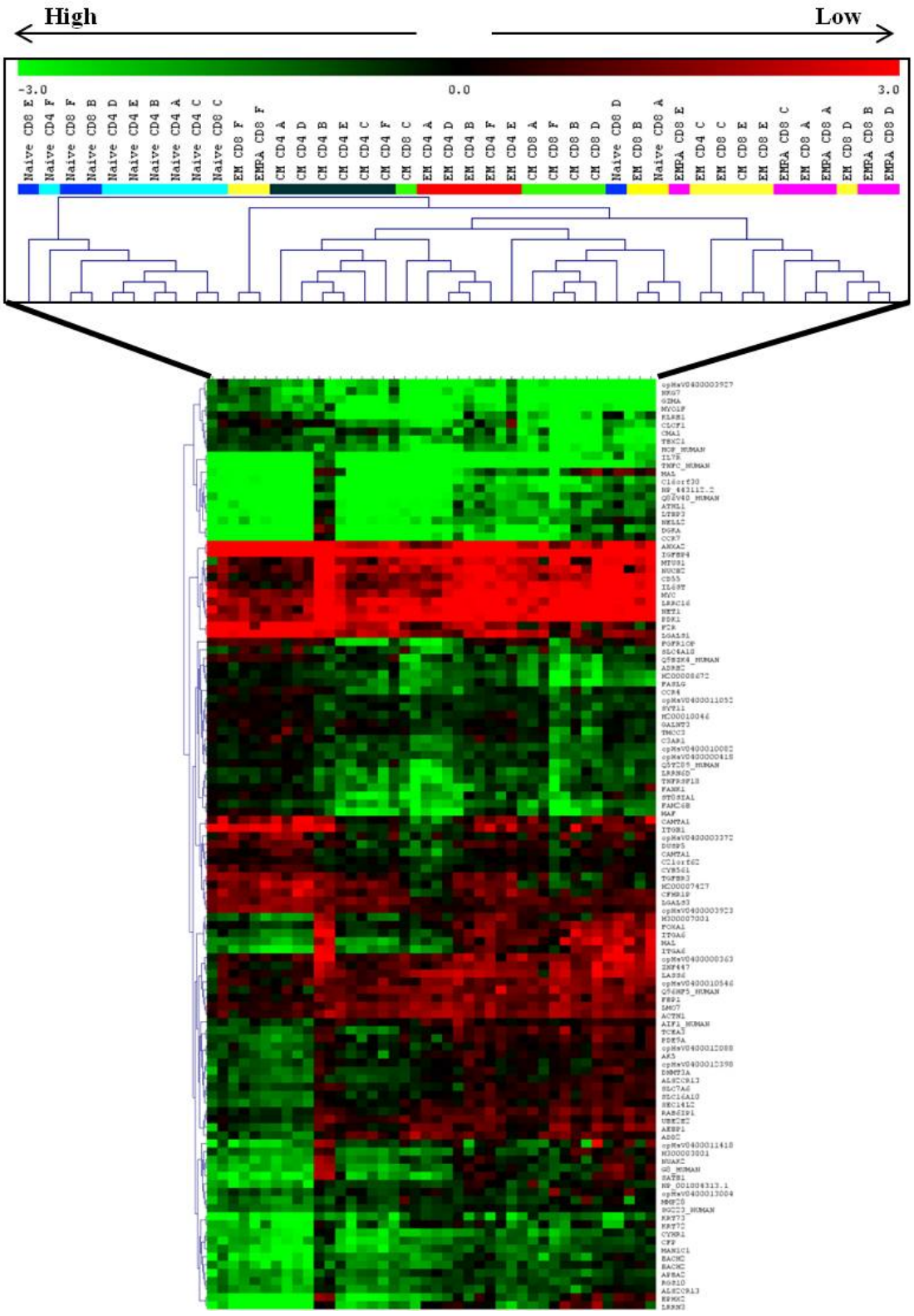

Figure 3.3. Comparing Naive, CM, EM and EMRA T cell populations from both the CD4$^+$ and CD8$^+$ T cell compartment. HCL using the gene list generated by SAM (1% FDR) comparing the four differentiation states without distinguishing between CD4$^+$ and CD8$^+$ populations. The HCL shows the clustering of the samples. Five samples are misclassified based on this clustering.

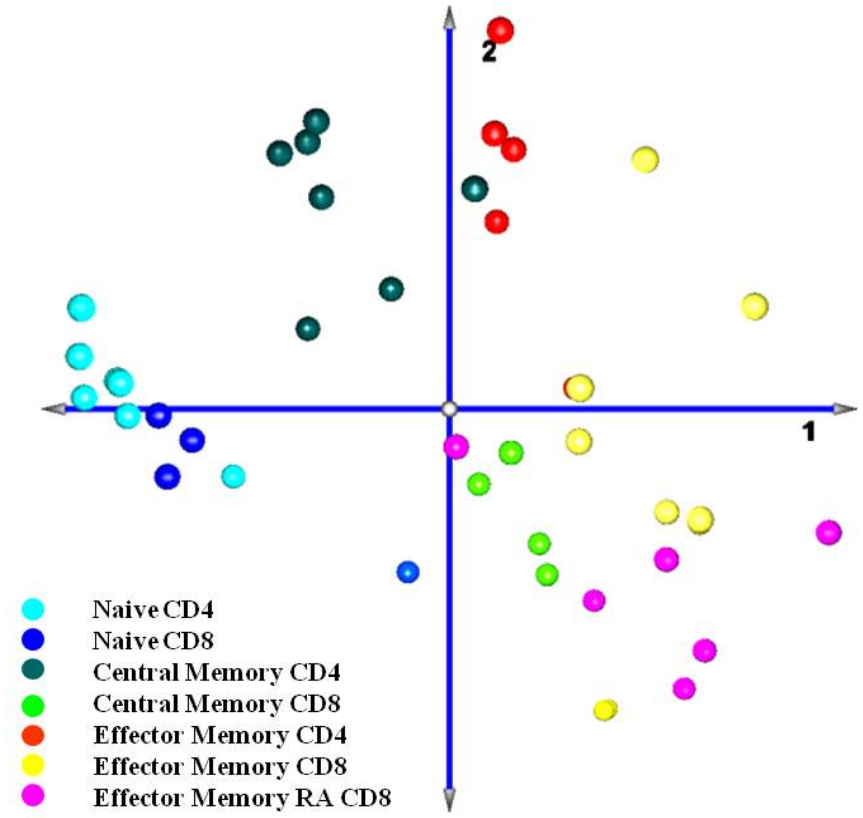

Figure 3.4. Comparing Naive, CM, EM and EMRA T cell populations from both the CD4$^+$ and CD8$^+$ T cell compartment. PCA visualising the clustering of the samples.

3.2.4 Comparing three differentiation states within the CD4$^+$ compartment

To generate a list of genes which are significantly differentially expressed between the three cell populations within the CD4$^+$ compartment a SAM was performed, dividing the samples into three groups. This generated a list of 226 genes with a FDR of 1% (Supplemental Table 2), Fig. 3.5A shows the HCL based on this gene list. The HCL reveals that these 226 genes allow very good clustering of the samples into their relevant differentiation states. All three groups branch off their own HCL branch, except for one EM sample which branched from the same arm as the CM samples. This did not result in mislabelling of the sample however

and as can be seen in the PCA (Fig. 3.5B) this does not have an impact on the visual representation of the clustering of the samples. The PCA shows that the naive population is the most different in its gene expression compared to the EM population. The CM population again showed an intermediate expression level of these genes to that of the naive and EM populations.

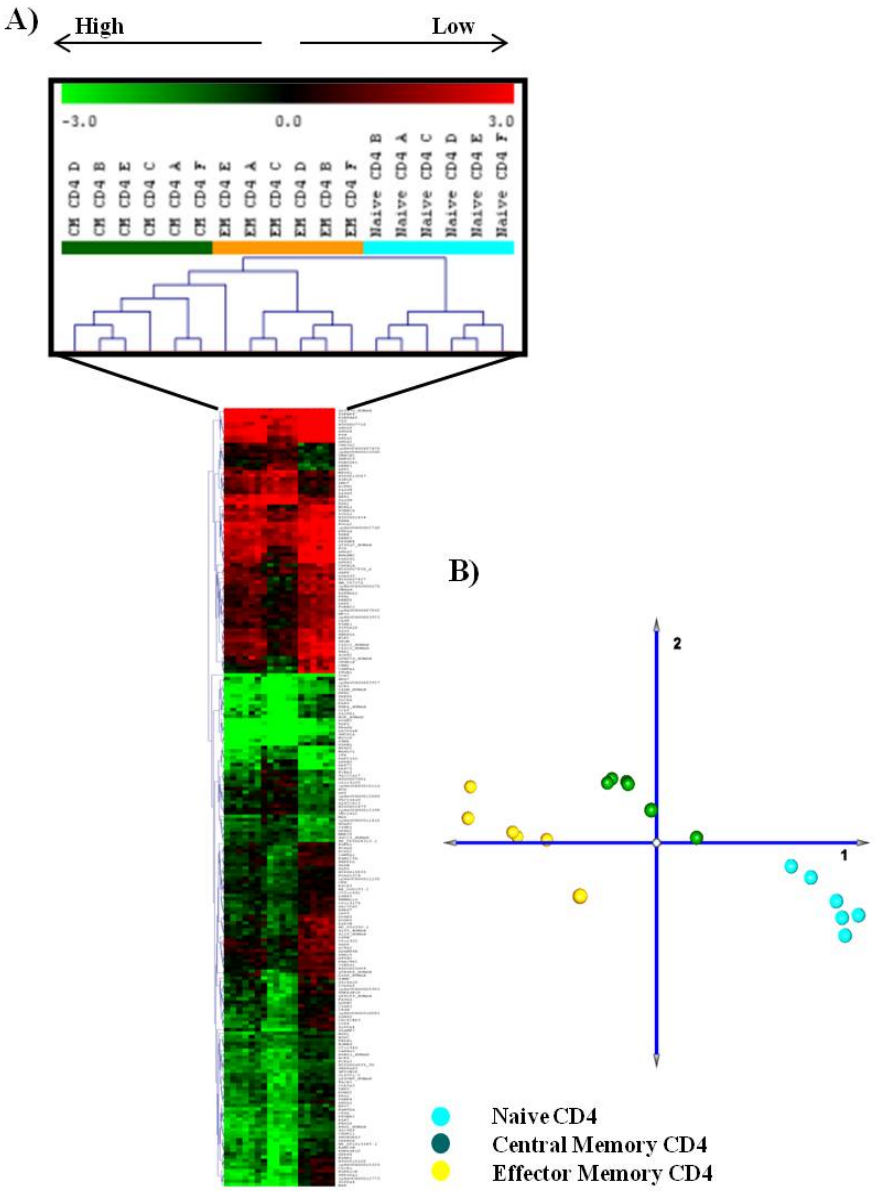

Figure 3.5. Comparing Naive, CM and EM T cell populations from the CD4$^+$ T cell compartment. SAM analysis resulted in a list of 226 significant genes (1%)FDR. **A)** HCL using the gene list generated by SAM, showing the clustering of the samples. **B)** PCA visualising the clustering of the samples.

To identify the genes significantly differently expressed between $CD4^+$ naive and CM populations, a paired SAM was executed. This meant that the naive and CM population from one donor were paired together in the analysis, to address any donor variability that may have been present. The paired SAM resulted in a list of 135 genes, with a FDR of 1% (Supplemental Table 3). The HCL in Fig. 3.6A clearly shows the ability of this gene list to separate the two populations from each other. Both populations clustered very tightly together on two separate arms of the HCL. The PCA (Fig. 3.6B) again shows two distinct clusters correlating to the two populations. Fig. 7A shows the 4 genes with the highest fold difference (> 2 fold) in the naive population compared to the CM population. The gene LRRN3 (Leucine-rich repeat neuronal protein 3) came up on this list as one of the genes with the highest fold difference between $CD4^+$ naive cells and $CD4^+$ CM cells. Fig. 3.7B shows the 10 genes with the highest fold difference (> 2 fold) in the CM population compared to the naive population. The two genes with the highest differential expression between CM $CD4^+$ T cells and naive $CD4^+$ T cells are KLRB1 (killer cell lectin-like receptor subfamily B member 1 or CD161) and FGFR1OP (CCR6 or CD196).

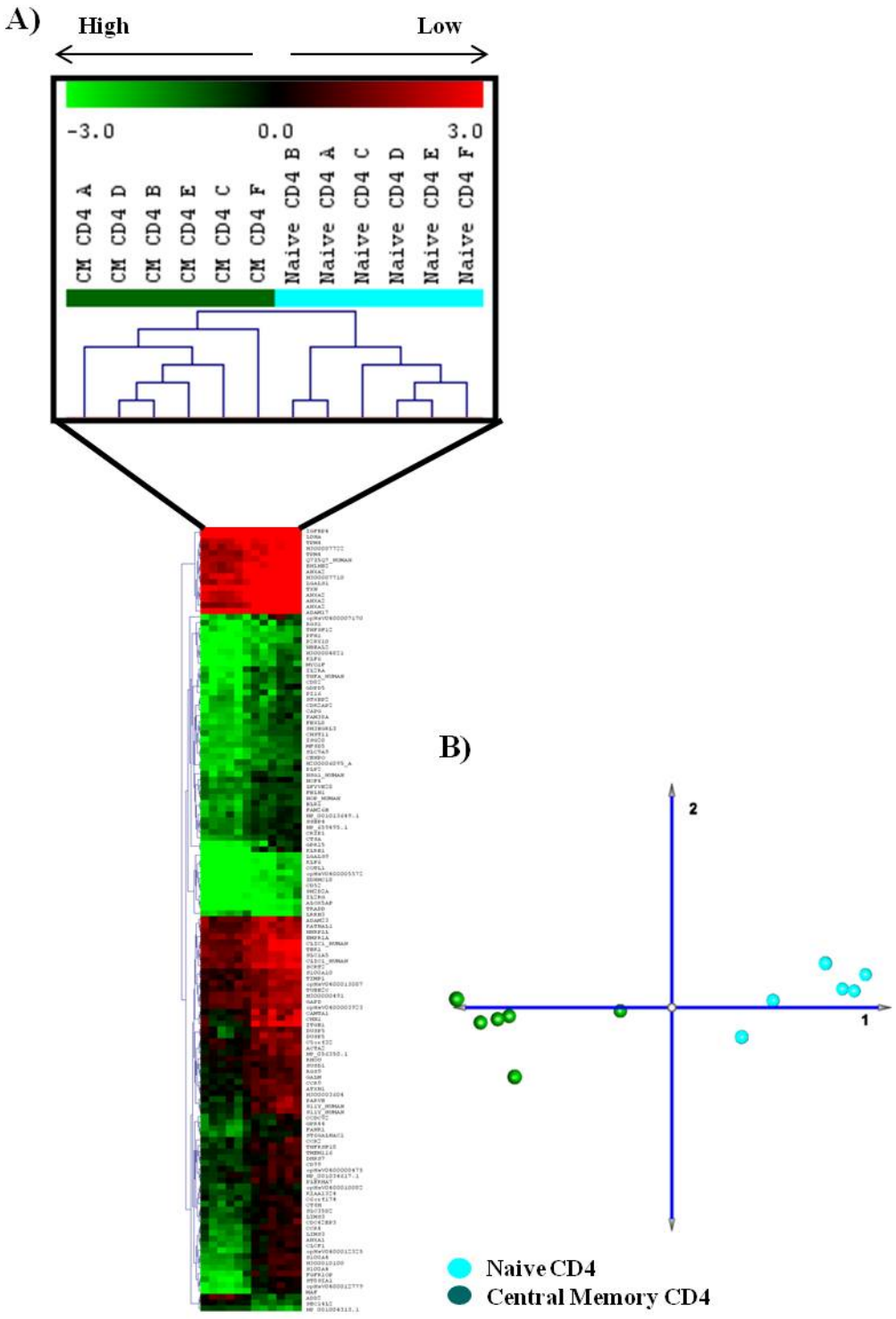

Figure 3.6. Comparing Naive and CM T cell populations from the CD4$^+$ T cell compartment. SAM analysis resulted in a list of 135 significant genes (1% FDR). **A)** HCL using the gene list generated by SAM, showing the clustering of the samples. **B)** PCA visualising the clustering of the samples.

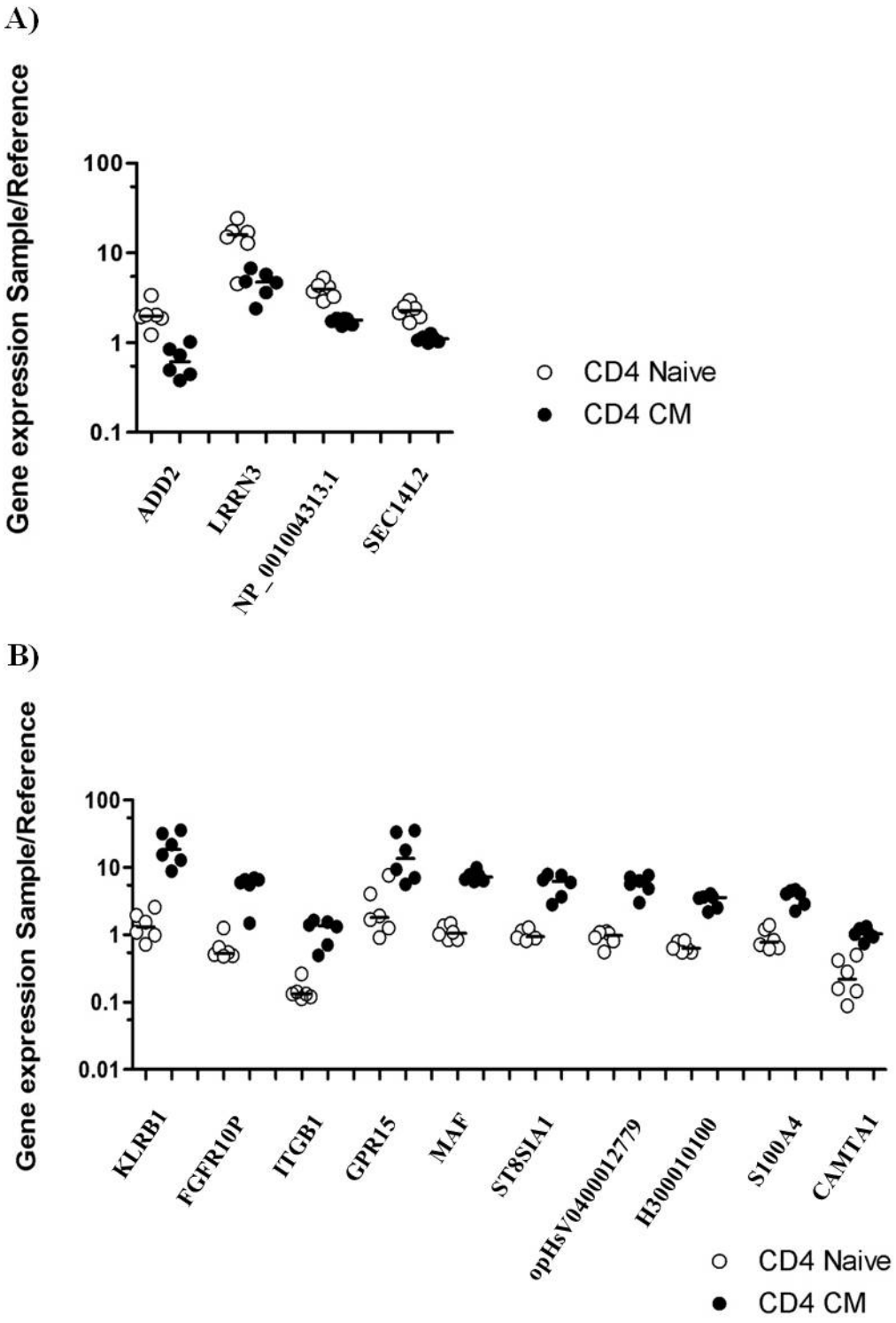

Figure 3.7. Genes with the highest fold difference from the gene list generated when comparing naive and CM T cell populations from the $CD4^+$ T cell compartment. The graphs show the expression levels for each donor for that gene on a log scale, with the bar indicating the median expression level. **A)** The four genes with the highest expression level (≥ 2 fold) in $CD4^+$ naive T cells compared to $CD4^+$ CM T cells. **B)** Ten genes with the highest expression level (≥ 2 fold) in $CD4^+$ CM cells compared to $CD4^+$ naive cells.

The same approach was used to identify genes which are differentially expressed between $CD4^+$ naive and EM populations. In this case the paired SAM resulted in a list of 279 genes (Supplemental Table 4) with significantly different gene expression between $CD4^+$ naive and $CD4^+$ EM T cell populations (1% FDR). The resulting HCL (Fig. 3.8A) shows the ability of this gene list to distinguish these two differentiation states based on their gene expression. The PCA (Fig. 3.8B) shows the two populations clustering apart from each other in concordance with the HCL. The 10 genes with the highest fold difference in $CD4^+$ naive T cells compared to $CD4^+$ EM T cells are shown in Fig. 3.9A. LRRN3 again is more highly expressed in $CD4^+$ naive T cells compared to the $CD4^+$ EM T cells (17.1 times higher expression). Fig. 3.9B shows the 10 genes with the highest fold difference in $CD4^+$ EM T cells compared to $CD4^+$ naive T cells. The two genes with the highest fold difference were KLRB1 (Killer cell lectin-like receptor) and GZMA (granzyme A) which are both genes involved in T cell effector function.

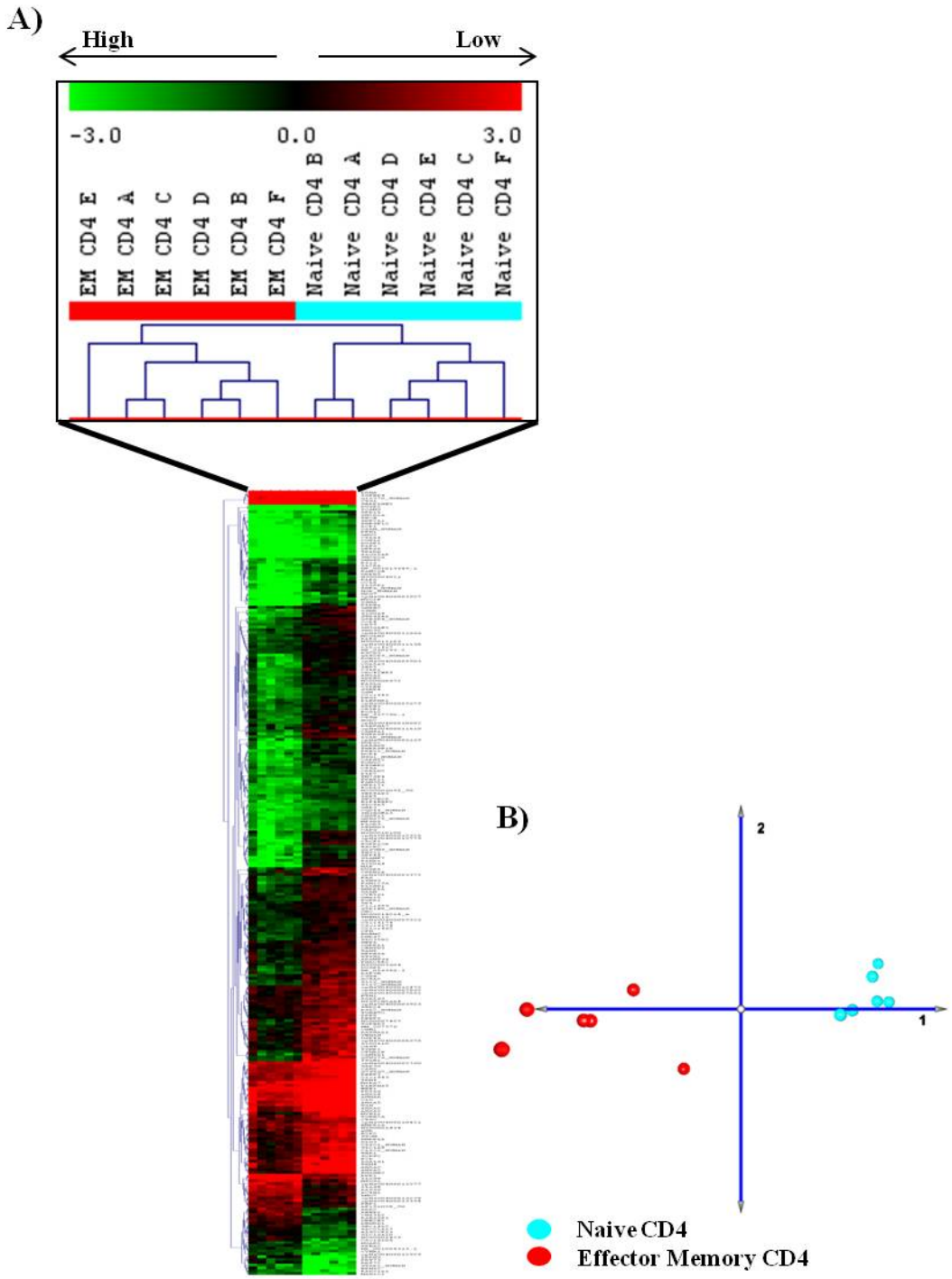

Figure 3.8. Comparing Naive and EM T cell populations from the CD4$^+$ T cell compartment. SAM analysis resulted in a list of 279 significant genes (1% FDR). **A)** HCL using the gene list generated by SAM, showing the clustering of the samples. **B)** PCA visualising the clustering of the samples.

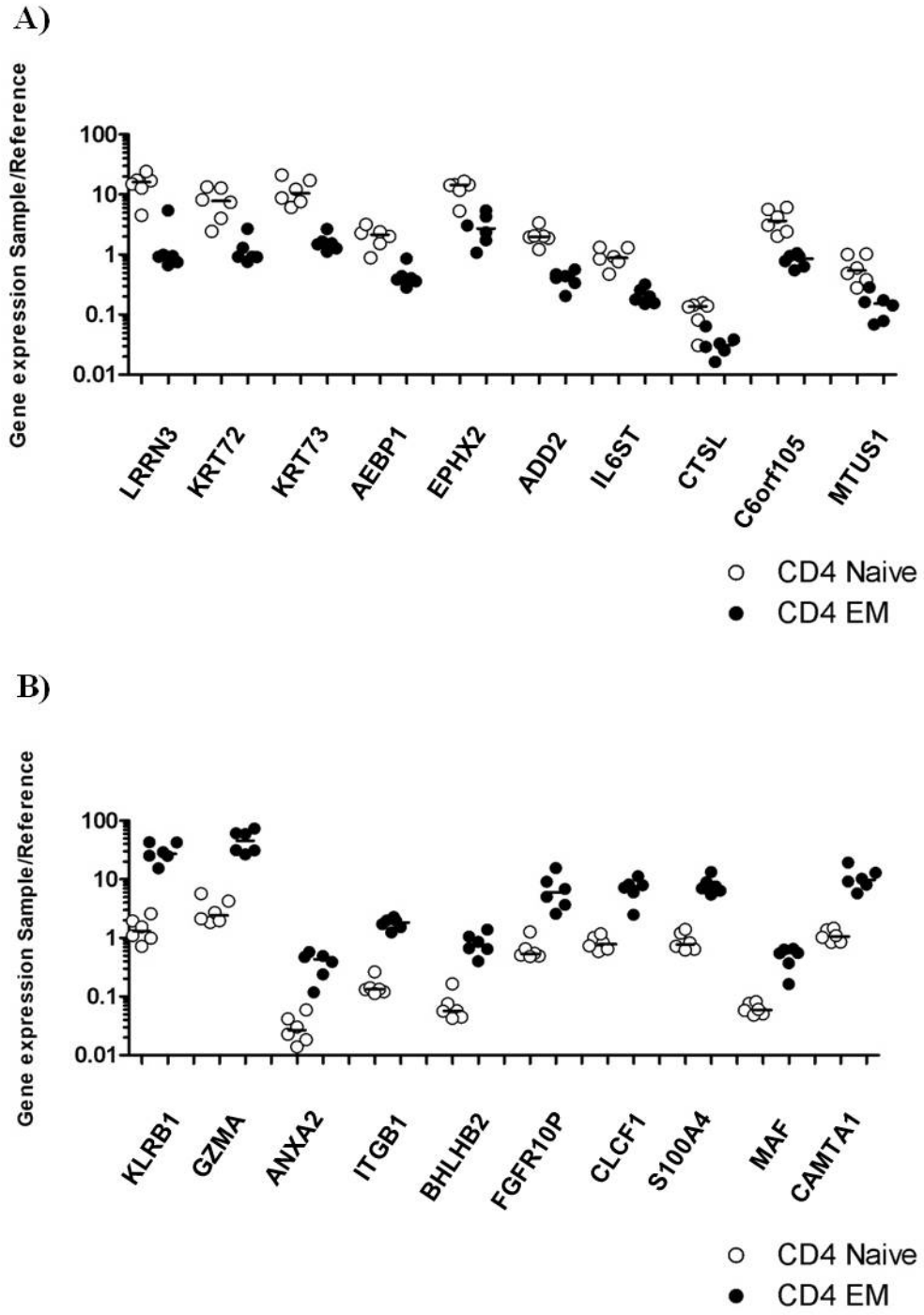

Figure 3.9. Genes with the highest fold difference from the gene list generated when comparing naive and EM T cell populations from the CD4$^+$ T cell compartment. The graphs show the expression levels for each donor for that gene on a log scale, with the bar indicating the median expression level**. A)** The ten genes with the highest expression level (≥ 2 fold) in CD4$^+$ naive T cells compared to CD4$^+$ EM T cells. **B)** Ten genes with the highest expression level (≥ 2 fold) in CD4$^+$ EM cells compared to CD4$^+$ naive cells.

The last comparison to be made within the $CD4^+$ compartment was between $CD4^+$ CM and EM populations and to this end a paired SAM was executed. The paired SAM resulted in a list of 40 genes with significantly different gene expression and a 1% FDR (Supplemental Table 5). The resulting HCL (Fig. 3.10A) shows the ability of this gene list to distinguish these two differentiation states based on their gene expression. The PCA (Fig. 3.10B) visualises the two populations clustering apart from each other. The 10 genes with the highest fold difference in $CD4^+$ CM T cells compared to $CD4^+$ EM T cells are shown in Fig. 3.11A. The genes with the highest fold difference between $CD4^+$ CM and $CD4^+$ EM populations were CCR7, LRRN3 and SELL (L-selectin or CD62L), both CCR7 and L-selectin are surface markers used by CM cells to regain entry into LNs. Fig. 3.11B shows the 10 genes with the highest fold difference in $CD4^+$ EM T cells compared to $CD4^+$ CM T cells. Within these 10 genes several genes associated with effector function can be found, such as SLAMF7 (SLAM family member 7 precursor, CD2-like receptor activating cytotoxic cells or CD319), NKG7 (Natural killer cell protein 7), GZMH (Granzyme H), GZMA (Granzyme A) and PFR1 (Perforin1).

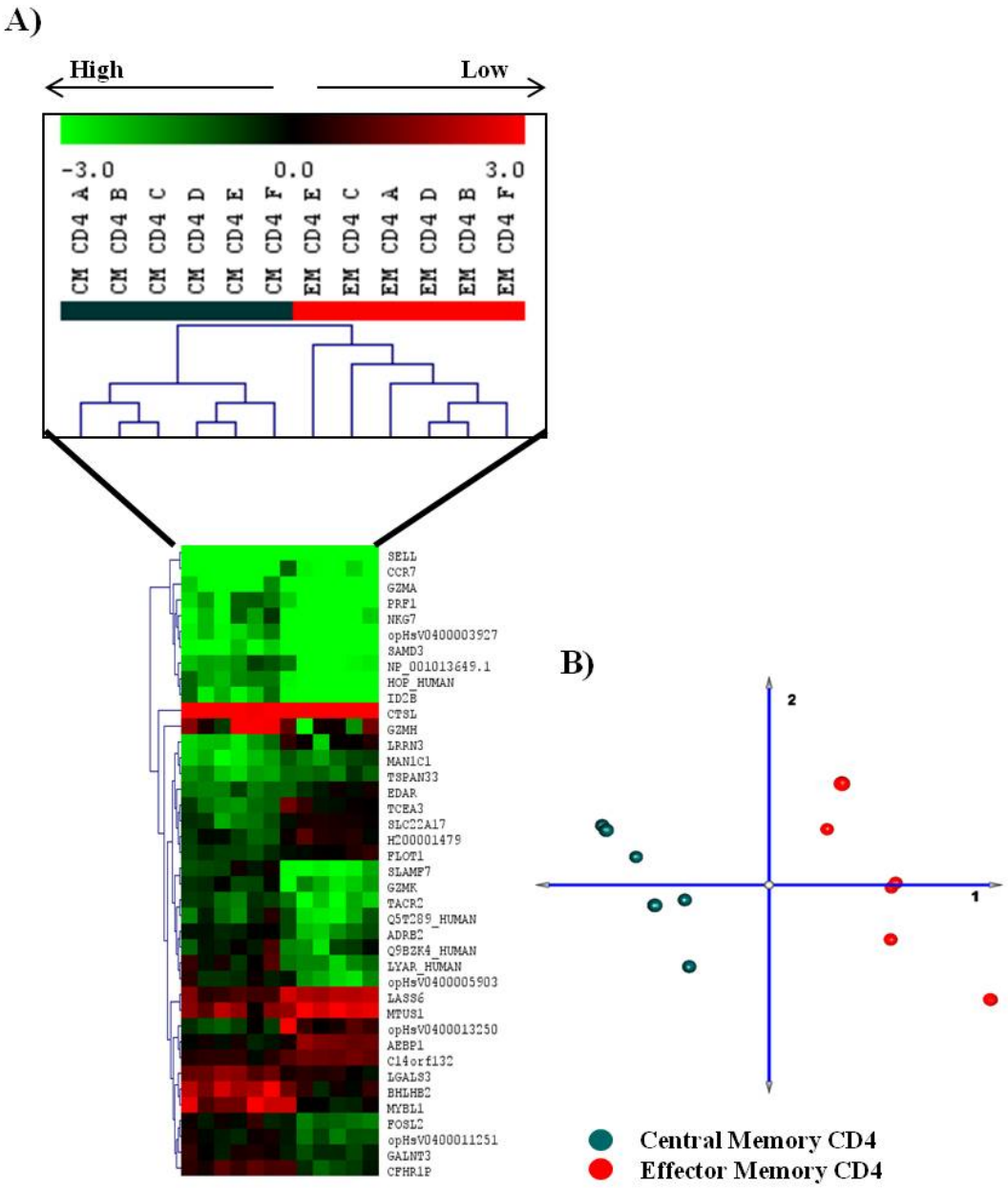

Figure 3.10. Comparing CM and EM T cell populations from the CD4$^+$ T cell compartment. SAM analysis resulted in a list of 40 significant genes (1% FDR). **A)** HCL using the gene list generated by SAM, showing the clustering of the samples. **B)** PCA visualising the clustering of the samples.

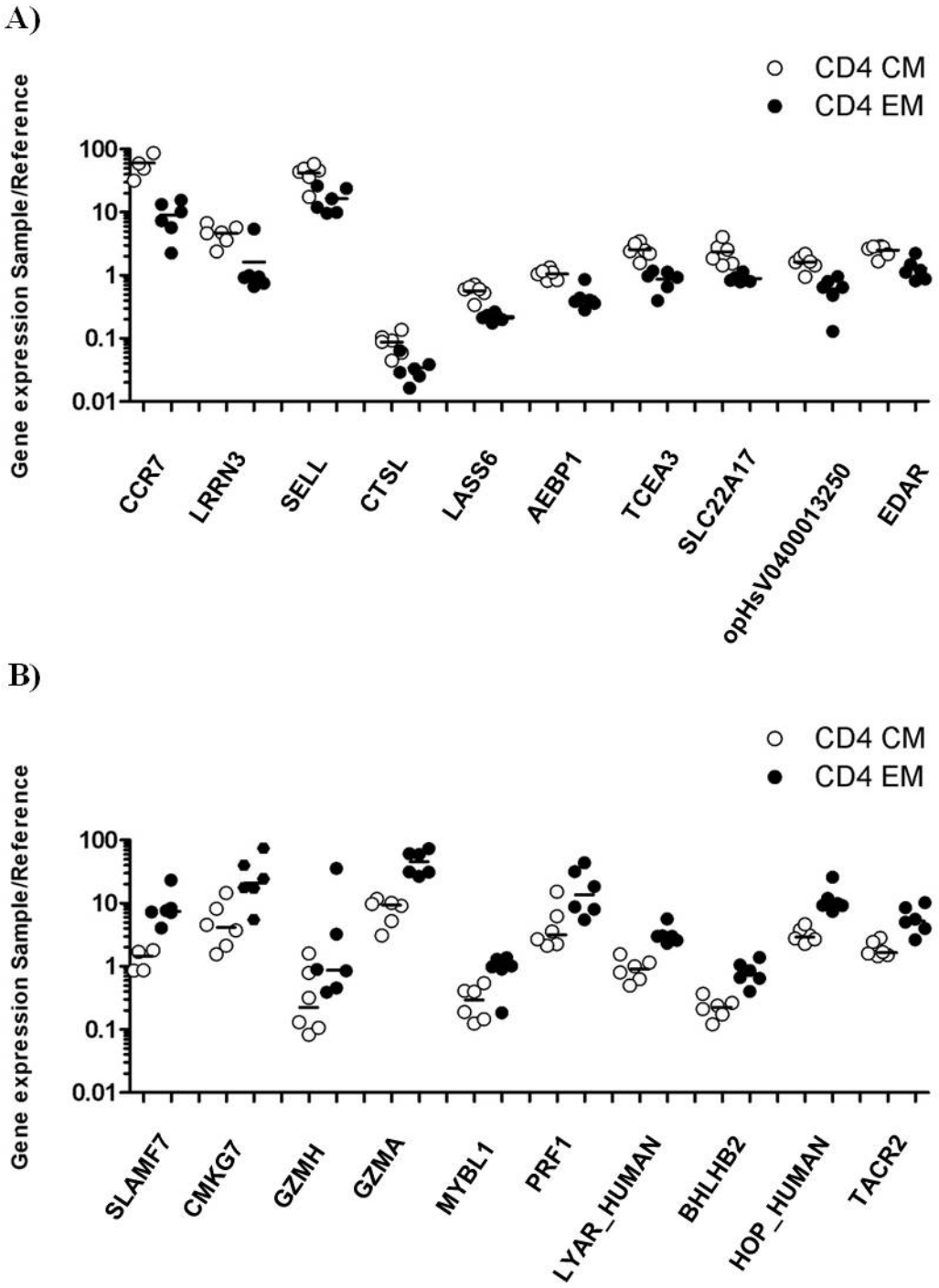

Figure 3.11. Genes with the highest fold difference from the gene list generated when comparing CM and EM T cell populations from the CD4$^+$ T cell compartment. The graphs show the expression levels for each donor for that gene on a log scale, with the bar indicating the median expression level. **A)** The ten genes with the highest expression level (≥ 2 fold) in CD4$^+$ CM T cells compared to CD4$^+$ EM T cells. **B)** Ten genes with the highest expression level (≥ 2 fold) in CD4$^+$ EM cells compared to CD4$^+$ CM cells.

3.2.5 Comparing four differentiation states within the $CD8^+$ compartment

To generate a list of significantly differentially expressed genes between the four cell populations within the $CD8^+$ compartment a SAM was performed, dividing the samples into four groups. This analysis resulted in a list of nine genes which were found to be expressed at significantly different levels between the four differentiation states (1% FDR, Supplemental Table 6). This list of genes was then used to cluster the samples together based on their gene expression profiles for these genes, shown in Fig. 3.12A as a HCL. Using these nine genes to cluster the samples resulted in five samples being misclassified. One CM sample clustered together with two naive samples, whereas another CM sample clustered together with the EM sample from the same donor (donor E). As was seen before in **3.2.3** distinguishing between the EM and EMRA populations proved difficult, which may be a result of the many shared functions between these two subsets. In this case three EM samples were misclassified as EMRA samples. Fig. 3.12B shows the resulting PCA which shows that the gene expression of the naive $CD8^+$ T cell population differed the most from the $CD8^+$ EM and EMRA T cell populations, with the gene expression levels of the CM population intermediate between the naive and effector populations.

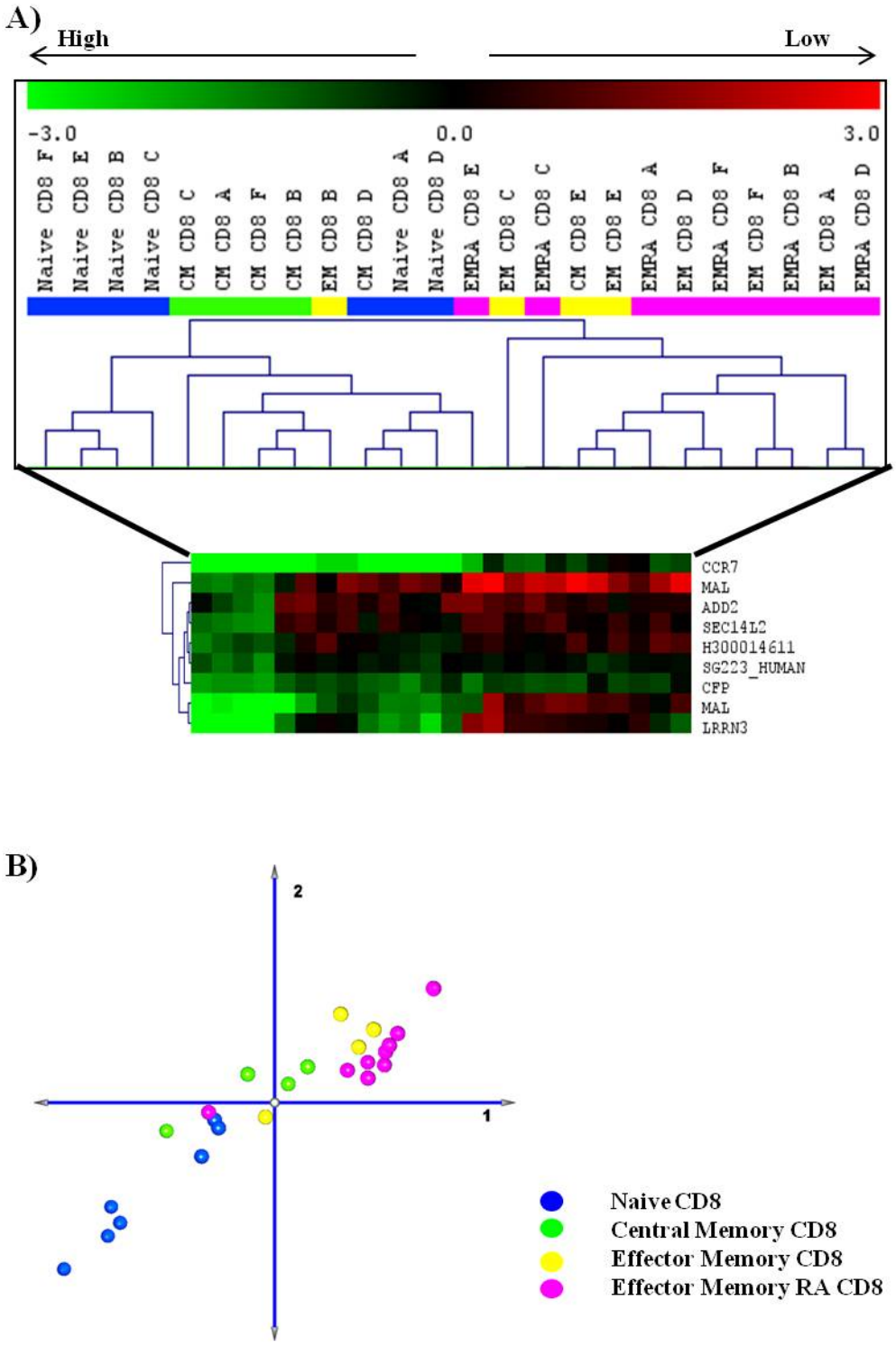

Figure 3.12. Comparing Naive, CM, EM and EMRA T cell populations from the CD8$^+$ T cell compartment. A) HCL using the gene list generated by SAM, showing the clustering of the samples. **B)** PCA visualising the clustering of the samples.

Comparing the CD8$^+$ naive and CM populations using a paired SAM resulted in a list of 4 genes, with a FDR of 1% (Supplemental Table 7). The HCL in Fig. 3.13A shows that based on the expression profiles of these four genes the samples can be divided into the two groups (naive or CM). The PCA (Fig. 3.13B) visualises the separation achieved using these four genes. The graph in Fig. 3.14 shows the fold difference between the four genes for the naive and CM populations. Three of the four genes (KRT72, MTMR8 and NP_689619.1) are found to be upregulated in the naive population compared to the CM population. The only gene upregulated (opHsV0400012617) in the CM population compared to the naive population shows a fold difference of 2.3.

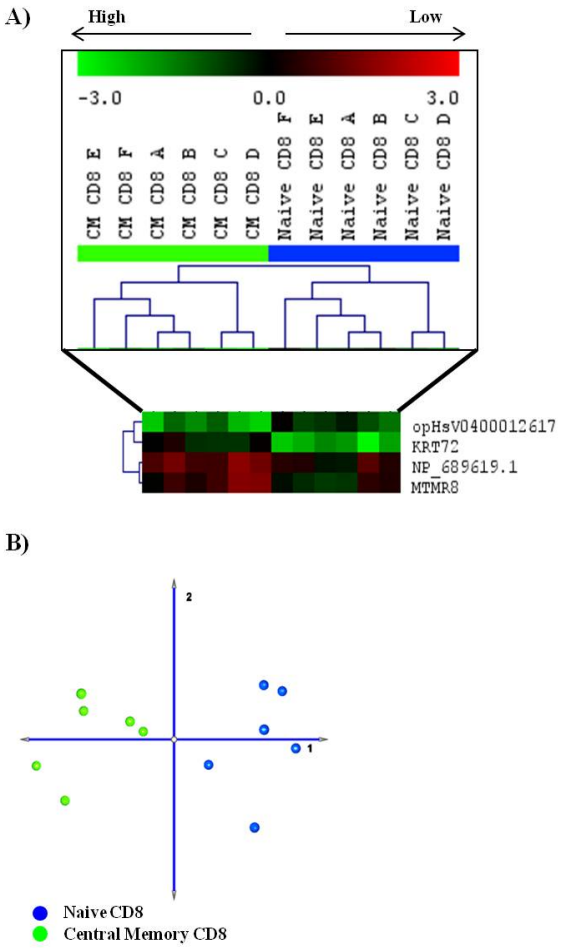

Figure 3.13. Comparing Naive and CM T cell populations from the CD8$^+$ T cell compartment. A) HCL using the gene list generated by SAM, showing the clustering of the samples. **B)** PCA visualising the clustering of the samples.

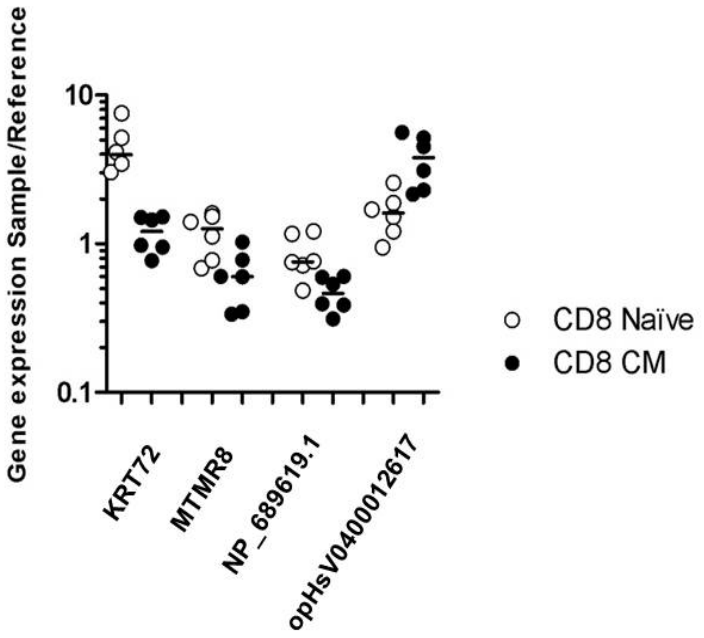

Figure 3.14. Genes with the highest fold difference from the gene list generated when comparing naive and CM T cell populations from the CD8$^+$ T cell compartment. The graphs show the expression levels for each donor for that gene on a log scale, with the bar indicating the median expression level. Three genes with the highest expression level (≥ 1.5 fold) in CD8$^+$ naive T cells compared to CD8$^+$ CM T cells. opHsV0400012617 is expressed ≥ 2 fold in CD8 CM than in CD8 naive cells.

Gene expression of CD8$^+$ naive and EM populations was then compared using a paired SAM, this resulted in a list of 23 genes with a FDR of 1% (Supplemental Table 8). The HCL in Fig. 3.15A shows that all samples are classified correctly using the expression profiles of these 23 genes, however two naive samples clustered off of the same branch as the EM samples. These two naive samples could be seen to cluster halfway in between the naive and EM populations in the PCA shown in Fig. 3.15B. This indicates that these two naive samples show an expression level intermediate between the naive phenotype and effector phenotype. The graph in Fig. 3.16 shows the 10 genes with the highest fold difference in expression between the naive and EM populations. All 23 genes from the SAM list were found to be upregulated at least 1.4 fold in the naive populations compared to the EM populations. The

gene with the highest fold difference in expression level was CCR7 with a 28.3 fold difference between naive and EM. LRRN3 again is more highly expressed in the naive population, as was seen within the $CD4^+$ compartment.

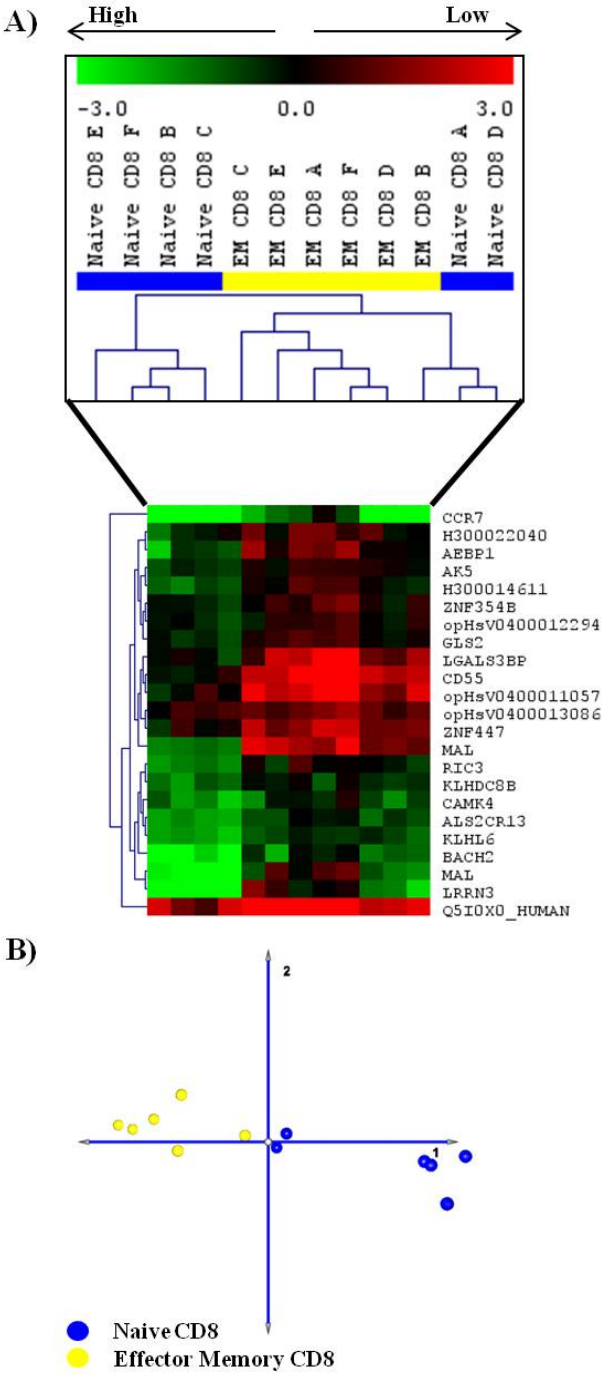

Figure 3.15. Comparing Naive and EM T cell populations from the $CD8^+$ T cell compartment. A) HCL using the gene list generated by SAM, showing the clustering of the samples. **B)** PCA visualising the clustering of the samples.

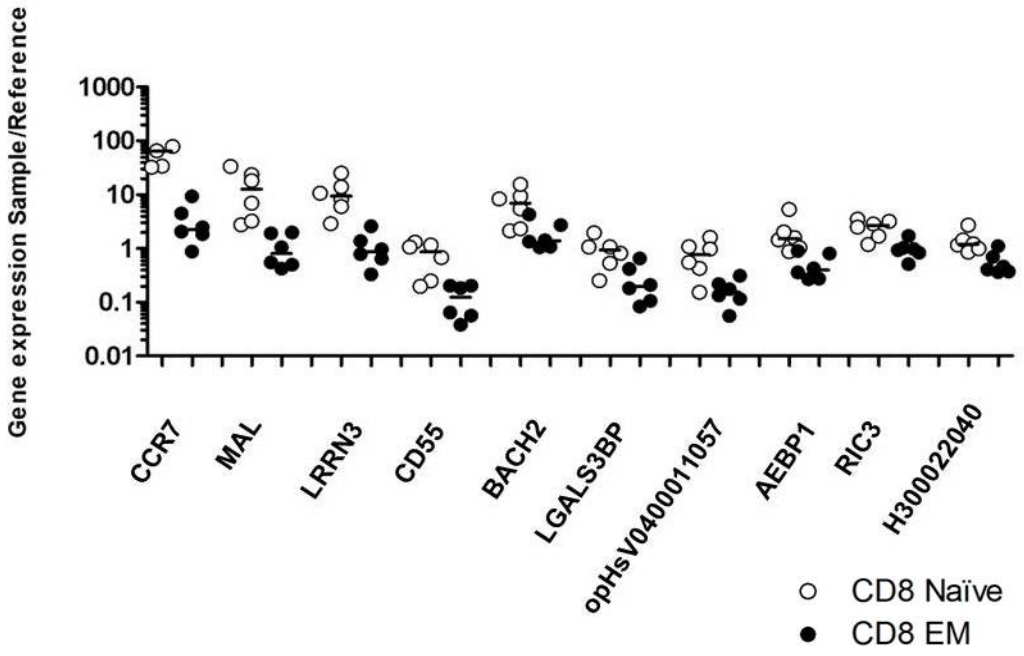

Figure 3.16. Genes with the highest fold difference from the gene list generated when comparing naive and EM T cell populations from the CD8$^+$ T cell compartment. The graphs show the expression levels for each donor for that gene on a log scale, with the bar indicating the median expression level**.** The graph shows the ten genes with the highest expression level (≥ 2 fold) in CD8$^+$ naive T cells compared to CD8$^+$ EM T cells.

Comparing CD8$^+$ naive and EMRA populations a SAM list of 24 genes, with a FDR of 1% (Supplemental Table 9) was generated. The HCL in Fig. 3.17A shows that all but one sample were correctly classified based on this gene list. Two naive samples are shown to branch off of the same HCL branch as the EMRA populations and one EMRA sample is classified as naive. The PCA in Fig. 3.17B shows the clustering of the samples and the two naive samples can be seen clustering closely to the EMRA samples. As was the case in the CD8$^+$ naive versus EM populations; all significant genes found in this comparison are upregulated in the naive samples compared to the EMRA samples. The ten genes with the highest fold difference are shown in Fig. 3.18.

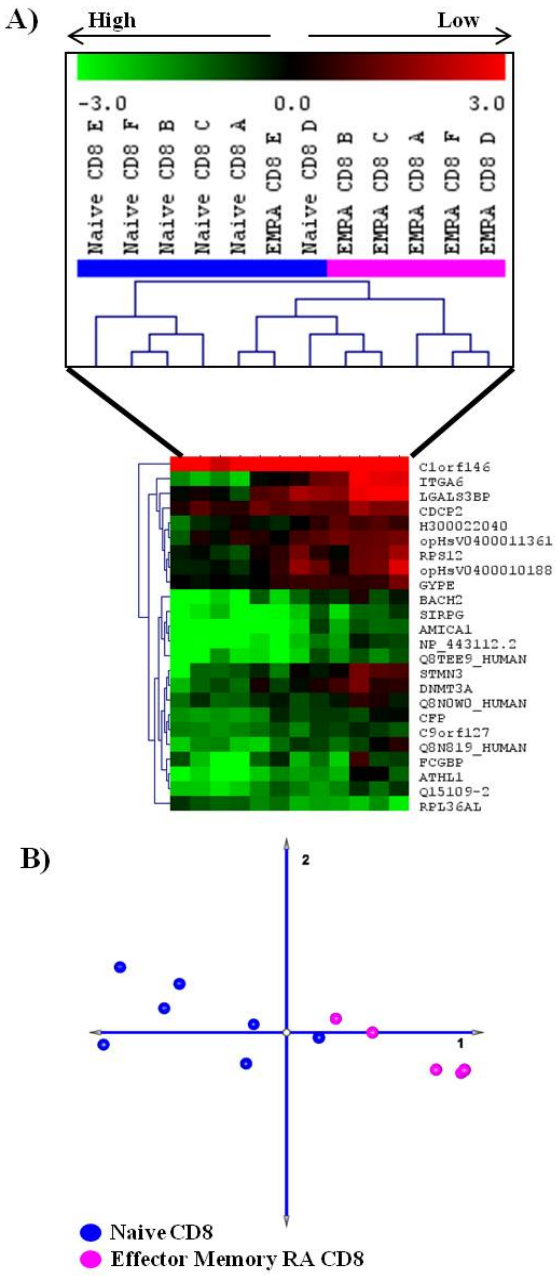

Figure 3.17. Comparing Naive and EMRA T cell populations from the CD8$^+$ T cell compartment. A) HCL using the gene list generated by SAM, showing the clustering of the samples**. B)** PCA visualising the clustering of the samples.

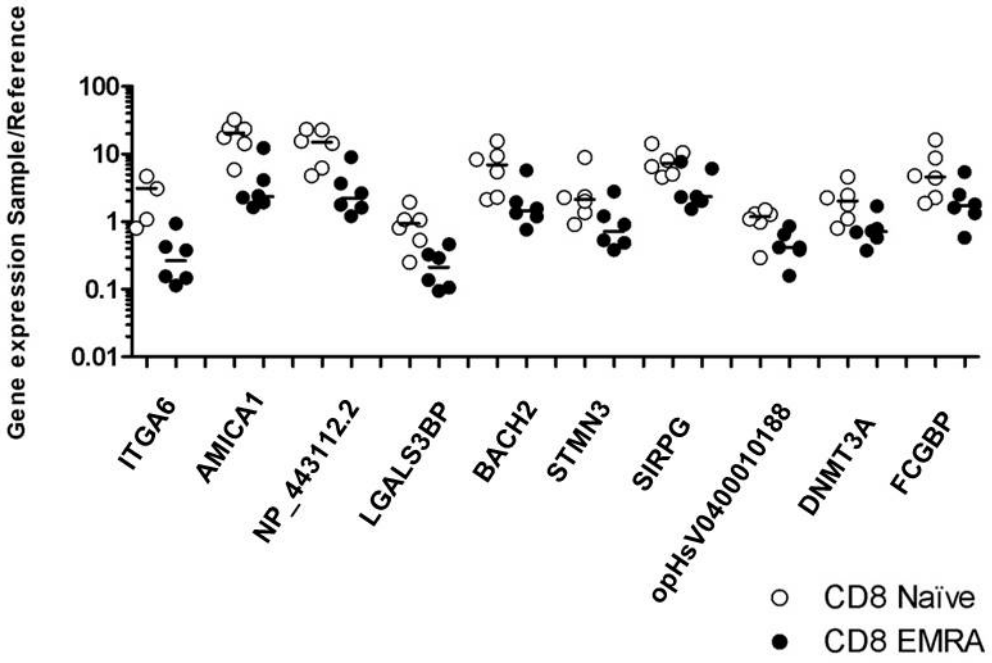

Figure 3.18. Genes with the highest fold difference from the gene list generated when comparing naive and EMRA T cell populations from the CD8$^+$ T cell compartment. The graphs show the expression levels for each donor for that gene on a log scale, with the bar indicating the median expression level**.** The ten genes with the highest expression level (≥ 2 fold) in CD8$^+$ naive T cells compared to CD8$^+$ EMRA T cells are shown.

The paired SAM used to identify the genes significantly differently expressed between CD8$^+$ CM and EM populations resulted in a list of 10 genes, with a FDR of 1% (Supplemental Table 10). The HCL in Fig**.** 3.19A shows the resulting clustering of the samples based on this gene list. The gene list allows all but one sample to be classified correctly, one EM sample was classified as a CM sample. Another conclusion which can be reached from looking at the HCL is that separating the two groups of samples into their respective groups is difficult, as the gene expression of the CD8$^+$ CM and EM T cell populations seems quite varied. This is also reflected in the PCA shown in Fig. 3.19B. The graph in Fig. 3.20 shows all five significant genes found using the paired SAM analysis. These five genes were found to be more than twofold up in the EM population compared to the CM population. GZMH and

KLRF1 (Killer cell lectin-like receptor subfamily F member 1) are both genes associated with effector function. A similar paired SAM analysis comparing $CD8^+$ CM to $CD8^+$ EMRA populations did not find any genes that were significantly different in their expression.

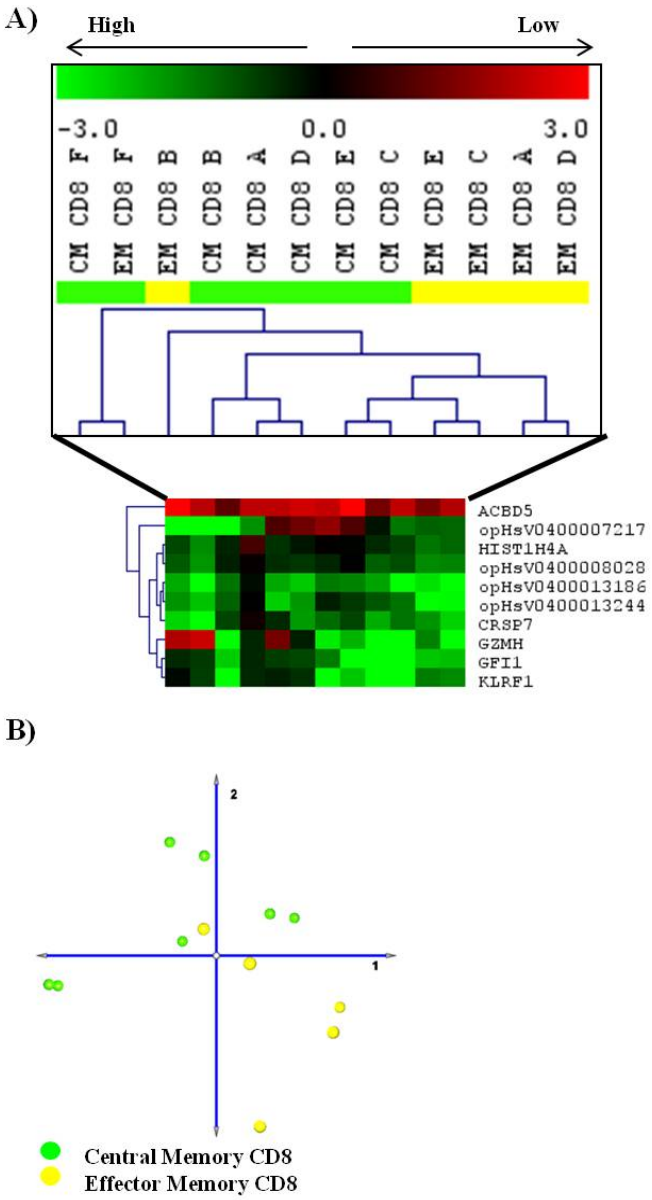

Figure 3.19. Comparing CM and EM T cell populations from the $CD8^+$ T cell compartment. A) HCL using the gene list generated by SAM, showing the clustering of the samples. **B)** PCA visualising the clustering of the samples.

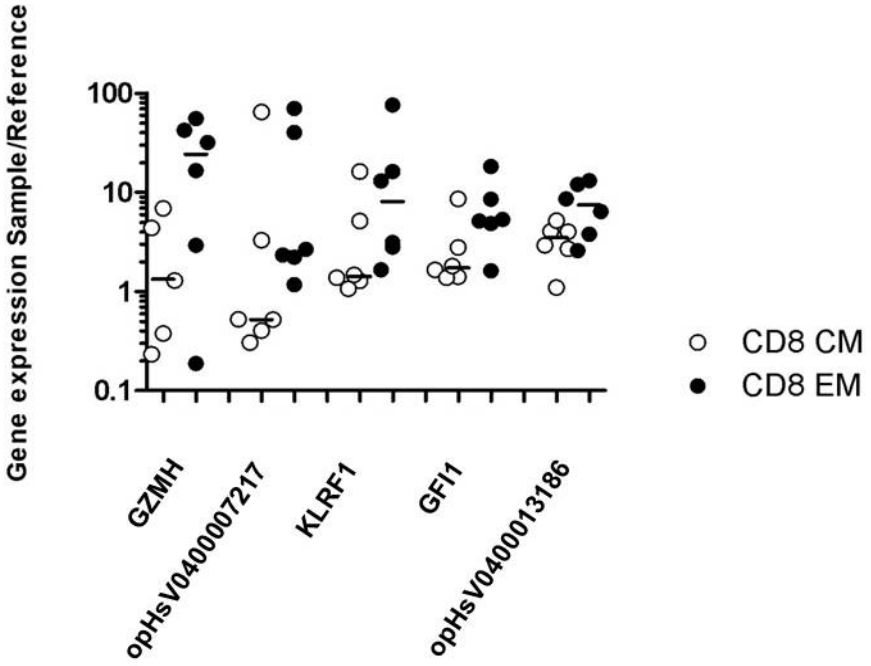

Figure 3.20. Genes with the highest fold difference from the gene list generated when comparing CM and EM T cell populations from the CD8$^+$ T cell compartment. The graphs show the expression levels for each donor for that gene on a log scale, with the bar indicating the median expression level. The ten genes with the highest expression level (≥ 2 fold) in CD8$^+$ CM T cells compared to CD8$^+$ EM T cells are shown.

Comparing the CD8$^+$ EM and EMRA populations resulted in a SAM list of two genes, with a FDR of 1% (Supplemental Table 11). The HCL in Fig. 3.21A shows the clustering of these samples based on these two genes. Two samples were misclassified using the SAM list, one EMRA sample clustered as an EM sample and one EM sample clustered together with the EMRA samples. The two genes found were upregulated more than 1.5 fold in the EM cell populations compared to the EMRA cell populations (Fig. 3.21B). ZNF563 was upregulated 1.7 times in CD8$^+$ EM T cells and opHsV0400008530 showed a fold difference of 1.3.

The two genes identified by this SAM comparison were unique to these two populations and did not show up in any other comparisons made.

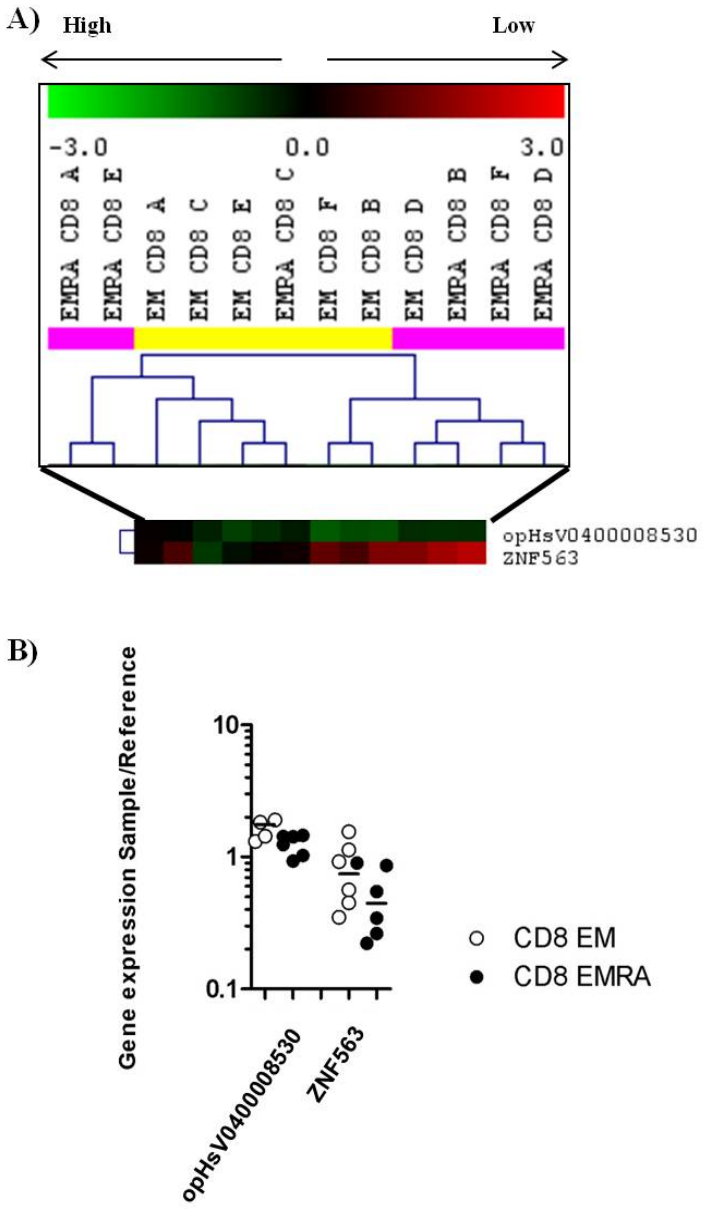

Figure 3.21. Comparing EM and EMRA T cell populations from the CD8$^+$ T cell compartment. A) HCL using the gene list generated by SAM, showing the clustering of the samples. **B)** Graph showing the fold difference in gene expression for the two genes significantly different between EM CD8$^+$ T cells and EMRA CD8$^+$ T cells. Both genes are more than 1 fold upregulated in EM CD8$^+$ T cells as opposed to EMRA CD8$^+$ T cells.

3.2.6 Comparing between $CD4^+$ and $CD8^+$ differentiation states

To identify the genes significantly differently expressed between $CD4^+$ naive and $CD8^+$ naive T cell populations, a paired SAM was executed. The $CD4^+$ naive and $CD8^+$ naive population from one donor were paired together in the analysis, to address any donor variability that may have been present. The paired SAM resulted in a list of 52 genes, with a FDR of 1% (Supplemental Table 12). The HCL in Fig. 3.22A shows that using these 52 genes results in perfect clustering of these two T cell populations, which is also shown in the PCA in Fig. 3.22B. The graph in Fig. 3.23A shows the 10 genes with the highest fold difference in the naive $CD4^+$ T cell populations compared to the $CD8^+$ naive T cell populations. CD4 was the gene with the highest fold difference (11.4) in $CD4^+$ naive cells compared to $CD8^+$ naive cells and the gene TSPAN18 (Tetraspanin-18) was upregulated 4.6 times. The graph in Fig. 3.23B shows the five genes with the highest fold difference in the naive $CD8^+$ T cell populations compared to the $CD4^+$ naive T cell populations. CD8β and CD8α were among these five genes with the highest fold difference in $CD8^+$ naive cells compared to $CD4^+$ naive cells as was KLRC4 (NKG2-D type II integral membrane protein or CD314), which is normally expressed on NK cells.

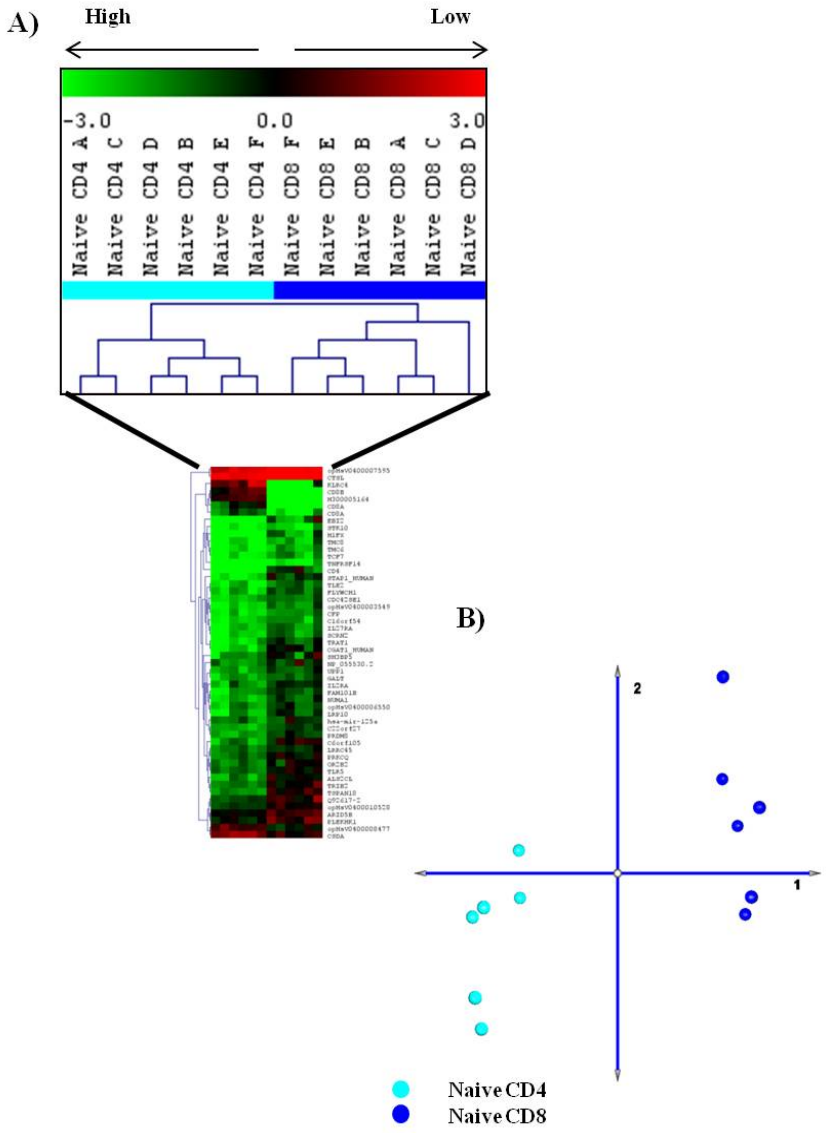

Figure 3.22. Comparing Naive CD4$^+$ and Naive CD8$^+$ T cell populations. A) HCL using the gene list generated by SAM, showing the clustering of the samples. **B)** PCA visualising the clustering of the samples.

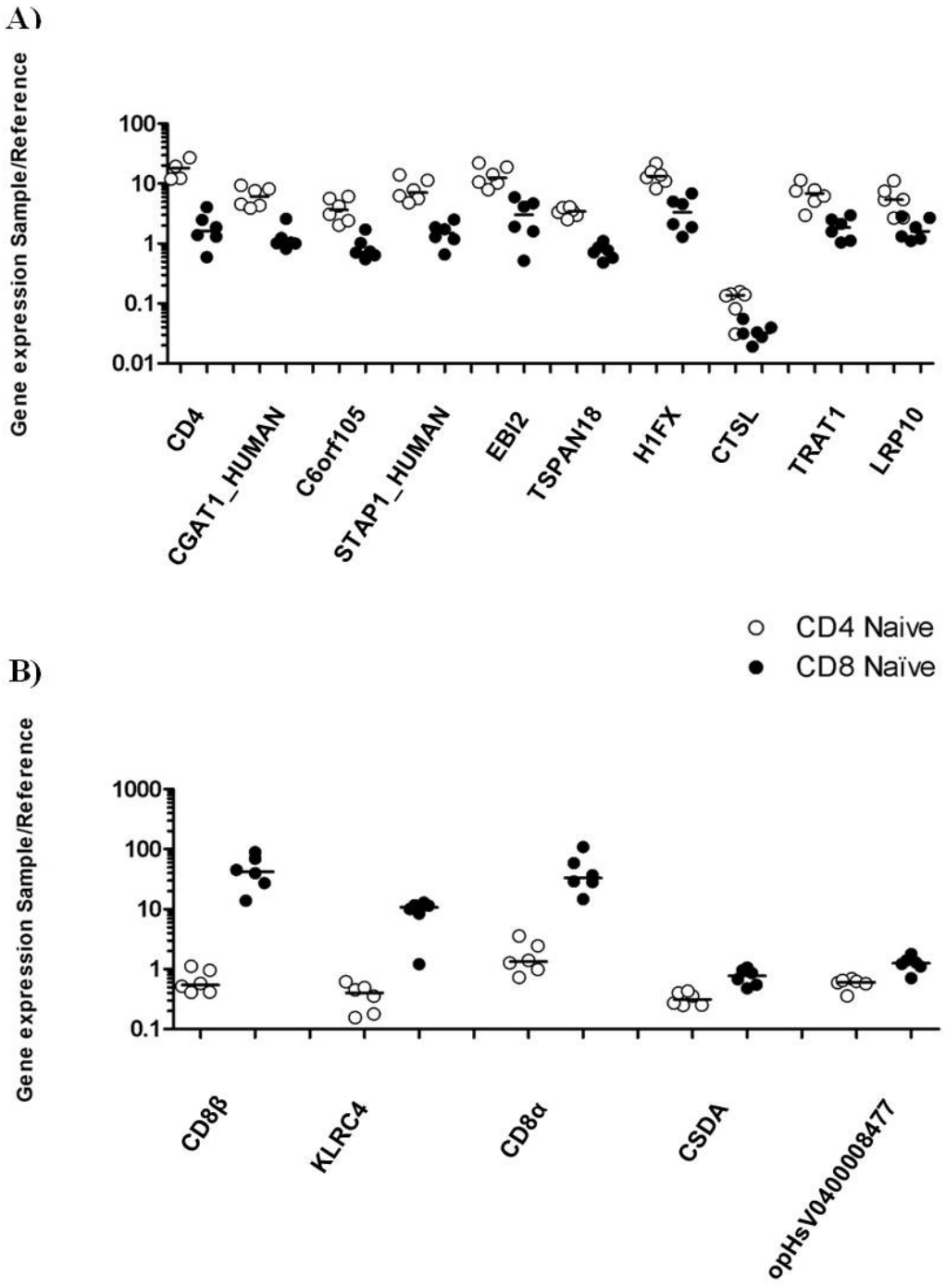

Figure 3.23. Genes with the highest fold difference from the gene list generated when comparing $CD4^+$ naive and $CD8^+$ naive T cell populations. The graphs show the expression levels for each donor for that gene on a log scale, with the bar indicating the median expression level**. A)** The ten genes with the highest expression level (≥ 2 fold) in $CD4^+$ naive T cells compared to $CD8^+$ naive T cells. **B)** Five genes with the highest expression level (≥ 2 fold) in $CD8^+$ naive cells compared to $CD4^+$ naive cells.

The paired SAM comparing $CD4^+$ CM and $CD8^+$ CM T cell populations resulted in a list of 735 genes, with a FDR of less than 1% (Supplemental Table 13). The HCL in Fig. 3.24A shows the resulting clustering of the samples based on these 735 genes. All samples were correctly classified; however one $CD8^+$ CM sample branched off of the separate arm for the $CD4^+$ CM samples. The PCA in Fig. 3.24B shows the separate clustering of the two groups and the one stray $CD8^+$ CM sample in between the $CD4^+$ CM samples. All 735 genes found in this analysis were upregulated more than 1.5 fold in $CD4^+$ CM populations compared to $CD8^+$ CM populations. The graph in Fig. 3.25 shows the 10 genes with the highest fold difference. CD4 was the gene with the highest fold difference (12.8) in $CD4^+$ CM cells compared to $CD8^+$ CM cells. TSPAN18 again was more highly expressed in the $CD4^+$ cells than in the $CD8^+$ cells (fold difference of 6.4), however since the 10 genes with the highest fold difference were all more than eight fold higher TSPAN18 is not represented in Fig. 25 (see Supplemental Table 13).

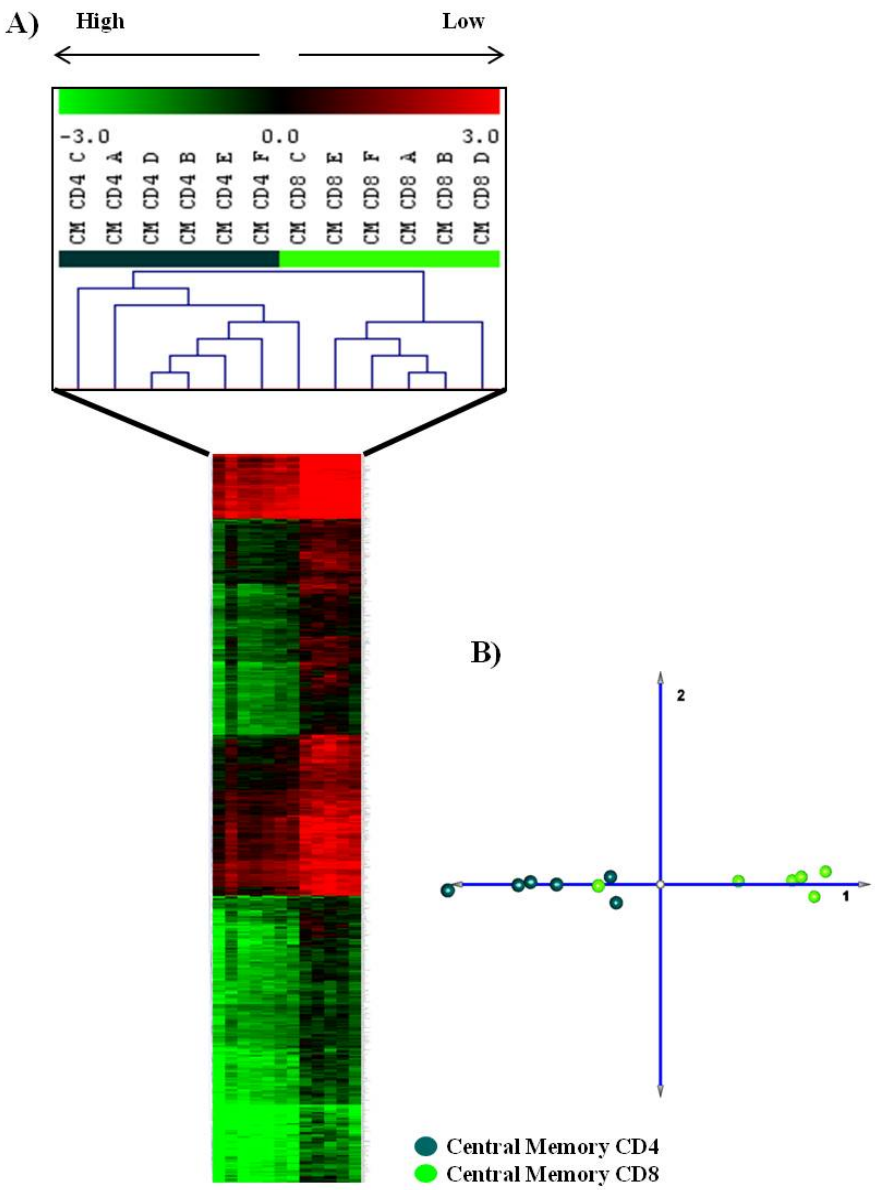

Figure 3.24. Comparing CM CD4$^+$ and CM CD8$^+$ T cell populations. A) HCL using the gene list generated by SAM, showing the clustering of the samples. **B)** PCA visualising the clustering of the samples.

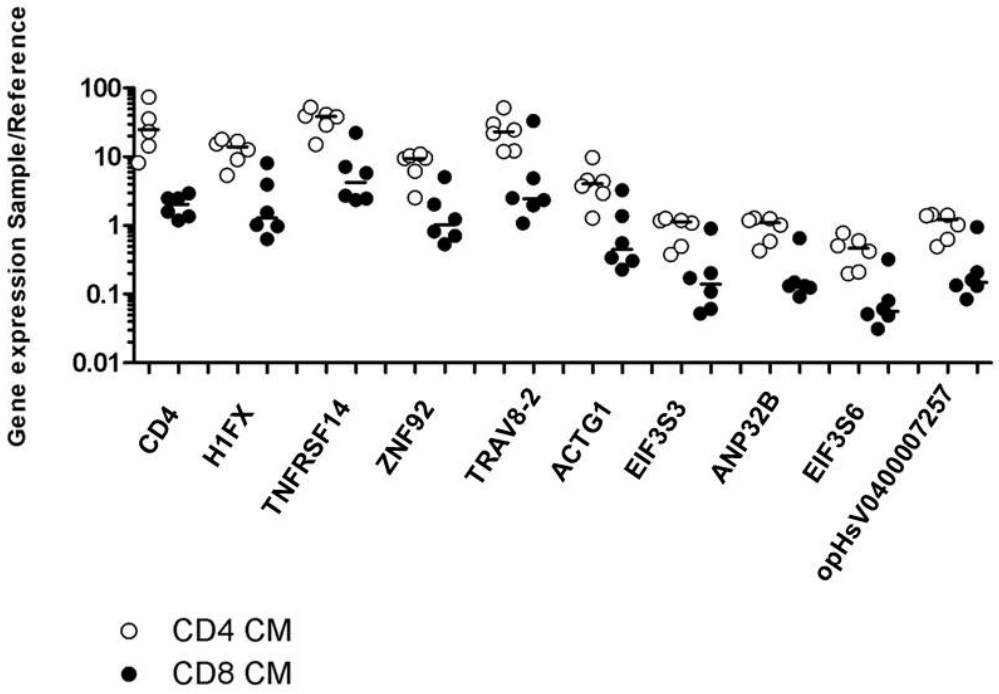

Figure 3.25. Genes with the highest fold difference from the gene list generated when comparing $CD4^+$ CM and $CD8^+$ CM T cell populations. The graphs show the expression levels for each donor for that gene on a log scale, with the bar indicating the median expression level. All 724 significant genes were found to be more than 1.5 fold upregulated in CM $CD4^+$ T cells than in CM $CD8^+$ T cells. This graph shows the 10 genes with the biggest fold difference (>2 fold).

Comparing the $CD4^+$ EM and $CD8^+$ EM T cell populations resulted in a list of 72 genes, with a FDR of less than 1% (Supplemental Table 14). The HCL in Fig. 3.26A shows the resulting clustering of the samples based on this gene list, all samples were correctly classified. The PCA in Fig. 3.26B shows the separation of the $CD4^+$ EM samples away from the $CD8^+$ EM samples. The graph in Fig. 3.27A shows the 10 genes with the highest fold difference in the CD4 EM populations. MAL (Myelin and lymphocyte protein or T-lymphocyte maturation-associated protein) was the gene with the highest fold difference (17.4) in $CD4^+$ EM cells compared to $CD8^+$ EM cells, CD4, IL-7R and IL-2RA followed and TSPAN18 was expressed higher (6.5 times) in $CD4^+$ EM than $CD8^+$ EM. The graph in Fig. 27B shows the

10 genes with the highest fold difference in the $CD8^+$ EM populations. CD8β was the gene with the highest fold difference (26.1) in $CD8^+$ EM compared to $CD4^+$ EM T cells.

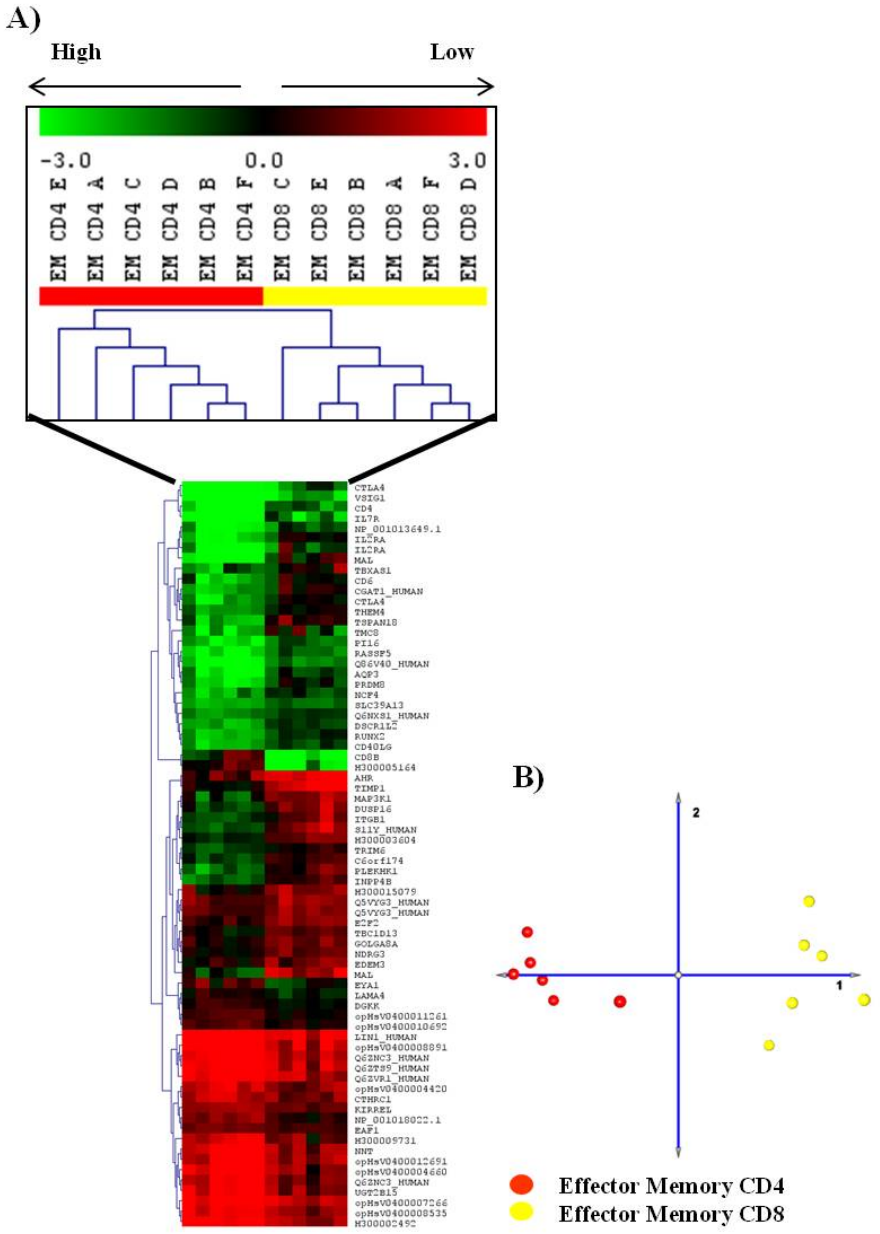

Figure 3.26. Comparing EM $CD4^+$ and EM $CD8^+$ T cell populations. A) HCL using the gene list generated by SAM, showing the clustering of the samples. **B)** PCA visualising the clustering of the samples.

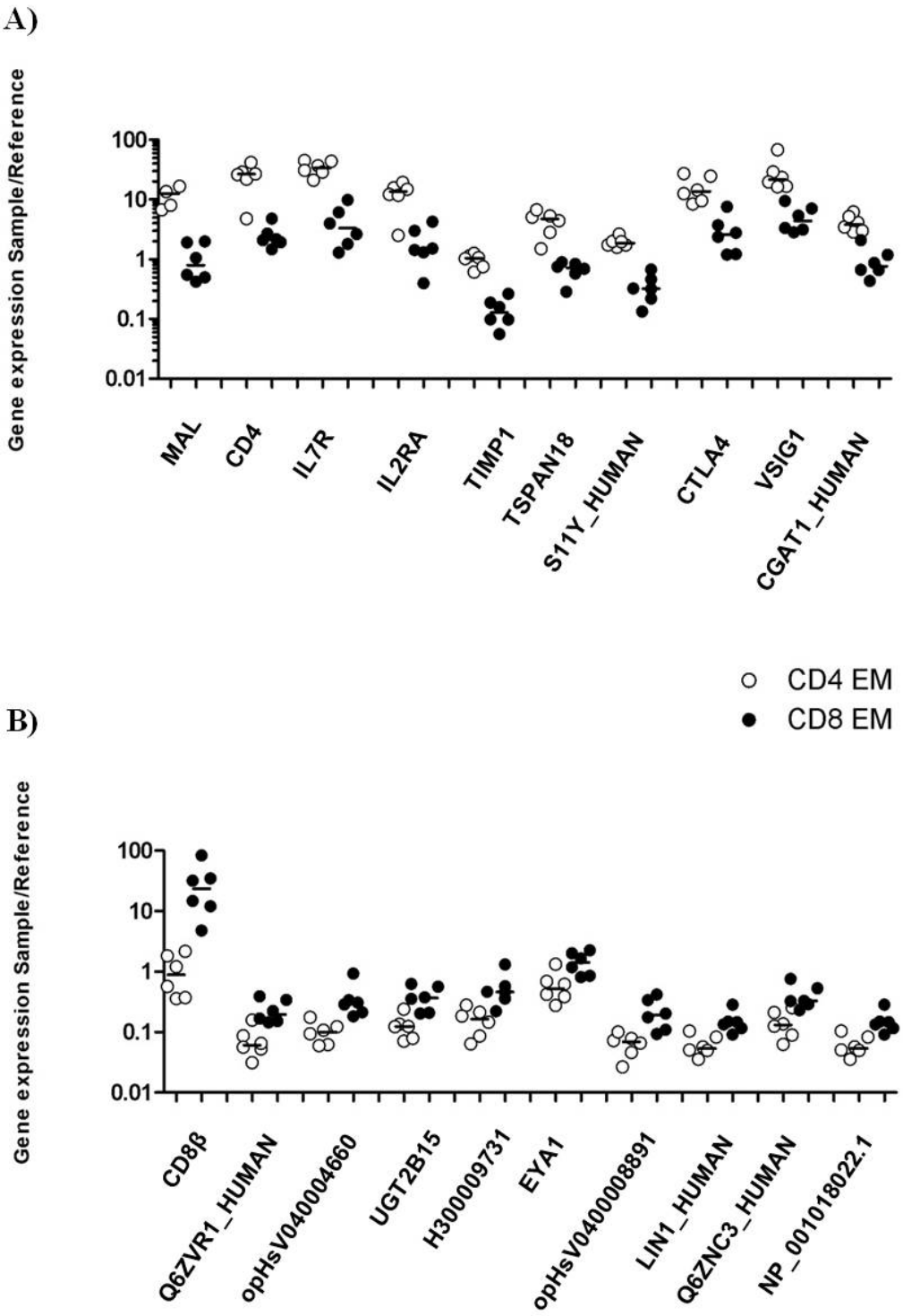

Figure 3.27. Genes with the highest fold difference from the gene list generated when comparing $CD4^+$ EM and $CD8^+$ EM T cell populations. The graphs show the expression levels for each donor for that gene on a log scale, with the bar indicating the median expression level. **A)** The ten genes with the highest expression level (≥ 2 fold) in $CD4^+$ EM T cells compared to $CD8^+$ EM T cells. **B)** Ten genes with the highest expression level (≥ 2 fold) in $CD8^+$ EM cells compared to $CD4^+$ EM cells.

3.2.7 Shared and unique genes in $CD4^+$ and $CD8^+$ differentiation pathways

To identify genes which were consistently different between $CD4^+$ and $CD8^+$ T cell populations the SAM lists generated when comparing $CD4^+$ T cell populations to $CD8^+$ T cell populations were compared, resulting in the identification of two genes consistently able to distinguish whether a cell was a $CD4^+$ or a $CD8^+$ T cell. These two genes were CD4 and TSPAN18 and their expression was higher in $CD4^+$ cells than in $CD8^+$ T cells. Tables 1, 2 and 3 show the genes which are shared between the three gene lists generated by the three possible comparisons when comparing the differentiation states between compartments ($CD4^+$ naive - $CD8^+$ naive, $CD4^+$ CM - $CD8^+$ CM and $CD4^+$ EM - $CD8^+$EM, represented in Fig. 3.28). Table 1 shows the genes shared between the comparisons $CD4^+$ naive/$CD8^+$ naive and $CD4^+$ CM/$CD8^+$ CM and that these shared genes are all upregulated in the $CD4^+$ populations. This indicates that either these genes are not expressed in $CD8^+$ T cell populations or just not as high as they are expressed in $CD4^+$ T cells. The fold difference CD4/CD8 is bigger in the CM comparison for 18 (out of 21) genes, indicating that there is a bigger difference in expression levels for these genes between the $CD4^+$ CM and $CD8^+$ CM populations.

A)

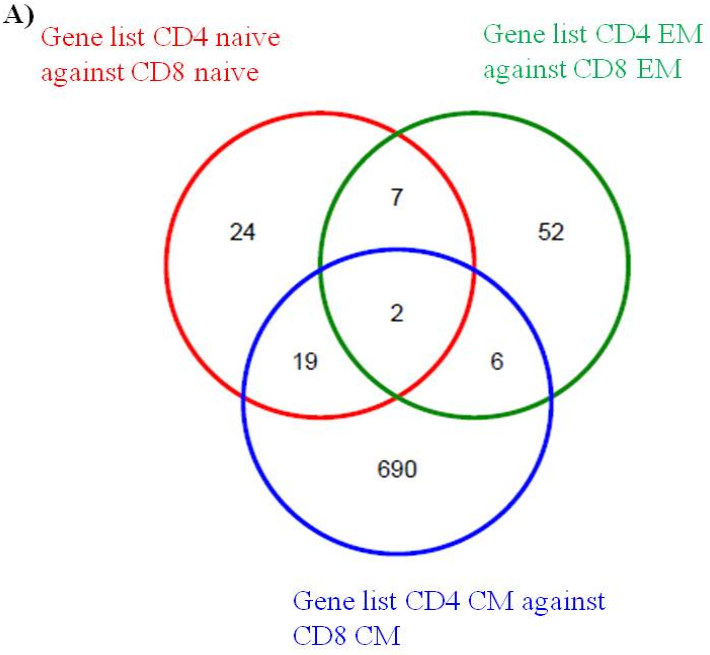

B)

Gene	CD4N/ CD8N	CD4CM/ CD8CM	CD4EM/ CD8EM	Description
CD4	11.37	12.82	12.44	T-cell surface glycoprotein CD4.
TSPAN18	4.64	6.25	6.54	Tetraspanin-18 (Tspan-18).

Figure 3.28. Unique and shared genes can be found when comparing the three differentiation states between the $CD4^+$ and $CD8^+$ compartments. The gene lists were generated by paired SAM analysis and subsequently analysed for any unique and shared genes. **A)** Venn diagram showing the shared and unique genes when comparing $CD4^+$ differentiation against $CD8^+$ differentiation. **B)** The two genes which are shared between all three comparisons, fold differences in each comparison and description of the genes are shown.

Gene Name	CD4N/ CD8N	CD4CM/ CD8CM	Description
C6orf105	4.94	2.73	Uncharacterized protein C6orf105.
CD4	11.37	12.82	T-cell surface glycoprotein CD4.
CDC42SE1	1.92	2.67	CDC42 small effector 1.
CFP	2.03	3.44	Properdin precursor (Factor P).
CTSL	4.26	2.99	Cathepsin L precursor.
EBI2	4.67	5.37	EBV-induced G-protein coupled receptor 2.
FAM101B	1.99	2.12	Protein FAM101B.
FLYWCH1	3.02	4.05	FLYWCH-type zinc finger 1 isoform a
H1FX	4.62	11.29	Histone H1x.
IL27RA	2.38	2.65	Interleukin-27 receptor subunit alpha.
LRP10	3.48	3.66	Low-density lipoprotein receptor-related protein 10.
NUMA1	2.52	4.44	Nuclear mitotic apparatus protein 1.
opHsV0400007595	1.74	2.10	Hypothetical gene supported by AK024248.
SH3BP5	2.70	5.15	SH3 domain-binding protein 5.
STAP1_HUMAN	4.73	4.24	Signal-transducing adaptor protein 1.
STK10	1.66	3.97	Serine/threonine-protein kinase 10, Lymphocyte-oriented kinase.
TMC6	2.74	3.04	Transmembrane channel-like protein 6.
TNFRSF14	2.83	10.44	Tumor necrosis factor receptor superfamily member 14.
TRIB2	2.90	6.17	Tribbles homolog 2 (TRB-2).
TSPAN18	4.64	6.25	Tetraspanin-18 (Tspan-18).
UPP1	1.62	2.57	Uridine phosphorylase 1.

Table 1. Genes shared between the comparisons $CD4^+$ naive versus $CD8^+$ naive and $CD4^+$ CM versus $CD8^+$ CM. These 21 genes are shared between the two comparisons made between the $CD4^+$ and $CD8^+$ differentiation states, fold differences in each comparison and description of the genes are shown.

Eight genes were shared between the comparisons $CD4^+$ naive/$CD8^+$ naive and $CD4^+$ EM/$CD8^+$ EM of these eight genes, one gene (CD8β) was expressed higher in $CD8^+$ T cells than in $CD4^+$ T cells (Table 2). Five genes (CD4, IL2RA, PLEKHK1, PRDM8 and TSPAN18) showed a bigger differential expression in $CD4^+$ EM/$CD8^+$ EM than in $CD4^+$ naive/$CD8^+$ naive. This indicates that the expression levels of these genes go up during $CD4^+$ T cell differentiation, but stay downregulated in $CD8^+$ T cells.

Another eight genes were shared between the SAM lists from comparisons $CD4^+$ CM/$CD8^+$ CM and $CD4^+$ EM/$CD8^+$ EM (Table 3), all of which were upregulated in the $CD4^+$ T cells. Six genes showed a higher differential gene expression in the gene list from the comparison $CD4^+$ EM/$CD8^+$ EM than in the comparison $CD4^+$ CM/$CD8^+$ CM. Of those six genes MAL and TIMP1 showed the highest difference, indicating that although both these genes are upregulated in the $CD4^+$ T cells when comparing to $CD8^+$ T cell populations their expression is also higher in EM $CD4^+$ T cells compared to CM $CD4^+$ T cells.

Gene Name	CD4N/ CD8N	CD4EM/ CD8EM	Description
CD4	11.37	12.44	T-cell surface glycoprotein CD4 precursor.
CD8B	0.01	0.04	T-cell surface glycoprotein CD8 beta chain.
CGAT1_HUMAN	5.55	4.99	Chondroitin beta-1,4-N-acetylgalactosaminyltransferase 1.
IL2RA	2.85	9.17	Interleukin-2 receptor alpha chain, CD25 antigen.
PLEKHK1	2.64	4.18	pleckstrin homology domain containing, family K member 1
PRDM8	2.06	4.52	PR domain zinc finger protein 8 (PR domain-containing protein 8).
TMC8	3.38	3.03	Transmembrane channel-like protein 8.
TSPAN18	4.64	6.54	Tetraspanin-18 (Tspan-18).

Table 2. Genes shared between the comparisons $CD4^+$ naive versus $CD8^+$ naive and $CD4^+$ EM versus $CD8^+$ EM. These eight genes are shared between the two comparisons made between the $CD4^+$ and $CD8^+$ differentiation states, fold differences in each comparison and description of the genes are shown.

Gene Name	CD4CM/ CD8CM	CD4EM/ CD8EM	Description
CD4	12.82	12.44	T-cell surface glycoprotein CD4 precursor.
CD6	3.73	3.83	T-cell differentiation antigen CD6.
H300003604	2.54	3.40	S100 CALCIUM BINDING-95.
MAL	7.19	17.36	Myelin and lymphocyte protein, T-lymphocyte maturation-associated protein.
Q86V40_HUMAN	4.96	2.94	Chromosome 2 open reading frame 89 (C2orf89), XM_059341.
S11Y_HUMAN	5.33	5.75	Putative S100 calcium-binding protein.
TIMP1	3.59	8.59	Metalloproteinase inhibitor 1.
TSPAN18	6.25	6.54	Tetraspanin-18 (Tspan-18).

Table 3. Genes shared between the comparisons $CD4^+$ CM versus $CD8^+$ CM and $CD4^+$ EM versus $CD8^+$ EM. These eight genes are shared between the two comparisons made between the $CD4^+$ and $CD8^+$ differentiation states, fold differences in each comparison and description of the genes are shown.

To identify genes shared during the differentiation of both $CD4^+$ and $CD8^+$ T cells, the SAM lists generated by comparing the differentiation states in either $CD4^+$ (three differentiation states) or $CD8^+$ (four differentiation states) were compared and seven conserved genes were found (Fig. 3.29 and 3.30). These seven genes are shared in both the $CD4^+$ and $CD8^+$ compartment when trying to distinguish between differentiation states. All seven genes showed highest expression in the naive populations and lowest expression in the EM populations (Fig. 3.30).

A)

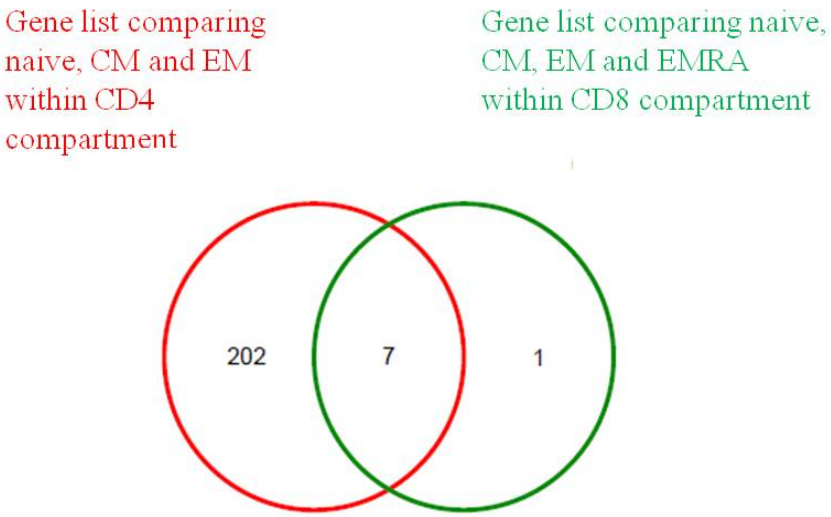

B)

Gene	Description
ADD2	Beta-adducin, Erythrocyte adducin subunit beta.
CCR7	C-C chemokine receptor type 7, CD197 antigen.
CFP	Properdin precursor, Factor P.
LRRN3	Leucine-rich repeat neuronal protein 3.
MAL	Myelin and lymphocyte protein, T-lymphocyte maturation-associated protein.
SEC14L2	SEC14-like protein 2.
SG223_HUMAN	Tyrosine-protein kinase SgK223.

Figure 3.29. Seven conserved genes can be found when comparing the gene lists generated to find the biggest difference between the differentiation states within the CD4$^+$ and CD8$^+$ compartments. The gene lists were generated by multiclass SAM analysis (three classes within CD4$^+$ compartment and four within the CD8$^+$ compartment) and subsequently analysed for any shared genes. **A)** Venn diagram showing the genes shared during CD4$^+$ and CD8$^+$ differentiation. **B)** Table showing the seven shared genes and their description.

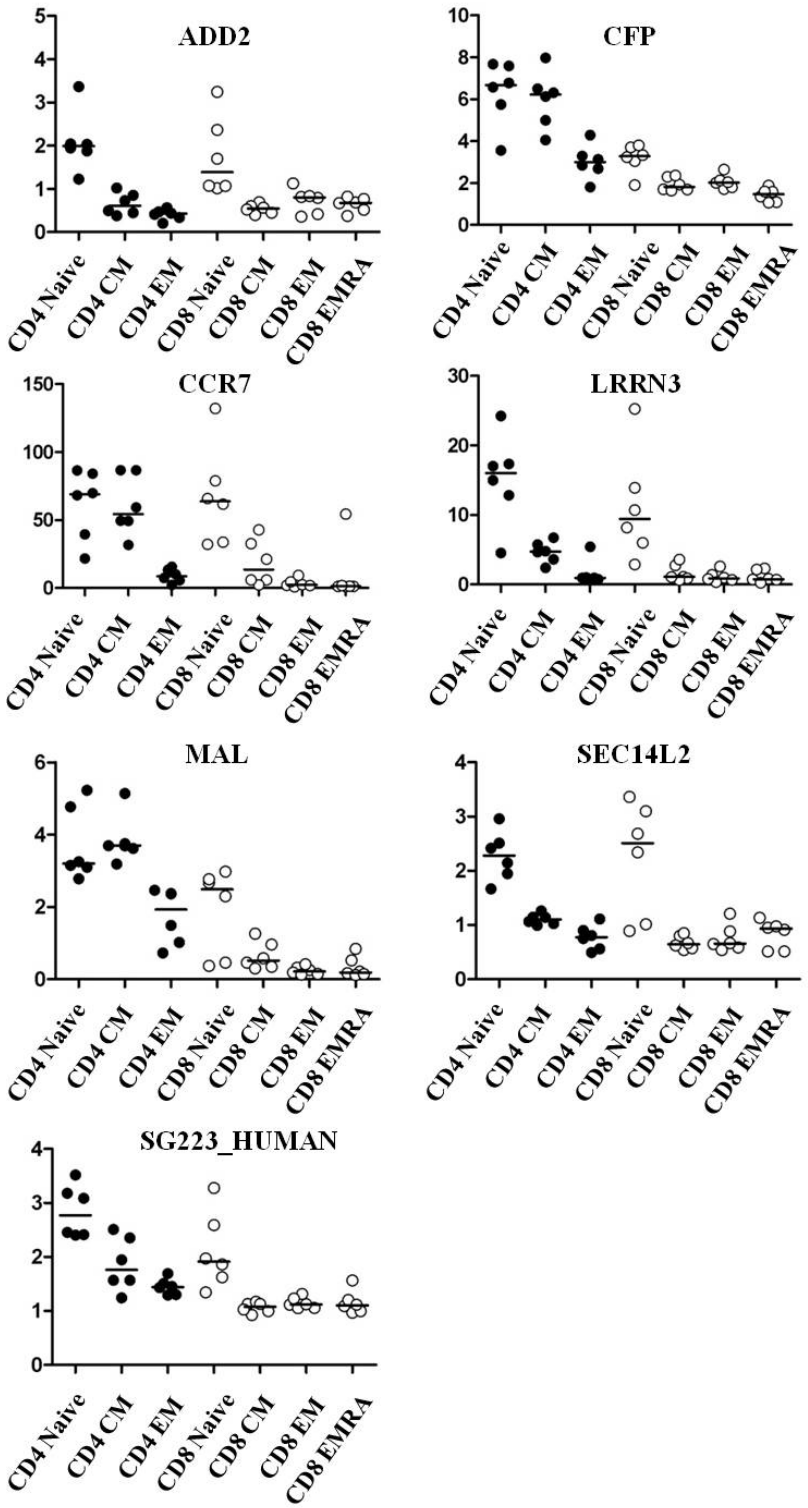

Figure 3.30. Seven conserved genes can be found when comparing the gene lists generated to find the biggest difference between the differentiation states within the $CD4^+$ and $CD8^+$ compartments. The gene lists were generated by SAM analysis and subsequently analysed for any shared genes.

3.3 Discussion.

T cell populations have been described using cell surface markers as well as intracellular markers (transcription factors) and the ability of the cells to produce cytokines [43;57;58;114]. Cell surface markers, such as CCR7, CD62L and CD45RA/RO, have been used to describe memory populations in both $CD4^+$ and $CD8^+$ T cells, however it is likely that within these seemingly homogenous populations there is a variety of cell types which have not been described yet [115]. Microarray analysis can be used to identify genes (and genetic profiles) which differ between T cell populations, but have not yet been described as having a role in T cell biology. Several studies have shown that microarray analysis is a useful strategy to utilise when trying to identify differences between cell populations sorted based on expression of surface markers [108;111;116-118]. The aim of the experiments in this chapter was to describe genes which are significantly different in their expression between the T cell populations based on CCR7 and CD45RA within the $CD4^+$ and $CD8^+$ compartments as well as genes which are shared in the differentiation process in both the $CD4^+$ and $CD8^+$ T cell compartments.

It is noticeable when analysing the various SAM gene lists generated in the different comparisons, that the number of differentially expressed genes in the $CD8^+$ compartment is lower than in the $CD4^+$ compartment. This might indicate that the four differentiation states within the $CD8^+$ compartment are very similar in their function. The lower amount of differentially expressed genes corresponds to the fact that in the literature $CD4^+$ T cells can be subdivided into many T helper subsets, whereas this has not been the case for the $CD8^+$ compartment. The variety of T helper populations within the memory populations of the $CD4^+$ compartment may result in many more differentially expressed genes within the $CD4^+$ compartment compared to the $CD8^+$ compartment. When going through the gene lists

generated it is noticeable that none of the $CD4^+$ T helper cell associated genes, such as T-bet and GATA-3 can be identified on the gene lists. This is also true for the typically Th1 or Th2 associated cytokines, such as IFNγ and IL-4, show up on the lists. This indicates that these cells are either present at too low a frequency or that these gene products are only expressed at relatively low levels. The genes which the array analysis has identified are therefore more likely to be genes shared by all $CD4^+$ T cell populations.

Microarray analysis identified several genes which are unique to the differentiation process within the $CD4^+$ or $CD8^+$ compartments as well as genes which are shared between the two compartments. The Venn diagram in Fig. 3.29 shows that there are seven genes which are shared between the gene lists generated when comparing the three differentiation states (naive, central memory and effector memory) between $CD4^+$ and $CD8^+$. These seven genes are involved in the differentiation process in both $CD4^+$ and $CD8^+$ T cells, CCR7 and LRRN3 are two genes from this list, which show differential expression levels as the cells differentiate (Fig. 3.30). Two genes (CD4 and TSPAN18) are shared between the lists generated when comparing the differentiation states from the CD4 compartment to those of the CD8 compartment (Fig. 3.28). This indicates that at least in our arrays the expression of these two genes is sufficient in determining whether a sample is from the $CD4^+$ T cell compartment or from $CD8^+$ T cell compartment.

Many of the genes identified in our gene lists have already been described in T cell biology, such as CD4, CD8, CCR7 and granzymes which supports the validity of finding other genes which have not yet been implicated in T cell biology.

CC-chemokine receptor 7 (CCR7) has been used to describe several T cell populations in combination with the surface marker CD45RA [114]. CCL19 and CCL21 are the only two ligands for this chemokine receptor and lymph nodes reticular fibroblasts in the T cell area produce CCL21 which then allows circulating naive and CM T cells entry into the LNs [119]. Whereas both naive and CM T cells express CCR7 and therefore can recirculate through peripheral lymphnodes, CCR7 expression is lost on the EM population [114]. As shown in figure 3.30, our results correspond with the literature, in that CCR7 expression from both $CD4^+$ and $CD8^+$ naive and CM T cells is higher than that found in the EM or EMRA populations.

L-selectin (SELL or CD62L) was among the 10 most differentially expressed genes between the $CD4^+$ CM and EM populations, with the highest expression found in the $CD4^+$ CM population. This corresponds with the described function of L-selectin as being expressed on the surface of both naive and CM populations for both the $CD4^+$ and the $CD8^+$ compartments. L-selectin allows these cells entry into LNs, by binding to its ligands, such as peripheral node addressins (PNAds) present on the surface of high endothelial venules within the LNs [120 121].

CCR6 is a chemokine receptor and its ligand is CCL20, CCR6 expression has an important role in mucosal immunity [122]. In our arrays CCR6 (or FGFR10P) is more highly expressed in both the $CD4^+$ CM and EM populations compared to the $CD4^+$ naive population. CCR6 and CCL20 are important in intestinal immunity. CCR6-mediated signals help to organize

lymphoid tissues such as Peyer's patches (PPs), mesenteric lymph nodes (MLNs) and gutassociated lymphoid tissue (GALT) by recruiting both lymphoid and myeloid cells. Expression of CCR6 has been described on both Th17 and Treg cells and this could correspond to the higher expression of CCR6 found in our arrays in the more differentiated cells.

TNFRSF14 (or Herpesvirus entry mediator, HVEM) belongs to a group of molecules involved in costimulation as well as inhibition of T cell responses. These proteins span the plasma membrane and their ligands are type II transmembrane proteins with intracellular N terminus domains [123]. OX-40 (CD134) and CD27 are both known members of the TNFRSF family and both are known to function as costimulatory molecules on T cells during T cell activation [123]. HVEM, however, can inhibit T cell activation by binding to coinhibitory receptors, such as B andT-lymphocyte attenuator (BTLA) or CD160 as well as as costimulate T cells by functioning as a receptor for LIGHT (homologous to LTs, exhibits inducible expression, and competes with HSV gD for herpesvirus entry mediator, a receptor expressed by T lymphocytes or TNSF14). Expression of TNFRSF14 was found to be more highly expressed on the $CD4^+$ CM population compared to its $CD8^+$ counterpart. Most T cells express TNFRSF14 on their cell surface and recently it has been shown that knocking out TNFRSF14 in a mouse model leads to a reduction in the amount of Th2 memory cells [124].

As described above CTLA-4 and CD28 are structurally related receptors present on the cell surface of T cells. Both receptors can bind to CD80 and CD86, but ligation of CTLA-4 leads to an inhibitory signal limiting T cell activation, whereas CD28 signalling functions as a costimulatory signal [51] [52].Furthermore, whereas CD28 expression on T cells is constitutive, CTLA-4 expression is induced by T cell stimulation via the TCR. CTLA-4 expression was

found to be higher in the $CD4^+$ EM population, when compared to the $CD8^+$ EM population. This higher expression could be due to the presence of Tregs within the $CD4^+$ compartment, with Tregs constitutively expressing CTLA-4.

Myelin and lymphocyte protein (MAL) was cloned from both human T cells as well as from cells in the nervous system, such as myelinating cells and oligodendrytes [125]. MAL was identified in our arrays as a differentially expressed gene within the CD8 compartment, comparing $CD8^+$ naive cells with $CD8^+$ EM cells, with expression being higher in the naive cells. It was also found to have higher expression in $CD4^+$ CM and EM T cells compared to their $CD8^+$ counterparts. MAL is a transmembrane protein and has been described to be a component of detergent insoluble complexes in myelinating and epithelial cells as well as in T cells [125]. In 2008 Antón *et al* showed that MAL was required for efficient Lck expression on the cell surface of T cells [126]. The MAL protein contains a MAL and related proteins for vesicle trafficking and membrane link (MARVEL) domain, which is present in proteins that are involved in membrane localisation events. Antón *et al* showed that Lck is transported to the plasma membrane of T cells in MAL expressing vesicles. When they used a Jurkat TCR-signalling impaired mutant, which did not express any MAL mRNA, they found that these cells also did not express any MAL protein. The mutant Jurkat cells were found to be unable to transport the TCR, ZAP-70 as well as LAT into the immunological synapse (IS). This same phenotype was found when MAL expression was knocked down in both wild type Jurkat cells as well as primary T cells by using MAL specific siRNA. Lck expression at the plasma membrane was found to be significantly lower in the mutant Jurkat cells, as well as in wild type Jurkat cells and primary cells treated with MAL specific siRNA. Expression of Lck was found to be concentrated at a specific intracellular location within the MAL deficient cells. Antón *et al* showed that MAL expression in T cells is needed for a specific Lck

transport pathway, required for Lck expression at the plasma membrane. A more recent paper from Antón *et al* (2011) describes a role for MAL in delivering proteins to the central supramolecular activation cluster (cSMAC), which forms on the T cell surface within the IS [127]. These data indicate an important role for MAL in T cell function and as figure 3.30 shows, MAL expression was found to be highest in the less differentiated cells from both $CD4^+$ and $CD8^+$ T cell compartments. The overall expression of MAL seems to be higher within the $CD4^+$ compartment, which could possibly correlate with the fact that the CD4 molecule is able to bind more Lck than the CD8 molecule.

The genes for perforin (PRF) and granzymes A and H (GZMA/H) were found to be more highly expressed in $CD4^+$ EM, when compared to $CD4^+$ CM T cells. This finding corresponds to the literature where it has been described that cytotoxic T cells express high levels of these proteins within their secretory granules [128]. When granzymes are synthesised they are inactive zymogens, when cleaved they become enzymatically active. Within the secretory granules the granzymes are in an acidic environment, but when released into the cytosol which has a pH of around 7, they become maximally active, since their pH optimum is at 7.5 [129]. Granzyme A can aid in T cell motility by cleaving several extracellular matrix proteins [128]. In total five human granzymes have been described (A, B, H, K and M), of which GZM A and GZM B are the most abundant [129]. Delivery of granzymes to the target cells is reliant on perforin created pores [130] [131]. Perforin itself is a calcium dependent pore forming protein of 67 kDa and it is present together with granzymes within the secrotory granules. There are two possible pathways described for how perforin aids granzyme delivery to the cytosol of the target cells. The first possibility is that the granules are secreted into the IS, where perforin forms a pore through the plasma membrane, allowing entry of the granzymes. The second possibility is that when the granules are secreted into the IS, they are

subsequently endocytosed by the target cell, after which perforin will form pores through the membrane of the granule into the cytosol of the target cell [131].

Tetraspanin18, which was found to be significantly more highly expressed in $CD4^+$ T cells, compared to $CD8^+$ T cells is a gene identified by our arrays which currently has no known function in T cell biology. A second gene which currently has not been implicated in T cell biology was LRRN3, which was found to mimic the expression of CCR7 in that it is highly expressed in naive T cells, drops in central memory T cells and is lowest in effector memory T cells. For both these genes there is no literature as to what their function might be in T cell biology. The family of tetraspanins has been implicated in organising the cell membrane resulting in coordinating signalling pathways and several groups have reported a role for tetraspanin microdomains in MHC-II clustering on APCs [73;82;132;133]. Unternaehrer *et al* (2007) described that CD9 on mouse DCs is involved in the multimerisation of MHC-II molecules on the cell surface and suggested that this multimerisation could enhance the ability of DCs to engage with the T cell receptor. They found that the absence of CD9 abrogated MHC-II clustering [134]. Kropshofer *et al* (2001) used an antibody against CDw78 microdomains on human cell lines and found that tetraspanins CD9, CD81 and CD82 associate with MHC-II in these microdomains. The function of tetraspanins on the cell surface of APCs seems to enhance the signal strength from loaded MHC-II molecules, the role of tetraspanin18 on the cell surface of $CD4^+$ T cells could have a similar function, in creating tetraspanin enriched domains containing CD4, costimulatory molecules and TCRs. Since Tspan18 expression is consistently higher in $CD4^+$ T cells compared to $CD8^+$ T cells it is possible Tspan18 actually clusters with the CD4 molecule on the cell surface. Another possibility is that Tspan18 associates specifically with a molecule which is only involved in $CD4^+$ T cell function and not $CD8^+$ T cell function. If a specific antibody against Tspan18

becomes available it could be possible to test whether this holds true by doing a co-imunoprecipitation assay with Tspan18.

LRRN3 has been implicated as a candidate gene for autism [135], because of its proximity to a marker which consistently showed up in screens of chromosome 7. The region 7q22-31 is suspected of containing a gene associated with autism. However it was concluded after genotyping that there is no genomic variation in the LRRN3 gene associated with autism and thus LRRN3 is in fact unlikely to be related to autism [135]. NLRR-3, which is the mouse ortholog of LRRN3 is highly expressed in the brain of mice and is thought to be important in the development of the murine nervous system. Studies in *Drosophila* also suggest that the LRR family is involved in target recognition and cell differentiation during the development of the neuronal network [136]. Haines *et al* (2005) describe NLRR-1 as possibly being involved in myogenesis. In their paper they also examined the expression of NLRR-2 and NLRR-3 during mouse development [137]. NLRR-3 was found to be highly expressed at 10.5 dpc in the trigeminal and facio-acoustic ganglia and in the migrating germ cells in the tail. Its expression in the neural tube was restricted to the developing motorhorn, whereas NLRR-2 expression could not be found during development. In adult mice NLRR-3 was highly expressed in brain and in lower levels in lung, kidney and liver. The NLRR family are proteins which are expressed on the cell surface and could be involved in cell adhesion or signalling [137]. Since LRRN3 consistently followed the same directionality as CCR7 it is possible that LRRN3 on T cells functions as a cell surface marker which is expressed on cells which need to be able to gain entry into LNs. To determine whether LRRN3 itself functions as a receptor which allows entry into LNs, a chemotaxis assay could be set up if a suitable antibody against LRRN3 becomes available.

ADD2 (Beta-adducin) shows up on two gene lists within the CD4 compartment, in the comparison naive against CM as well as in the comparison naive against EM. In both

comparisons its expression is higher in the naive population. ADD2 is a subunit of the adducin cytoskeleton protein [138;139]. Yenerel *et al* (2005) found that during *in vitro* erythroid differentiation of human cells expression of ADD3 was higher than ADD2 expression at day 8, but by day 10 this had reversed. This data suggests that ADD3 is needed in early erythroid differentiation whereas ADD2 is needed in later stages of differentiation. In our arrays the expression of ADD2 highly expressed in the naive CD4 T cells compared to the differentiated CM and EM populations. If ADD2 has a similar role on T cells as Yeneral *et al* (2005) describe for red blood cells, it could be that during T cell maturation in the thymus a similar switch of ADD3 and ADD2 occurs, reaching highest levels of ADD2 in the naive cells which are then released into the periphery [139]

AEBP1 (adipocyte enhancer binding protein 1) and MTUS1 (mitochondrial tumor suppressor 1 isoform 3) are shared between the gene lists generated when comparing $CD4^+$ naive T cells to EM and CM to EM cells. In these comparisons, both genes were more highly expressed on naive or CM cells respectively. Ro *et al* (2007) describe a role for AEBP1 in energy homeostasis of mice [140]. Rodrigues-Ferreira *et al* (2009) describe a correlation between MTUS1 downregulation and breast cancer tumours which are highly proliferative [141].

S100A4 (S100 calcium binding protein A4) shows up in the comparisons naive versus CM and naive versus EM and in both cases the gene is expressed more highly in the more differentiated cells. Haining *et al* (2008) also identified S100A4 as a differentially expressed gene, in studies addressing a transcriptional signature of human $CD8^+$ memory cell differentiation which is shared by T and B cells [108]. S100A4 has been described to enhance the motility of cancer cells by its interaction with myosin-IIA, Haining *et al* (2008) suggest that its function on more differentiated cells could be to enhance their ability to migrate [108;142]. MYO1F (Myosin-If), also found to be upregulated in previous studies, showed the same trend as S100A4, in that it is more highly expressed in the more differentiated $CD4^+$ T

cells. Kim *et al* (2006) showed that mice deficient in Myo1f have increased adhesion and reduced mobility [143].

BHLHB2 (class B helix-loop-helix protein 2) can be found in all three gene lists generated when comparing the three differentiation states within the $CD4^+$ compartment. Spontaneous activation of T cells occurs in mice deficient in the transcription factor Stra13 (BHLHB2) and these mice go on to develop autoimmunity [108;144]. Haining *et al* (2008) suggest that increased expression of BHLHB2 in the more differentiated cells could be needed for quiescence [108]. Indeed BHLHB2 expression was found to be highest in the more differentiated $CD4^+$ EM population. Based on the results discussed in this chapter a list of 96 genes was generated to validate the array results by Real Time PCR.

Based on our data two possible models of T cell differentiation can be suggested, a linear model of T cell differentiation and a non-linear model of T cell differentiation (Fig. 3.31 and 3.32). Several models for T cell differentiation have been proposed before; Kallies (2008) suggests a pathway for $CD8^+$ T cell differentiation which is similar to the non-linear model of T cell differentiation shown in Fig. 3.31 [145]. Kalies suggests that differential expression of transcription factors and responsiveness to cytokines results in the development of distinct T cell populations. Kallies' model is based on expression levels of the cytokines IL-2 and IL-12 and transcription factors T-bet, Eomes and Blimp-1, he suggests that low levels of IL-2 and IL-12 in the environment skew naive T cells to memory precursor effector cells (MPECs), which express low levels of T-bet, Eomes and Blimp-1. The MPECs can then give rise to long lived memory cells (central memory) and long lived effector cells (effector memory). High levels of IL-2 and IL-12 will skew the naive cells towards short lived effector cells. Chang *et al* (2007) suggest that the occurrence of distinct differentiated T cells is a result of

asymmetric cell division [146]. A naive T cell is activated by an antigen presenting cell (APC) and this results in the formation of an immunological synapse containing $CD4^+$ and $CD8^+$ T cell coreceptors, adhesion molecules and cytokine receptors. The interaction between the T cell and the APC lasts for several hours and could therefore last during cell division. They suggest that the daughter cell near the immunological synapse gives rise to effector cells, whereas the cell derived from the distal end differentiates into memory cells [146]. Catron *et al* (2006) suggest yet another possibility as to how central memory cells arise. First they assessed what the dynamics of naive T cell circulation were when naive $CD4^+$ T cells specific for the I-Eα MHC-II molecule were injected into wildtype C57BL/6 recipient mice which lack this antigen. Naive cells were shown to quickly enter lymph nodes using CD62L, where they remained for a day before returning to the circulation. Their subsequent experiments identified two populations. The first is a resident population, which was not affected by blocking CD62L with an antibody, had gone through more than six cell divisions and the majority of which did not express either CD62L or CCR7. The second population, the late-arriving population, could be blocked by anti-CD62L treatment, had undergone one to six cell divisions and expressed both CD62L and CCR7 at high levels. The features of the late-arriving cell population suggest that these could be central memory cells, whereas the resident population shares the features of an effector population [147].

A)

ADD2	+++	++	+
CCR7	+++	++	+
CFP	+++	++	+
LRRN3	+++	++	+
MAL	+++	++	+
SEC14L2	+++	++	+
SG223_HUMAN	+++	++	+

B)

BACH2	+++	+	+
CD55 [3]	+++	+	+
EPHX2 [2]	+++	++	+
IL6ST [2]	+++	+	+
KRT72	++	+	+
KRT73	++	+	+
LASS6	++	+	+
L-Selectin	+++	+++	+
Tspan33	+++	++	+
CTLA4 [1]	+	++	++
GZMA	-	+	+++
GZMK	-	+	+++
IL2RA [1]	+	++	++
IL7R [1]	++	+++	+++
ITGB1 [2]	-	++	+++
KLRB1 [2]	-	++	+++
MAF [2]	-	++	+++
PRF1	+	+	++
S100A4 [2]	+	++	+++
SLAMF7	-	-	+

Figure 3.31. Linear model of T cell differentiation based on gene expression profiles. The genes shown are all on the lists generated by (paired) SAM analysis and subsequently analysed for similar expression patterns as the cells differentiate. **A)** Seven genes shared during differentiation within the $CD4^+$ and $CD8^+$ T cell compartments show a clear pattern of reduced expression in the more differentiated subpopulations. **B)** Two sets of genes showing a clear pattern of switching off or on of genes as the cells differentiate. [1] Change only seen in $CD4^+$ T cells. [2] More pronounced difference in $CD4^+$ T cells. [3] More pronounced difference in $CD8^+$ T cells.

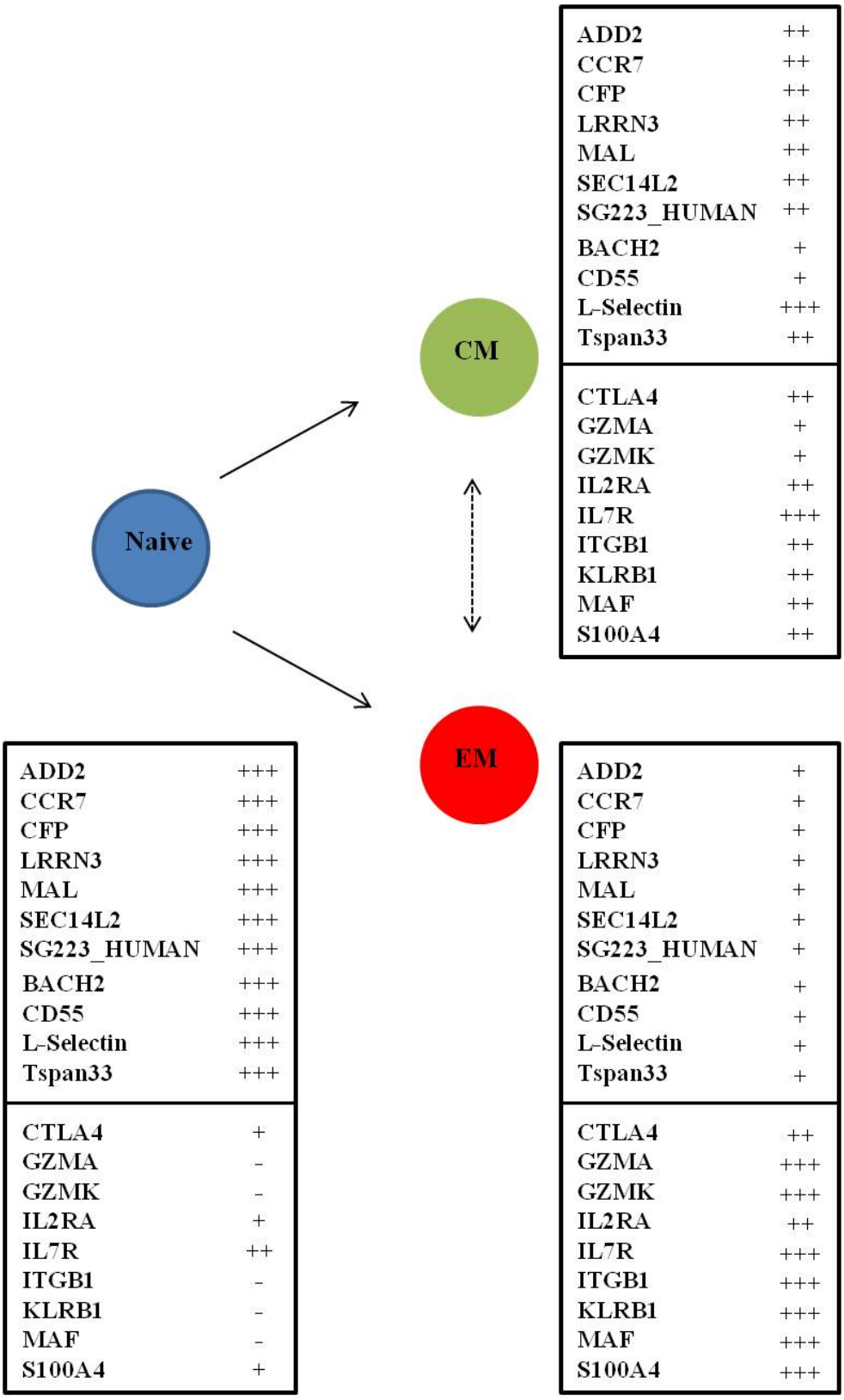

Figure 3.32. Non-linear model of T cell differentiation based on gene expression profiles. The genes shown are all on the lists generated by (paired) SAM analysis and subsequently analysed for similar expression patterns as the cells differentiate. Genes in top box show a clear pattern of reduced expression in the more differentiated subpopulations. Genes in the bottom box show a clear pattern of switching on as the cells differentiate.

The gene expression patterns described in this chapter cannot by themselves point to which of these three described theories of T cell differentiation is true for the populations analysed. It is also not necessarily the case that these three differentiation pathways are mutually exclusive of each other. What our data does suggest is that for many of the genes shared when comparing between the naive, CM and EM populations for both $CD4^+$ and $CD8^+$ T cell populations the CM population shows gene expression levels intermediate to those of the naive and the EM populations. This suggests to us that these genes could very well be important in the fine-tuning which results in the different differentiation states. Fig. 3.31 and 3.32 both show the seven genes which are shared when comparing the SAM gene lists generated through the comparisons of differentiation states in either $CD4^+$ (three differentiation states) or $CD8^+$ (four differentiation states). It is clear that these genes show the highest expression in the naive population and lowest in the EM population. This indicates that in both $CD4^+$ and $CD8^+$ T cells there are several important genes which need to be switched off or downregulated during the differentiation of a naive T cell into an EM T cell. The genes in Fig. 3.31B are selected from the SAM lists of all comparisons specifically looking for genes which show a trend. It shows that apart from those seven shared genes there are another nine genes which follow the same trend of highest expression in naive T cells and lowest in EM T cells. There are also 11 genes which follow the opposite gene expression in that their expression is highest in EM cells and lowest in the naive cells, many of which are known to be involved in effector function (such as the granzymes and perforin). Both a linear model and a non-linear model of differentiation could be supported by our data. Naive T cells could give rise to CM T cells by downregulation of some genes and upregulation of several others, after which the CM T cells could continue the downregulation and upregulation of the same genes and give rise to the EM population which would be in line with a linear pathway of differentiation. However a non-linear model of differentiation is

also supported by our gene expression patterns and incorporating the asymmetric model of differentiation we could postulate that a naive T cell can give rise to both a CM and an EM T cell. The late-arriving cell model of differentiation could also be used in conjunction with our non-linear model of differentiation, where a naive T cell encounters antigen in the lymph node and is activated to give rise to an EM cell and a subsequent naive T cell to arrive to the site of antigen presentation is stimulated to give rise to a CM T cell. Our data cannot exclude the possibility of 'inter-differentiation' where a CM cell could differentiate into an EM cell and vice versa.

Chapter Four

Validating Gene Expression Profiles of $CD4^+$ and $CD8^+$ T Cell Populations by Real Time PCR Analysis

4 VALIDATING GENE EXPRESSION PROFILES OF CD4+ AND CD8+ T CELL POPULATIONS BY REAL TIME PCR ANALYSIS

4.1 Introduction

The results from the previous chapter showed that a number of shared and unique genes could be identified when comparing $CD4^+$ and $CD8^+$ T cell populations. To validate the results from the microarray analysis a list of 96 genes was chosen from the different Significance Analysis of Microarray (SAM) lists generated by all the different comparisons. These 96 genes included two housekeeping genes, ribosomal RNA 18S and GAPDH.

Quantitative Real Time polymerase chain reaction (PCR) is a more accurate way of utilising PCR analysis to quantify the expression level of a certain gene in a sample. The addition of fluorescent probes to Real Time PCR allows accurate measurement of a fluorescent signal during the PCR reaction, hence the addition Real Time [109]. Real Time PCR has been used to validate gene expression results obtained from microarray analysis because it allows the researcher to focus on several specific genes with a more quantitative technique. Wang *et al* (2008) compared the gene expression profiles of bulk $CD4^+$ and $CD8^+$ T cells against each other as well as against the total $CD3^+$ population; gene expression between these three populations was found to be largely conserved, but not identical. They then used Real Time PCR to validate their microarray results and found that the Real Time PCR data for several selected genes corresponded with the microarray data. By comparing the log ratios of the timepoint/0 hour calculated for both the PCR data and the microarray data on an x/y-plot, the correlation between the data sets could be visualised [110]. Chtanova *et al* (2001) used microarray analysis to compare the gene expression profiles of murine $CD4^+$ Th1 and Th2

cells and $CD8^+$ type 1 and type 2 T cells. Type 1 $CD8^+$ T cells are thought to arise by exposure to IL-12, whereas type 2 $CD8^+$ T cells require IL-4. The populations analysed were shown to exhibit differential expression of cytokine, growth factor and transcription factor genes; which was validated through Real Time PCR analysis [111]. To date Real Time PCR remains the gold standard for validating microarray results [109;112].

TaqMan low density arrays (LDAs) are customisable 384-well micro fluidic cards designed to be used with the Applied Biosystems 7900HT Fast Real-Time PCR System. Each LDA can be used to perform 384 real-time PCR reactions on one to eight samples simultaneously. To validate the gene expression profiles found in Chapter 3, 96 genes were selected from the SAM lists generated in Chapter 3 and a specific LDA was created with each card containing four repeats.

The aim of the experiments in this chapter was to validate the gene expression values identified through the microarray results by analysing the gene expression values of 96 specific genes through micro fluidic Real Time PCR (Supplemental Table 1).

4.2 Results

4.2.1 Sorting $CD4^+$ and $CD8^+$ T cell populations based on CCR7 and CD45RA for gene expression analysis on microfluidic cards

$CD4^+$ and $CD8^+$ T cell populations were sorted based on expression of CCR7 and CD45RA. In the sorting protocol for the $CD4^+$ T cells monocytes were excluded by adding an antibody against CD14 (Fig. 4.1A). $CD8^+$ T cell populations were sorted based on CD8β expression which allowed the analysis of CD8αβ T cells only and excluded any NK cells which express CD8α as a homodimer on their cell surface (Fig. 4.1B). The resulting sorted populations were all more than 95% pure. Sorting gates used differed slightly from the gates used to analyse the purities of the sorts. During the sort a very tight gate was set around the population of interest, to ensure the purest populations possible; when analysing the purities a gate which was slightly bigger than the sorting gate could therefore be used.

Five healthy donors were used to sort five replicates of each population, two donors which had been analysed in the microarray experiment and three new donors. The mRNA of 100,000 cells from each population was reverse transcribed and the resulting cDNA was then used to run on a micro fluidic card. The relative quantity of signal per gene was calculated by setting thresholds within the logarithmic phase of the PCR for the control gene (18S) and the target gene. The cycle number (Ct) at which the threshold was reached was then determined. The Ct for the target gene was subtracted from the Ct for the control gene and the relative quantity was calculated as $2^{-\Delta CT}$.

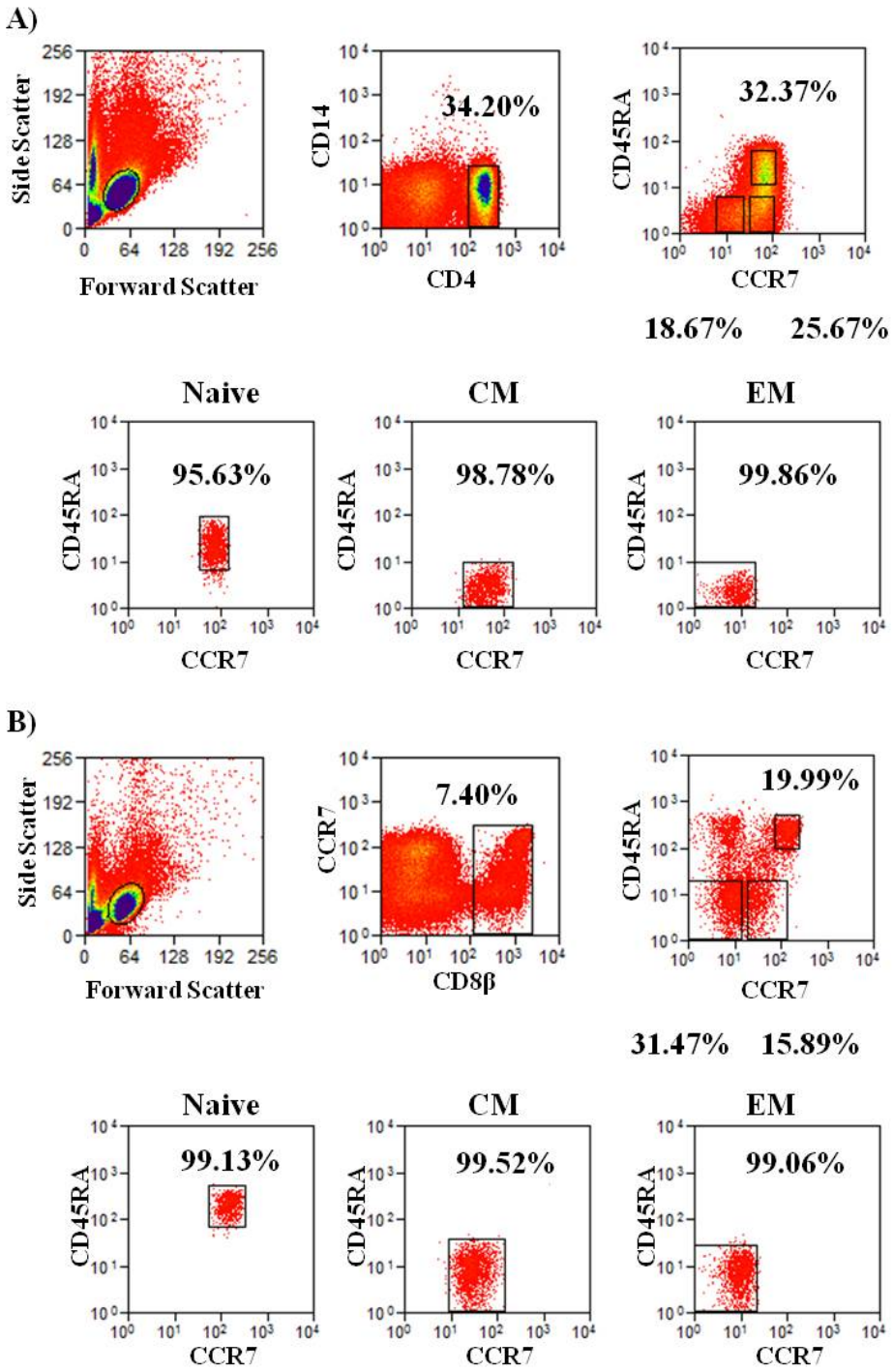

Figure 4.1. Sorting $CD4^+$ and $CD8^+$ T cell populations based on the expression CCR7 and CD45RA. The populations were sorted from five healthy donors. Representative plots show the gating strategy used during the sort and representative percentages of each population are shown. **A)** A representative sort for $CD4^+$ T cell populations is shown, representative purities for the sorted populations are also shown. **B)** A representative sort for $CD8^+$ T cell populations is shown, representative purities for the sorted populations are also shown.

4.2.2 Gene expression profiles identified through microarray correspond with the expression found through Real Time PCR analysis

To analyse the correlation between the microarray results from Chapter 3 and the micro fluidic card results, the gene expression profiles for the 96 genes selected for validation were compared. The microarray data were available as a log 2 ratio of reference/sample, whereas the Real Time PCR data was available as a relative quantity value. Since the PCR data did not have a reference sample run alongside, which would enable calculating the log 2 ratio of reference/sample for the PCR data, a different approach was used to analyse correlation between microarray results and PCR results. For each comparison made, the fold differences were calculated for both the array data and the PCR data; these were then converted to a log 2 scale, because the range of the fold differences was too high to be represented well on a linear scale (Supplementary Table 1). The log 2 value of the fold difference from the PCR data (Fig. 4.2 *x*-axis) was then plotted against the log 2 value of the fold difference from the array data (Fig. 4.2 *y*-axis). The plots in Fig. 4.2 clearly show that the data from PCR and array for the 96 genes which were selected for validation correlate to each other.

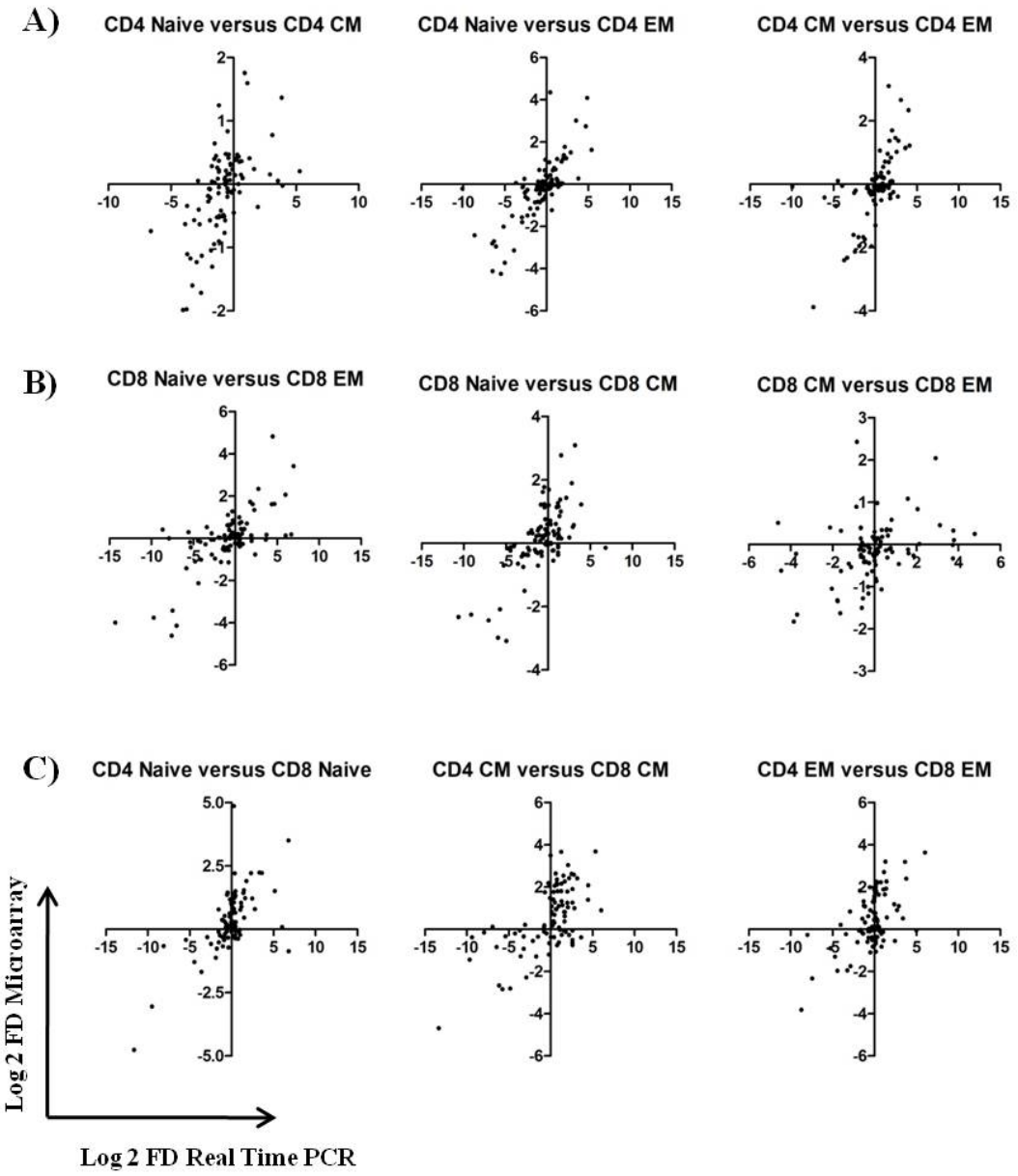

Figure 4.2. Comparing the log 2 fold differences from the Real Time PCR data to the log 2 fold differences from the array analysis. The fold differences for each comparison made, were calculated for both the microarray data and the Real Time PCR data; the log 2 value of both data sets were plotted against each other to show any correlation. The comparisons made within the $CD4^+$ T cell compartment are shown in **A)** The comparisons made within the $CD8^+$ T cell compartment are shown in **B)** and the comparisons made when comparing the $CD4^+$ T cell populations to the $CD8^+$ T cell populations are shown in **C)**.

4.2.3 Comparing the three differentiation states without distinguishing between the $CD4^+$ and $CD8^+$ T cell compartment

To assess genes which are shared during differentiation of both $CD4^+$ and $CD8^+$ T cell populations a SAM analysis was performed; the samples were divided into the three differentiation states: naive, central memory (CM) and effector memory (EM). The samples were not divided between $CD4^+$ and $CD8^+$; therefore each SAM group contained 10 samples (five $CD4^+$ populations and five $CD8^+$ populations). This analysis resulted in a SAM gene list of 34 genes which differed significantly in their expression between the differentiated T cell populations and a false discovery rate (FDR) of 1% (Table 1). The median values of the relative quantities (RQs) for the three cell populations as well as the fold differences between the three populations are shown. CCR7, LRRN3 (Leucine-rich repeat neuronal protein 3) and L-Selectin (SELL) are all more highly expressed in the naive and CM samples compared to the EM samples. CXCR5 was shown to have highest expression in the CM population, with the lowest expression found in the naive population. GZMA (granzyme A) and PRF1 (perforin) were most highly expressed in the EM populations of both $CD4^+$ and $CD8^+$ T cells.

Detector	Median Naive	Median CM	Median EM	Naive / CM	Naive/ EM	CM/ EM	
KLRC4	1.14174E-05	1.502E-06	3.7434E-07	7.6	30.5	4.01	
NGFRAP1	1.99604E-06	3.408E-07	1.9449E-07	5.86	10.26	1.75	
LRRN3	6.26286E-06	1.496E-06	8.3141E-08	4.19	75.33	17.99	
TSPAN33	1.94453E-06	1.022E-06	4.8781E-07	1.9	3.99	2.09	
CCR7	3.61864E-05	2.276E-05	2.5131E-06	1.59	14.4	9.06	
SELL	6.17424E-05	4.511E-05	1.5146E-05	1.37	4.08	2.98	
LASS6	1.6341E-06	1.325E-06	3.8709E-07	1.23	4.22	3.42	
TLE2	2.30954E-06	1.971E-06	1.1154E-06	1.17	2.07	1.77	
SLC22A17	6.95652E-07	6.226E-07	7.197E-08	1.12	9.67	8.65	
MED26	5.83135E-07	8.747E-07	9.0828E-07	0.67	0.64	0.96	
EHD1	8.06504E-06	1.441E-05	1.4649E-05	0.56	0.55	0.98	
GAPDH	1.64481E-05	3.328E-05	4.067E-05	0.49	0.4	0.82	
LTBP4	9.2022E-07	1.914E-06	2.2848E-06	0.48	0.4	0.84	
TSPAN18	3.37098E-06	7.092E-06	8.451E-06	0.48	0.4	0.84	
MINK1	5.40541E-06	1.21E-05	1.18E-05	0.45	0.46	1.03	
TSPAN17	6.8609E-07	1.586E-06	2.0846E-06	0.43	0.33	0.76	
GPR183	7.81576E-06	1.944E-05	2.2156E-05	0.4	0.35	0.88	
CD81	6.99335E-06	1.761E-05	2.2338E-05	0.4	0.31	0.79	
TSPAN5	1.20514E-06	3.111E-06	2.7959E-06	0.39	0.43	1.11	
SH3BP5	4.88374E-06	1.305E-05	1.4101E-05	0.37	0.35	0.93	
CD63	5.01517E-06	1.52E-05	1.8748E-05	0.33	0.27	0.81	
PRF1	4.77547E-07	1.514E-06	6.2908E-06	0.32	0.08	0.24	
CD151	2.08315E-06	6.669E-06	7.4879E-06	0.31	0.28	0.89	
TSPAN2	2.57403E-07	1.135E-06	1.511E-06	0.23	0.17	0.75	
GNLY	3.37879E-08	1.665E-07	5.4012E-06	0.2	0.01	0.03	
PRDM8	4.24102E-07	2.205E-06	2.7855E-06	0.19	0.15	0.79	
CD82	2.50903E-06	1.455E-05	1.0204E-05	0.17	0.25	1.43	
KLRG1	5.80401E-07	3.625E-06	8.3333E-06	0.16	0.07	0.43	
CXCR5	7.72281E-07	5.087E-06	1.1253E-06	0.15	0.69	4.52	
GFI1	4.02429E-10	2.676E-09	1.1355E-08	0.15	0.04	0.24	
BHLHE40	6.68568E-07	5.223E-06	1.4849E-05	0.13	0.05	0.35	
MYBL1	9.54545E-08	9.911E-07	2.2372E-06	0.1	0.04	0.44	
GZMA	5.35863E-08	1.415E-06	4.863E-06	0.04	0.01	0.29	
F2R	4.02429E-10	3.388E-08	9.6954E-08	0.01	0	0.35	

Table 1. Comparing the gene expression of sorted naive, central memory (CM) and effector memory (EM) $CD4^+$ and $CD8^+$ T cell populations. SAM analysis resulted in a list of 34 significant genes (1% FDR).

4.2.4 Comparing the three differentiation states within the CD4$^+$ T cell compartment

To generate a list of genes which are significantly differentially expressed between the three cell populations within the CD4$^+$ compartment a SAM was performed, dividing the samples into three groups. This generated a list of 26 genes with a FDR of 1% (Table 2), Fig. 4.3A shows the HCL based on this gene list. The HCL reveals that these 26 genes allow good clustering of the samples into their relevant differentiation states. The PCA (Fig. 4.3B) visualises the clustering of the samples. The PCA shows that the naive and CM populations are the most similar in their gene expression compared to the EM population.

Detector	Median CD4 Naive	Median CD4 CM	Median CD4 EM	CD4 Naive/ CM	CD4 Naive/ EM	CD4 CM/ EM
KLRC4	1.3E-08	9.09E-10	2.358E-08	14.3	0.55	0.04
LRRN3	3.02E-06	1.63E-06	1.04E-07	1.85	29.06	15.69
TLE2	3.65E-06	2.22E-06	1.091E-06	1.64	3.35	2.04
CCR7	4.81E-05	3.47E-05	4.167E-06	1.38	11.54	8.33
TCEA3	8.55E-06	6.54E-06	2.02E-06	1.31	4.23	3.24
STAP1	1.23E-06	1.12E-06	3.049E-07	1.1	4.03	3.67
SLC22A17	7.94E-07	7.25E-07	1.06E-07	1.1	7.48	6.83
LASS6	1.48E-06	1.74E-06	3.247E-07	0.85	4.56	5.36
TSPAN10	8.26E-10	1E-09	2.591E-10	0.83	3.19	3.86
CFP	2.39E-07	3.86E-07	2.653E-07	0.62	0.9	1.46
TSPAN16	4.05E-10	9.09E-10	2.591E-10	0.45	1.56	3.51
TSPAN1	4.05E-10	9.09E-10	2.591E-10	0.45	1.56	3.51
TSPAN11	4.05E-10	9.09E-10	2.591E-10	0.45	1.56	3.51
TSPAN8	4.05E-10	9.09E-10	2.591E-10	0.45	1.56	3.51
TNFRSF25	4.05E-10	9.09E-10	2.591E-10	0.45	1.56	3.51
TSPAN17	6.58E-07	1.87E-06	1.431E-06	0.35	0.46	1.31
SH3BP5	5.13E-06	1.68E-05	1.471E-05	0.31	0.35	1.14
KLRG1	7.58E-07	2.52E-06	4.762E-06	0.3	0.16	0.53
PRDM8	5.49E-07	2.22E-06	3.155E-06	0.25	0.17	0.7
CD82	2.68E-06	1.62E-05	2.07E-05	0.17	0.13	0.78
TSPAN2	2.67E-07	1.9E-06	1.961E-06	0.14	0.14	0.97
CXCR5	8.4E-07	6.49E-06	1.091E-06	0.13	0.77	5.95
MYBL1	8.77E-08	9.52E-07	1.3E-06	0.09	0.07	0.73
F2R	4.05E-10	5.24E-09	3.175E-08	0.08	0.01	0.16
BHLHE40	4.61E-07	6.21E-06	1.471E-05	0.07	0.03	0.42
TSPAN5	6.67E-07	9.71E-06	3.247E-06	0.07	0.21	2.99

Table 2. Comparing the gene expression of sorted naive, central memory (CM) and effector memory (EM) $CD4^+$ T cell populations. SAM analysis resulted in a list of 26 significant genes (1% FDR).

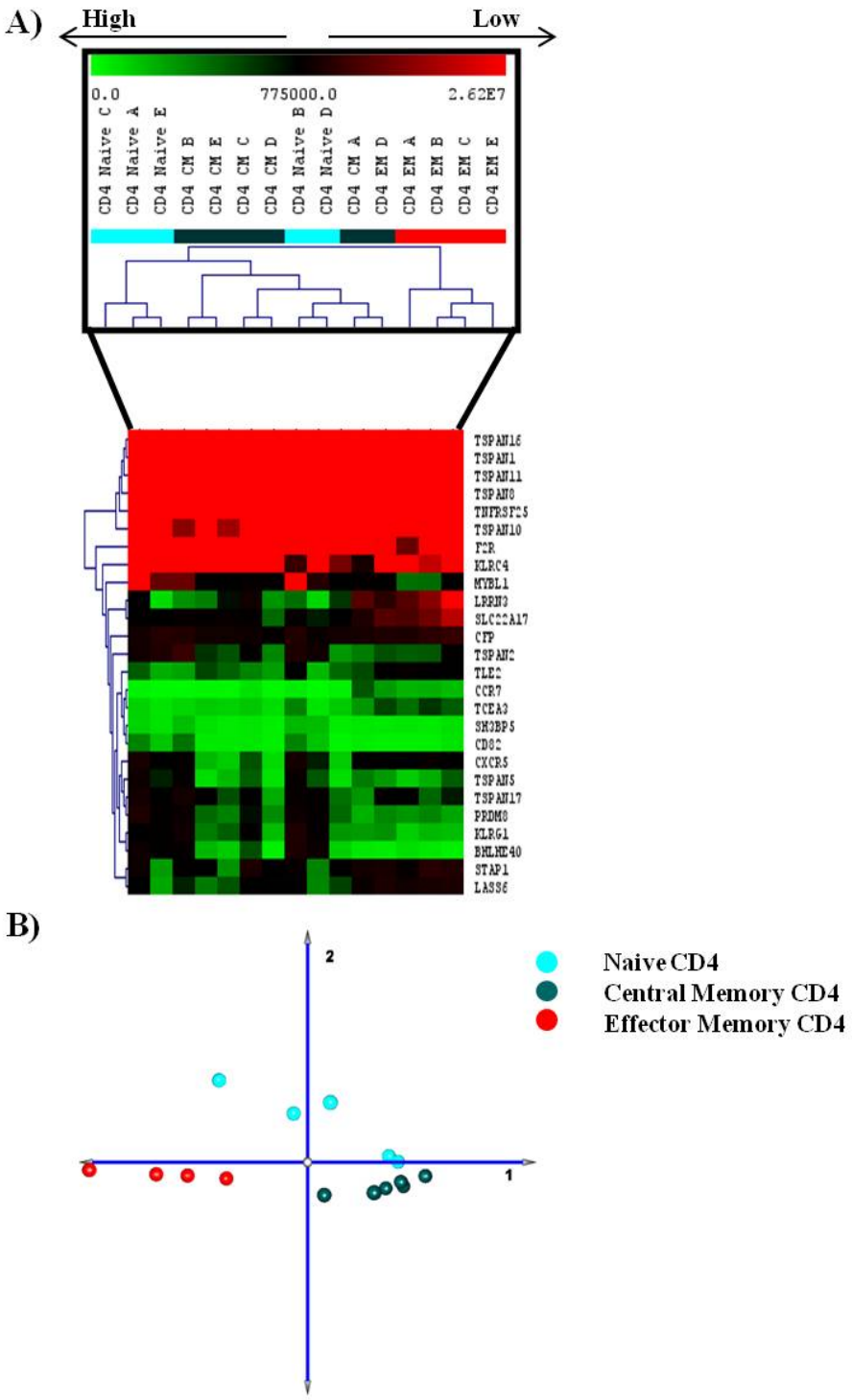

Figure 4.3. Comparing the gene expression of sorted naive, central memory (CM) and effector memory (EM) CD4$^+$ T cell populations. The populations were sorted from five healthy donors. SAM analysis resulted in a list of 26 significant genes (>1% FDR). **A)** The HCL shows how the samples cluster based on the gene expression of these 26 genes. **B)** The PCA visualises the clustering seen in the HCL.

To identify the genes significantly differently expressed between $CD4^+$ naive and CM populations, a paired SAM was executed. This means that the naive and CM population from one donor were paired together in the analysis, to address any donor variability that may have been present. The paired SAM resulted in a list of 12 genes, with a FDR of 1% (Table 3). All 12 genes were more highly expressed in the $CD4^+$ CM population than in the $CD4^+$ naive population, with tetraspanin5 (TSPAN5), BHLHE40 (also known as BHLHB2, basic helix-loop-helix protein B2), F2R (coagulation factor II (thrombin) receptor) and MYBL1 (Myb-related protein A) showing more than tenfold higher expression in the $CD4^+$ CM population.

Detector	Median CD4 Naive	Median CD4 CM	CD4 Naive/CM	CD4 CM/Naive
TSPAN18	6.41E-06	1.03E-05	0.62	1.61
CFP	2.39E-07	3.861E-07	0.62	1.61
TSPAN17	6.58E-07	1.869E-06	0.35	2.84
SH3BP5	5.13E-06	1.681E-05	0.31	3.28
PRDM8	5.49E-07	2.222E-06	0.25	4.04
CD82	2.68E-06	1.621E-05	0.17	6.05
TSPAN2	2.67E-07	1.901E-06	0.14	7.13
CXCR5	8.4E-07	6.494E-06	0.13	7.73
MYBL1	8.77E-08	9.524E-07	0.09	10.86
F2R	4.05E-10	5.236E-09	0.08	12.93
BHLHE40	4.61E-07	6.211E-06	0.07	13.48
TSPAN5	6.67E-07	9.709E-06	0.07	14.56

Table 3. Comparing the gene expression of sorted naive and central memory (CM) $CD4^+$ T cell populations. SAM analysis resulted in a list of 12 significant genes (1% FDR).

The same approach was used to identify genes which are differentially expressed between $CD4^+$ naive and EM populations. In this case the paired SAM resulted in a list of 16 genes (Table 4) with significantly different gene expression between $CD4^+$ naive and $CD4^+$ EM T cell populations (1% FDR). LRRN3 and CCR7 were the genes with the highest fold difference between the $CD4^+$ naive population and the $CD4^+$ EM population. The genes with the highest fold difference between the $CD4^+$ EM and $CD4^+$ naive population were F2R and BHLHE40.

The last comparison to be made within the $CD4^+$ compartment was between $CD4^+$ CM and EM populations and to this end a paired SAM was executed. The paired SAM resulted in a list of 20 genes with significantly different gene expression and a 1% FDR (Table 5). All genes except for one were more highly expressed in the $CD4^+$ CM compared to the $CD4^+$ EM population. Surprisingly the gene which was more highly expressed in the $CD4^+$ EM population was CD8α, with over fivefold fold difference. LRRN3 was the gene with the highest fold difference between the $CD4^+$ CM population and the $CD4^+$ EM population.

Detector	Median CD4 Naive	Median CD4 EM	CD4 Naive/EM	CD4 EM/Naive
LRRN3	3.021E-06	1E-07	29.06	0.03
CCR7	4.808E-05	4.2E-06	11.54	0.09
SLC22A17	7.937E-07	1.1E-07	7.48	0.13
NGFRAP1	1.65E-06	3.2E-07	5.1	0.2
LASS6	1.479E-06	3.2E-07	4.56	0.22
TCEA3	8.547E-06	2E-06	4.23	0.24
STAP1	1.23E-06	3E-07	4.03	0.25
TLE2	3.65E-06	1.1E-06	3.35	0.3
TSPAN3	1.669E-06	8.8E-07	1.89	0.53
TSPAN17	6.579E-07	1.4E-06	0.46	2.17
SH3BP5	5.128E-06	1.5E-05	0.35	2.87
PRDM8	5.495E-07	3.2E-06	0.17	5.74
TSPAN2	2.667E-07	2E-06	0.14	7.35
CD82	2.681E-06	2.1E-05	0.13	7.72
BHLHE40	4.608E-07	1.5E-05	0.03	31.91
F2R	4.049E-10	3.2E-08	0.01	78.41

Table 4. Comparing the gene expression of sorted naive and effector memory (EM) $CD4^+$ T cell populations. SAM analysis resulted in a list of 16 significant genes (1% FDR).

Detector	Median CD4 CM	Median CD4 EM	CD4 CM/EM	CD4 EM/CM
LRRN3	1.631E-06	1.04E-07	15.69	0.06
NGFRAP1	3.937E-06	3.236E-07	12.17	0.08
CCR7	3.472E-05	4.167E-06	8.33	0.12
SLC22A17	7.246E-07	1.06E-07	6.83	0.15
CXCR5	6.494E-06	1.091E-06	5.95	0.17
LASS6	1.739E-06	3.247E-07	5.36	0.19
TSPAN10	1E-09	2.591E-10	3.86	0.26
STAP1	1.12E-06	3.049E-07	3.67	0.27
TSPAN11	9.091E-10	2.591E-10	3.51	0.28
TSPAN1	9.091E-10	2.591E-10	3.51	0.28
TSPAN8	9.091E-10	2.591E-10	3.51	0.28
TSPAN16	9.091E-10	2.591E-10	3.51	0.28
TNFRSF25	9.091E-10	2.591E-10	3.51	0.28
TCEA3	6.536E-06	2.02E-06	3.24	0.31
TRIB2	4.63E-05	1.49E-05	3.11	0.32
TLE2	2.222E-06	1.091E-06	2.04	0.49
TSPAN3	1.431E-06	8.85E-07	1.62	0.62
CFP	3.861E-07	2.653E-07	1.46	0.69
FLYWCH1	1.961E-06	1.57E-06	1.25	0.8
CD8A	1.441E-07	8.197E-07	0.18	5.69

Table 5. Comparing the gene expression of sorted central memory (CM) and effector memory (EM) $CD4^+$ T cell populations. SAM analysis resulted in a list of 20 significant genes (1% FDR).

4.2.5 Comparing the three differentiation states within the $CD8^+$ T cell compartment

To generate a list of genes which are significantly differentially expressed between the three cell populations within the $CD8^+$ compartment a SAM was performed, dividing the samples into three groups. This analysis resulted in a list of 22 genes which were found to be expressed at significantly different levels between the three differentiation states (1% FDR, Table 6). NGFRAP1 (nerve growth factor receptor (TNFRSF16) associated protein 1) was found to have the highest expression in $CD8^+$ naive T cells and its expression dropped down as the cells differentiate. LRRN3, CCR7 and L-selectin were also all expressed highest on

$CD8^+$ naive T cells and their expression was lowest in $CD8^+$ EM T cells. GNLY (granulysin), F2R, GZMK, SLAMF7 (SLAM family member 7) and GZMA were all upregulated in the more differentiated populations compared to the naive population.

Detector	Median CD8 Naive	Median CD8 CM	Median CD8 EM	CD8 Naive/ CM	CD8 Naive/ EM	CD8 CM/ EM
NGFRAP1	2.74E-06	1.81E-07	4.4E-08	15.12	62.74	4.15
LRRN3	8.85E-06	9.71E-07	7.2E-08	9.12	123.01	13.5
SLC22A17	6.67E-07	2.25E-07	5.1E-08	2.96	13	4.39
CCR7	3.53E-05	1.22E-05	1.6E-06	2.9	21.8	7.52
SELL	6.67E-05	2.99E-05	0.00001	2.23	6.67	2.99
CD63	7.19E-06	1.65E-05	2.3E-05	0.44	0.31	0.7
CD81	6.94E-06	2.51E-05	3.7E-05	0.28	0.19	0.68
PRF1	9.9E-07	4.95E-06	1.7E-05	0.2	0.06	0.29
TSPAN18	1.31E-06	6.8E-06	5.3E-06	0.19	0.25	1.29
SH3BP5	1.94E-06	1.01E-05	1.3E-05	0.19	0.14	0.75
PRDM8	2.54E-07	1.46E-06	2.7E-06	0.17	0.1	0.55
TSPAN2	1.33E-07	9.71E-07	9.7E-07	0.14	0.14	1
GPR183	1.82E-06	1.41E-05	1.3E-05	0.13	0.14	1.09
CDKN1A	8.33E-08	6.58E-07	9.9E-07	0.13	0.08	0.66
CD82	1.32E-06	1.17E-05	7.8E-06	0.11	0.17	1.5
KLRG1	2.72E-07	4.33E-06	1.3E-05	0.06	0.02	0.33
GFI1	3.4E-10	9.35E-09	1.4E-08	0.04	0.02	0.65
GZMA	6.37E-08	1.99E-06	8.2E-06	0.03	0.01	0.24
SLAMF7	3.82E-08	0.000002	6.8E-06	0.02	0.01	0.29
GZMK	1.15E-07	1.53E-05	2.7E-05	0.0075	0.0042	0.56
F2R	3.95E-10	2.21E-07	3.4E-07	0.0018	0.0012	0.66
GNLY	5.99E-10	9.43E-07	1.2E-05	0.0006	0.00005	0.08

Table 6. Comparing the gene expression of sorted naive, central memory (CM) and effector memory (EM) $CD8^+$ T cell populations. SAM analysis resulted in a list of 22 significant genes (1% FDR).

Comparing the $CD8^+$ naive and CM populations using a paired SAM resulted in a list of 14 genes, with a FDR of 1% (Table 7). All genes were found to be upregulated more than twofold in the $CD8^+$ CM T cells compared to the $CD8^+$ naive T cells. The genes with the highest fold difference were mostly associated with effector function, such as GZMA, GZMK and PRF1. CXCR5 was found to be more than fourfold more highly expressed in the $CD8^+$ CM T cells compared to the $CD8^+$ naive T cells.

Detector	Median CD8 Naive	Median CD8 CM	CD8 Naive/CM	CD8 CM/Naive
MINK1	5.263E-06	1.23E-05	0.43	2.34
CD81	6.944E-06	2.51E-05	0.28	3.62
CXCR5	7.042E-07	3.34E-06	0.21	4.75
PRF1	9.901E-07	4.95E-06	0.2	5
TSPAN18	1.311E-06	6.8E-06	0.19	5.19
PRDM8	2.538E-07	1.46E-06	0.17	5.75
GPR183	1.821E-06	1.41E-05	0.13	7.74
CDKN1A	8.333E-08	6.58E-07	0.13	7.89
CD82	1.319E-06	1.17E-05	0.11	8.87
GFI1	3.401E-10	9.35E-09	0.04	27.48
GZMA	6.369E-08	1.99E-06	0.03	31.21
SLAMF7	3.817E-08	0.000002	0.02	52.4
GZMK	1.149E-07	1.53E-05	0.01	133.03
F2R	3.953E-10	2.21E-07	0.0018	559.73

Table 7. Comparing the gene expression of sorted naive and central memory (CM) CD8$^+$ T cell populations. SAM analysis resulted in a list of 14 significant genes (1% FDR).

Gene expression of CD8$^+$ naive and EM populations was then compared using a paired SAM, this resulted in a list of 23 genes with a FDR of 1% (Table 8). Four of these genes were found to be upregulated (> 2 fold) in the CD8$^+$ naive population compared to the CD8$^+$ EM population, these were LRRN3, NGFRAP1, CCR7 and CRTAM (cytotoxic and regulatory T cell molecule).

The paired SAM used to identify the genes significantly differently expressed between CD8$^+$ CM and EM populations resulted in a list of 12 genes, with a FDR of 1% (Table 9). The genes with the highest fold difference between the CD8$^+$ CM population and the CD8$^+$ EM population were LRRN3, NGFRAP1 and IL-2RA (IL-2 receptor α chain). GZMH, KLRF1 (killer cell lectin-like receptor subfamily F, member 1) and Tspan15 (tetraspanin 15) were all more than tenfold more highly expressed in the CD8$^+$ EM population compared to the CD8$^+$ CM population.

Detector	Median CD8 Naive	Median CD8 EM	CD8 Naive/EM	CD8 EM/Naive
LRRN3	8.85E-06	7.19E-08	123.01	0.01
NGFRAP1	2.74E-06	4.37E-08	62.74	0.02
CCR7	3.534E-05	1.62E-06	21.8	0.05
CRTAM	3.559E-06	1.68E-06	2.12	0.47
TSPAN5	1.241E-06	2.57E-06	0.48	2.07
CD63	7.194E-06	2.34E-05	0.31	3.26
CD151	2.342E-06	8.26E-06	0.28	3.53
TSPAN18	1.311E-06	5.29E-06	0.25	4.04
CD81	6.944E-06	3.7E-05	0.19	5.33
CD82	1.319E-06	7.81E-06	0.17	5.92
SH3BP5	1.942E-06	1.35E-05	0.14	6.95
GPR183	1.821E-06	1.29E-05	0.14	7.08
TSPAN2	1.33E-07	9.71E-07	0.14	7.3
PRDM8	2.538E-07	2.66E-06	0.1	10.48
CDKN1A	8.333E-08	9.9E-07	0.08	11.88
PRF1	9.901E-07	1.69E-05	0.06	17.06
GFI1	3.401E-10	1.43E-08	0.02	42.06
KLRG1	2.717E-07	1.31E-05	0.02	48.23
GZMA	6.369E-08	8.2E-06	0.01	128.69
SLAMF7	3.817E-08	6.8E-06	0.01	178.23
GZMK	1.149E-07	2.75E-05	0.004184	239.01
F2R	3.953E-10	3.37E-07	0.001174	851.85
GNLY	5.988E-10	1.22E-05	4.91E-05	20365.85

Table 8. Comparing the gene expression of sorted naive and effector memory (EM) CD8$^+$ T cell populations. SAM analysis resulted in a list of 23 significant genes (1% FDR).

Detector	Median CD8 CM	Median CD8 EM	CD8 CM/EM	CD8 EM/CM
LRRN3	9.70874E-07	7.19424E-08	13.5	0.07
NGFRAP1	1.81159E-07	4.36681E-08	4.15	0.24
IL2RA	1.02041E-06	5.81395E-07	1.76	0.57
CD63	1.65017E-05	2.34192E-05	0.7	1.42
GZMK	1.52905E-05	2.74725E-05	0.56	1.8
NKG7	8.92857E-06	2.77778E-05	0.32	3.11
SLAMF7	0.000002	6.80272E-06	0.29	3.4
PRF1	4.9505E-06	1.68919E-05	0.29	3.41
GZMA	1.98807E-06	8.19672E-06	0.24	4.12
TSPAN15	2.38095E-07	3.19489E-06	0.07	13.42
KLRF1	1.63934E-07	2.36967E-06	0.07	14.45
GZMH	6.66667E-07	1.62075E-05	0.04	24.31

Table 9. Comparing the gene expression of sorted central memory (CM) and effector memory (EM) CD8$^+$ T cell populations. SAM analysis resulted in a list of 12 significant genes (1% FDR).

4.2.6 Comparing between $CD4^+$ and $CD8^+$ differentiation states

To find genes which differed in their expression between $CD4^+$ and $CD8^+$ T cell differentiation states, three separate SAM analyses were done comparing the $CD4^+$ naive population to the $CD8^+$ naive population, the $CD4^+$ CM population to the $CD8^+$ CM population and the $CD4^+$ EM population to the $CD8^+$ EM population. Comparing the $CD4^+$ naive and $CD8^+$ naive T cell populations to each other resulted in a SAM list of 10 genes, with a FDR of 1% (Table 10). Only two of the ten significant genes were upregulated in the $CD8^+$ naive population compared to the $CD4^+$ naive population, namely CRTAM and TSPAN32. CD4, TSPAN9 and GPR183 were the genes with the highest fold difference (>10 fold) between the $CD4^+$ naive population and the $CD8^+$ naive population.

Detector	Median CD4 Naive	Median CD8 Naive	CD4 Naive/ CD8 Naive	CD8 Naive/ CD4 Naive
CD4	1.58E-05	1.45E-07	109	0.01
TSPAN9	8.7E-08	1.35E-09	64.43	0.02
GPR183	2.19E-05	1.82E-06	12.01	0.08
TSPAN18	6.41E-06	1.31E-06	4.89	0.2
TRIB2	1.25E-05	4.57E-06	2.74	0.37
SH3BP5	5.13E-06	1.94E-06	2.64	0.38
CD82	2.68E-06	1.32E-06	2.03	0.49
SUSD4	1.97E-06	0.000001	1.97	0.51
TSPAN32	2.39E-06	6.99E-06	0.34	2.92
CRTAM	1.64E-07	3.56E-06	0.05	21.71

Table 10. Comparing the gene expression of sorted naive $CD4^+$ and naive $CD8^+$ T cell populations. SAM analysis resulted in a list of 10 significant genes (1% FDR).

The SAM comparing $CD4^+$ CM and $CD8^+$ CM T cell populations resulted in a list of 33 genes, with a FDR of less than 1% (Table 11). Six of the 33 genes were upregulated in the $CD8^+$ CM compared to the $CD4^+$ CM population, amongst which were CD8α and CD8β. CD4 showed the highest fold difference between the $CD4^+$ CM and the $CD8^+$ CM population, followed by NGFRAP1.

Comparing the $CD4^+$ EM and $CD8^+$ EM T cell populations resulted in a list of 21 genes, with a FDR of less than 1% (Table 12). Four of these genes were more highly expressed in the $CD4^+$ EM population, namely CD4, IL-2RA, NGFRAP1 and TRIB2 (tribbles homolog 2) all of which were more than twofold more highly expressed. Among the genes upregulated in the $CD8^+$ EM population were many genes associated with effector functions, such as KLRC4 (killer cell lectin-like receptor subfamily C, member 4, also known as NKG2F), NKG7 (natural killer cell group 7 sequence), GZMH and PRF1. CD8α and CD8β were also upregulated in the $CD8^+$ EM population.

Detector	Median CD4 CM	Median CD8 CM	CD4 CM/ CD8 CM	CD8 CM/ CD4 CM
CD4	1.57E-05	3.91E-07	40.19	0.02
NGFRAP1	3.94E-06	1.81E-07	21.73	0.05
TSPAN6	1.09E-07	8.85E-09	12.32	0.08
IL2RA	9.17E-06	1.02E-06	8.99	0.11
EDAR	1.17E-06	1.66E-07	7.04	0.14
CTLA4	4.78E-06	7.04E-07	6.79	0.15
TSPAN11	9.09E-10	1.51E-10	6.02	0.17
TSPAN1	9.09E-10	1.51E-10	6.02	0.17
TSPAN12	9.09E-10	1.51E-10	6.02	0.17
TSPAN16	9.09E-10	1.51E-10	6.02	0.17
TSPAN8	9.09E-10	1.51E-10	6.02	0.17
TNFRSF25	9.09E-10	1.51E-10	6.02	0.17
TRIB2	4.63E-05	8.26E-06	5.6	0.18
GPR183	6.41E-05	1.41E-05	4.54	0.22
SUSD4	3.15E-06	6.94E-07	4.54	0.22
TRAT1	0.0001	2.4E-05	4.18	0.24
TSPAN5	9.71E-06	2.37E-06	4.1	0.24
CFP	3.86E-07	9.8E-08	3.94	0.25
TLR5	4.2E-07	1.07E-07	3.93	0.25
KRT73	3.37E-07	1.06E-07	3.18	0.31
TSPAN15	7.46E-07	2.38E-07	3.13	0.32
LASS6	1.74E-06	6.67E-07	2.61	0.38
TCEA3	6.54E-06	2.75E-06	2.38	0.42
TSPAN31	1.54E-06	7.19E-07	2.14	0.47
TSPAN2	1.9E-06	9.71E-07	1.96	0.51
TLE2	2.22E-06	1.32E-06	1.68	0.59
CD82	1.62E-05	1.17E-05	1.39	0.72
MED26	6.33E-07	1.07E-06	0.59	1.69
PRF1	5.92E-07	4.95E-06	0.12	8.37
CSDA	3.3E-07	3.94E-06	0.08	11.93
CD8B	7.04E-08	1.75E-05	0.004021	248.69
CD8A	1.44E-07	0.000116	0.001246	802.31
KLRC4	9.09E-10	9.43E-06	9.64E-05	10377.36

Table 11. Comparing the gene expression of sorted central memory (CM) $CD4^+$ and CM $CD8^+$ T cell populations. SAM analysis resulted in a list of 33 significant genes (1% FDR).

Detector	Median CD4 EM	Median CD8 EM	CD4 EM/ CD8 EM	CD8 EM/ CD4 EM
CD4	1.721E-05	2.68E-07	64.2	0.02
IL2RA	7.143E-06	5.81E-07	12.29	0.08
NGFRAP1	3.236E-07	4.37E-08	7.41	0.13
TRIB2	1.49E-05	5.59E-06	2.67	0.37
CD63	1.639E-05	2.34E-05	0.7	1.43
SCRN2	1.988E-06	3.36E-06	0.59	1.69
TSPAN15	1.441E-06	3.19E-06	0.45	2.22
CD81	1.52E-05	3.7E-05	0.41	2.44
GZMA	3.226E-06	8.2E-06	0.39	2.54
KLRG1	4.762E-06	1.31E-05	0.36	2.75
GZMK	8.197E-06	2.75E-05	0.3	3.35
SLAMF7	9.259E-07	6.8E-06	0.14	7.35
PRF1	2.222E-06	1.69E-05	0.13	7.6
CSDA	1.869E-07	1.77E-06	0.11	9.47
F2R	3.175E-08	3.37E-07	0.09	10.61
GZMH	9.804E-07	1.62E-05	0.06	16.53
NKG7	1.29E-06	2.78E-05	0.05	21.53
CRTAM	4.348E-08	1.68E-06	0.03	38.66
CD8A	8.197E-07	0.000142	0.01	172.8
CD8B	6.667E-08	1.71E-05	0.0039	256.41
KLRC4	2.358E-08	0.00001	0.0024	424

Table 12. Comparing the gene expression of sorted effector memory (EM) CD4$^+$ and effector memory (EM) CD8$^+$ T cell populations. SAM analysis resulted in a list of 21 significant genes (1% FDR).

4.2.7 Shared and unique genes in CD4$^+$ and CD8$^+$ differentiation pathways

To identify genes shared during differentiation of both CD4$^+$ and CD8$^+$ T cell populations the SAM lists generated when comparing the naive, CM and EM populations within the CD4$^+$ and CD8$^+$ compartments were compared. This resulted in nine genes which were found to be shared between these comparisons (Fig. 4.4). As can be seen in the figure all nine genes showed a pattern in which the CM population exhibits an intermediate gene expression to the naive and EM populations. This pattern suggests that these genes are important in the differentiation from a naive T cell to a CM or EM T cell in both the CD4$^+$ and CD8$^+$ T cell compartment.

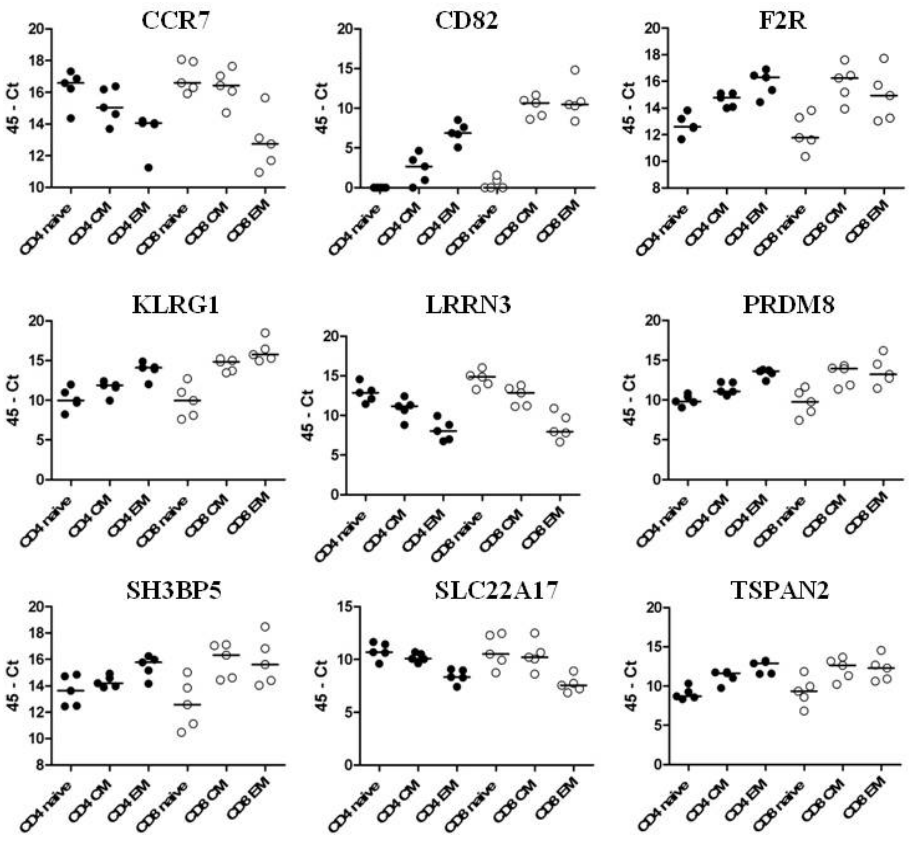

Figure 4.4. Nine shared genes can be found when comparing the differentiation of $CD4^+$ and $CD8^+$ T cell populations. When analysing the SAM lists generated when comparing the naive, central memory (CM) and effector memory (EM) populations within the $CD4^+$ and $CD8^+$ compartments, nine genes were found to be shared.

When trying to identify genes which were consistently different between $CD4^+$ and $CD8^+$ T cell populations the SAM lists generated when comparing the $CD4^+$ naive to $CD8^+$ naive, $CD4^+$ CM to $CD8^+$ CM and $CD4^+$ EM to $CD8^+$ EM were compared to each other. One gene, TRIB2, was found to be shared (Fig. 4.5). This suggests that this gene is consistently differentially expressed between all $CD4^+$ and $CD8^+$ T cell populations.

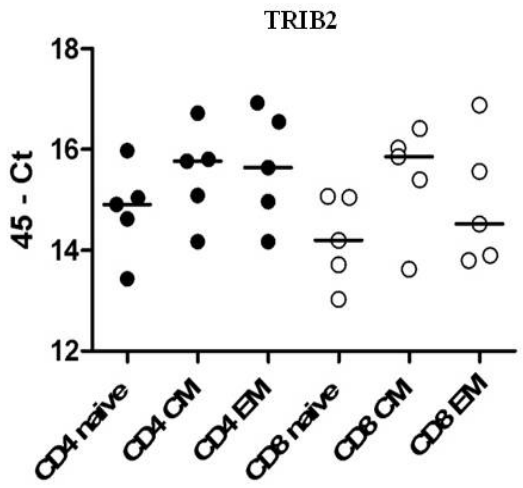

Figure 4.5. One shared gene can be found when comparing the differentiation states of $CD4^+$ and $CD8^+$ T cell. When analysing the SAM lists generated when comparing the $CD4^+$ naive to $CD8^+$ naive, $CD4^+$ central memory (CM) to $CD8^+$ CM and $CD4^+$ effector memory (EM) to $CD8^+$ EM one gene was found to be shared.

4.3 Discussion

The results from the previous Chapter suggested a pathway shared between $CD4^+$ and $CD8^+$ T cells during differentiation. Real Time PCR has been used as the gold standard for validating gene expression levels and to validate the microarray analysis of the $CD4^+$ and $CD8^+$ T cell populations 96 genes were selected from the gene lists generated in Chapter 3 and tested by Real Time PCR. Real Time PCR has the advantage over microarrays in that it is a highly reproducible and more quantitative way and it allows the testing of more samples than would be possible by microarray analysis (Fig. 4.6). Large scale microarray analysis is a useful tool to analyse large quantities of genes at the same time and identifying genes of interest, to validate and follow up on such genes a more specific microarray can be designed which might contain genes from the same gene family as a gene of interest. Real Time PCR analysis can then be used to validate the gene expression identified through array analysis, as it is a more quantitative technique as well as allowing the researcher to analyse a larger sample pool.

Microarray analysis of the T cell populations within the $CD4^+$ and $CD8^+$ compartment identified tetraspanin18 as a differentially expressed gene between $CD4^+$ and $CD8^+$ T cells. The Real Time PCR data of these same T cell populations did not show this difference to the same extent. Instead, whereas Tspan18 expression by microarray analysis was consistently found to be higher in $CD4^+$ naive, CM and EM T cell populations when compared to their $CD8^+$ counterparts, the Real Time PCR analysis showed that this was not the case when comparing $CD4^+$ CM to $CD8^+$ CM. In the Real Time PCR samples expression of Tspan18 was found to be higher in the $CD8^+$ CM population compared to the $CD4^+$ CM population. In

both the naive and EM populations Tspan18 expression was again found to be higher in the $CD4^+$ compartment. Protty et al (2009) analysed the expression of tetraspanins in platelets and found that CD9, CD63, CD151 and Tspan9 were expressed on platelets. They also analysed expression of the 33 different tetraspanins in various human cell types and found that when comparing $CD4^+$ helper T cells to cytotoxic $CD8^+$ T cells, Tspan18 was also more highly expressed in the $CD4^+$ T cells compared to the $CD8^+$ T cells [148]. This data strengthens our initial finding of higher Tspan18 expression in the $CD4^+$ T cell compartment. Based on our identification of Tspan18 in our microarray analysis, tetraspanin family members were included in our Real Time PCR validation experiments. This allowed us to identify that several tetraspanins were differentially expressed during T cell differentiation, such as CD81 and CD82; both of which show increased expression in the more differentiated cells of both the $CD4^+$ and the $CD8^+$ compartment. CD9 expression seemed to be lowest on the $CD4^+$ CM population, with $CD4^+$ naive and EM cells expressing similar levels of CD9. Within the $CD8^+$ compartment CD9 expression did not significantly differ between the three populations.

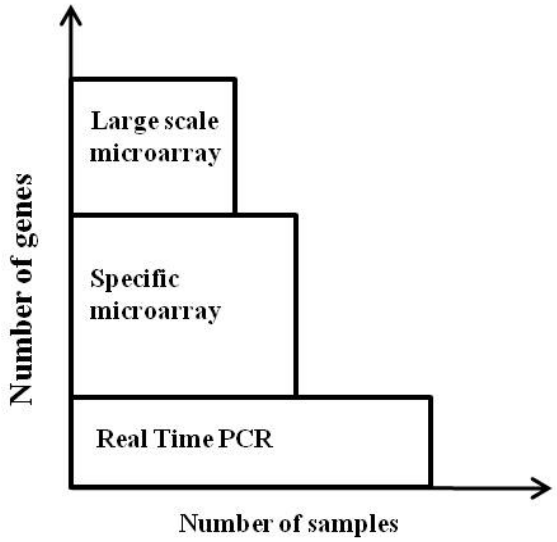

Figure 4.6. Comparing microarray analysis to Real Time PCR analysis. Large scale microarray analysis allows analysis of large quantities of genes at the same time and identifying genes of interest. Validation and follow up on such genes can be done with a more specific microarray designed to contain genes from the same gene family as a gene of interest. Real Time PCR analysis is then used as the gold standard to validate the gene expression identified through array analysis, as it is a more quantitative technique as well as it allows the researcher to analyse a larger sample pool.

Real Time PCR analysis of genes selected from the microarray data resulted, as expected, in several differentially expressed genes. One of which was KLRC4, also known as NKG2F and found to be raised in $CD8^+$ EM T cells. KLRC4 is a member of the NKG2 family of C-type lectins. MHC-Ib molecule HLA-E functions as a ligand for the receptor encoded by these genes and its binding results in an inhibitory signal to the cells expressing the receptor, mainly NK cells and some T cells [149]. Some family members can also send an activation signal when recognising MHC molecules and whether a receptor is inhibitory or activating corresponds to the characteristics of their cytoplasmic or transmembrane domains [150;151]. NKG2A contains an immunorecptor tyrosine-based inhibition motif (ITIM) in its cytoplasmic tail which upon activation results in a inhibitory signal. Family members with activating capabilities have a truncated cytoplasmic domain, therefore lacking the ITIMs, these

receptors associate with adaptor molecules (*e.g.* DAP12) which contain immunoreceptor tyrosine-based activation motifs (ITAMs) [150;151].

The transcript for KLRC4 has been identified in studies however Kim *et al* (2004) are the first to describe protein expression of KLRC4 in NK cells by performing immunoprecipitation and immunoblotting [149;152]. KLRC4 has a high homology with NKG2C, which binds to DAP12, prompting them to assess whether KLRC4 could also bind to DAP12. The mouse pro-B cell line Ba/F3 was transfected with either NKG2C as a control or with KLRC4 as well as with an ecotropic retrovirus encoding human DAP12 with a Flag epitope attached to allow identification on the cell surface. Subsequent immunoprecipitation with an anti-Flag antibody and immunoblotting showed that KLRC4 was able to bind to DAP12. Further analysis revealed that the KLRC4-DAP12 complex was not expressed on the cell surface. The association of KLRC4 with DAP12 suggests that it could have a role in cell activation. Somewhat contradictory is the fact that KLRC4 contains an ITIM motif in its cytoplasmic tail, which could suggest that KLRC4 could have a role in cell activation as well as a cell activation inhibitory role. The data in this chapter shows KLRC4 is differentially expressed on T cell populations, being the most highly expressed gene in four SAM gene lists. When comparing the differentiation states without distinguishing between $CD4^+$ and $CD8^+$ T cell populations, its expression is highest in the naive populations and drops down as the cells differentiate. KLRC4 also comes up as differentially expressed between the naive, CM and EM populations within the $CD4^+$ compartment; however within the $CD4^+$ compartment its expression is highest on the EM population and lowest on the CM population (Fig. 4.7). When comparing the differentiation states between compartments, KLRC4 is shown to be more highly expressed in $CD8^+$ CM and EM T cell populations compared to the $CD4^+$ CM and EM T cell populations respectively. It is clear that $CD8^+$ T cells express higher levels of KLRC4 which corresponds with some reports of expression of

previously thought to be NK cell specific markers on $CD8^+$ T cell populations, indicating the possibility of these cells to express a receptor which is thought to be associated with the innate immune response.

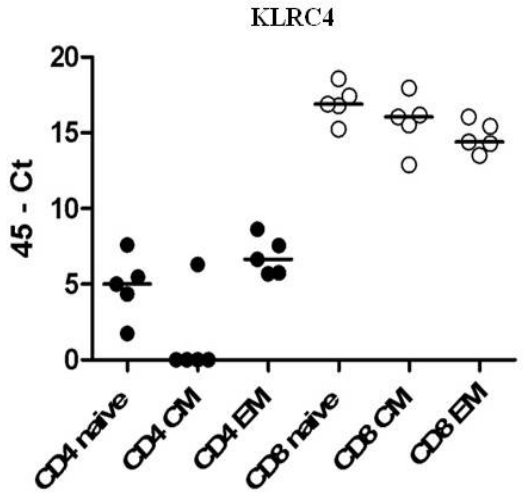

Figure 4.7. KLRC4 gene expression is highest on $CD8^+$ T cell populations. KLRC4, also known as NKG2F, is a member of the NKG2 family of C-type lectins.

NGFRAP1 (Bex3) interacts with the p75 neurotrophin receptor (p75NTR), which is a member of the tumor necrosis facor receptor family. NGFRAP1 interaction with p75NTR modulates nerve growth factor (NGF) signalling through NFκB which can result in regulation of cell cycle, apoptosis and differentiation in neuronal tissue [153;154]. NGFRAP1 encodes p75NTR associated cell death executor (NADE) which binds to the death domain of p75NTR in response to NGF resulting in apoptosis of neuronal cells.

NGFRAP1 is identified in several of the SAM lists when comparing the differentiation states of $CD4^+$ and $CD8^+$ T cells. When comparing the differentiation states without distinguishing between $CD4^+$ and $CD8^+$ T cells, NGFRAP1 is shown to have the highest expression on naive T cells and lowest in the EM T cells (Table 1). It shows this same expression pattern when comparing the three differentiation states within the $CD8^+$ T cell compartment (Table

6). Comparing its expression between $CD4^+$ and $CD8^+$ T cell populations shows that in both compartments the expression is lowest in the EM population (Table 4, 5, 8 and 9) in the $CD8^+$ compartment expression is highest in the naive population, while its expression level in $CD4^+$ naive cells is similar to that of $CD4^+$ CM cells (Fig. 4.8). If naive and CM T cells express high levels of NGFRAP1 this may make them more susceptible to p75NTR mediated apoptosis, which would indicate a pathway for controlling naive and CM T cell responses.

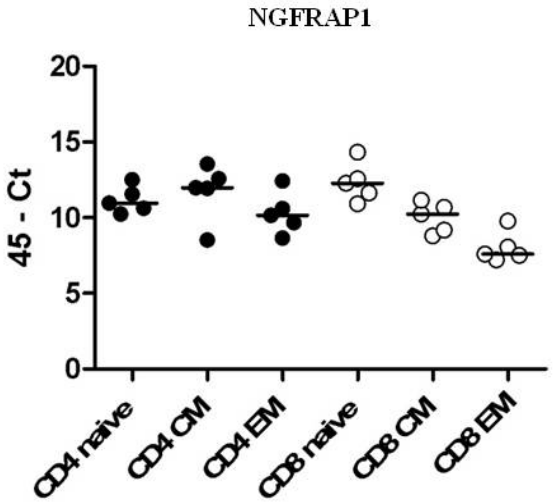

Figure 4.8. NGFRAP1 gene expression is lowest on EM $CD4^+$ and $CD8^+$ T cell populations. NGFRAP1 binds p75 neurotrophin receptor (p75NTR), a member of the tumor necrosis facor receptor family, this binding can result in apoptosis.

SLC22A17 (Solute carrier family 22 member 17) is also known as brain type organic cation transporter (BOCT) in mice and Miharada *et al* (2007) suggest that the human homolog might be a receptor for lipocalin 2 (LCN2 or 24p3) [155]. As a protection mechanism mamalian cells remove iron from the environment to prevent it from being used for bacterial cell growth. LCN2 is a secreted member of the lipocalin family of proteins and has been implicated in iron trafficking in and out of the cell. LCN2 on its own cannot bind iron, but it can bind iron through binding with a small molecular weight bacterial siderophore, which is

an iron chelator [156]. Internalisation of LCN2 bound to iron leads to the prevention of apoptosis, whereas LCN2 internalised without bound iron leads to apoptosis as a result of LCN2 shuttling iron out of the cell [156;157]. The expression of SLC22A17 (BOCT) in our data is highest in the naive populations of both $CD4^+$ and $CD8^+$ T cells and lowest on the EM population. SLC22A17 does not come up as significantly different when comparing the naive population to the CM population in both the $CD4^+$ and $CD8^+$ T cell compartment, indicating that these cell populations express similar levels of this gene (Fig. 4.9). If this high expression of SLC22A17 correlates with the cell surface expression of the LCN2 receptor, this could indicate a pathway for naive and CM T cell populations to perform a task more commonly associated with innate immune cells, suggesting an evolutionary link.

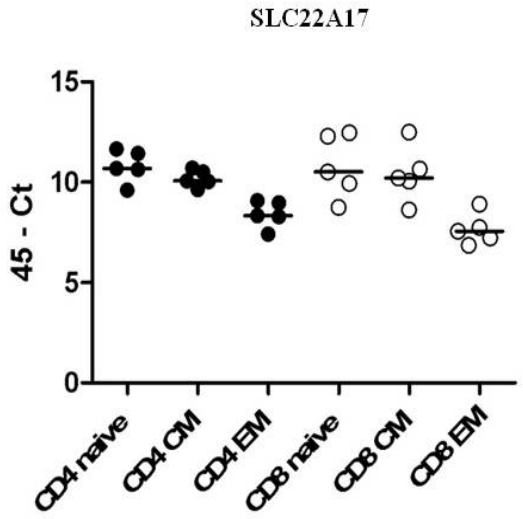

Figure 4.9. SLC22A17 gene expression is lowest on EM $CD4^+$ and $CD8^+$ T cell populations. SLC22A17 encodes the receptor for lipocalin 2, which is involved in iron trafficking.

Microarray analysis identified CXCR5 as a differentially expressed gene when comparing the three differentiation states within the $CD4^+$ compartment as well as in the comparison between $CD4^+$ naive T cells and $CD4^+$ CM T cells. Its expression was found to be highest on

$CD4^+$ CM T cells. CXCR5 is the chemokine receptor for CXCL13 which is expressed on all B cells as well as on $CD4^+$ follicular helper cells (T_{FH}). T_{FH} cells can be found within the B cell area of secondary lymphoid organs where they help generate an effective B cell response by supporting antibody production and isotype class switching [58;158]. The Real Time PCR data for CXCR5 showed that the difference between $CD4^+$ naive and $CD4^+$ CM T cells identified in the array analysis is maintained, but it also shows that $CD8^+$ CM T cells also express high levels of CXCR5 (Fig. 4.10). The higher expression on $CD4^+$ CM T cells could correspond to the T_{FH} cell population, but the higher expression on $CD8^+$ CM T cells has not been described before. Quigley *et al* (2007) describe a $CD8^+CXCR5^+$ T cell population in human tonsil B cell follicles as well as peripheral blood which does not express any CCR7. They describe these cells as early effector cells because of the lack of CCR7 expression combined with their ability to produce IFNγ and GZMA. Stimulation of these cells *in vitro* led to the upregulation of receptors needed for interaction with B cells, such as CD70 and OX40. They found that $CD8^+CXCR5^+$ T cells could support tonsil B cell survival and IgG production [158]. The cell surface expression of CXCR5 on the $CCR7^+CD45RA^-CD8^+$ CM T cells will have to be analysed to examine whether the high expression found in the mRNA levels of these cells corresponds to the protein levels. If $CD8^+$ CM T cells indeed express high levels of CXCR5 on their cell surface, these $CD8^+CXCR5^+$ CM T cells could provide B cell help, as do T_{FH} cells; with the exception that $CD8^+CXCR5^+$ CM T cells will be able to respond to different antigens presented on MHC class I molecules as opposed to T_{FH} cells which respond to antigen presented on MHC class II molecules.

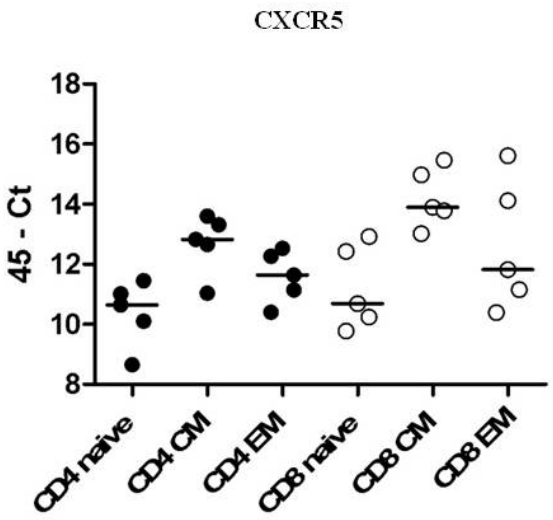

Figure 4.10. CXCR5 gene expression is highest on both $CD4^+$ and $CD8^+$ CM T cell populations. CXCR5 expression is associated with $CD4^+$ follicular T helper cells (T_{FH}).

The results in this Chapter show that the data collected through microarray analysis in Chapter 3 could be validated through Real Time PCR analysis, providing proof that more extensive analysis of the potential new target genes identified by microarray analysis is needed to ascertain their role in T cell biology.

Chapter Five

Expression of Tetraspanin Family Members on $CD4^+$ and $CD8^+$ T Cell Populations

5 EXPRESSION OF TETRASPANIN FAMILY MEMBERS ON CD4+ AND CD8+ T CELL POPULATIONS

5.1 Introduction

The purpose of analysing gene expression profiles of different subsets of T cell was to identify genes or gene families associated with specific subsets and which may be involved in differentiation of T cells and T cell function. Several family members of the tetraspanin family were identified by microarray and Real Time PCR as showing differential expression on $CD4^+$ and $CD8^+$ T cell subsets. Tetraspanins are a family of membrane spanning proteins, consisting of 33 family members in humans and mouse [73;74]. They consist of four transmembrane domains, a small and a large extracellular loop and two short intracellular amino and carboxyl tails. Many tetraspanins are posttranslationally modified by the addition of palmitate to the cysteine residues closest to the membrane. This addition of palmitate allows the formation of tetraspanin-enriched microdomains (TEMs) at the cell surface. Tetraspanins have been implicated in having a role in many biological functions, such as cell activation, membrane fusion, adhesion, differentiation and metastasis [78;79;80;81;82]. CD9 has been described to be involved in membrane fusion, metastasis suppression and sperm-egg fusion [80;81;83] and CD81 in cell migration, hepatitis C infection and also membrane fusion [84] [80] [85] [89]. CD63 is highly expressed on late endosomes and exosomes [78]. Several binding partners which tetraspanins associate with on the cell surface have been identified; Yanez-Mo *et al* (2008) showed direct association of CD9 with ICAM-1 as well as recruitment of VCAM-1 into TEMs by its association with CD151 [87;88]. CD151 is also described to associate with

α3β1 and α6β4 and by doing so is involved in regulating integrin-dependent cell morphology, migration and adhesion [86].

In the previous chapters various members of the tetraspanin family showed differential expression based on their mRNA in T cell populations. Using microarray analysis tetraspanin18 was shown to consistently be able to distinguish between $CD4^+$ and $CD8^+$ T cell populations. We wished to determine whether the surface expression of tetraspanins corresponded to the mRNA data from the microarray and Real Time PCR; to date however there is no working monoclonal or polyclonal antibody against tetraspanin18. I therefore analysed the cell surface expression of the tetraspanin family members where antibodies were available. The analysis of tetraspanin family member gene expression via Real Time PCR indicated that CD81 and CD82 showed differential gene expression along the T cell differentiation pathway, therefore antibodies against these tetraspanins were included in the flow cytometry analysis. Antibodies against CD9, CD37, CD53, CD63 and CD151 were also included. CD53, like CD63 has been described in the endocytic pathway [8]. CD9 was found to show a biphasic expression on both $CD4^+$ and $CD8^+$ T cell populations and therefore the possible function of CD9 on T cells was also examined.

5.2 Results

5.2.1 Expression of tetraspanin CD9 on human $CD4^+$ and $CD8^+$ T cell populations is biphasic

Peripheral Blood Mononuclear Cells (PBMC) were isolated from fresh heparinised blood. The cells were subsequently stained for the markers CD4, CD8, CCR7, CD45RA and CD9 and analysed by flow cytometry. Fig. 5.1 shows the expression levels of CD9 on $CD4^+$ T cell populations based on CCR7 and CD45RA. As described above, the markers CCR7 and CD45RA allow the distinction of several T cell populations within the $CD4^+$ T cell compartment, namely naive ($CCR7^+CD45RA^+$), central memory ($CCR7^+CD45RA^-$) and effector memory ($CCR7^-CD45RA^-$). The top part of Fig. 5.1 shows representative plots showing the gating strategy used to analyse the data. The percentage CD9 positive cells in each differentiation state (based on an isotype control) varied between donors, however a trend can be detected showing that the CM population has the lowest level of expression compared to the naive and EM populations (Fig. 5.3).

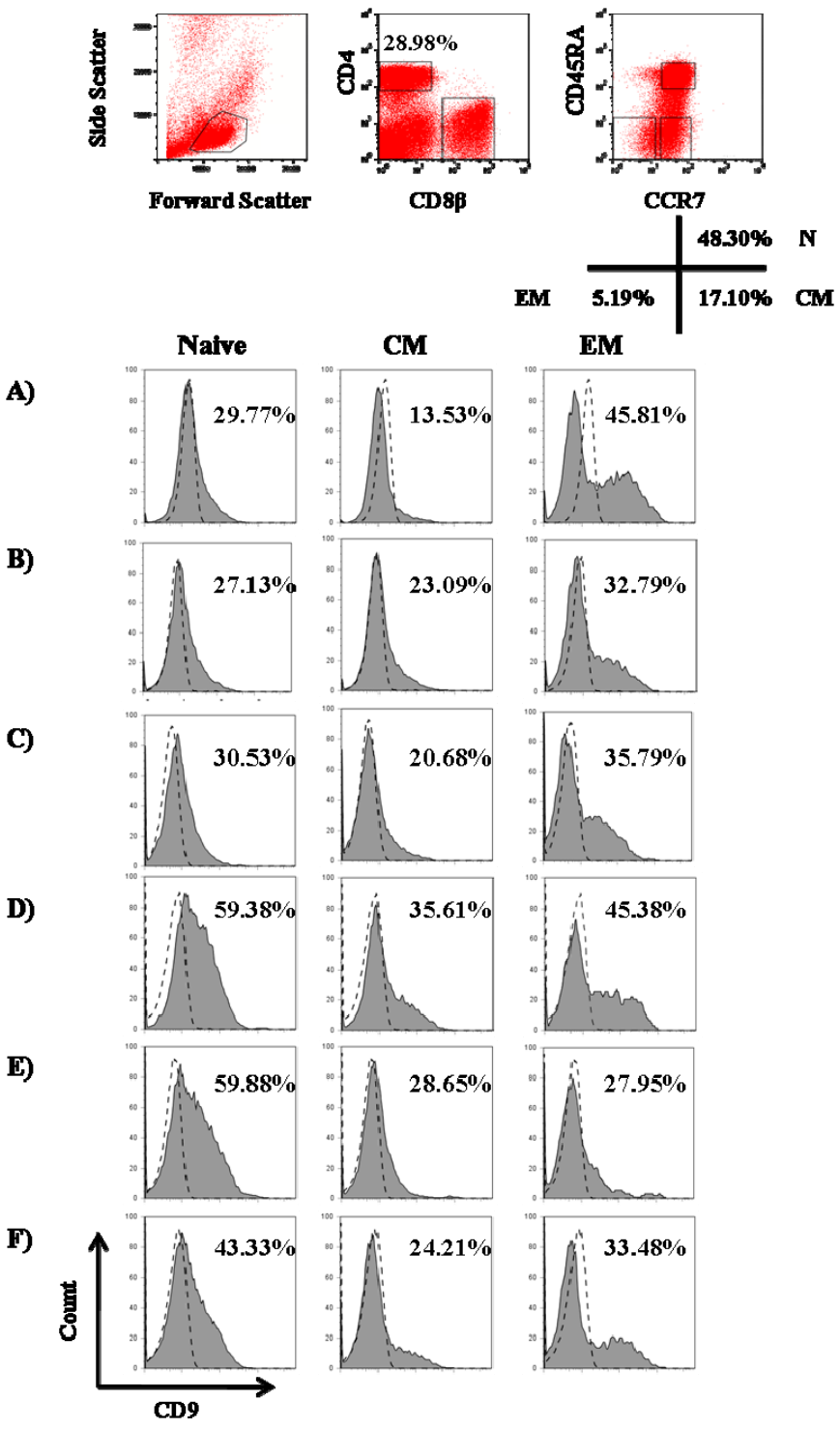

Figure 5.1. CD9 expression on CD4$^+$ T cell populations is varied between donors as well as differentiation states. CD9 expression on CD4$^+$ T cell populations was analysed by FACS for six different donors, the letters A-F denote the 6 different donors, percentage positive cells based on isotype control, indicated by dotted line.

Fig. 5.2 shows the expression levels of CD9 on $CD8^+$ T cell populations based on CCR7 and CD45RA. Again some variation can be seen in the expression levels of CD9 on the four differentiation states between the six donors, however a trend can be seen in which CD9 expression goes down as the cells differentiate. The naive population has the highest expression levels, the CM and EM populations show similar levels of expression and the EMRA population expresses the least CD9 on its cell surface (Fig. 5.3). The change in CD9 expression between the naive and EMRA populations of the $CD8^+$ T cell compartment is statistically significant as determined by Kruskal-Wallis test with a Dunns post test (p=0.0154 for change in MFI and p=0.0051 for change in percentage positive cells).

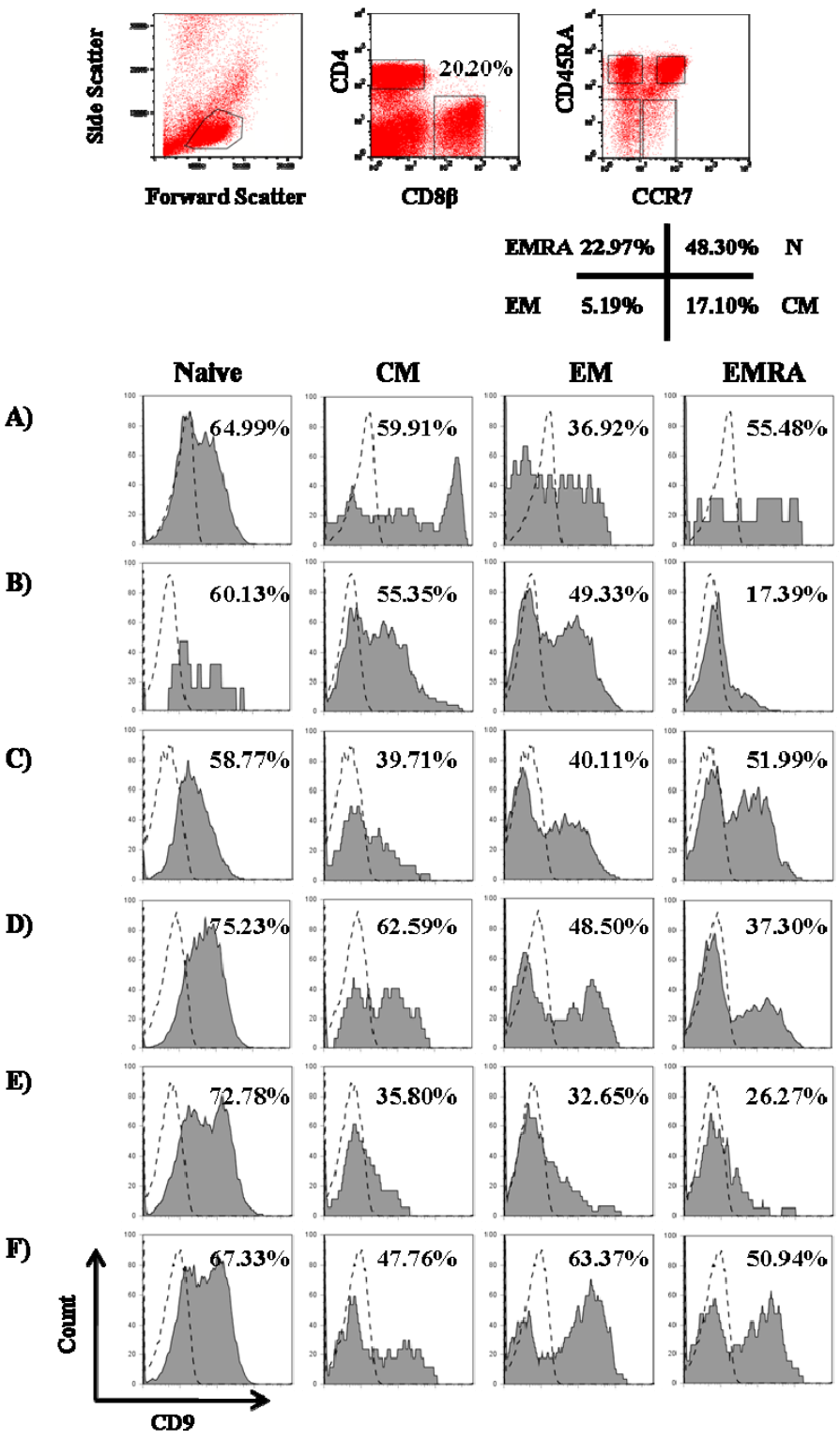

Figure 5.2. CD9 expression on CD8$^+$ T cell populations is varied between donors as well as differentiation states. CD9 expression on CD8$^+$ T cell populations was analysed by FACS for six different donors, the letters A-F denote the 6 different donors, percentage positive cells based on isotype control, indicated by dotted line.

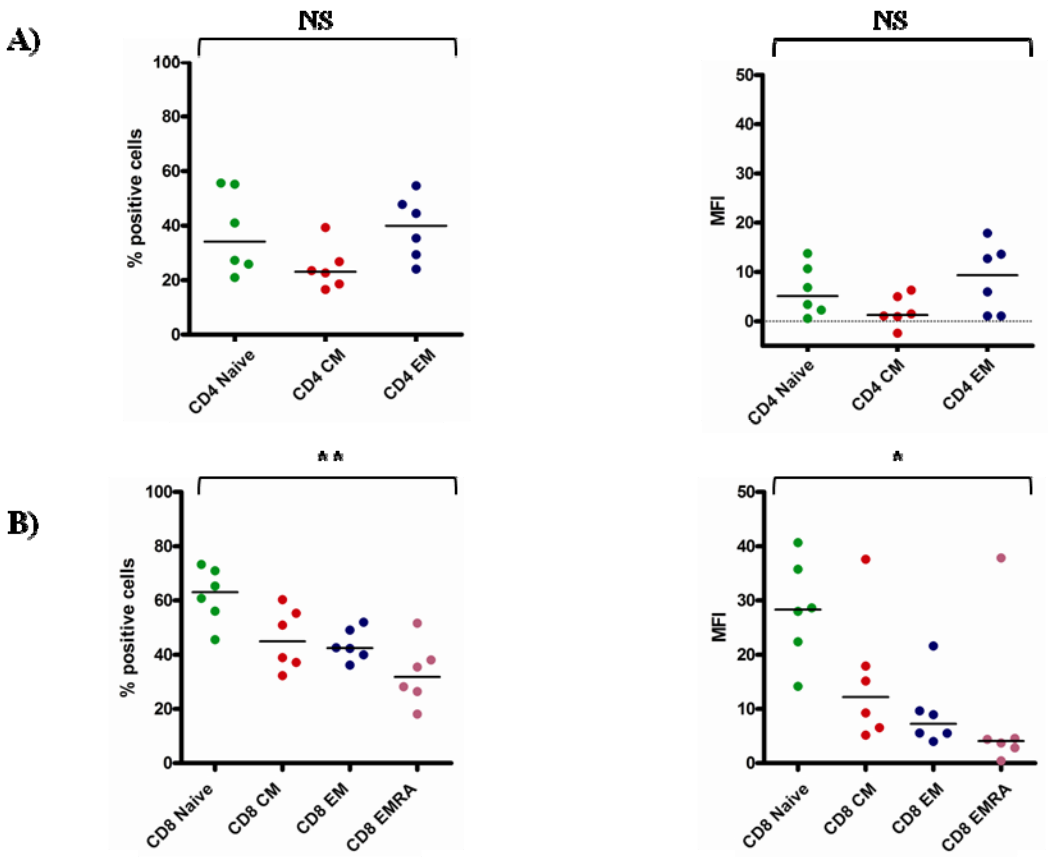

Figure 5.3. CD9 expression on CD4+ and CD8 + T cell populations is varied between differentiation states. The statistical significant differences were identified by Kruskal-Wallis with a Dunns post test. **A)** The percentage of CD9 positive cells and the mean fluorescence intensity (MFI) in the CD4+ T cell populations. **B)** The percentage of CD9 positive cells and the mean fluorescence intensity (MFI) in the CD8+ T cell populations (*=*p* 0.0154, **=*p* 0.0051).

5.2.2 CD37 is not expressed on $CD4^+$ and $CD8^+$ T cell populations

Fig. 5.4A shows representative plots for the CD37 expression on $CD4^+$ T cell populations. The top part of the figure shows the gating strategy used to analyse the data, cells were gated on their forward and side scatter profiles and subsequently on their CD4, CD45RA and CCR7 expression. As can be seen in the figure, the $CD4^+$ T cells do not express any CD37 on their cell surface (compared to the isotype control). Fig. 5.4B shows representative plots for the

expression of CD37 on CD8 T cell populations and as was the case with the $CD4^+$ populations, the $CD8^+$ T cells do not express any CD37 on their cell surface.

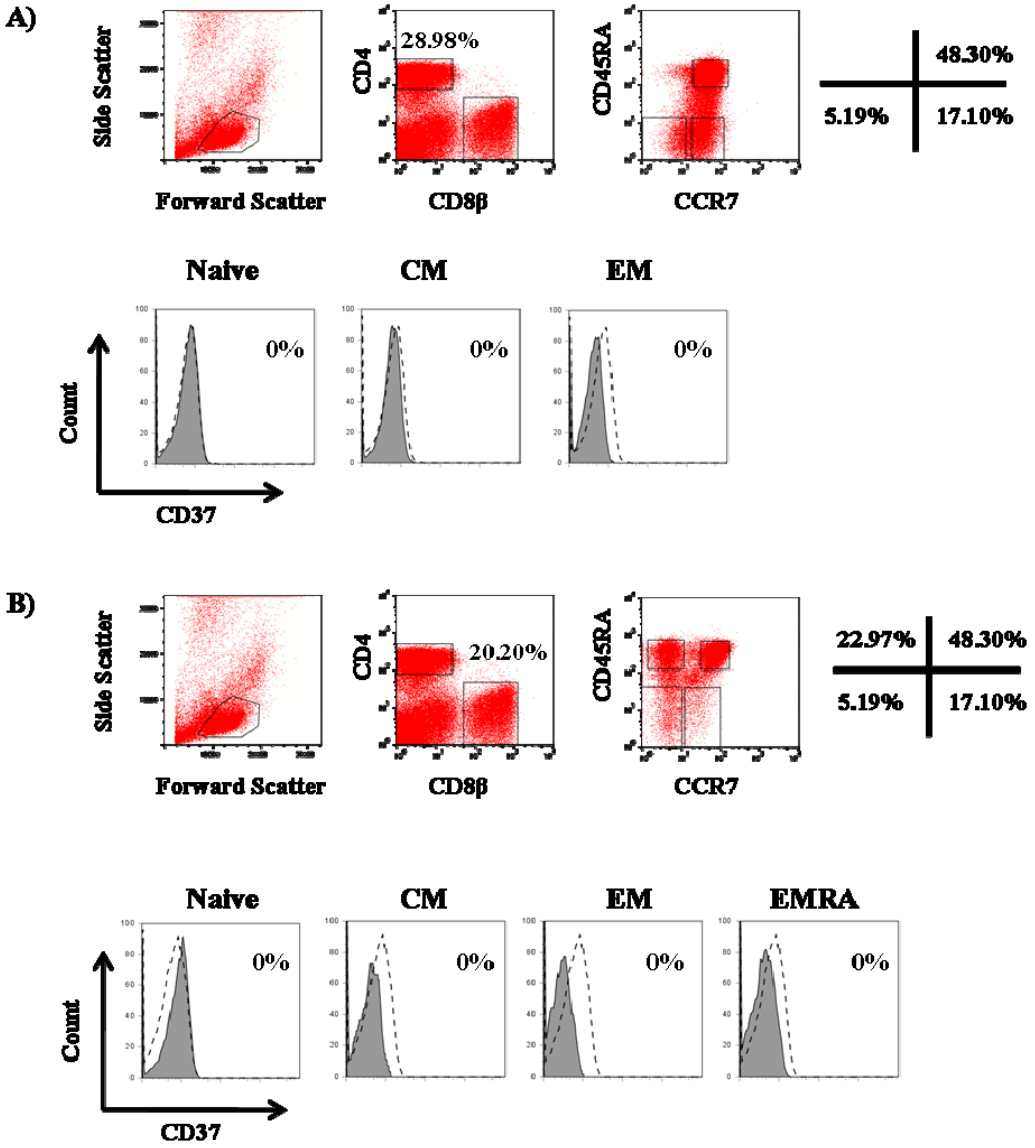

Figure 5.4. CD37 is not expressed on $CD4^+$ and $CD8^+$ T cell populations. CD37 expression on $CD4^+$ and $CD8^+$ T cell populations was analysed by FACS for six different donors, percentage positive cells based on isotype control, indicated by dotted line. **A)** Representative plot showing the CD37 expression on $CD4^+$ T cell populations. **B)** Representative plot showing the CD37 expression on $CD8^+$ T cell populations.

5.2.3 CD53 and CD63 expression on $CD8^+$ T cell populations increases during differentiation

Fig. 5.5A shows representative plots for the CD53 expression on $CD4^+$ T cell populations. The top part of the figure shows the gating strategy used to analyse the data, cells were gated on their forward and side scatter profiles and subsequently on their CD4, CD45RA and CCR7 expression. The CD53 expression on $CD4^+$ T cells seemed stable during differentiation (Fig. 5.6A). Fig. 5.5B shows the CD53 expression on $CD8^+$ T cell populations and the expression of CD53 on the cell surface seemed to increase as the cells become more differentiated (Fig. 5.6). The increase in CD53 expression on the $CD8^+$ T cells as they differentiate from naive to the EM and EMRA populations is statistically different, as determined by Kruskall-Wallis with a Dunns post test (p=0.0119 for change in MFI and p=0.0107 for change in percentage positive cells).

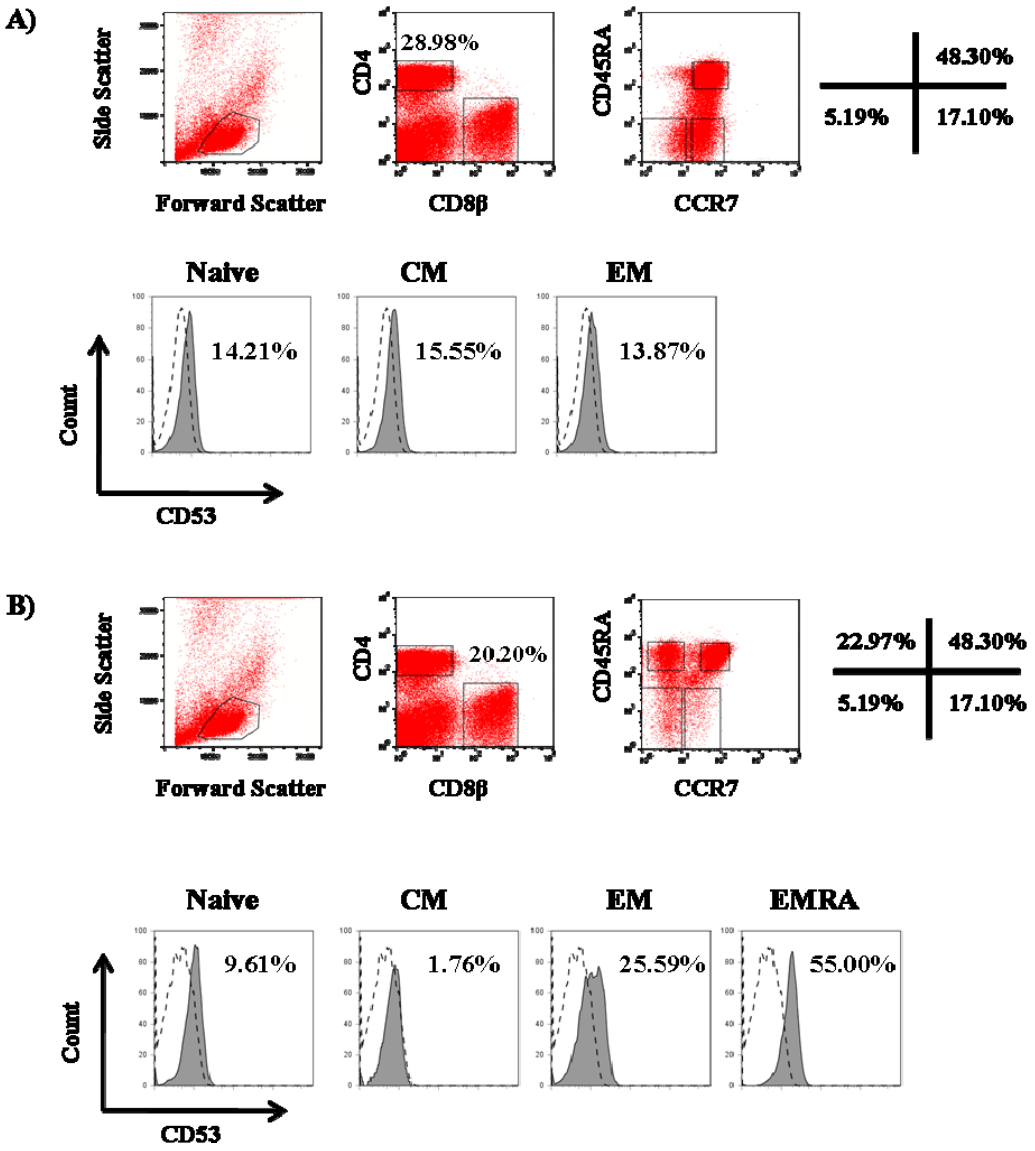

Figure 5.5. CD53 expression on $CD4^+$ and $CD8^+$ T cell populations. CD53 expression on $CD4^+$ and $CD8^+$ T cell populations was analysed by FACS for six different donors, percentage positive cells based on isotype control, indicated by dotted line. **A)** Representative plot showing the CD53 expression on $CD4^+$ T cell populations. **B)** Representative plot showing the CD53 expression on $CD8^+$ T cell populations.

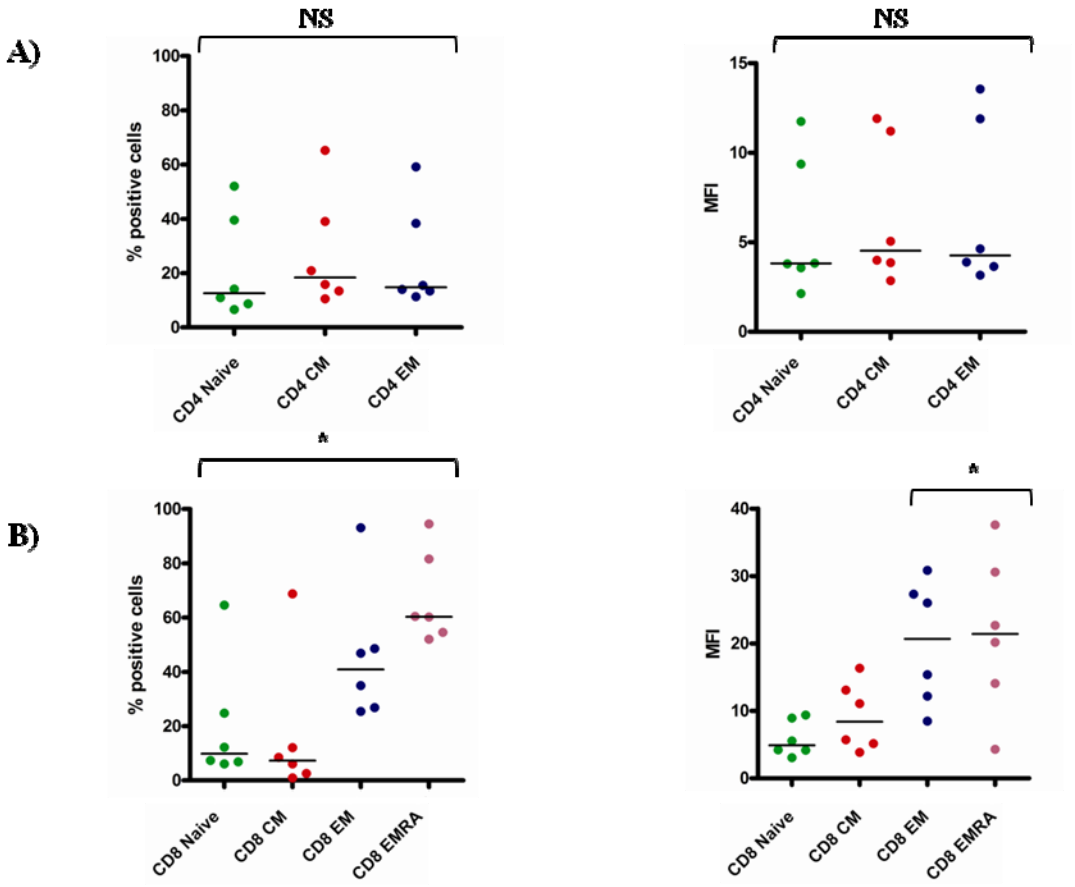

Figure 5.6. CD53 expression on CD4$^+$ T cell populations stays similar as the cells differentiate, but the expression increases during differentiation on CD8$^+$ T cell populations. The statistical significant differences were identified by Kruskal-Wallis with a Dunns post test. **A)** The percentage of CD53 positive cells and the mean fluorescence intensity (MFI) in the CD4$^+$ T cell populations. **B)** The percentage of CD53 positive cells and the mean fluorescence intensity (MFI) in the CD8$^+$ T cell populations (*=*p* 0.0107 for % positive cells, *=*p* 0.0119 for MFI).

Fig. 5.7A shows representative plots for the CD63 expression on CD4$^+$ T cell populations. The top part of the figure shows the gating strategy used to analyse the data, cells were gated on their forward and side scatter profiles and subsequently on their CD4, CD45RA and CCR7 expression. The expression of CD63 on the cell surface of CD4$^+$ T cells seemed stable during differentiation (percentage positive cells and MFI represented in Fig. 5.8A). As was the case with the CD53 expression on CD4$^+$ T cells, the MFI of the populations did not change as the cells differentiated (Fig. 5.8A). Fig. 5.7B shows that CD63 expression on the cell surface of

$CD8^+$ T cell populations showed a slight increase as the cells become more differentiated, however this increase seen in the percentage $CD63^+$ cells is not significant (Fig. 5.8A). The slight increase in both percentage of positive cells and MFI on the more differentiated $CD8^+$ T cell populations is not a statistically significant increase.

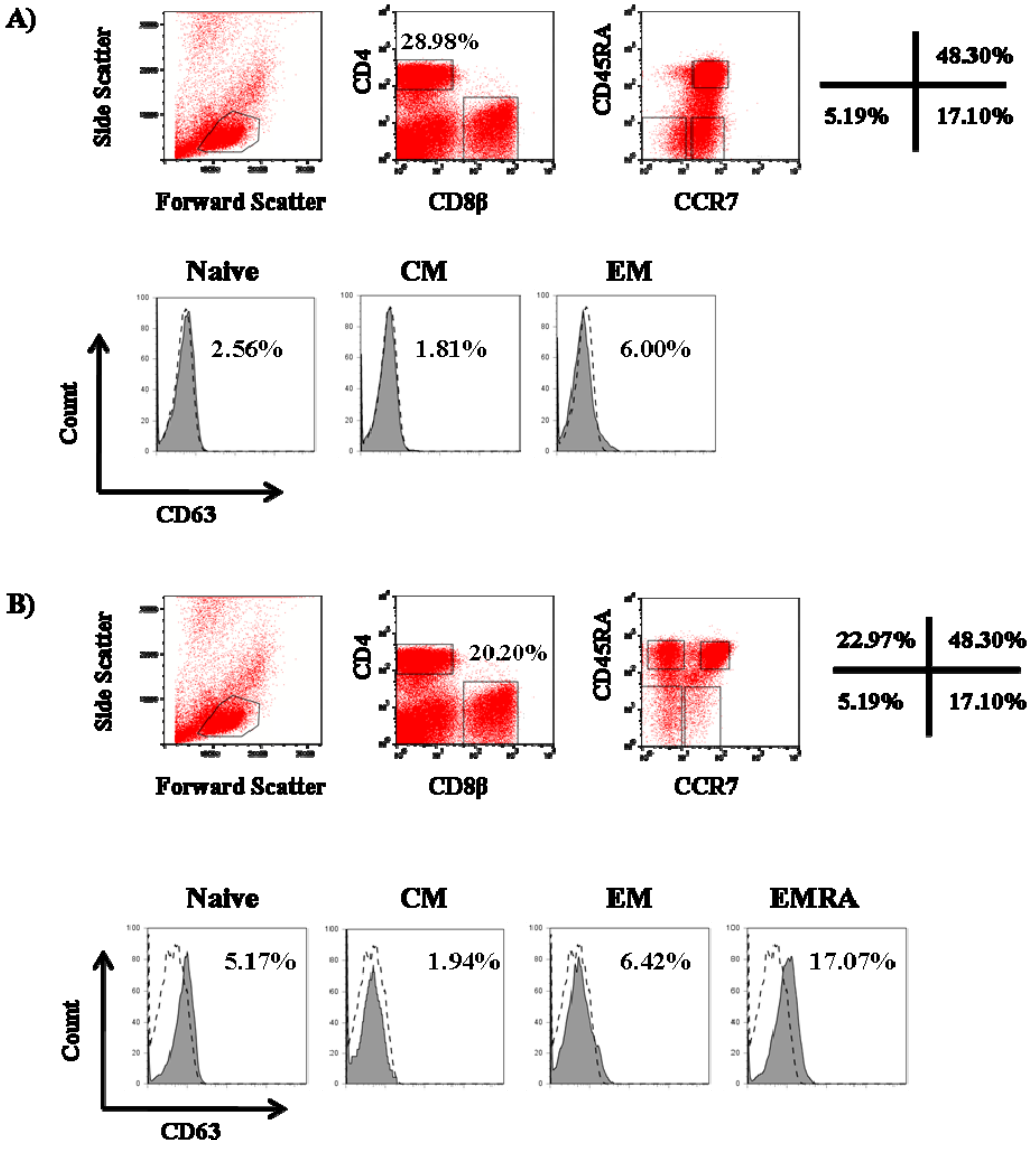

Figure 5.7. CD63 is expressed at low levels on $CD4^+$ and $CD8^+$ T cell populations. CD63 expression on $CD4^+$ and $CD8^+$ T cell populations was analysed by FACS for six different donors, percentage positive cells based on isotype control, indicated by dotted line. **A)** Representative plot showing the CD63 expression on $CD4^+$ T cell populations. **B)** Representative plot showing the CD63 expression on $CD8^+$ T cell populations.

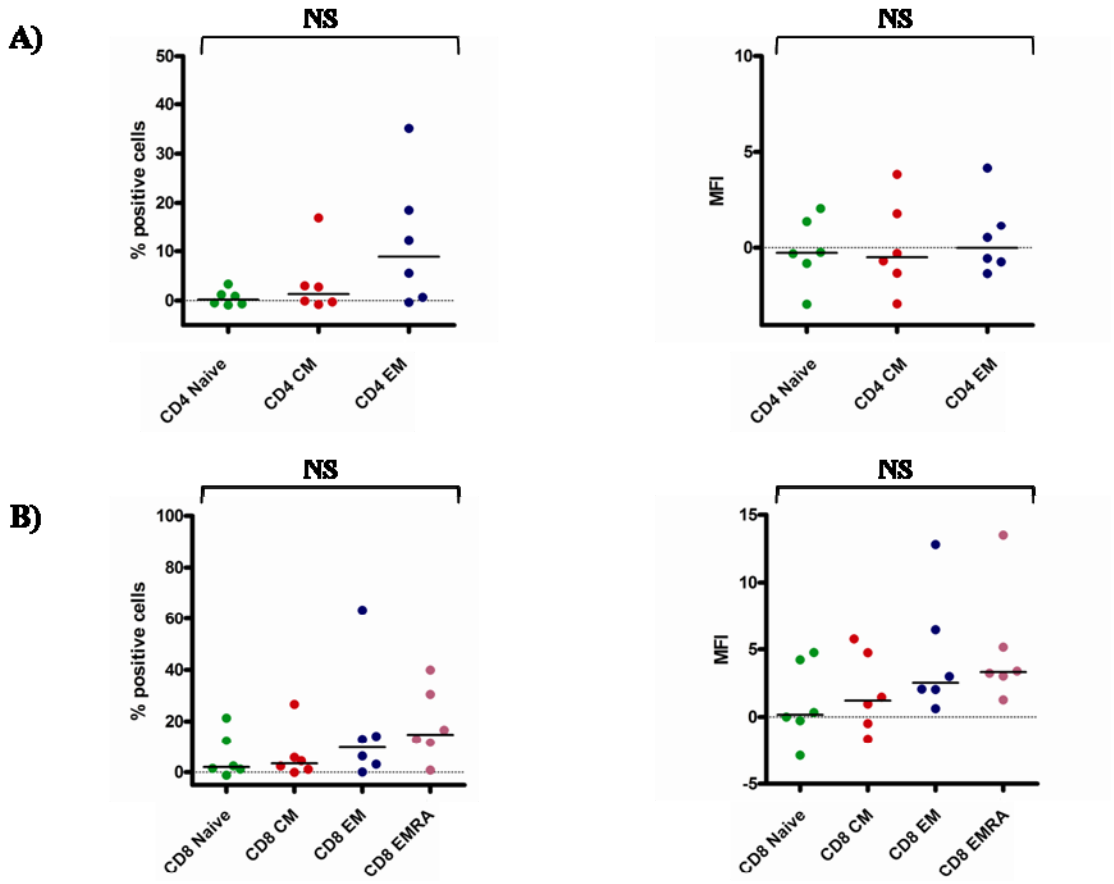

Figure 5.8. CD63 expression on $CD4^+$ T cell populations stays similar as the cells differentiate, but the expression increases during differentiation on $CD8^+$ T cell populations. The statistical significant differences were identified by Kruskal-Wallis with a Dunns post test.. **A)** The percentage of CD63 positive cells and the mean fluorescence intensity (MFI) in the $CD4^+$ T cell populations. **B)** The percentage of CD63 positive cells and the mean fluorescence intensity (MFI) in the $CD8^+$ T cell populations.

5.2.4 CD81 is expressed at high levels in both $CD4^+$ and $CD8^+$ T cell populations

Fig. 5.9A shows representative plots for the CD81 expression on $CD4^+$ T cell populations. The top part of the figure shows the gating strategy used to analyse the data, cells were gated on their forward and side scatter profiles and subsequently on their CD4, CD45RA and CCR7 expression. The CD81 expression on $CD4^+$ T cells seemed to stay stable as the cells differentiated (Fig. 5.10A). Fig. 5.9B shows the expression of CD81 on $CD8^+$ T cell populations. The $CD8^+$ T cells show a slight increase in CD81 expression as they differentiated (percentage positive cells and MFI shown in Fig. 5.10B). No statistical difference could be found in the percentage positive cells comparing all populations. The change in MFI between naive and EM populations is statistically different (Kruskal-Wallis with a Dunns post test, p=0.0383), however the median values between the more differentiated CM, EM and EMRA populations did not differ much.

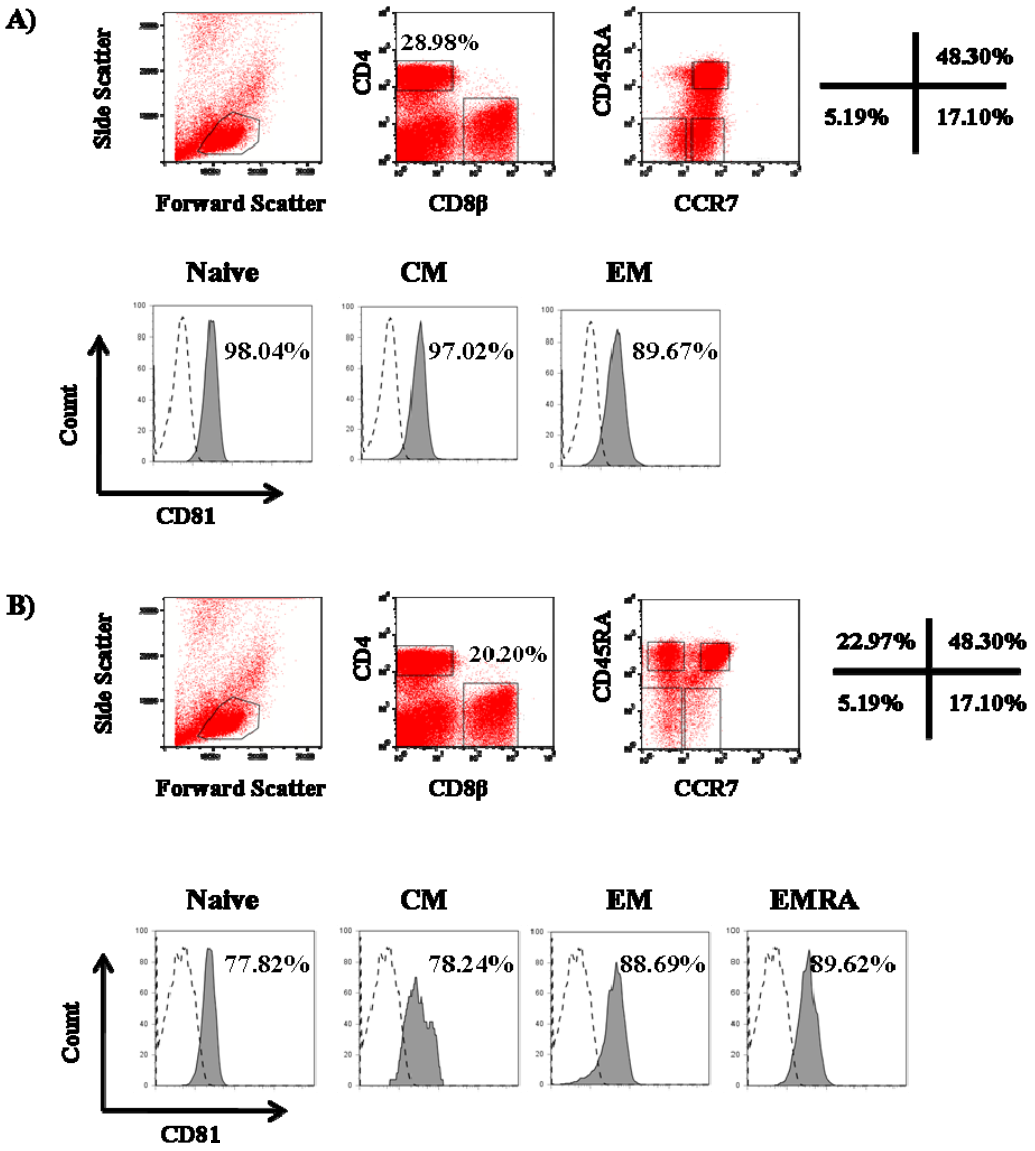

Figure 5.9. CD81 is expressed at high levels both on $CD4^+$ and $CD8^+$ T cell populations. CD81 expression on $CD4^+$ and $CD8^+$ T cell populations was analysed by FACS for six different donors, percentage positive cells based on isotype control, indicated by dotted line. **A)** Representative plot showing the CD81 expression on $CD4^+$ T cell populations. **B)** Representative plot showing the CD81 expression on $CD8^+$ T cell populations.

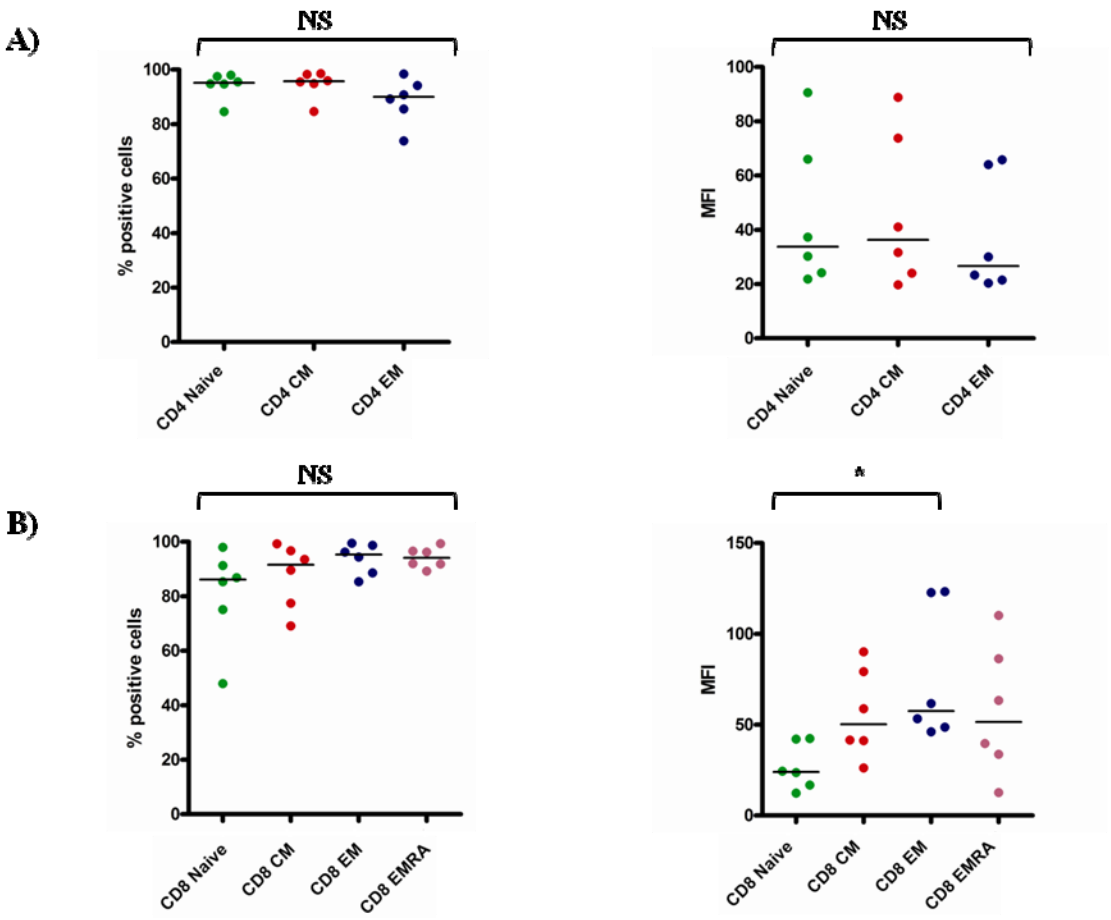

Figure 5.10. CD81 is expressed at high levels in both $CD4^+$ and $CD8^+$ T cell populations. The statistical significant differences were identified by Kruskal-Wallis with a Dunns post test. **A)** The percentage of CD81 positive cells and the mean fluorescence intensity (MFI) in the $CD4^+$ T cell populations. **B)** The percentage of CD81 positive cells and the mean fluorescence intensity (MFI) in the $CD8^+$ T cell populations (*=*p* 0.0383).

5.2.5 CD82 is expressed at very high levels on $CD4^+$ T cell populations and its expression decreases on $CD8^+$ T cells as they differentiate

Fig. 5.11A shows representative plots for the CD82 expression on $CD4^+$ T cell populations. The top part of the figure shows the gating strategy used to analyse the data, cells were gated on their forward and side scatter profiles and subsequently on their CD4, CD45RA and CCR7 expression. The percentage CD82 positive cells was ≥ 95% on all three differentiation states, however the amount of CD82 expressed on the cell surface of CD82 positive cells (represented by the MFI) showed lowest expression of CD82 on the naive population, whereas the CM and EM populations showed the highest MFI (Fig. 5.12A). The change in CD82 expression on the $CD4^+$ T cells as they differentiate from naive to the CM and EM populations is statistically different, as determined by Kruskall-Wallis with a Dunns post test (p=0.00097 for change in MFI and p=0.0008 for change in percentage positive cells). Fig. 5.11B shows the CD82 expression on $CD8^+$ T cell populations and the expression of CD82 seemed to decrease as the cells differentiate. Both the percentage positive cells and the MFI readings showed the highest expression levels of CD82 on the CM population and the lowest expression on the EMRA population (Fig. 5.12B). The change in CD82 expression between the CM and EMRA $CD8^+$ T cells is statistically different, as determined by Kruskall-Wallis with a Dunns post test (p=0.0035 for change in MFI and p=0.0004 for change in percentage positive cells).

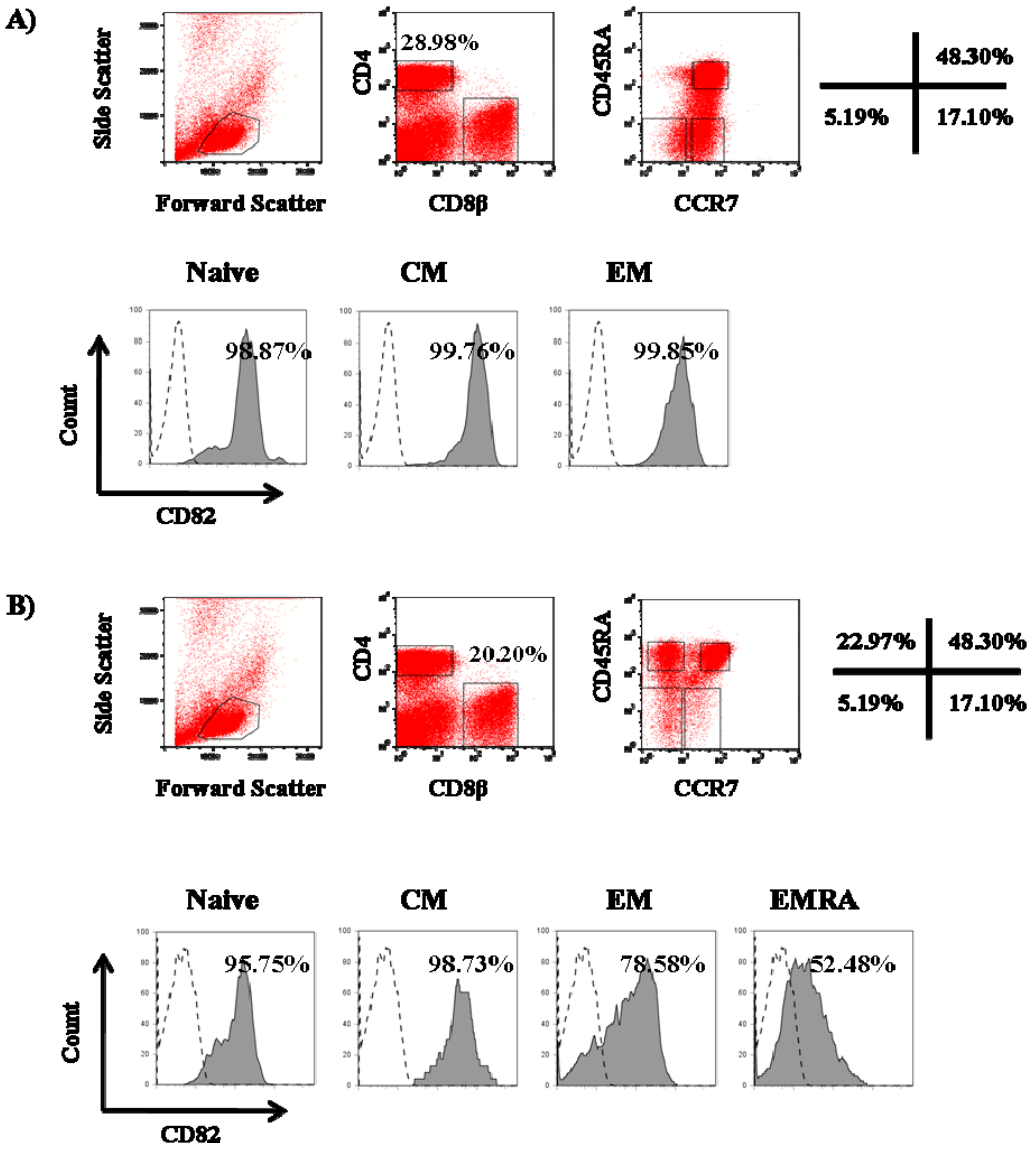

Figure 5.11. CD82 is expressed at high levels on both $CD4^+$ and $CD8^+$ T cell populations. CD82 expression on $CD4^+$ and $CD8^+$ T cell populations was analysed by FACS for six different donors, percentage positive cells based on isotype control, indicated by dotted line. **A)** Representative plot showing the CD82 expression on $CD4^+$ T cell populations. **B)** Representative plot showing the CD82 expression on $CD8^+$ T cell populations.

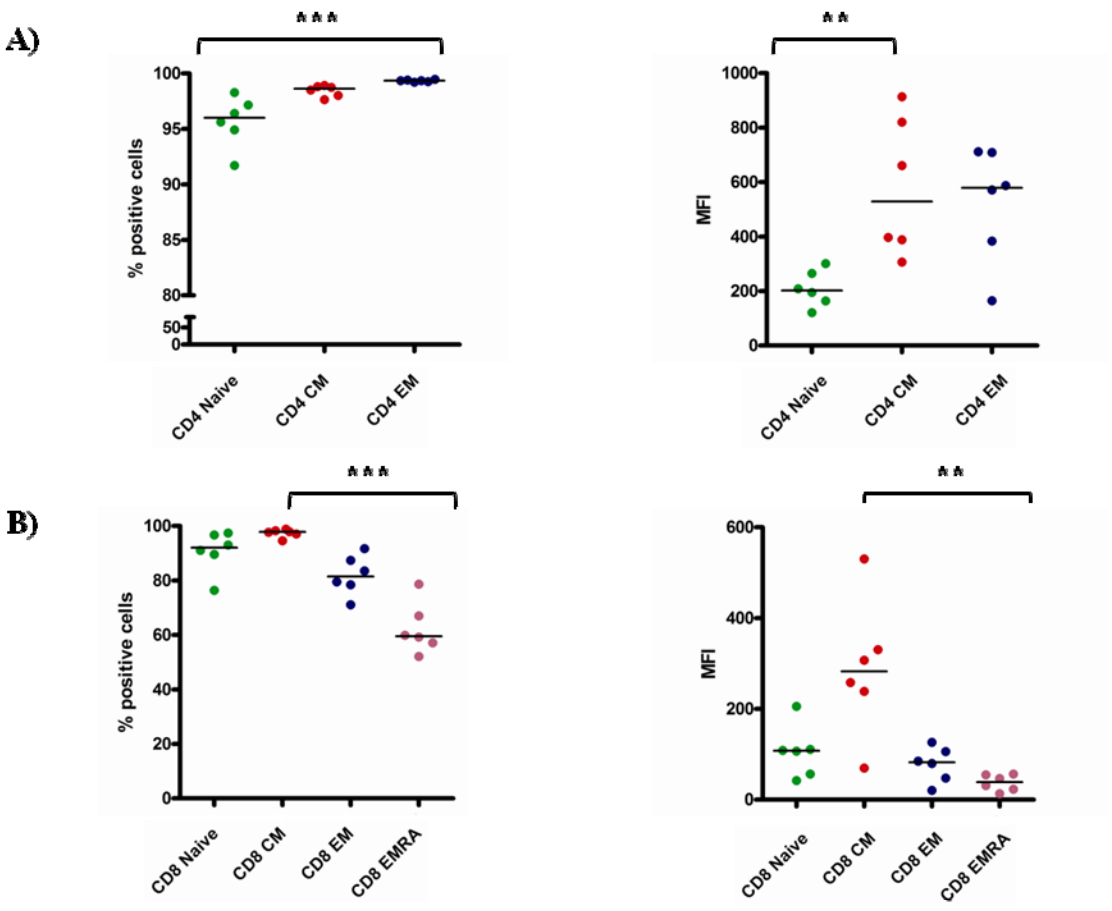

Figure 5.12. CD82 is expressed at very high levels on CD4$^+$ T cell populations and its expression decreases on CD8$^+$ T cells as they differentiate. The statistical significant differences were identified by Kruskal-Wallis with a Dunns post test. **A)** The percentage of CD82 positive cells and the mean fluorescence intensity (MFI) in the CD4$^+$ T cell populations (**=*p* 0.0097, ***=*p* 0.0008). **B)** The percentage of CD82 positive cells and the mean fluorescence intensity (MFI) in the CD8$^+$ T cell populations (**=*p* 0.0035, ***=*p* 0.0004).

5.2.6 CD151 expression is highest on $CD4^+$ and $CD8^+$ EM T cell populations

Fig. 5.13A shows representative plots for the CD151 expression on $CD4^+$ T cell populations. The top part of the figure shows the gating strategy used to analyse the data, cells were gated on their forward and side scatter profiles and subsequently on their CD4, CD45RA and CCR7 expression. The expression of CD151 on $CD4^+$ T cell populations is shown to go from almost no expression on $CD4^+$ naive T cells to > 40% positive cells in the EM population. The highest expression of CD151 could be found on the $CD4^+$ EM cells (Fig. 5.14). The change in CD151 expression on the $CD4^+$ T cells as they differentiate from naive to the EM and population is statistically different, as determined by Kruskall-Wallis with a Dunns post test (p=0.0043 for the change in percentage positive cells). The expression of CD151 on $CD8^+$ T cell populations showed a similar trend (Fig. 5.13B and 5.14B), although there seemed to be a bigger spread between donors in the $CD8^+$ compartment. The increase in CD151 expression on the $CD8^+$ T cells as they differentiate from naive to the EM population is statistically different, as determined by Kruskall-Wallis with a Dunns post test (p=0.0372 for change in MFI).

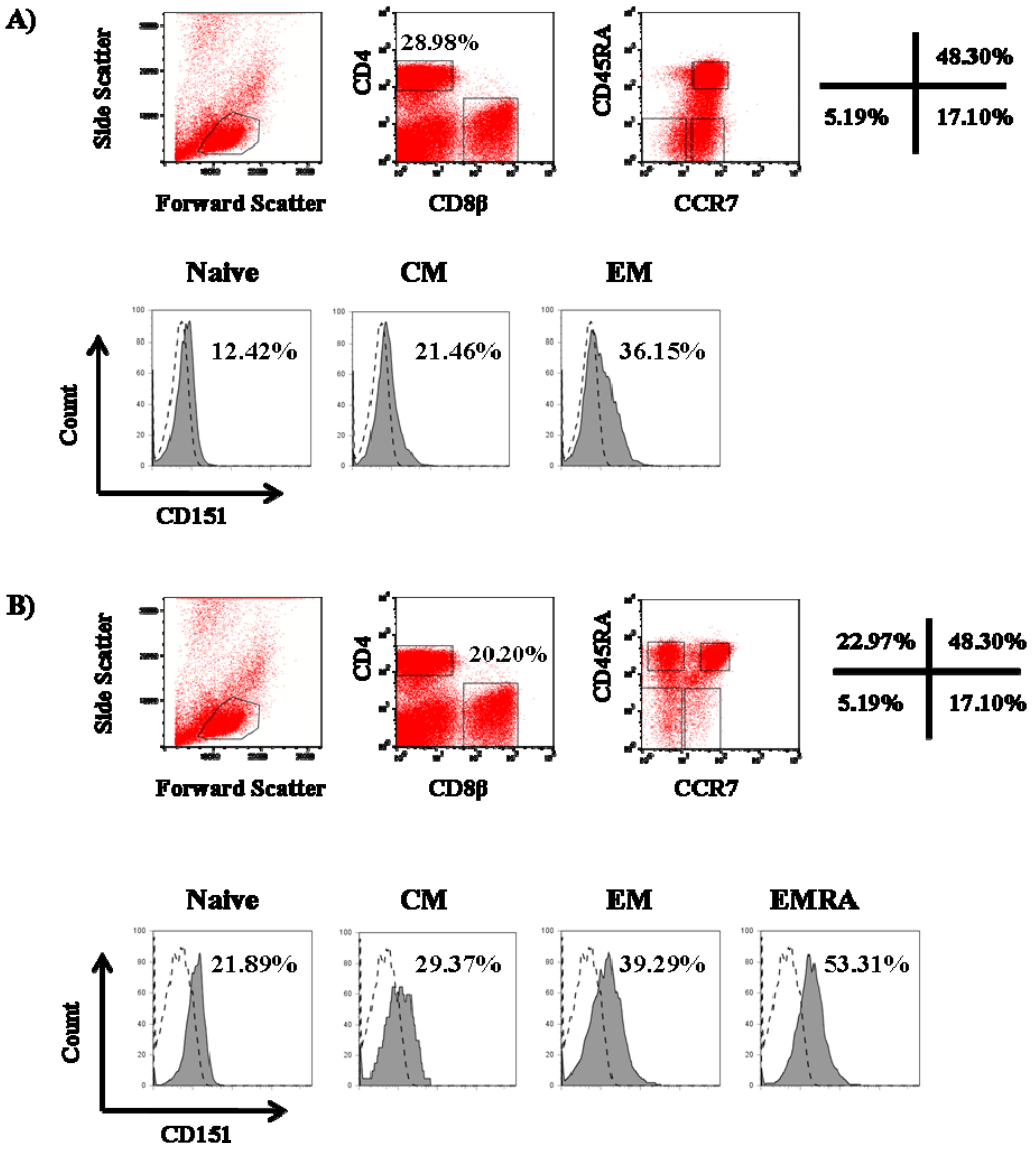

Figure 5.13. CD151 is expressed at low levels on both $CD4^+$ and $CD8^+$ T cell populations. CD151 expression on $CD4^+$ and $CD8^+$ T cell populations was analysed by FACS for six different donors, percentage positive cells based on isotype control, indicated by dotted line. **A)** Representative plot showing the CD151 expression on $CD4^+$ T cell populations. **B)** Representative plot showing the CD151 expression on $CD8^+$ T cell populations.

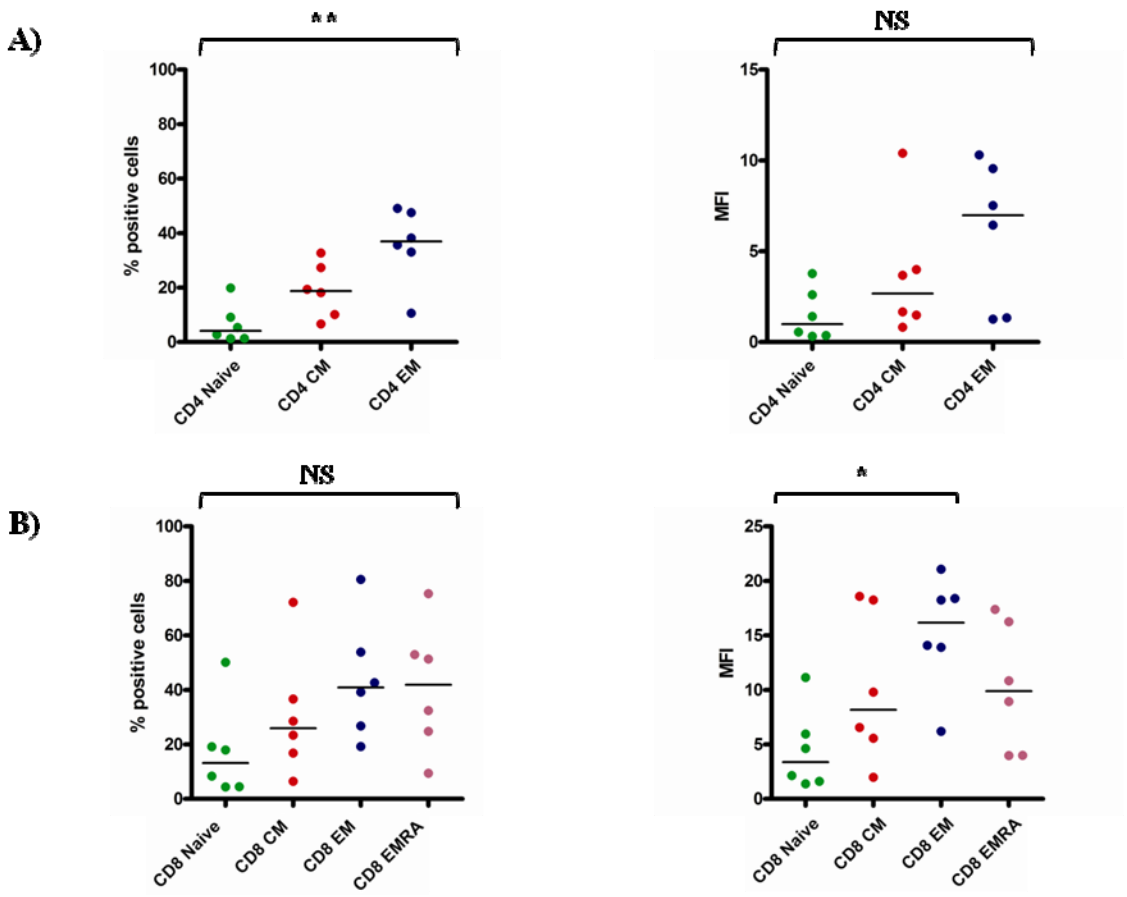

Figure 5.14. CD151 expression goes up in both CD4$^+$ and CD8$^+$ T cell populations as they differentiate. The statistical significant differences were identified by Kruskal-Wallis with a Dunns post test. **A)** The percentage of CD151 positive cells and the mean fluorescence intensity (MFI) in the CD4$^+$ T cell populations (**=*p* 0.0043). **B)** The percentage of CD151 positive cells and the mean fluorescence intensity (MFI) in the CD8$^+$ T cell populations (*=*p* 0.0372).

5.2.7 Expression of tetraspanins on the cell surface of $CD4^+$ or $CD8^+$ T cell populations is not altered when comparing populations based on CD27 and CD45RA or CCR7 and CD45RA

As described before different surface markers can be used to divide $CD4^+$ and $CD8^+$ T cell populations into several distinct differentiation states. CD27 is another marker which when used in conjunction with CD45RA describes naive, CM, EM and EMRA populations. To check if any difference in the expression of the tetraspanin panel could be found when using CD27 instead of CCR7 to divide the cells into the four populations, the cells were stained with both CCR7 and CD27 as well as CD4, CD8β and CD45RA. As can be seen in Fig. 5.15 and 5.16 the expression of the tetraspanins on the four populations for both $CD4^+$ and $CD8^+$ T cells follows the same expression pattern regardless of which antibody was used to identify the populations. This indicates that $CD4^+$ and $CD8^+$ populations based on CCR7 and CD27 are homogeneous in their tetraspanin expression and one can conclude from this that these two cell surface markers therefore are identifying the same populations.

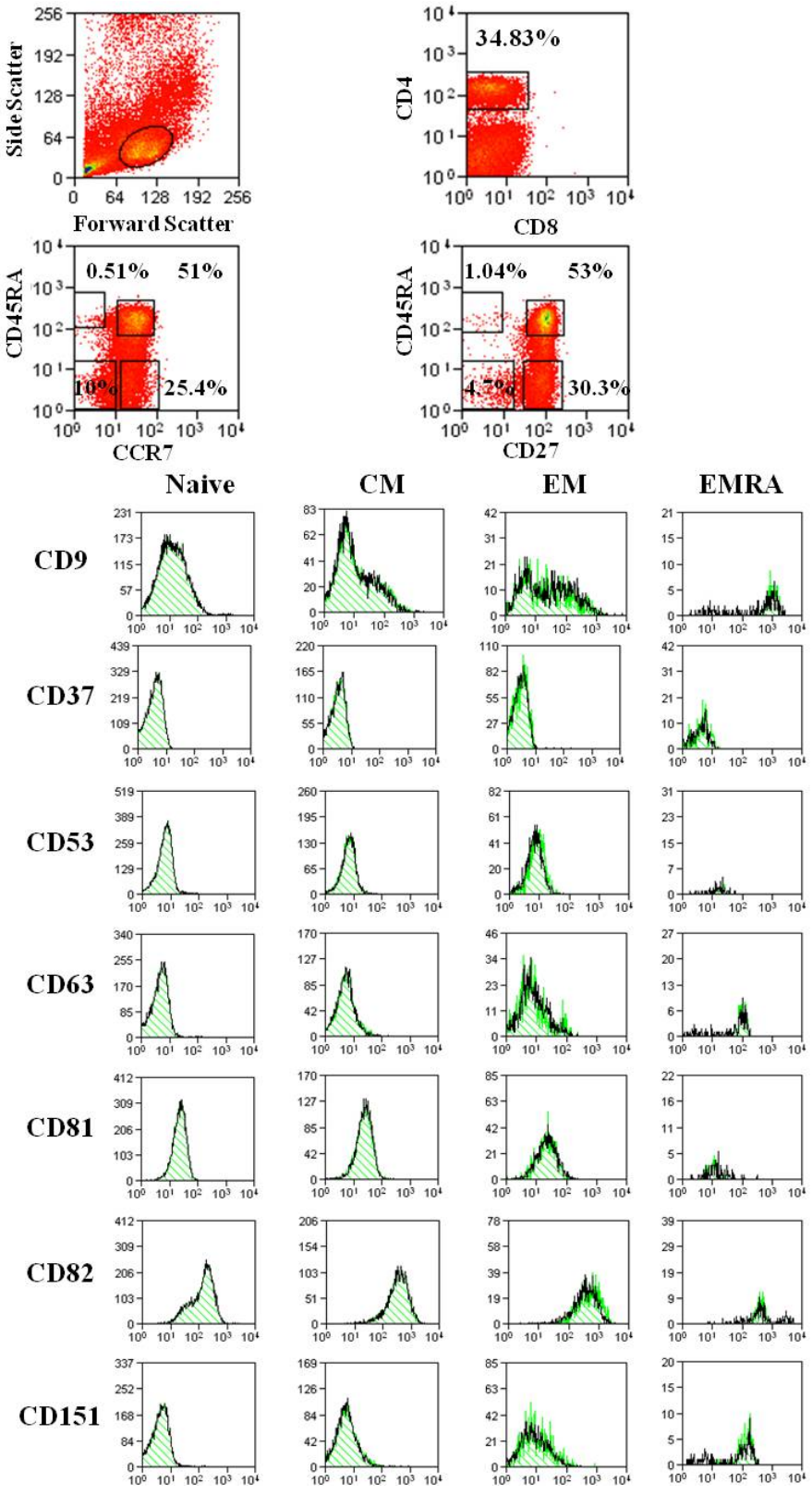

Figure 5.15. Tetraspanin expression on CD4$^+$ T cell populations based on CCR7 (black) or CD27 (green) does not differ. The expression of the different tertaspanins is the same in the populations based on CCR7 as in those based on CD27 expression.

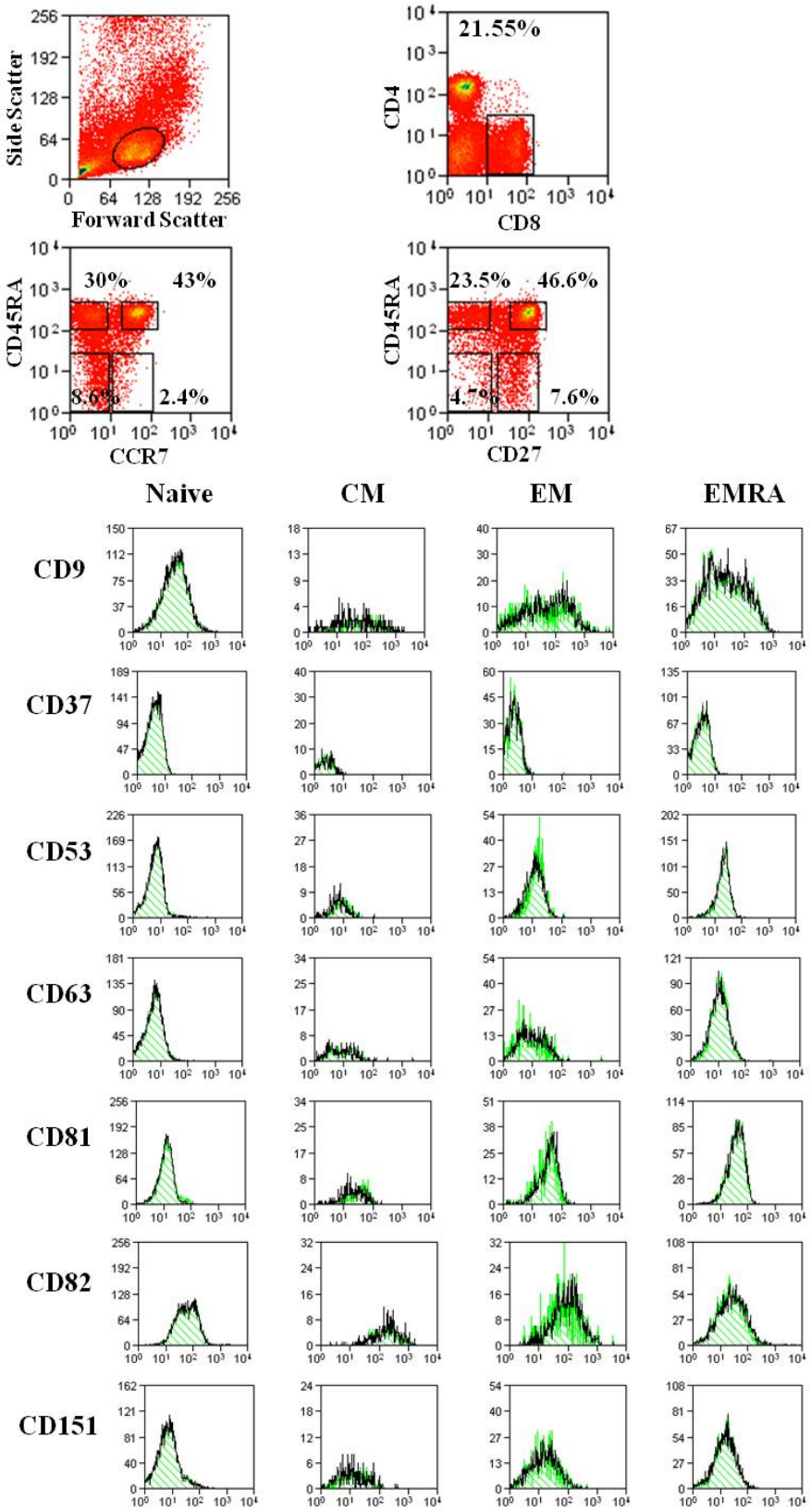

Figure 5.16. Tetraspanin expression on CD8$^+$ T cell populations based on CCR7 (black) or CD27 (green) does not differ. The expression of the different tertaspanins is the same in the populations based on CCR7 as in those based on CD27 expression.

5.2.8 CD9 negative and CD9 positive cells within $CD4^+$ and $CD8^+$ T cell populations do not differ in the ability to produce cytokines

To examine the possible consequence of the biphasic expression of CD9 on the different $CD4^+$ and $CD8^+$ T cell populations (Fig. 5.1 and 5.2), the ability of these cells to produce cytokines was tested. Six different donors were used, their PBMCs were stimulated with PMA/ionomycin in the presence of Brefeldin A for 3 hours after which they were fixed and permeabilised and the intracellular cytokines were detected using specific antibodies. The cytokines identified were IFN-γ, IL-17 and IL-22. Fig. 5.17A shows the flow cytometry from a representative donor for $CD4^+$ T cell populations. The top part of the figure shows the gating strategy used to analyse the data and the histograms show the expression of CD9 for the naive, CM and EM populations. The bottom part of Fig. 5.17A shows the expression of CD9 (x-axis) against IFN-γ (y-axis), as expected the ability to produce cytokine upon stimulation was lowest in the naive cells, increased in the CM and was highest in the EM cells. Fig. 5.17B shows the percentage IFN-γ production of CD9 negative cells and CD9 positive cells from all six donors. The figure shows that there is no significant difference in the ability of CD9 negative and CD9 positive T cells to produce cytokine within the $CD4^+$ compartment. The same trend was found for the ability of these cells to produce IL-17 and IL-22 (data not shown).

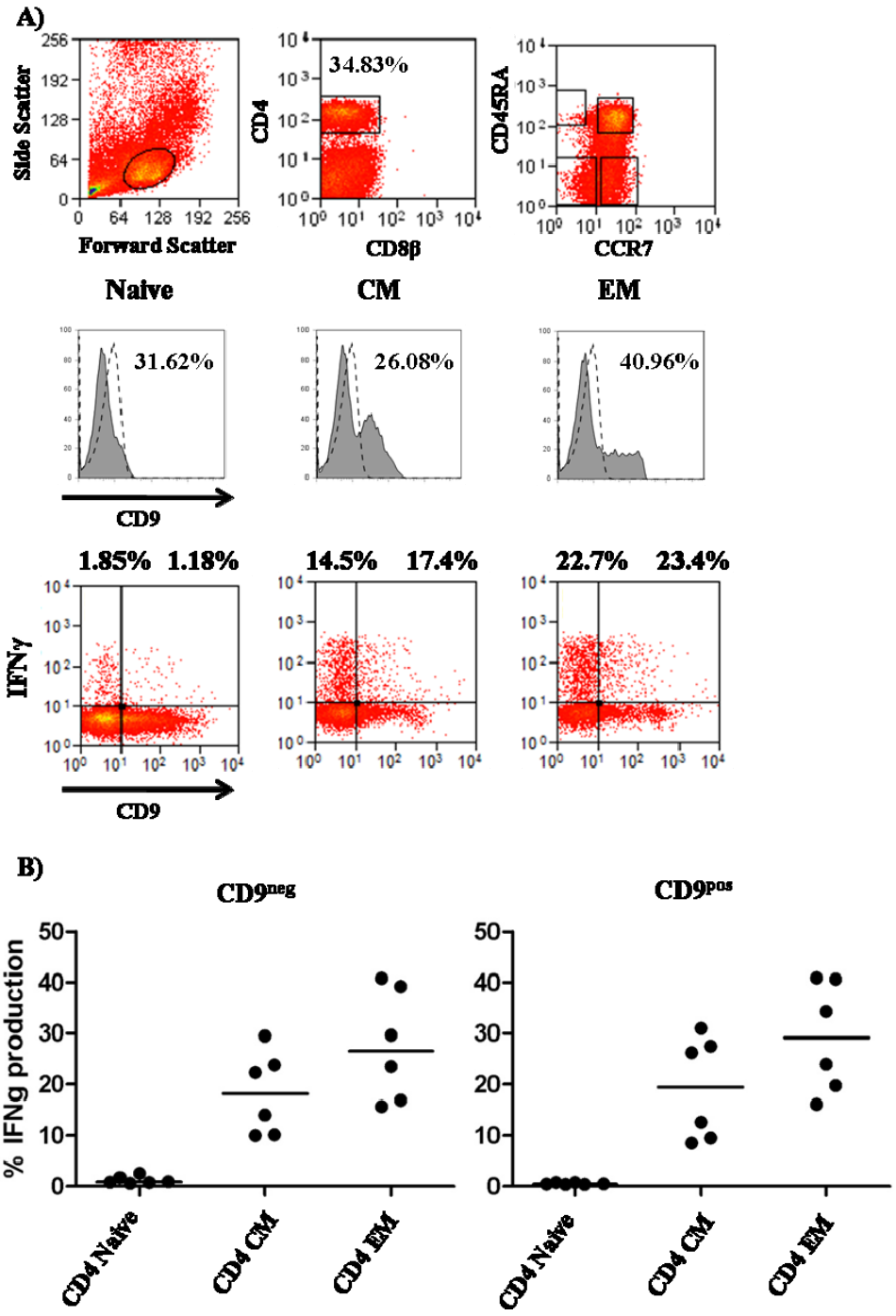

Figure 5.17. No difference between CD9 negative and CD9 positive cells IFN γ production in CD4$^+$ T cell populations. A) Representative plot (n=6) of the IFN γ production of CD9 negative and CD9 positive cells in CD4$^+$ T cell populations. Dotted line indicates isotype control. **B)** The percentage of IFN γ production in the CD9 negative (left) and CD9 positive cells (right) CD4$^+$ T cell populations.

Fig. 5.18A shows the flow cytometry stain from a representative donor for $CD8^+$ T cell populations. The top part of the figure shows the gating strategy used to analyse the data and the histograms show the expression of CD9 for the naive, CM, EM and EMRA populations. The bottom part of Fig. 5.18A shows the expression of CD9 (x-axis) against IFN-γ (y-axis), as can be seen the ability to produce cytokine upon stimulation was lowest in the naive cells, increased in the CM, was highest in the EM cells and dropped down slightly in the EMRA population. The figure shows that the percentage of IFN-γ producing cells in the CD9 negative population is slightly higher than in the CD9 positive T cells. Even though $CD8^+$ cells are known to have a more limited repertoire of cytokine production and preferentially produce IFN-γ, the production of IL-17 and IL-22 was still analysed. The production of IL-17 and IL-22 was found to not significantly differ between the CD9 negative and CD9 positive populations for both the $CD4^+$ and the $CD8^+$ compartment (data not shown).

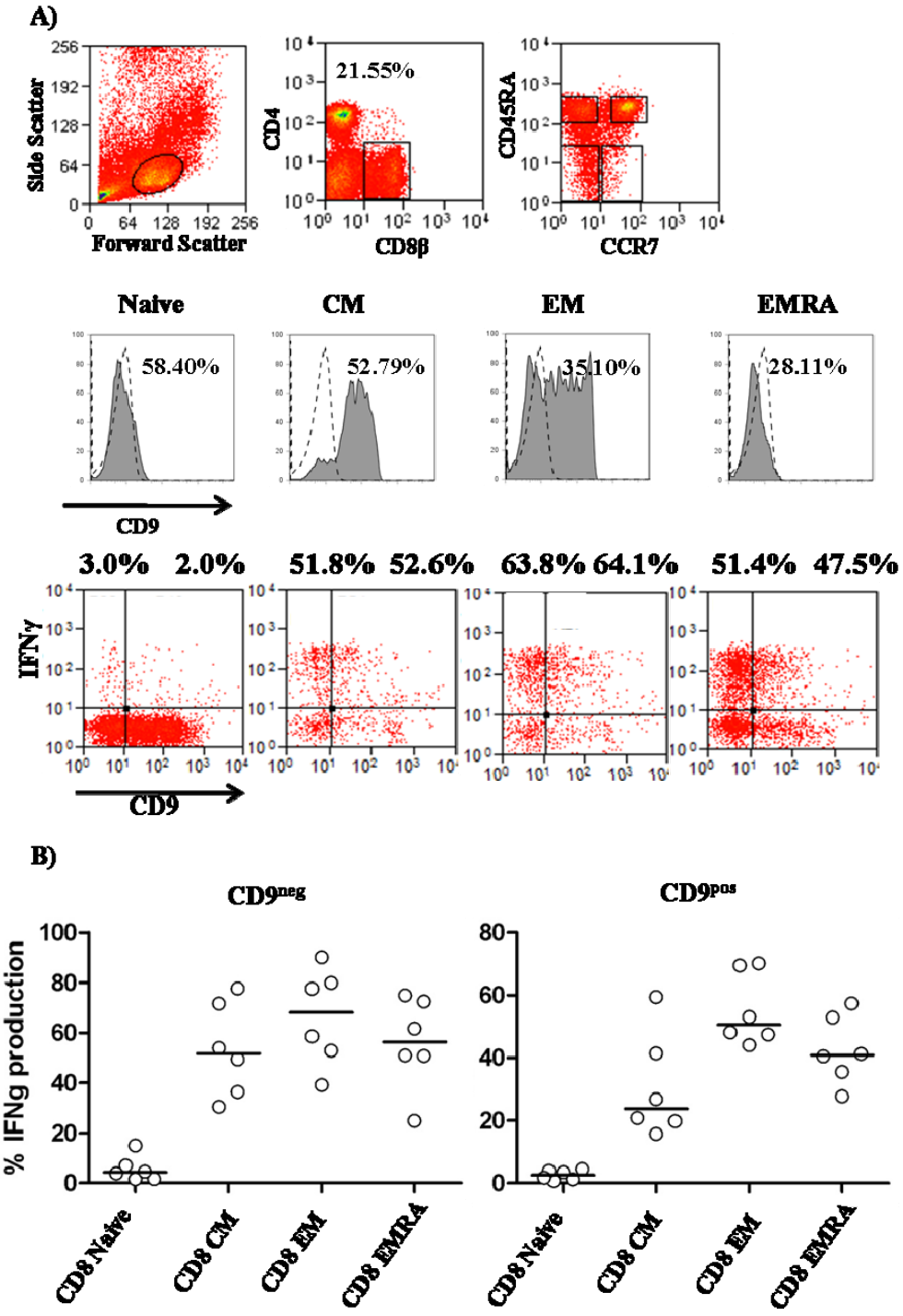

Figure 5.18. No difference between CD9 negative and CD9 positive cells IFN γ production in CD8$^+$ T cell populations. A) Representative plot (*n*=6) of the IFN γ production of CD9 negative and CD9 positive cells in CD8$^+$ T cell populations. Dotted line indicates isotype control. **B)** The percentage of IFN γ production in the CD9 negative (left) and CD9 positive cells (right) CD8$^+$ T cell populations.

5.2.9 CD9 expression on sorted $CD4^+$ CM and EM T cell populations

To analyse the effect of cellular activation on CD9 negative T cells, CD9 negative populations were sorted from $CD4^+$ CM and EM populations for two donors. The cells were then seeded at 10,000-70,000 cells/well and were either stimulated with α-CD3/α-CD28 beads and cultured, or not stimulated and cultured, after which their CD9 expression was assessed. Fig. 5.19A shows the sorting strategy used to sort $CD4^+$ CM $CD9^-$ cells, representative flow cytometry plots are shown. The cells were gated on size and granularity, the expression of CD4 and $CCR7^+CD45RA^-$. An isotype control (IgGκ) for the CD9 antibody (Fig. 5.19A first histogram) was used to establish specific staining for CD9 (Fig. 5.19A second histogram). Fig. 5.19B shows representative purities for CD4, the CM population and subsequently the sorted $CD9^-$ population. Compared to the purity on day 0 a subtle increase in $CD9^+$ cells could be seen for both the unstimulated and the stimulated cultured cells at day 2. The number of $CD9^+$ cells on day 8 returned to a similar percentage positive cells as on day 0. Fig. 5.20A shows the percentage CD9 positive cells from one sort for the CM $CD9^-$ sorted population in culture (a technical replicate is shown for day 2). Fig. 5.20A shows that especially the stimulated cells increased their CD9 expression after two days in culture, but that this increased expression has disappeared at day 8 in culture. Fig. 5.20B shows the percentage CD9 positive cells from a second sort for the CM $CD9^-$ sorted population in culture. An increase in CD9 positive cells can be seen in the stimulated cells after two days in culture. For this second sort, there was no day 8 time point to corroborate the drop back to day 0 CD9 expression levels seen in the first experiment.

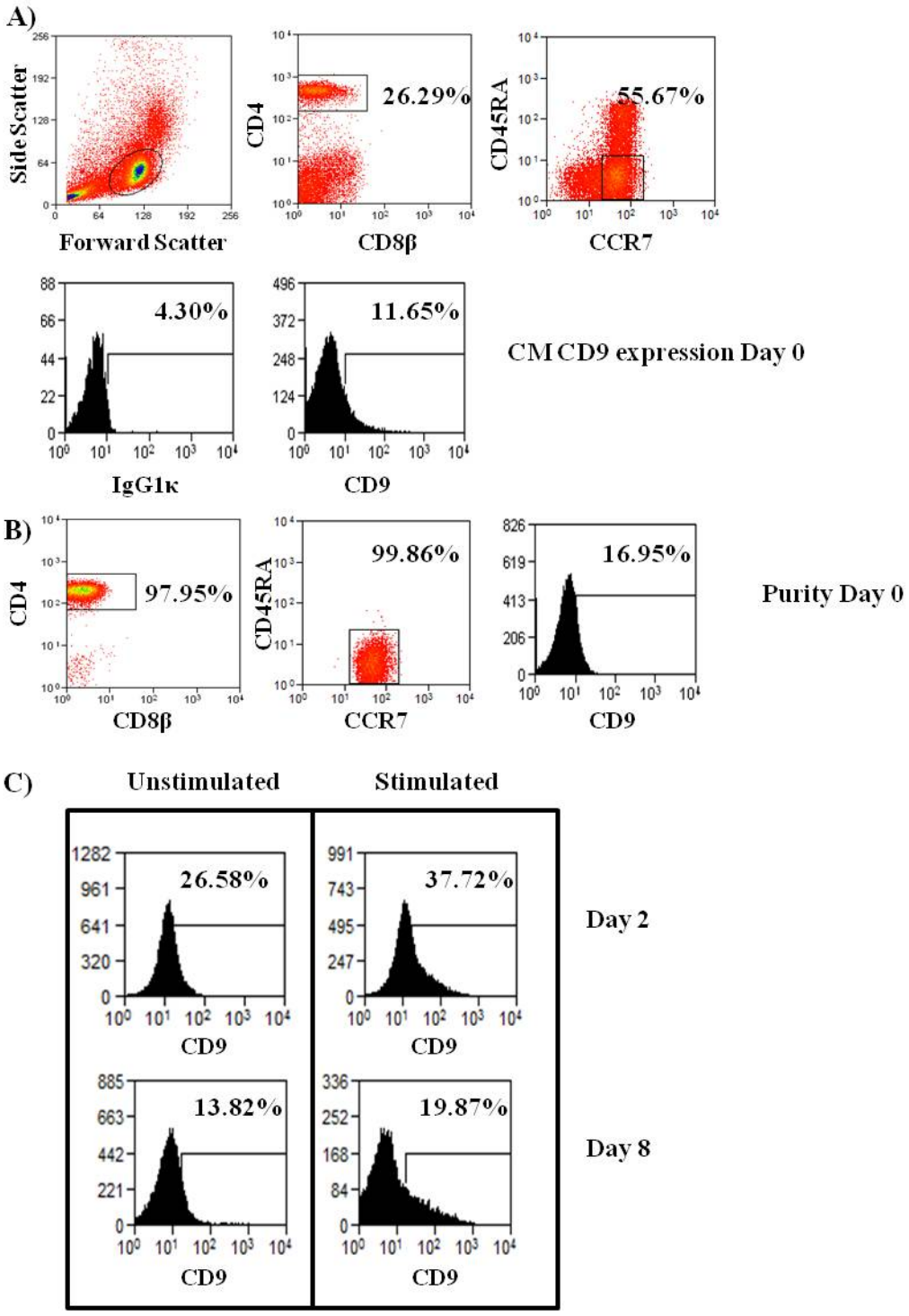

Figure 5.19. Sorted CD4$^+$ central memory (CM) CD9 negative sorted populations. Cells were sorted and cultured for 2 and 8 days, either unstimulated or stimulated with α-CD3/α-CD28 beads on day 0. CD9 expression was assessed after day 2 and day 8 in culture. Percentage positive cells based on isotype control. **A)** Sorting strategy used to sort CD4$^+$ CM CD9$^-$ T cells. Histograms show isotype control and purity on day 0. **B)** CD9 expression on sorted CD4$^+$ CM T cells on day 2 or day 8 in culture.

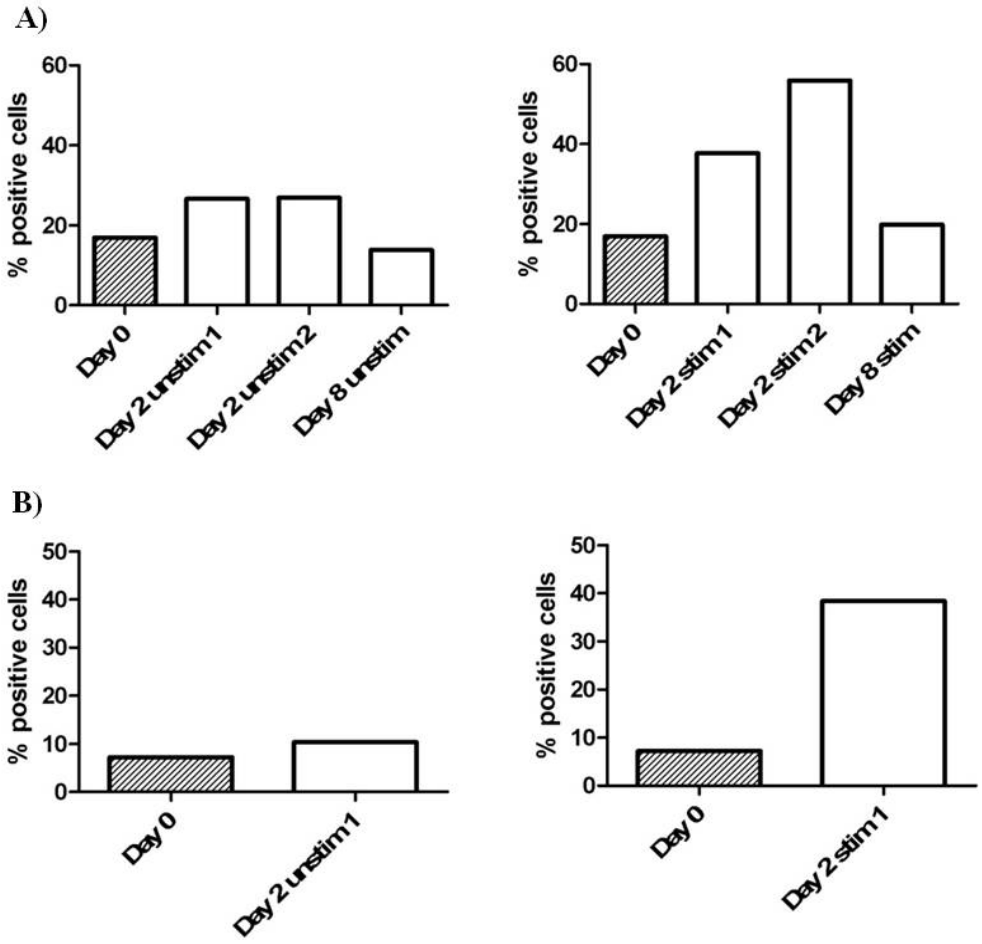

Figure 5.20. Percentage positive cells of sorted CD4$^+$ central memory (CM) CD9 negative populations in culture. Cells were sorted and cultured for 2 and 8 days, either unstimulated or stimulated with α-CD3/α-CD28 beads on day 0. CD9 expression was assessed after day 2 and day 8 in culture. Percentage positive cells based on isotype control. **A)** CD9 expression on CD4$^+$ CM T cells in culture from first experiment, a technical repeat for day 2 is included. **B)** CD9 expression on CD4$^+$ CM T cells in culture from second experiment.

Fig. 5.21A shows the sorting strategy used to sort CD4$^+$ EM CD9$^-$ cells, representative flow cytometry plots are shown. The cells were gated on size and granularity, the expression of CD4 and CCR7$^+$CD45RA$^-$. An isotype control (IgGκ) for the CD9 antibody (Fig. 5.21A first histogram) was used to establish specific staining for CD9 (Fig. 21A second histogram). Fig. 5.21B shows representative purities for CD4, the EM population and subsequently the sorted CD9$^-$ population. Compared to the purity of day 0 the percentage CD9 positive cells

increased substantially after two days in culture (Fig. 5.21C), this held true for both the unstimulated and (to a lesser extent) stimulated cells. After eight days in culture, the CD9 expression was back to a similar level as on day 0. Fig. 5.22A summarises the flow cytometry data for the first experiment and it is clear that CD9 expression was increased on day 2 and dropped back down on day 8. The increase in CD9 expression was higher in the unstimulated cells than in the stimulated cells. This increase in CD9 expression was also clear in the second experiment (Fig. 5.22B).

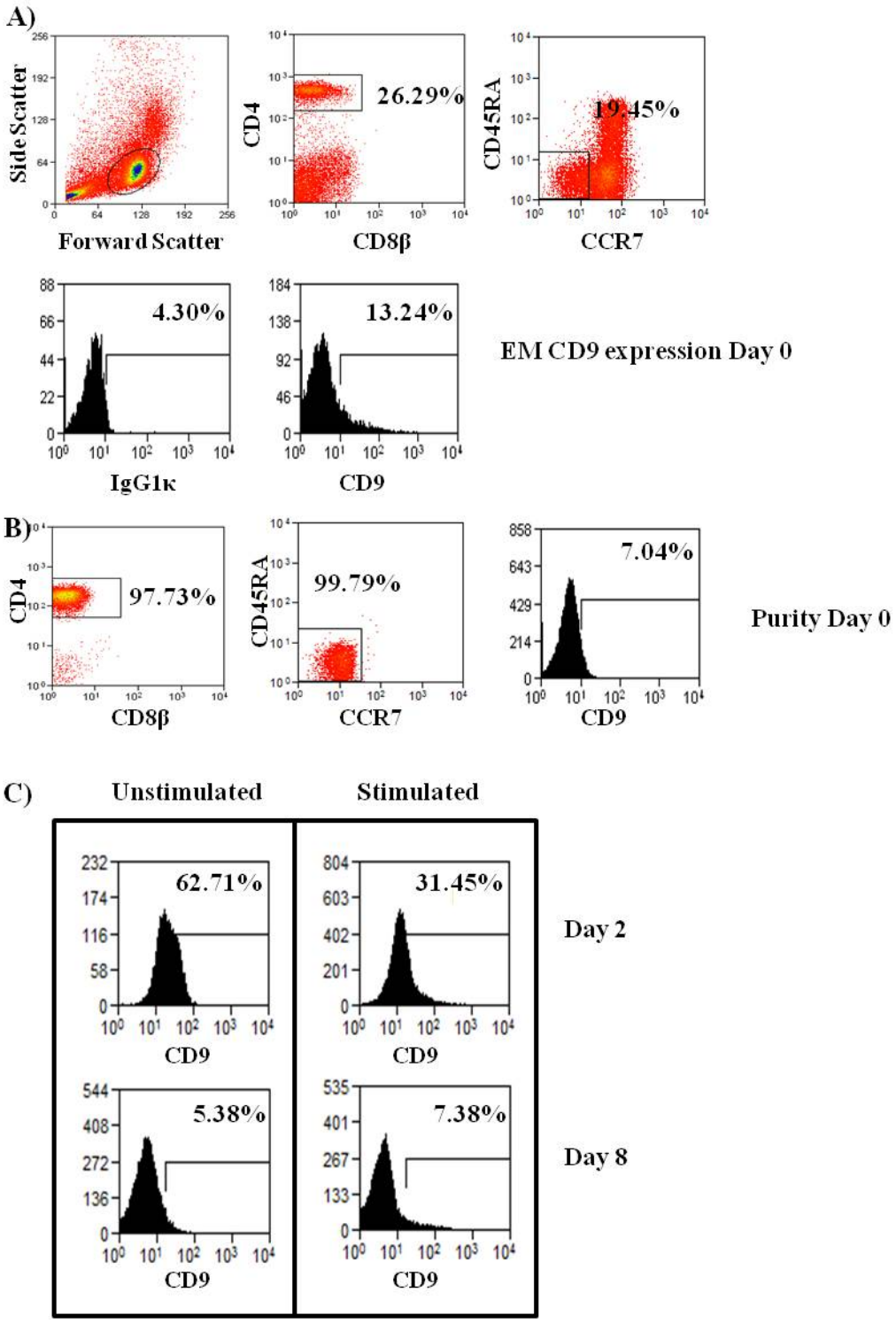

Figure 5.21. Sorted CD4$^+$ effector memory (EM) CD9 negative sorted populations. Cells were sorted and cultured for 2 and 8 days, either unstimulated or stimulated with α-CD3/α-CD28 beads on day 0. CD9 expression was assessed after day 2 and day 8 in culture. Percentage positive cells based on isotype control. **A)** Sorting strategy used to sort CD4$^+$ EM CD9$^-$ T cells. Histograms show isotype control and purity on day 0. **B)** CD9 expression on sorted CD4$^+$ EM T cells on day 2 or day 8 in culture.

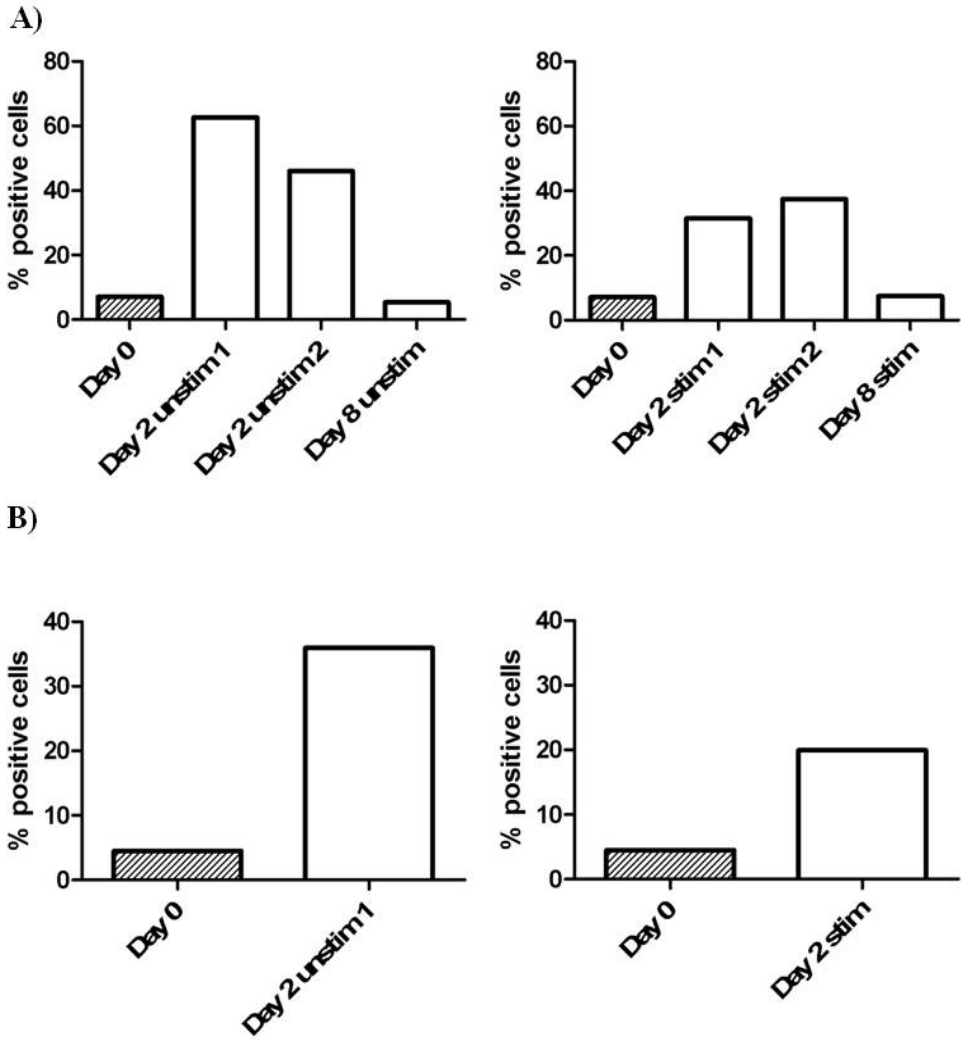

Figure 5.22. Percentage positive cells of sorted CD4$^+$ effector memory (EM) CD9 negative populations in culture. Cells were sorted and cultured for 2 and 8 days, either unstimulated or stimulated with α-CD3/α-CD28 beads on day 0. CD9 expression was assessed after day 2 and day 8 in culture. Percentage positive cells based on isotype control. **A)** CD9 expression on CD4$^+$ EM T cells in culture from first experiment, a technical repeat for day 2 is included. **B)** CD9 expression on CD4$^+$ EM T cells in culture from second experiment.

5.3 Discussion

The aim of the experiments in this chapter was to correlate the cell surface expression of tetraspanins on $CD4^+$ and $CD8^+$ T cell populations with their mRNA levels identified in these cells by microarray and Real Time PCR. Tetraspanins have been implicated in organising the cell membrane resulting in coordinating signalling pathways and several groups have reported a role for tetraspanin microdomains in MHC II clustering on APCs [73;82;132;133]. The experiments in this chapter show that the family of tetraspanins shows differential expression patterns on both $CD4^+$ and $CD8^+$ T cell populations.

In most cases the expression levels measured by microarray, Real Time PCR and flow cytometry corresponded very well (Fig. 5.23 A and B) indicating that for most tetraspanins mRNA levels and cell surface expression do not differ too much. For CD37 cell surface expression was undetectable above an isotype control (Fig. 5.4 and 5.23A), but was detectable at mRNA level on both microarray and Real Time PCR. The cell surface expression of CD9 detected by flow cytometry corresponded with the mRNA levels identified through microarray and Real Time PCR.

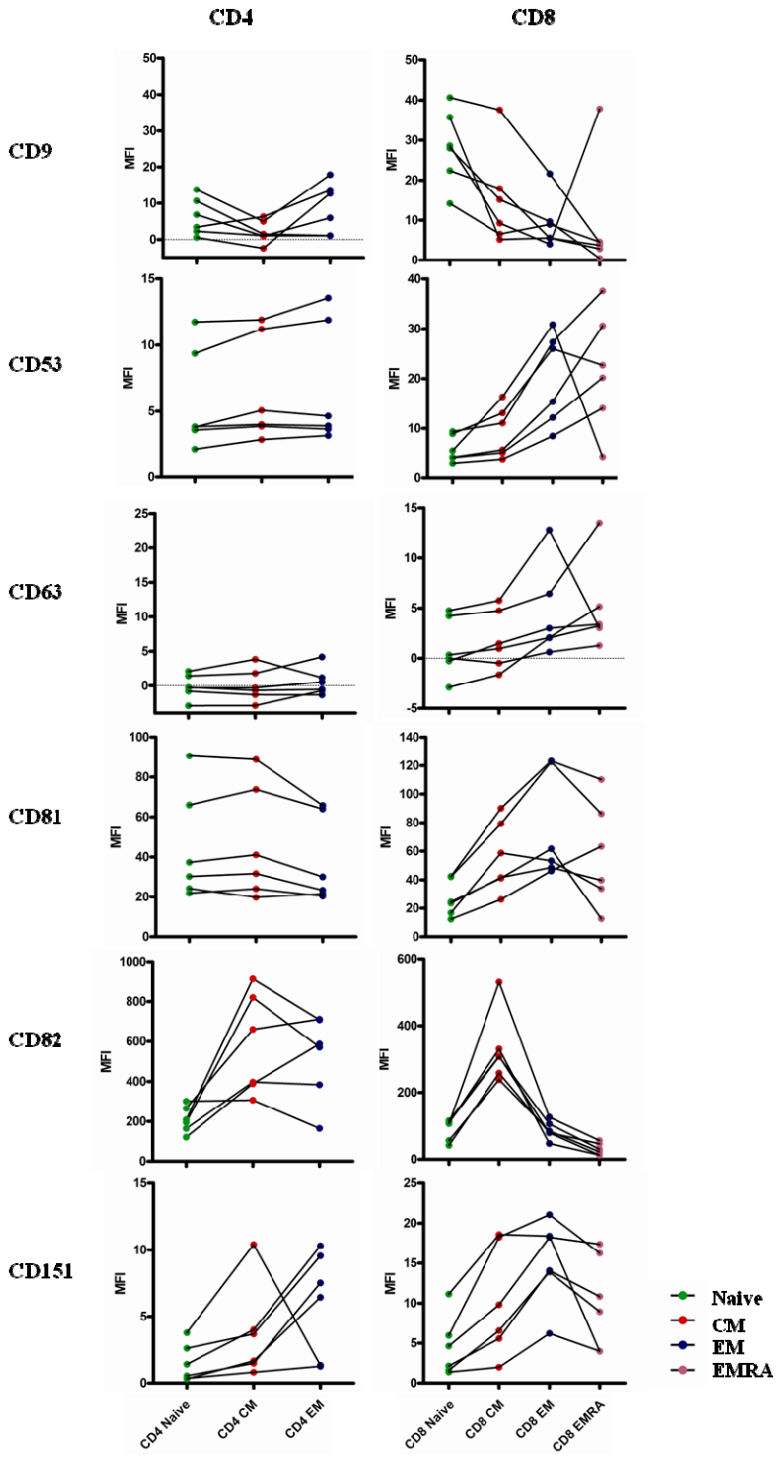

Figure 5.23. Summary of tetraspanin expression on CD4$^+$ and CD8$^+$ T cell populations. Trends in expression levels, based on the median fluorescence intensity values from flow cytometry data, are summarised for each tetraspanin.

Tetraspanins have been described to be expressed on endosomes, which are formed by budding of endocytic vesicles from the plasma membrane and on multivesicular bodies

(MVBs) [78]. MVBs can mature into lysosomes, which can fuse with the plasma membrane when triggered, turning them into exosomes. Tetraspanins CD53 and CD63 have been described to be highly expressed on exosomes [78;159]. Exosomes can transfer lipids and proteins, deliver mRNA or in the case of cytotoxic T cells deliver perforins and granzymes. CD63 has been described to be mainly localised on the lysosomes of resting platelets, but after platelet activation CD63 expression is increased on the cell surface [159]. The data in this chapter shows that for $CD8^+$ T cells the expression of CD53 and CD63 goes up in the more differentiated cells (Fig. 5.23). This increased expression of these tetraspanins on the more mature cells of the EM and EMRA populations could be due to the fact that these two populations are capable of exerting effector functions by releasing cytotoxic lysosomes. The CD53 and CD63 expression on the cell surface could reflect a stage in the recirculation to the plasma membrane from endosomes/exosomes.

CD151 regulates cell migration through its interaction with the integrin α3β1 and α6β4 and its involvement in matrix metalloproteinases (MMP) expression [81]. After CD151 knockdown in a carcinoma cell line the expression levels of several MMPs were reduced. The CD151 knockdown cells also had impairment in their mobility and in α3β1 internalisation. The importance of CD151 in integrin trafficking was shown by mutating the sorting motif of CD151 resulting in reduced α3β1, α5β1 and α6β1 endocytosis and accumulation of these integrins in intracellular compartments. The expression of CD151 on both $CD4^+$ and $CD8^+$ T cells was shown to be highest on the EM and EMRA populations (Fig. 5.23) and these cells need to be able to migrate into tissues. CD151's involvement in integrin trafficking and the fact that memory T cells are known to show a higher and more varied expression of integrins than the naive population, could correlate with the increased CD151 expression found on the more differentiated cells [81]. In cultured human umbilical vein endothelial cells (HUVEC)

CD151 expression was found mostly on endosomes/exosomes, which could indicate that similar to CD53 and CD63, the increased expression of CD151 on the EM and EMRA T cell populations could be due to recirculation between endosomes and plasma membrane [160 161].

Unternaehrer *et al* (2007) described that CD9 on mouse DCs is involved in the multimerisation of MHC-II molecules on the cell surface and suggested that this multimerisation could enhance the ability of DCs to engage with the T cell receptor [134]. They found that MHC-II formed clusters on the cell surface of DCs, but not B blasts. They then focussed on the expression of several tetraspanins known to be predominantly expressed on the surface of cells. CD81 was expressed at high levels on B blasts, but not on DCs. Whereas CD9 was expressed at high levels on the DCs and not on B blasts. When they transfected BM derived DCs from $CD9^{-/-}$ mice with a I-E-GFP construct and tested I-A/I-E clustering by using I-A or I-E beads, they found that in the absence of CD9 MHC-II clustering was abrogated. To test whether CD9 was indeed capable of directing MHC-II clustering on the cell surface, a B cell line which does not express CD9 was transfected with a CD9 construct and this resulted in I-E coimmunoprecipitating with I-A. Kropshofer *et al* (2001) used an antibody against CDw78 microdomains on human cell lines and found that tetraspanins CD9, CD81 and CD82 associate with MHC-II in these microdomains [133].

When sorted CD9 negative cells from $CD4^{+}$ CM or EM T cells were cultured *in vitro*, an increase in CD9 positive cells was found after two days in culture (Fig. 5.19-22). This increase in CD9 positive cells disappeared after prolonged culture of these cells without restimulation (8 days in culture). The increase in CD9 positive cells after stimulation could indicate CD9 involvement on recently activated T cells. As Unternaehrer *et al* (2007) show,

CD9 on DCs is involved in clustering of MHC-II molecules. In resting cells the cell membrane is thought to be in a liquid disordered state (Ld) in which the cell surface molecules are spread across the plasma membrane evenly [162;163]. After activation the cell surface molecules needed for activation are packed more densely and in a more organised fashion into liquid ordered states (Lo) resembling rafts. Gordon-Alonso *et al* (2006) describe CD9 and CD81 involvement in HIV-1 induced membrane fusion, showing that adding antibodies against CD9 and CD81 to human T cell lines results in an increase of viral entry into the cell [80]. They suggest two possible ways for CD9 and CD81 to enhance HIV-1 induced membrane fusion, firstly indirect by enhancing T cell activation, through their involvement in different signalling pathways in T cells (such as the activation of protein kinase C). Adding antibodies against CD81 has been shown to stimulate T cells and activated T cells are more susceptible to HIV-1 infection. The direct pathway for CD9 and CD81 to enhance HIV-1 entry could be through the organising function of tetraspanins on the cell surface, shuttling co-receptors and TCRs together to form activation rafts. If CD9 expression on the sorted CD9 negative $CD4^+$ T cell populations is involved in recent activation of the cells, I propose a model of CD9 involvement in $CD4^+$ T cell activation (Fig. 5.24) where CD9 recruits molecules to form an immunological synapse. In a resting T cell the molecules are relatively equally distributed across the plasma membrane (Fig. 5.24A). After an APC presents antigen on its MHC molecule and this is recognised by the TCR on the T cell surface CD9 could start shuttling co-receptors such as CD4 and CD28 and linker for T cell activation (LAT) into the immunological synapse (Fig. 5.24B). To test whether CD9 is indeed present in the immunological synapse, I propose an experiment in which sorted CD9 negative $CD4^+$ T cell populations (CM or EM) are stimulated *in vitro* with α-CD3-α-CD28 magnetic beads (Fig. 5.25). The activated T cells are then homogenised using nitrogen cavitation, lysing the cells while leaving the plasma membrane bound to the magnetic bead intact. Through

Western Blot analysis and Real Time PCR, it can then be determined whether CD9 is present in the immunological synapse after activation, this experiment was adapted from Zech *et al* [164]. The production of cytokines by CD9 negative and positive $CD4^+$ and $CD8^+$ T cells was shown to not differ (Fig. 5.17 and 5.18); this indicates that CD9 could still be involved in the activation status of these cells, but its expression does not convey any differences in cytokine production.

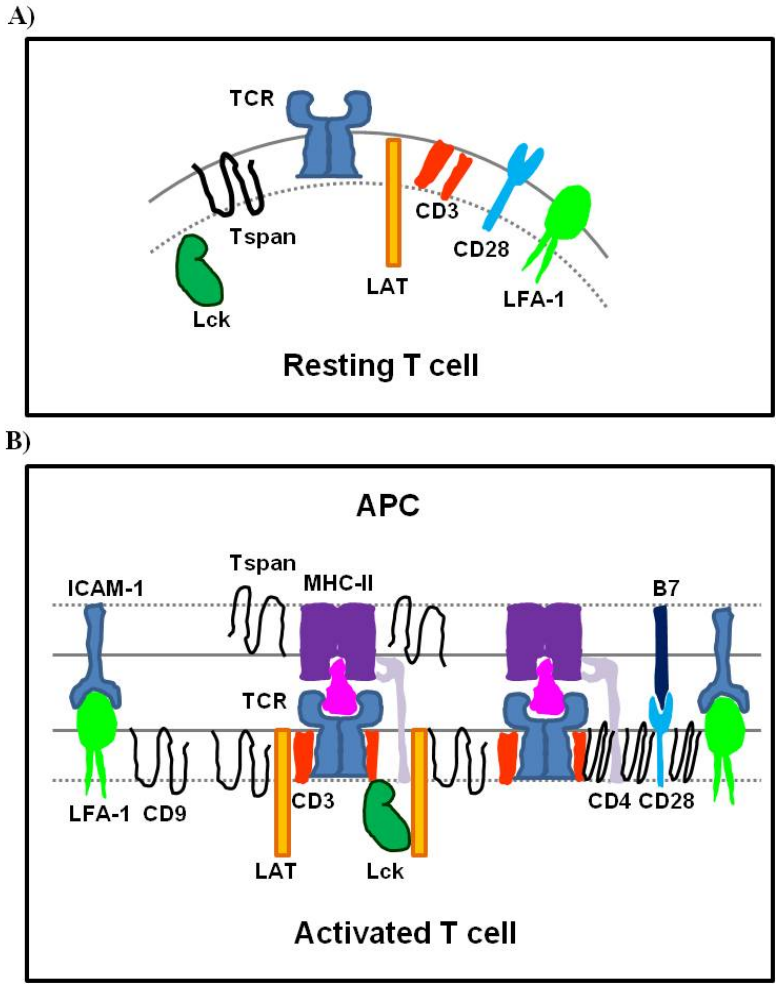

Figure 5.24. Model of CD9 involvement on recently activated CD4$^+$ T cell populations. **A)** The cell membrane of resting T cells may contain small rafts of proteins. **B)** When activated by an antigen presenting cell (APC) clusters of T cell receptors (TCRs) and CD3 with signalling proteins such as LAT and Lck can form. Tetraspanin CD9 could be involved in forming these rafts.

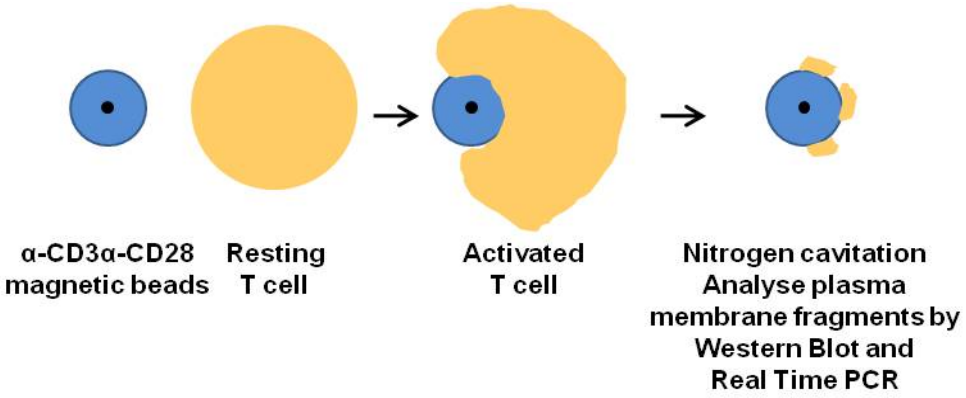

Figure 5.25. Model of analysing CD9 involvement on recently activated CD4$^+$ T cell populations. Sorted CD4$^+$ T cells are incubated with α-CD3/α-CD28 magnetic beads, the T cell gets activated after which the cell is lysed by nitrogen cavitation, leaving the plasma membrane bound to the magnetic bead intact. The bound plasma membrane can than be analysed through Western Blot and Real Time PCR to identify whether CD9 is involved in these activation rafts.

CD81 has been described to have an antiproliferative effect on B cells where it is part of a complex with CD21, CD19 and Leu13 [79]. On human thymocytes CD81 has been shown to associate with both the CD4 and the CD8 co-receptors and the addition of an anti-CD81 antibody resulted in adhesion of the cells. The anti-CD81 triggered adhesion could be blocked by anti-LFA-1 and anti-ICAM-1 antibodies, suggesting that this adhesion is caused by these molecules. Crosslinking of CD81 on thymocytes resulted in a costimulatory signal to CD3 and subsequent proliferation, but each of the antibodies to CD3 or CD81 on their own had no proliferative effect on the cells [79;98]. The data in this chapter shows the percentage CD81 positive CD4$^+$ T cells slightly decreases as the cells mature, whereas a slight increase can be seen on the percentage CD81 positive CD8$^+$ T cells as they differentiate (Fig. 5.23). When looking at the MFI of the positive cells though, it is noticeable that the amount of CD81 on the positive cells does not change significantly (Fig 5.10), except between CD8$^+$ populations (p = 0.0383). This suggests that in both CD4$^+$ and CD8$^+$ T cells throughout differentiation the naive cells and the antigen experienced CM, EM and EMRA populations

express similar levels of CD81 on their cell surface. Todd *et al* (1996) cultured thymocytes in the presence of an antibody against CD81, which resulted in the upregulation of the activation markers CD69 and CD25 [98]. They found that the majority of the $CD69^+$ cells cultured in the presence of anti-CD81 had a $CD4^-CD8^+$ phenotype. This could suggest that CD81 has an important role in $CD8^+$ T cell generation in the thymus and possibly in the more differentiated $CD8^+$ T cells. $CD8^+$ T cells might need CD81 expression to become more easily activated and increase their proliferation; it is possible that CD9 performs a similar function on $CD4^+$ T cells.

The results from Chapter 5 show that several tetraspanin family members display differential expression on the T cell surface. CD9 expression was found to show a biphasic expression pattern on both $CD4^+$ and $CD8^+$ T cells. An increase in CD9 positive cells was found after two days in culture (Fig. 5.19-22) when sorted CD9 negative cells from $CD4^+$ CM or EM T cells were cultured *in vitro*; this increase in CD9 positive cells disappeared after prolonged culture of these cells without restimulation (8 days in culture). The increase in CD9 positive cells after stimulation could possibly indicate CD9 involvement on recently activated T cells, however there was no difference in the production of cytokines by CD9 negative and positive $CD4^+$ and $CD8^+$ T cells (Fig. 5.17 and 5.18). This result does not exclude CD9 involvement in the activation status of these cells, but its expression does not seem to convey a difference in cytokine production.

Chapter Six

General Discussion

6 GENERAL DISCUSSION

6.1 Introduction

$CD4^+$ and $CD8^+$ T cells are important mediators of the adaptive immune response and they can be subdivided into several populations based on the expression of cell surface markers and transcription factors as well as the ability to produce cytokines. The principle of using gene expression profiles to analyse previously described cell populations has been successfully used in several studies, resulting in the identification of several target genes and cell type specific gene expression profiles [108;110;117]. The aim of this study was to analyse the gene expression of sorted $CD4^+$ and $CD8^+$ T cell populations based on the expression of CCR7 and CD45RA to identify gene profiles for these cell populations as well as genes of interest to be analysed further.

During the course of this thesis I have shown that by using microarray analysis on sorted $CD4^+$ and $CD8^+$ T cell populations shared and distinct genes can be found. The gene expression profiles analysed suggested a linear pathway of differentiation for these populations; they could not exclude a divergent differentiation pathway necessarily. I have also provided evidence that the data generated through microarray analysis could be validated by Real Time PCR. Furthermore the role of the tetraspanin gene family of interest, which arose from the microarray data was analysed for $CD4^+$ and $CD8^+$ T cells, indicating the differential involvement of tetraspanins at various stages of T cell differentiation.

The finding of gene expression profiles relating to naive, central memory (CM) and effector memory (EM) T cell populations for both $CD4^+$ and $CD8^+$ T cells can be of importance when examining T cell mediated diseases in humans. The profiles identified in this study are

specific to a steady-state condition, with no inflammation present; however the fact that these genes have proved to be important in distinguishing between T cell populations at a steady-state implies that they could also be important in a disease setting. The genes identified in this thesis could reflect a baseline expression level which changes when the immune system is activated against a pathogen and returns to baseline after antigen clearance. It would therefore be interesting to analyse the gene expression of these cell populations in a disease setting.

The tetraspanin gene family has been described to be involved in many important cellular processes, such as cell activation, adhesion and differentiation [77;165;166]. Several tetraspanins show wide distribution on many different cell types (*e.g.* CD81 on most human tissues), whereas others show a more restricted level of expression (*e.g.* CD37 on B cells). Tetraspanins are known to associate with other molecules such as integrins, signalling enzymes as well as other tetraspanins [77;165]. The many interactions that tetraspanins can form suggest their involvement in the plasma membrane as molecular facilitators which organise the membrane into tetraspanin enriched domains (TEMs) upon activation. Differential expression levels of tetraspanins found in this study indeed suggest a role for tetraspanins in T cell activation, migration and lysosomal function. The fact that tetraspanins are capable of forming homodimers and heterodimers suggests that there might be some redundancy in the function of different tetraspanins.

6.2 A shared differentiation pathway for $CD4^+$ and $CD8^+$ T cell populations based on CCR7 and CD45RA

The results from Chapters 3 and 4 suggest several genes which can be used to distinguish between naive, central memory and effector memory T cell populations. These genes suggest a linear pathway of differentiation, but they do not exclude a non-linear pathway of differentiation (Fig. 3.32 and 3.33). One of the limitations of microarray analysis is the generation of a large data set, which on its own is not biologically significant. Further experiments leading on from microarray data are always needed to examine the function of target genes identified. The genes identified in this study will need to be analysed more extensively to ascertain their function in T cell biology. Another factor to consider is that the cell populations analysed in this thesis were all collected under non-inflammatory conditions, from healthy donors. The populations analysed were therefore in a resting state and how their behaviour in rest relates to that which occurs under inflammatory conditions cannot be ascertained from this study. Based on the results from the gene expression analysis I would suggest an adaptation to our models of differentiation described in Chapter 3 (Fig. 6.1, 3.32 and 3.33). During acute inflammation naive T cells are activated and give rise to short lived effector T cells, capable of producing inflammatory cytokines as well as releasing vesicles containing granzymes and perforin. Memory T cells can either be formed during this same acute inflammation stage and persist over longer periods of time, or they arise at the end of the expansion state by late-arriving naive T cells. The late arriving naive T cells can differentiate along a linear pathway of differentiation or a non-linear pathway to give rise to long lived CM and EM T cell populations.

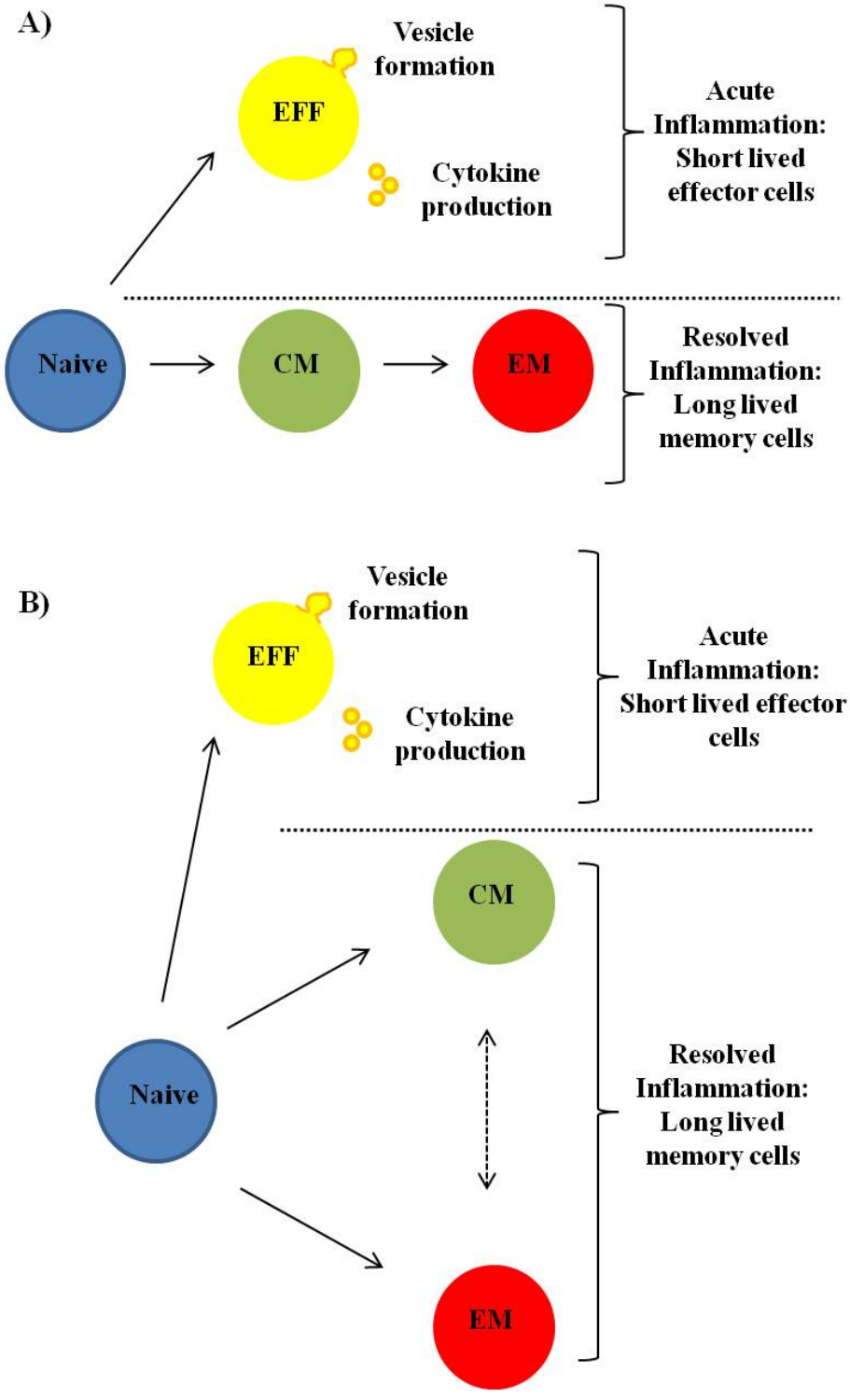

Figure 6.1. Adapted linear and non-linear models of T cell differentiation to reflect active inflammation and resolved inflammation conditions. A naive T cell is activated and gives rise to short lived effector T cells, which produce cytokines and release vesicles with effector molecules such as granzymes and perforin. As the inflammation is resolved central memory (CM) and effector memory (EM) T cells arise either in a linear pathway of differentiation **(A)** or a non-linear pathway **(B)**.

There are several restrictions when examining immune mediated diseases in humans, such as the localised nature of some inflammatory responses. This restricts the access to samples required to further characterise the disease; the rheumatoid joint is an example of such a restricted access site. Not only the access to the site of inflammation can be limiting, but also the sample size after collection can be restricting. Chaussabel *et al* (2010) discuss the idea that gene expression analysis of peripheral blood cells can be used to identify potential biomarkers for disease as well as provide more insight in the pathogenesis of disease (Fig. 6.2) [167;168]. The gene expression profiles described in Chapter 3 for naive, CM and EM T cells could provide specific gene profiles to analyse in a disease setting. Chaussabel *et al* (2010) postulate that peripheral blood cells upon their circulation through the body between central and peripheral lymphoid organs as well as migrating to and from sites of inflammation come into contact with multiple environmental cues. These environmental cues can then result in an altered phenotype and genotype of these peripheral blood cells which can be measured by flow cytometry as well as gene expression analysis [167]. Comparing the gene expression of a steady state to that which occurs during an infection can lead to the identification of biomarkers as well as gene expression profiles specific to a disease. McKinney *et al* (2010) for example used transcriptome analysis to identify two subgroups of $CD8^+$ T cells in a cohort of 32 patients with antineutrophil cytoplasmic antibody (ANCA)-associated vasculitis (AAV). They found that the gene expression profile of one of the $CD8^+$ subgroups corresponded to a poorer prognosis for patients [169]. Pascual *et al* (2008) studied rheumatic diseases in children and identified IFN and IL-1 as important genes in systemic lupus erythematosus (SLE) and systemic onset juvenile arthritis (SoJIA), respectively [168]. These studies underline the possibility of using gene expression analysis within a disease setting allowing the identification of prognostic gene expression profiles as well as disease specific markers.

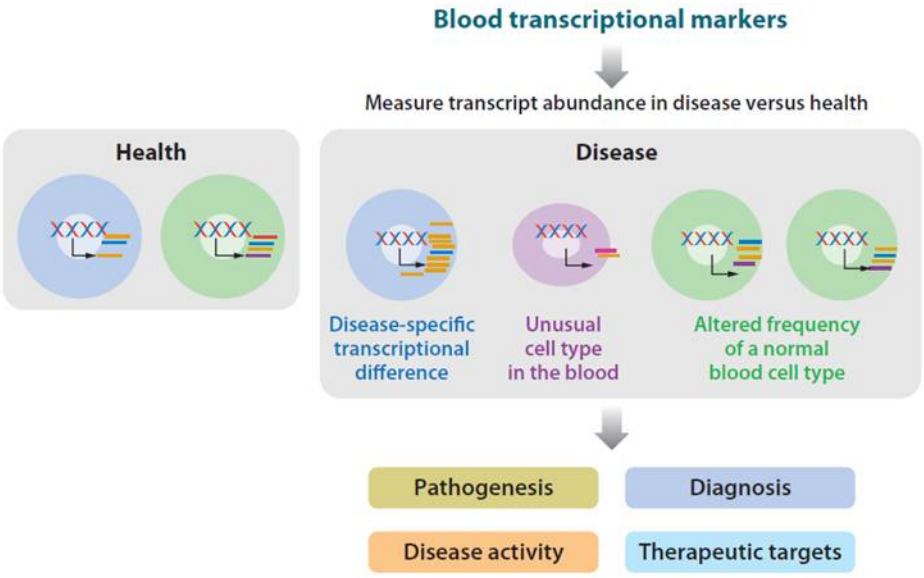

Figure 6.2. Graphical representation of how gene expression analysis of peripheral blood cells can be important in identifying disease related transcriptional changes, adapted from Pascual *et al* (2010). Comparing gene expression profiles in health to those collected from cells in a disease setting can provide important information on disease severity, prognosis, potential diagnoses and therapeutic targets.

6.3 Differential expression of tetraspanin family members on $CD4^+$ and $CD8^+$ T cell populations

Tetraspanins have been implicated in many biological processes and it is therefore not surprising that several family members are shown to have differential expression on different T cell populations. Many tetraspanins, however, exhibit overlapping functions in their ability to organise tetraspanin enriched microdomains (TEMs). CD9, CD53, CD63, CD81 and CD151 were shown to have differential cell surface expression on T cell populations, as well as TSPAN18 on mRNA level. CD53 and CD63, which are known to be expressed on MVBs, expression increased as the cells differentiated correlating with the increased potential of

those cells to produce vesicles. CD9 and CD81 expression seem to follow opposite expression patterns on $CD4^+$ and $CD8^+$ T cells as they differentiate, with CD9 expression going up in $CD4^+$ T cells, but down in $CD8^+$ and CD81 expression going down on $CD4^+$ T cells but up in $CD8^+$. This could suggest a role for CD9 in $CD4^+$ T cell activation and CD81 in $CD8^+$ T cell activation. CD9 and CD81 might bind to CD4 and CD8 respectively, or bind to an unknown CD4 specific or CD8 specific cell surface molecule, resulting in the enhancement of T cell activation. This includes the possibility CD9 and CD81 organise the plasma membrane around the TCR-co-stimulatory molecule complex which could enhance T cell activation.

It would be interesting, however, to analyse the differential tetraspanin expression found on human T cells more in depth. The experiment I suggest in Chapter 5 to analyse the involvement of CD9 in $CD4^+$ T cell activation, can easily be used for analysing CD81's possible role in $CD8^+$ T cell activation. The differential tetraspanin expression found on T cells in this study, as was the case with the gene expression profiles, were assessed during steady state conditions. It would be interesting to see if these particular tetraspanins, which show differential expression under non-inflammatory conditions exhibit the same expression patterns during disease. Tetraspanins have been implicated in several disease settings, such as CD9 and CD81 in HIV-1 induced membrane fusion, CD82 as a tumour suppressor and CD151 as a promoter of tumour progression [80;81] and it would therefore be interesting to analyse the expression of these tetraspanins on the CCR7/CD45RA based T cell populations in peripheral blood of patients with these different diseases.

6.4 Future work leading from this study

The aim of this study was to examine lineage relationships between human $CD4^+$ and $CD8^+$ T cell populations based on CCR7 and CD45RA. Through microarray analysis gene expression profiles could be assembled to distinguish between sorted human $CD4^+$ and $CD8^+$ T cell populations. These gene expression profiles show that the central memory population consistently shows expression values intermediate to the naive and the effector memory populations. As described before this suggests a linear pathway of differentiation, but does not exclude a non-linear pathway. To analyse which of these pathways is involved in the generation of differentiated T cell populations, I suggest an adaptation of Schepers *et al* (2008) method for cellular barcoding [170]. Schepers *et al* (2008) generated a retroviral plasmid library, with each plasmid containing the GFP gene as well as a unique barcode formed by a random stretch of 98 bp of noncoding DNA. Cells of interest can be retrovirally transduced and their progeny analysed by a barcode microarray. To use this strategy for further analysis of the data generated in this thesis, there are two models which can be followed; an *in vitro* human model and an *in vivo* mouse model. For the *in vitro* human model sorted $CD4^+$ or $CD8^+$ human naive T cells will be labelled using the Schepers *et al* barcoding method; the cells are then stimulated *in vitro* using αCD3/αCD28 beads. Cells are collected on day 0 as well as after 48 hrs, 7 days and 14 days after which CM and EM populations are sorted based on the expression of CCR7 and CD45RA. The RNA and genomic DNA of these cells are than extracted to be analysed by Real Time PCR and barcode microarray respectively. The Real Time PCR analysis will include the genes identified in this thesis and the barcode microarray will allow analysis of the progeny of the naive population from day 0. These data can then be correlated to each other to allow a conclusion to be made on which pathway of

differentiation naive T cells follow to give rise to their differentiated progeny and whether their progeny corresponds with the cell types in steady state conditions.

The second model I suggest is to analyse the differentiation of naive T cells in an *in vivo* mouse model. This involves validating the gene expression profiles generated in this thesis using murine T cell populations. Sorted $CD4^+$ and $CD8^+$ T cell populations from spleen and lymph node based on CCR7 or CD62L and CD44 expression are analysed by Real Time PCR for their expression of the genes identified in the human model. If these genes can be validated, naive OT-I T cells can be labelled with a barcode, after which they are injected back into the mice which are then challenged with ovalbumin (OVA). At day 7 after the OVA challenge the spleen and lymph nodes of these mice are collected and the cells are sorted based on CCR7/CD62L and CD44 expression. The samples are split in two; one for RNA extraction and a second for genomic DNA extraction. The RNA is used in the analysis of the gene expression profiles of these cells, whereas the genomic DNA is put on the barcode microarrays. Subsequent analysis of the results from those tests will show whether the cells which are formed after antigenic challenge of naive T cells correspond to the CM and EM populations described based on the genes identified in this study; as well as how they relate to a single naive progenitor cell.

LRRN3 consistently showed highest expression levels on naive T cells and lowest on EM T cells, similar to the expression pattern of CCR7 and L-Selectin. Since LRRN3 has not yet been described in T cell biology, it would be interesting to identify the role of LRRN3 on T cells. The fact that LRRN3 follows the expression levels of chemokine receptors involved into gaining entry into LNs (CCR7 and L-selectin) might suggest that LRRN3 has a similar role on T cells, however leucine rich repeats (LRRs) have also been described in pattern

recognition receptors (PRRs) such as TLRs [115]. The higher expression of LRRN3 on naive T cells could suggest a way for naive T cells to recognise antigen, independent of MHC presentation, and a crossover between innate and adaptive immunity. The first experiment to identify LRRN3's role in T cells would be to assess whether LRRN3 is actually expressed on the cell surface. This would be easiest with an antibody, but as no antibody against LRRN3 is available as of yet, I would suggest constructing a plasmid containing GFP labelled LRRN3 and transfecting naive T cells which are already known to express it at mRNA level. The expression of LRRN3 can then be analysed by flow cytometry to assess whether LRRN3 expression can be found at the cell surface. If LRRN3 is found to be expressed at the cell surface, a cell type identified by Real Time PCR not to have any LRRN3 expression can be transfected with the construct. If LRRN3 functions as a PRR it might respond to one of the known ligands for TLRs. The transfected cells would therefore be incubated with known TLR ligands after which the possible interaction between LRRN3 and a ligand can be assessed by immunoprecipitation using an antibody against GFP.

CXCR5 expression was found to be highest on both $CD4^+$ and $CD8^+$ CM T cell populations, to analyse whether this high expression level of CXCR5 mRNA corresponds to high expression of CXCR5 on the cell surface, flow cytometry analysis can be done. If the cell surface expression of CXCR5 corresponds to the mRNA levels, it would be interesting to investigate the function of CXCR5 on these cell populations. $CD4^+$ T_{FH} cells continuously express CXCR5 at high levels on their cell surface and high expression levels found on $CD4^+$ CM T cells could correspond to this cell population. High expression of CXCR5 on $CD8^+$ CM T cells has not been described before and it would therefore be interesting to further investigate the function of CXCR5 on these cells. To determine whether $CXCR5^+CD8^+$ CM T cells can maintain B cell survival, I suggest sorting $CXCR5^+CD8^+$ CM T cells as well as B

cells from the same donor and co-culturing these cells together. B cells would be co-cultured with $CD4^+$ T_{FH} cells or B cells cultured alone as a control. After seven days in culture the cells will be stained for flow cytometry analysis of CXCR5, CD8 and CD19 expression as well as a stain to exclude dead cells. The supernatant of the co-cultures will be analysed for IgG expression to analyse whether $CXCR5^+CD8^+$ CM T cells can support B cell production of IgG.

Taken together these data identified gene expression profiles for $CD4^+$ and $CD8^+$ T cell populations, as well as identifying several genes of interest whose role in T cell biology should be studied further. However, transcriptome analysis could not identify populations of T cells encapsuled within our sorted populations, such as subsets based on cytokine expression. These subsets may become more apparent in a disease setting. In conclusion, transcriptome analysis has shown great potential in identifying genes specific to individual T cells subsets. Future studies should concentrate on both global gene profiles and individual gene analysis in such subsets.

Chapter Seven

Reference List

7 REFERENCE LIST

1. Moser M, Leo O. Key concepts in immunology. Vaccine 2010;28 Suppl 3:C2-13.

2. Biron CA. More things in heaven and earth: defining innate and adaptive immunity. Nat.Immunol. 2010;11:1080-1082.

3. Dempsey PW, Vaidya SA, Cheng G. The art of war: Innate and adaptive immune responses. Cell Mol.Life Sci. 2003;60:2604-2621.

4. Paust S, Senman B, von Andrian UH. Adaptive immune responses mediated by natural killer cells. Immunol.Rev. 2010;235:286-296.

5. Joffre O, Nolte MA, Sporri R, Reis e Sousa. Inflammatory signals in dendritic cell activation and the induction of adaptive immunity. Immunol.Rev. 2009;227:234-247.

6. Dunkelberger JR, Song WC. Complement and its role in innate and adaptive immune responses. Cell Res. 2010;20:34-50.

7. Auffray C, Sieweke MH, Geissmann F. Blood monocytes: development, heterogeneity, and relationship with dendritic cells. Annu.Rev.Immunol. 2009;27:669-692.

8. Giebel B, Beckmann J. Asymmetric cell divisions of human hematopoietic stem and progenitor cells meet endosomes. Cell Cycle 2007;6:2201-2204.

9. Beckmann J, Scheitza S, Wernet P, Fischer JC, Giebel B. Asymmetric cell division within the human hematopoietic stem and progenitor cell compartment: identification of asymmetrically segregating proteins. Blood 2007;109:5494-5501.

10. Doulatov S, Notta F, Eppert K et al. Revised map of the human progenitor hierarchy shows the origin of macrophages and dendritic cells in early lymphoid development. Nat.Immunol. 2010;11:585-593.

11. Kondo M, Weissman IL, Akashi K. Identification of clonogenic common lymphoid progenitors in mouse bone marrow. Cell 1997;91:661-672.

12. Akashi K, Traver D, Miyamoto T, Weissman IL. A clonogenic common myeloid progenitor that gives rise to all myeloid lineages. Nature 2000;404:193-197.

13. Dorshkind K. Not a split decision for human hematopoiesis. Nat.Immunol. 2010;11:569-570.

14. Yin T, Li L. The stem cell niches in bone. J.Clin.Invest 2006;116:1195-1201.

15. Suda T, Arai F, Hirao A. Hematopoietic stem cells and their niche. Trends Immunol. 2005;26:426-433.

16. Calvi LM, Adams GB, Weibrecht KW et al. Osteoblastic cells regulate the haematopoietic stem cell niche. Nature 2003;425:841-846.

17. Zhang J, Niu C, Ye L et al. Identification of the haematopoietic stem cell niche and control of the niche size. Nature 2003;425:836-841.

18. Kopp HG, Avecilla ST, Hooper AT, Rafii S. The bone marrow vascular niche: home of HSC differentiation and mobilization. Physiology.(Bethesda.) 2005;20:349-356.

19. Witte MH, Jones K, Wilting J et al. Structure function relationships in the lymphatic system and implications for cancer biology. Cancer Metastasis Rev. 2006;25:159-184.

20. Boehm T, Bleul CC. The evolutionary history of lymphoid organs. Nat.Immunol. 2007;8:131-135.

21. Blum KS, Pabst R. Keystones in lymph node development. J.Anat. 2006;209:585-595.

22. Drayton DL, Liao S, Mounzer RH, Ruddle NH. Lymphoid organ development: from ontogeny to neogenesis. Nat.Immunol. 2006;7:344-353.

23. Randall TD, Carragher DM, Rangel-Moreno J. Development of secondary lymphoid organs. Annu.Rev.Immunol. 2008;26:627-650.

24. Cupedo T, Mebius RE. Cellular interactions in lymph node development. J.Immunol. 2005;174:21-25.

25. Hoorweg K, Cupedo T. Development of human lymph nodes and Peyer's patches. Semin.Immunol. 2008;20:164-170.

26. Link A, Vogt TK, Favre S et al. Fibroblastic reticular cells in lymph nodes regulate the homeostasis of naive T cells. Nat.Immunol. 2007;8:1255-1265.

27. Balogh P, Fisi V, Szakal AK. Fibroblastic reticular cells of the peripheral lymphoid organs: unique features of a ubiquitous cell type. Mol.Immunol. 2008;46:1-7.

28. Fu YX, Chaplin DD. Development and maturation of secondary lymphoid tissues. Annu.Rev.Immunol. 1999;17:399-433.

29. Ohl L, Henning G, Krautwald S et al. Cooperating mechanisms of CXCR5 and CCR7 in development and organization of secondary lymphoid organs. J.Exp.Med. 2003;197:1199-1204.

30. Ruddle NH, Akirav EM. Secondary lymphoid organs: responding to genetic and environmental cues in ontogeny and the immune response. J.Immunol. 2009;183:2205-2212.

31. Vinuesa CG, Linterman MA, Goodnow CC, Randall KL. T cells and follicular dendritic cells in germinal center B-cell formation and selection. Immunol.Rev. 2010;237:72-89.

32. Carpenter AC, Bosselut R. Decision checkpoints in the thymus. Nat.Immunol. 2010;11:666-673.

33. Rothenberg EV. Cell lineage regulators in B and T cell development. Nat.Immunol. 2007;8:441-444.

34. Dervovic D, Zuniga-Pflucker JC. Positive selection of T cells, an in vitro view. Semin.Immunol. 2010;22:276-286.

35. Aliahmad P, Kaye J. Commitment issues: linking positive selection signals and lineage diversification in the thymus. Immunol.Rev. 2006;209:253-273.

36. Singer A, Adoro S, Park JH. Lineage fate and intense debate: myths, models and mechanisms of CD4- versus CD8-lineage choice. Nat.Rev.Immunol. 2008;8:788-801.

37. Hosoya T, Maillard I, Engel JD. From the cradle to the grave: activities of GATA-3 throughout T-cell development and differentiation. Immunol.Rev. 2010;238:110-125.

38. Sprent J, Surh CD. T cell memory. Annu.Rev.Immunol. 2002;20:551-579.

39. Weninger W, Manjunath N, von Andrian UH. Migration and differentiation of CD8+ T cells. Immunol.Rev. 2002;186:221-233.

40. Laudanna C, Alon R. Right on the spot. Chemokine triggering of integrin-mediated arrest of rolling leukocytes. Thromb.Haemost. 2006;95:5-11.

41. Rocha B, Tanchot C. The Tower of Babel of CD8+ T-cell memory: known facts, deserted roads, muddy waters, and possible dead ends. Immunol.Rev. 2006;211:182-196.

42. Dutton RW, Bradley LM, Swain SL. T cell memory. Annu.Rev.Immunol. 1998;16:201-223.

43. Sallusto F, Lenig D, Forster R, Lipp M, Lanzavecchia A. Two subsets of memory T lymphocytes with distinct homing potentials and effector functions. Nature 1999;401:708-712.

44. Surh CD, Boyman O, Purton JF, Sprent J. Homeostasis of memory T cells. Immunol.Rev. 2006;211:154-163.

45. Vogt AB, Spindeldreher S, Kropshofer H. Clustering of MHC-peptide complexes prior to their engagement in the immunological synapse: lipid raft and tetraspan microdomains. Immunol.Rev. 2002;189:136-151.

46. van der Merwe PA, Davis SJ. Molecular interactions mediating T cell antigen recognition. Annu.Rev.Immunol. 2003;21:659-684.

47. Vyas JM, Van der Veen AG, Ploegh HL. The known unknowns of antigen processing and presentation. Nat.Rev.Immunol. 2008;8:607-618.

48. Guy CS, Vignali DA. Organization of proximal signal initiation at the TCR:CD3 complex. Immunol.Rev. 2009;232:7-21.

49. Baine I, Abe BT, Macian F. Regulation of T-cell tolerance by calcium/NFAT signaling. Immunol.Rev. 2009;231:225-240.

50. Alarcon B, Mestre D, Martinez-Martin N. The immunological synapse: a cause or consequence of T-cell receptor triggering? Immunology 2011;133:420-425.

51. Bour-Jordan H, Esensten JH, Martinez-Llordella M et al. Intrinsic and extrinsic control of peripheral T-cell tolerance by costimulatory molecules of the CD28/ B7 family. Immunol.Rev. 2011;241:180-205.

52. Felix NJ, Suri A, Salter-Cid L et al. Targeting lymphocyte co-stimulation: from bench to bedside. Autoimmunity 2010;43:514-525.

53. Swain SL, Agrewala JN, Brown DM et al. CD4+ T-cell memory: generation and multi-faceted roles for CD4+ T cells in protective immunity to influenza. Immunol.Rev. 2006;211:8-22.

54. Bourgeois C, Tanchot C. Mini-review CD4 T cells are required for CD8 T cell memory generation. Eur.J.Immunol. 2003;33:3225-3231.

55. Bevan MJ. Helping the CD8(+) T-cell response. Nat.Rev.Immunol. 2004;4:595-602.

56. Rocha B, Tanchot C. Towards a cellular definition of CD8+ T-cell memory: the role of CD4+ T-cell help in CD8+ T-cell responses. Curr.Opin.Immunol. 2004;16:259-263.

57. Zhou L, Chong MM, Littman DR. Plasticity of CD4+ T cell lineage differentiation. Immunity. 2009;30:646-655.

58. Yu D, Batten M, Mackay CR, King C. Lineage specification and heterogeneity of T follicular helper cells. Curr.Opin.Immunol. 2009;21:619-625.

59. Akbar AN, Vukmanovic-Stejic M, Taams LS, Macallan DC. The dynamic co-evolution of memory and regulatory CD4+ T cells in the periphery. Nat.Rev.Immunol. 2007;7:231-237.

60. Pillai V, Karandikar NJ. Human regulatory T cells: a unique, stable thymic subset or a reversible peripheral state of differentiation? Immunol.Lett. 2007;114:9-15.

61. Liston A, Rudensky AY. Thymic development and peripheral homeostasis of regulatory T cells. Curr.Opin.Immunol. 2007;19:176-185.

62. Amyes E, Hatton C, Montamat-Sicotte D et al. Characterization of the CD4+ T cell response to Epstein-Barr virus during primary and persistent infection. J.Exp.Med. 2003;198:903-911.

63. Amyes E, McMichael AJ, Callan MF. Human CD4+ T cells are predominantly distributed among six phenotypically and functionally distinct subsets. J.Immunol. 2005;175:5765-5773.

64. Roman E, Miller E, Harmsen A et al. CD4 effector T cell subsets in the response to influenza: heterogeneity, migration, and function. J.Exp.Med. 2002;196:957-968.

65. Lu L, Cantor H. Generation and regulation of CD8(+) regulatory T cells. Cell Mol.Immunol. 2008;5:401-406.

66. Kondo T, Takata H, Takiguchi M. Functional expression of chemokine receptor CCR6 on human effector memory CD8(+) T cells. Eur.J.Immunol. 2007;37:54-65.

67. Takata H, Takiguchi M. Three memory subsets of human CD8+ T cells differently expressing three cytolytic effector molecules. J.Immunol. 2006;177:4330-4340.

68. Hamann D, Baars PA, Rep MH et al. Phenotypic and functional separation of memory and effector human CD8+ T cells. J.Exp.Med. 1997;186:1407-1418.

69. Appay V, Dunbar PR, Callan M et al. Memory CD8+ T cells vary in differentiation phenotype in different persistent virus infections. Nat.Med. 2002;8:379-385.

70. Monteiro M, Evaristo C, Legrand A, Nicoletti A, Rocha B. Cartography of gene expression in CD8 single cells: novel. Blood 2007;109:2863-2870.

71. Noble A, Zhao ZS, Cantor H. Suppression of immune responses by CD8 cells. II. Qa-1 on activated B cells stimulates CD8 cell suppression of T helper 2 responses. J.Immunol. 1998;160:566-571.

72. Najafian N, Chitnis T, Salama AD et al. Regulatory functions of CD8+. J.Clin.Invest 2003;112:1037-1048.

73. Berditchevski F, Odintsova E. Tetraspanins as regulators of protein trafficking. Traffic. 2007;8:89-96.

74. Boucheix C, Rubinstein E. Tetraspanins. Cell Mol.Life Sci. 2001;58:1189-1205.

75. Wright MD, Moseley GW, van Spriel AB. Tetraspanin microdomains in immune cell signalling and malignant disease. Tissue Antigens 2004;64:533-542.

76. Charrin S, le Naour F, Silvie O et al. Lateral organization of membrane proteins: tetraspanins spin their web. Biochem.J. 2009;420:133-154.

77. Hemler ME. Tetraspanin functions and associated microdomains. Nat.Rev.Mol.Cell Biol. 2005;6:801-811.

78. Pols MS, Klumperman J. Trafficking and function of the tetraspanin CD63. Exp.Cell Res. 2009;315:1584-1592.

79. Levy S, Todd SC, Maecker HT. CD81 (TAPA-1): a molecule involved in signal transduction and cell adhesion in the immune system. Annu.Rev.Immunol. 1998;16:89-109.

80. Gordon-Alonso M, Yanez-Mo M, Barreiro O et al. Tetraspanins CD9 and CD81 modulate HIV-1-induced membrane fusion. J.Immunol. 2006;177:5129-5137.

81. Zoller M. Tetraspanins: push and pull in suppressing and promoting metastasis. Nat.Rev.Cancer 2009;9:40-55.

82. Khandelwal S, Roche PA. Distinct MHC class II molecules are associated on the dendritic cell surface in cholesterol-dependent membrane microdomains. J.Biol.Chem. 2010;285:35303-35310.

83. Rubinstein E, Ziyyat A, Wolf JP, le Naour F, Boucheix C. The molecular players of sperm-egg fusion in mammals. Semin.Cell Dev.Biol. 2006;17:254-263.

84. Chambrion C, le Naour F. The tetraspanins CD9 and CD81 regulate CD9P1-induced effects on cell migration. PLoS.One. 2010;5:e11219.

85. Andre M, Morelle W, Planchon S et al. Glycosylation status of the membrane protein CD9P-1. Proteomics. 2007;7:3880-3895.

86. van Spriel AB, Figdor CG. The role of tetraspanins in the pathogenesis of infectious diseases. Microbes.Infect. 2010;12:106-112.

87. Yanez-Mo M, Barreiro O, Gordon-Alonso M, Sala-Valdes M, Sanchez-Madrid F. Tetraspanin-enriched microdomains: a functional unit in cell plasma membranes. Trends Cell Biol. 2009;19:434-446.

88. Yanez-Mo M, Barreiro O, Gonzalo P et al. MT1-MMP collagenolytic activity is regulated through association with tetraspanin CD151 in primary endothelial cells. Blood 2008;112:3217-3226.

89. van Spriel AB, Sofi M, Gartlan KH et al. The tetraspanin protein CD37 regulates IgA responses and anti-fungal immunity. PLoS.Pathog. 2009;5:e1000338.

90. Powner D, Kopp PM, Monkley SJ, Critchley DR, Berditchevski F. Tetraspanin CD9 in cell migration. Biochem.Soc.Trans. 2011;39:563-567.

91. Miyado K, Yamada G, Yamada S et al. Requirement of CD9 on the egg plasma membrane for fertilization. Science 2000;287:321-324.

92. Jegou A, Ziyyat A, Barraud-Lange V et al. CD9 tetraspanin generates fusion competent sites on the egg membrane for mammalian fertilization. Proc.Natl.Acad.Sci.U.S.A 2011;108:10946-10951.

93. Takeda Y, He P, Tachibana I et al. Double deficiency of tetraspanins CD9 and CD81 alters cell motility and protease production of macrophages and causes chronic obstructive pulmonary disease-like phenotype in mice. J.Biol.Chem. 2008;283:26089-26097.

94. Koumangoye RB, Sakwe AM, Goodwin JS, Patel T, Ochieng J. Detachment of breast tumor cells induces rapid secretion of exosomes which subsequently mediate cellular adhesion and spreading. PLoS.One. 2011;6:e24234.

95. Petersen SH, Odintsova E, Haigh TA et al. The role of tetraspanin CD63 in antigen presentation via MHC class II. Eur.J.Immunol. 2011;41:2556-2561.

96. Shoham T, Rajapaksa R, Boucheix C et al. The tetraspanin CD81 regulates the expression of CD19 during B cell development in a postendoplasmic reticulum compartment. J.Immunol. 2003;171:4062-4072.

97. Boismenu R, Rhein M, Fischer WH, Havran WL. A role for CD81 in early T cell development. Science 1996;271:198-200.

98. Todd SC, Lipps SG, Crisa L, Salomon DR, Tsoukas CD. CD81 expressed on human thymocytes mediates integrin activation and interleukin 2-dependent proliferation. J.Exp.Med. 1996;184:2055-2060.

99. Takeda Y, Li Q, Kazarov AR et al. Diminished metastasis in tetraspanin CD151-knockout mice. Blood 2011;118:464-472.

100. Sadej R, Romanska H, Kavanagh D et al. Tetraspanin CD151 regulates transforming growth factor beta signaling: implication in tumor metastasis. Cancer Res. 2010;70:6059-6070.

101. Haeuw JF, Goetsch L, Bailly C, Corvaia N. Tetraspanin CD151 as a target for antibody-based cancer immunotherapy. Biochem.Soc.Trans. 2011;39:553-558.

102. Wright MD, Geary SM, Fitter S et al. Characterization of mice lacking the tetraspanin superfamily member CD151. Mol.Cell Biol. 2004;24:5978-5988.

103. Yang YH, Speed T. Design issues for cDNA microarray experiments. Nat.Rev.Genet. 2002;3:579-588.

104. Olson NE. The microarray data analysis process: from raw data to biological significance. NeuroRx. 2006;3:373-383.

105. Holmes S, He M, Xu T, Lee PP. Memory T cells have gene expression patterns intermediate between naive and effector. Proc.Natl.Acad.Sci.U.S.A 2005;102:5519-5523.

106. Du X, Tang Y, Xu H et al. Genomic profiles for human peripheral blood T cells, B cells, natural killer cells, monocytes, and polymorphonuclear cells: comparisons to ischemic stroke, migraine, and Tourette syndrome. Genomics 2006;87:693-703.

107. Palmer C, Diehn M, Alizadeh AA, Brown PO. Cell-type specific gene expression profiles of leukocytes in human peripheral blood. BMC.Genomics 2006;7:115.

108. Haining WN, Ebert BL, Subrmanian A et al. Identification of an evolutionarily conserved transcriptional signature of CD8 memory differentiation that is shared by T and B cells. J.Immunol. 2008;181:1859-1868.

109. Canales RD, Luo Y, Willey JC et al. Evaluation of DNA microarray results with quantitative gene expression platforms. Nat.Biotechnol. 2006;24:1115-1122.

110. Wang M, Windgassen D, Papoutsakis ET. Comparative analysis of transcriptional profiling of CD3+, CD4+ and CD8+ T cells identifies novel immune response players in T-cell activation. BMC.Genomics 2008;9:225.

111. Chtanova T, Kemp RA, Sutherland AP, Ronchese F, Mackay CR. Gene microarrays reveal extensive differential gene expression in both CD4(+) and CD8(+) type 1 and type 2 T cells. J.Immunol. 2001;167:3057-3063.

112. Vanguilder HD, Vrana KE, Freeman WM. Twenty-five years of quantitative PCR for gene expression analysis. Biotechniques 2008;44:619-626.

113. Reiner SL. Development in motion: helper T cells at work. Cell 2007;129:33-36.

114. Sallusto F, Geginat J, Lanzavecchia A. Central memory and effector memory T cell subsets: function, generation, and maintenance. Annu.Rev.Immunol. 2004;22:745-763.

115. Haining WN, Wherry EJ. Integrating genomic signatures for immunologic discovery. Immunity. 2010;32:152-161.

116. Peixoto A, Evaristo C, Munitic I et al. CD8 single-cell gene coexpression reveals three different effector types present at distinct phases of the immune response. J.Exp.Med. 2007;204:1193-1205.

117. Chtanova T, Newton R, Liu SM et al. Identification of T cell-restricted genes, and signatures for different T cell responses, using a comprehensive collection of microarray datasets. J.Immunol. 2005;175:7837-7847.

118. Haining WN, Angelosanto J, Brosnahan K et al. High-throughput gene expression profiling of memory differentiation in primary human T cells. BMC.Immunol. 2008;9:44.

119. Forster R, Davalos-Misslitz AC, Rot A. CCR7 and its ligands: balancing immunity and tolerance. Nat.Rev.Immunol. 2008;8:362-371.

120. Barthel SR, Gavino JD, Descheny L, Dimitroff CJ. Targeting selectins and selectin ligands in inflammation and cancer. Expert.Opin.Ther.Targets. 2007;11:1473-1491.

121. Laubli H, Borsig L. Selectins promote tumor metastasis. Semin.Cancer Biol. 2010;20:169-177.

122. Ito T, Carson WF, Cavassani KA, Connett JM, Kunkel SL. CCR6 as a mediator of immunity in the lung and gut. Exp.Cell Res. 2011;317:613-619.

123. del Rio ML, Lucas CL, Buhler L, Rayat G, Rodriguez-Barbosa JI. HVEM/LIGHT/BTLA/CD160 cosignaling pathways as targets for immune regulation. J.Leukoc.Biol. 2010;87:223-235.

124. Soroosh P, Doherty TA, So T et al. Herpesvirus entry mediator (TNFRSF14) regulates the persistence of T helper memory cell populations. J.Exp.Med. 2011;208:797-809.

125. Frank M. MAL, a proteolipid in glycosphingolipid enriched domains: functional implications in myelin and beyond. Prog.Neurobiol. 2000;60:531-544.

126. Anton O, Batista A, Millan J et al. An essential role for the MAL protein in targeting Lck to the plasma membrane of human T lymphocytes. J.Exp.Med. 2008;205:3201-3213.

127. Anton OM, Andres-Delgado L, Reglero-Real N, Batista A, Alonso MA. MAL protein controls protein sorting at the supramolecular activation cluster of human T lymphocytes. J.Immunol. 2011;186:6345-6356.

128. Trapani JA. Granzymes: a family of lymphocyte granule serine proteases. Genome Biol. 2001;2:REVIEWS3014.

129. Heutinck KM, ten Berge IJ, Hack CE, Hamann J, Rowshani AT. Serine proteases of the human immune system in health and disease. Mol.Immunol. 2010;47:1943-1955.

130. Voskoboinik I, Dunstone MA, Baran K, Whisstock JC, Trapani JA. Perforin: structure, function, and role in human immunopathology. Immunol.Rev. 2010;235:35-54.

131. Kondos SC, Hatfaludi T, Voskoboinik I et al. The structure and function of mammalian membrane-attack complex/perforin-like proteins. Tissue Antigens 2010;76:341-351.

132. Buschow SI, Nolte-'t Hoen EN, van NG et al. MHC II in dendritic cells is targeted to lysosomes or T cell-induced exosomes via distinct multivesicular body pathways. Traffic. 2009;10:1528-1542.

133. Kropshofer H, Spindeldreher S, Rohn TA et al. Tetraspan microdomains distinct from lipid rafts enrich select peptide-MHC class II complexes. Nat.Immunol. 2002;3:61-68.

134. Unternaehrer JJ, Chow A, Pypaert M, Inaba K, Mellman I. The tetraspanin CD9 mediates lateral association of MHC class II molecules on the dendritic cell surface. Proc.Natl.Acad.Sci.U.S.A 2007;104:234-239.

135. Hutcheson HB, Olson LM, Bradford Y et al. Examination of NRCAM, LRRN3, KIAA0716, and LAMB1 as autism candidate genes. BMC.Med.Genet. 2004;5:12.

136. Battye R, Stevens A, Perry RL, Jacobs JR. Repellent signaling by Slit requires the leucine-rich repeats. J.Neurosci. 2001;21:4290-4298.

137. Haines BP, Gupta R, Jones CM, Summerbell D, Rigby PW. The NLRR gene family and mouse development: Modified differential display PCR identifies NLRR-1 as a gene expressed in early somitic myoblasts. Dev.Biol. 2005;281:145-159.

138. Bianchi G, Ferrari P, Staessen JA. Adducin polymorphism: detection and impact on hypertension and related disorders. Hypertension 2005;45:331-340.

139. Yenerel MN, Sundell IB, Weese J, Bulger M, Gilligan DM. Expression of adducin genes during erythropoiesis: a novel erythroid promoter for ADD2. Exp.Hematol. 2005;33:758-766.

140. Ro HS, Zhang L, Majdalawieh A et al. Adipocyte enhancer-binding protein 1 modulates adiposity and energy homeostasis. Obesity.(Silver.Spring) 2007;15:288-302.

141. Rodrigues-Ferreira S, Di TA, Dimitrov A et al. 8p22 MTUS1 gene product ATIP3 is a novel anti-mitotic protein underexpressed in invasive breast carcinoma of poor prognosis. PLoS.One. 2009;4:e7239.

142. Li ZH, Bresnick AR. The S100A4 metastasis factor regulates cellular motility via a direct interaction with myosin-IIA. Cancer Res. 2006;66:5173-5180.

143. Kim SV, Mehal WZ, Dong X et al. Modulation of cell adhesion and motility in the immune system by Myo1f. Science 2006;314:136-139.

144. Seimiya M, Wada A, Kawamura K et al. Impaired lymphocyte development and function in Clast5/Stra13/DEC1-transgenic mice. Eur.J.Immunol. 2004;34:1322-1332.

145. Kallies A. Distinct regulation of effector and memory T-cell differentiation. Immunol.Cell Biol. 2008;86:325-332.

146. Chang JT, Palanivel VR, Kinjyo I et al. Asymmetric T lymphocyte division in the initiation of adaptive immune responses. Science 2007;315:1687-1691.

147. Catron DM, Rusch LK, Hataye J, Itano AA, Jenkins MK. CD4+ T cells that enter the draining lymph nodes after antigen injection participate in the primary response and become central-memory cells. J.Exp.Med. 2006;203:1045-1054.

148. Protty MB, Watkins NA, Colombo D et al. Identification of Tspan9 as a novel platelet tetraspanin and the collagen receptor GPVI as a component of tetraspanin microdomains. Biochem.J. 2009;417:391-400.

149. Kim DK, Kabat J, Borrego F et al. Human NKG2F is expressed and can associate with DAP12. Mol.Immunol. 2004;41:53-62.

150. Hofer E, Sobanov Y, Brostjan C, Lehrach H, Duchler M. The centromeric part of the human natural killer (NK) receptor complex: lectin-like receptor genes expressed in NK, dendritic and endothelial cells. Immunol.Rev. 2001;181:5-19.

151. Trowsdale J, Barten R, Haude A et al. The genomic context of natural killer receptor extended gene families. Immunol.Rev. 2001;181:20-38.

152. Brostjan C, Bellon T, Sobanov Y, Lopez-Botet M, Hofer E. Differential expression of inhibitory and activating CD94/NKG2 receptors on NK cell clones. J.Immunol.Methods 2002;264:109-119.

153. Naderi A, Teschendorff AE, Beigel J et al. BEX2 is overexpressed in a subset of primary breast cancers and mediates nerve growth factor/nuclear factor-kappaB inhibition of apoptosis in breast cancer cell lines. Cancer Res. 2007;67:6725-6736.

154. Kendall SE, Ryczko MC, Mehan M, Verdi JM. Characterization of NADE, NRIF and SC-1 gene expression during mouse neurogenesis. Brain Res.Dev.Brain Res. 2003;144:151-158.

155. Miharada K, Hiroyama T, Sudo K et al. Lipocalin 2-mediated growth suppression is evident in human erythroid and monocyte/macrophage lineage cells. J.Cell Physiol 2008;215:526-537.

156. Devireddy LR, Gazin C, Zhu X, Green MR. A cell-surface receptor for lipocalin 24p3 selectively mediates apoptosis and iron uptake. Cell 2005;123:1293-1305.

157. Richardson DR. 24p3 and its receptor: dawn of a new iron age? Cell 2005;123:1175-1177.

158. Quigley MF, Gonzalez VD, Granath A, Andersson J, Sandberg JK. CXCR5+. Eur.J.Immunol. 2007;37:3352-3362.

159. Zhang F, Kotha J, Jennings LK, Zhang XA. Tetraspanins and vascular functions. Cardiovasc.Res. 2009;83:7-15.

160. Sincock PM, Fitter S, Parton RG et al. PETA-3/CD151, a member of the transmembrane 4 superfamily, is localised to the plasma membrane and endocytic system of endothelial cells, associates with multiple integrins and modulates cell function. J.Cell Sci. 1999;112 (Pt 6):833-844.

161. Liu L, He B, Liu WM et al. Tetraspanin CD151 promotes cell migration by regulating integrin trafficking. J.Biol.Chem. 2007;282:31631-31642.

162. Harder T, Rentero C, Zech T, Gaus K. Plasma membrane segregation during T cell activation: probing the order of domains. Curr.Opin.Immunol. 2007;19:470-475.

163. Gaus K, Chklovskaia E, Fazekas de St GB, Jessup W, Harder T. Condensation of the plasma membrane at the site of T lymphocyte activation. J.Cell Biol. 2005;171:121-131.

164. Zech T, Ejsing CS, Gaus K et al. Accumulation of raft lipids in T-cell plasma membrane domains engaged in TCR signalling. EMBO J. 2009;28:466-476.

165. Schroder J, Lullmann-Rauch R, Himmerkus N et al. Deficiency of the tetraspanin CD63 associated with kidney pathology but normal lysosomal function. Mol.Cell Biol. 2009;29:1083-1094.

166. Imhof I, Gasper WJ, Derynck R. Association of tetraspanin CD9 with transmembrane TGF{alpha} confers alterations in cell-surface presentation of TGF{alpha} and cytoskeletal organization. J.Cell Sci. 2008;121:2265-2274.

167. Chaussabel D, Pascual V, Banchereau J. Assessing the human immune system through blood transcriptomics. BMC.Biol. 2010;8:84.

168. Pascual V, Allantaz F, Patel P et al. How the study of children with rheumatic diseases identified interferon-alpha and interleukin-1 as novel therapeutic targets. Immunol.Rev. 2008;223:39-59.

169. McKinney EF, Lyons PA, Carr EJ et al. A CD8+ T cell transcription signature predicts prognosis in autoimmune disease. Nat.Med. 2010;16:586-91, 1p.

170. Schepers K, Swart E, van Heijst JW et al. Dissecting T cell lineage relationships by cellular barcoding. J.Exp.Med. 2008;205:2309-2318.

Chapter Eight

Appendix

8 APPENDIX

Please see enclosed CD for appendix data

8.1 Chapter Three Supplemental Table 1

8.2 Chapter Three Supplemental Table 2

8.3 Chapter Three Supplemental Table 3

8.4 Chapter Three Supplemental Table 4

8.5 Chapter Three Supplemental Table 5

8.6 Chapter Three Supplemental Table 6

8.7 Chapter Three Supplemental Table 7

8.8 Chapter Three Supplemental Table 8

8.9 Chapter Three Supplemental Table 9

8.10 Chapter Three Supplemental Table 10

8.11 Chapter Three Supplemental Table 11

8.12 Chapter Three Supplemental Table 12

8.13 Chapter Three Supplemental Table 13

8.14 Chapter Three Supplemental Table 14

8.15 Chapter Three Supplemental Table 15

Normalised microarray results for all samples

8.16 Chapter Four Supplemental Table 1